The role of ASPP2 in intestinal cell polarity and homeostasis

Sofia Koch

A thesis submitted in fulfillment of the requirements for the degree of

Doctor of Philosophy

Wolfson College

Ludwig Institute for Cancer Research, ORCB

Nuffield Department of Clinical Medicine

University of Oxford

Hilary 2013

DECLARATION

All the work presented in this thesis is the result of my own work and does not constitute part of any other thesis unless stated otherwise. The work here described was performed while I was a graduate student at the Ludwig Institute for Cancer Research, under the supervision of Professor Xin Lu.

Number of words: 48 023 + bibliography

The Paradox of Life:

A bit beyond perception's reach
I sometimes believe I see
that Life is two locked boxes, each
containing the other's key.

Piet Hein (1905-1996)

The role of ASPP2 in intestinal cell polarity and homeostasis

Sofia Koch, Wolfson College, DPhil in Clinical Medicine, Hillary 2013

ABSTRACT

The intestinal epithelium is an important model that integrates various biological processes, including cell proliferation, cell differentiation and inflammation. Recent evidence has linked intestinal homeostasis with cell polarity. ASPP2, a known tumor suppressor, has been implicated in the maintenance of epithelial integrity. In this thesis, how ASPP2 is involved in intestinal epithelial cell polarity, and whether its function modulates the epithelial homeostasis in the intestine is examined.

For this purpose, the intestinal epithelia of transgenic Balb/c ASPP2 Δexon3 and ASPP2 conditional knockout mice were studied. The expression of ASPP2 under energetic stress was investigated, and the consequences of the loss of ASPP2 in a DSS-challenged mouse model were evaluated. ASPP2 was found to be localized at the tight junctions in the intestinal epithelium. The loss of ASPP2 in the intestine resulted in epithelial disorganization, and compromised epithelial cell turnover by promoting cell proliferation and influencing Notch-regulated differentiation. Interaction between ASPP2 and the LKB1 complex was also observed, and the expression and localization of ASPP2 was proven to be influenced by glucose levels in an AMPK-dependent manner. Various signs of intestinal inflammation were detected in ASPP2-null mice, and the increased susceptibility of these mice to develop DSS-induced colitis further supported the observations.

Overall, ASPP2 was identified as a gatekeeper of the intestinal tight junctions, and new insights into the complex involvement of ASPP2 in cell metabolism and intestinal inflammation were uncovered.

ACKNOWLEDGEMENTS

Every time I was asked to define my experience as a PhD student I would immediately remember the feeling of enjoying a roller coaster ride. With my one way ticket I have now finished the most exciting ride of my life. This would have never been so pleasant and memorable without you all.

Xin, thank you for guiding me throughout these years and, most of all, thank you for believing in me and for giving me the confidence and motivation when I most needed.

To my beautiful family, the biggest thank you for all the love and support. Mami, I am so thankful for all your patience and wise words. Distance seemed a lot smaller with your daily therapeutic love. Papi, thank you for teaching me the word Science and for always making me feel I am the greatest. To my sister and brother, thank you for 3471 miles of support, optimism and confidence even when science is not your biggest pation. Love you.

Special friends, you painted my life with beautiful colors during these years. Your visits, phone calls and emails, put a smile on my face every day. Martinha, your daily "good morning" will be forever in my heart! Thank you for being close to me for the past 22 years. Gui, a million times thank you for being my loveliest fan, for believing I could make it and, most importantly, for inspiring me. "Eu sei, eu sei/ Que a vida devia ser bem melhor e será/ Mas isso não importa que eu repita/ É bonita, é bonita/ E é bonita...". Felipe, thank you so much for your support, friendship and long conversations, which gave me the peace and courage to keep moving on. Morgan, four years and 5437 miles later I thank you for always being close to me. Joana, thank you for rescuing me every time I was feeling lonely. Visiting you in

London was always the best plan. Ju, finding you again brought fresh air to my life in Oxford. Thank you for your sweet words and for being just like me.

Oxfamily, you made my PhD so much easier! Jasmin, Melania, Mara, Jorgito, Luca, Anna, Chris, Mario, Ludo, Zinaida, Emma, Ewa, Anna, Emmanouela, Paul, Alex, Cristiano, Massimo, Lara, Francisca, Rui and Elisa thank you for all your help, support, conversations, parties, ethnic dinners, pub crawls and road trips. For the good and bad moments, I know I could always count on you!

Finally, but not less important, a big thank you to Indi, Mark, Douglas and Kelly. My work was in very good hands all these years because of you. Million times thank you.

TABLE OF CONTENTS

CHAPTER 1 – INTRODUCTION **16**

1.1 - Development and homeostasis in the intestine **16**

1.1.1 – Biology of the intestinal epithelium 16

1.1.2 – Stem cell renewal and cell turnover 19

1.1.3 – Signalling pathways involved in intestinal development 21

1.1.3.1 – The Notch signalling pathway 21

1.1.3.2 – The Wnt signalling pathway 25

1.2 - Epithelial cell polarity **29**

1.2.1 – The epithelial cell architecture 29

1.2.2 – Crosstalk between cell polarity complexes 30

1.2.3 – Tight junctional proteins and their biological importance 34

1.2.3.1 – Cell polarity proteins and pathogens 36

1.2.3.2 – Cell polarity proteins and cancer 37

1.3 - Inflammation in the intestinal epithelium **39**

1.3.1 – Host-bacterial relationships in the intestinal epithelium 39

1.3.2 – Keeping commensal bacteria under surveillance 40

1.3.3 – Intestinal immune response 44

1.3.4 – Inflammation and epithelial cell polarity: a vicious cycle 47

1.3.5 – Inflammatory bowel diseases 48

1.4 – Tumorigenesis in the intestine **51**

1.4.1 – Tumor suppressors in colorectal cancer 51

1.4.1.1 – Adenomatous polyposis coli (APC) 51

1.4.1.2 – p53 53

1.4.2 – Sporadic colorectal cancer vs. colitis-associated cancer 55

1.4.2.1 – Inflammation and CAC initiation 57

1.5 – LKB1 – The intestinal tumour suppressor **62**

1.5.1 – LKB1 and Peutz-Jeghers syndrome 62

1.5.2 – Structure and regulation of LKB1 63

1.5.3 – LKB1 and p53 partnership 66

1.5.4 – LKB1 and cell metabolism 67

1.5.5 – LKB1 and cell polarity 69

1.6 – The ASPP family of proteins **70**

1.6.1 – Discovery and characterization 70

1.6.2 – Expression and biological function *in vivo* 73

1.6.3 – ASPP proteins in cancer 79

1.6.4 – ASPP2 and cell polarity 80

AIMS OF THE STUDY **81**

CHAPTER 2 – MATERIALS AND METHODS **84**

2.1 – Materials **84**

2.1.1 – Reagents 84

2.1.2 – SDS-Poliacrylamide gels 94

2.1.3 – Antibodies 95

2.1.4 – Cell lines 97

2.2 – Methods **98**

2.2.1 – Tissue culture 98

2.2.2 – DNA and RNA techniques 100

2.2.3 – Protein manipulation 103

2.2.4 – Cell-based assays 106

2.2.5 – Mouse work 109

2.2.6 – Dextran sulphate sodium-induced colitis 117

2.2.6.1 – Experimental setup 117
2.2.6.2 – Histological grading 118
2.2.7 – Human tissue samples 119
2.2.8 – Data analysis 119

CHAPTER 3 – ASPP2 DEFICIENCY COMPROMISES THE MORPHOLOGY AND INTEGRITY OF THE INTESTINAL EPITHELIUM 120

3.1 – Introduction 120

3.2 – Results 122

3.2.1 – ASPP2 is located at the epithelial tight junctions in both duodenum and colon 122
3.2.2 – ASPP2 deficiency leads to cell disorganization and shortening of crypt structure 126
3.2.3 – An absence of ASPP2disrupts the epithelium in colon but not in duodenum 135
3.2.4 – Goblet cell lineage is impaired in ASPP2$^{\Delta 3/\Delta 3}$ intestine 134
3.2.5 – The number of Paneth cells is increased in ASPP2 deficient mice 137
3.2.6 – ASPP2 deficiency does not affect enteroendocrine and absorptive cell lineages 141
3.2.7 – Notch target gene Hes5 is upregulated in ASPP2$^{\Delta 3/\Delta 3}$ duodenum 144
3.2.8 – ASPP2 deficiency results in an increased proliferation in Intestinal epithelium *in vivo* 147
3.2.9 – ASPP2 deficiency promotes proliferation of *ex vivo* intestinal organoids culture 152
3.2.10 – ASPP2 deficient mice show increased apoptosis in the duodenal epithelium 156

3.3 – Summary and brief discussion 160

CHAPTER 4 – ASPP2 IS AFFECTED BY GLUCOSE STARVATION: A LINK TO LKB1 164

4.1 – Introduction 164

4.2 – Results 167

4.2.1 – ASPP2 expression is altered under glucose deprivation conditions 167

4.2.2 – Under glucose deprivation conditions, the expression of ASPP2 is dependent on AMPK activation 171

4.2.3 – Deletion of ASPP2 influences LKB1 cellular location and AMPK activation 174

4.2.4 – LKB1 expression interferes with ASPP2 location 179

4.2.5 – ASPP2 interacts with the LKB1 complex 181

4.2.6 – The interaction between ASPP2 and PP1 is weaker upon glucose starvation 187

5.3 – Summary and brief discussion 189

CHAPTER 5 – ASPP2 DEFICIENCY INCREASES SUSCEPTIBILITY TO COLONIC INFLAMMATION 191

5.1 – Introduction 191

5.2 – Results 193

5.2.1 – ASPP2-deficient mice show evidence of intestinal inflammation 193

5.2.2 – $ASPP2^{loxP/loxP}$; Cre^{+} mice are more susceptible to developing DSS-induced colitis 201

5.2.3 – ASPP2 is downregulated in colonic epithelia of Crohn's patients 212

5.2.4 – ASPP2 expression and cellular localization are modulated by TNFα production and hypoxic conditions 215

5.2.5 – Normal localization of ASPP2 is disrupted in the colon of *Helicobacter hepaticus* infected mice 222

5.2.6 – ASPP2 deficient mice are susceptible to chronic DSS-induced colitis 225

5.3 – Summary **230**

CHAPTER 6 – DISCUSSION AND FUTURE PLANS **232**

6.1 – ASPP2, Notch and Wnt signaling: crosstalk *in vivo* 232

6.2 – ASPP2 and the intestinal epithelium: one role, different outcomes 237

6.3 – ASPP2: a putative link between cell polarity and metabolism 238

6.4 – ASPP2: the gatekeeper in cell polarity and intestinal inflammation 243

BIBLIOGRAPHY **247**

LIST OF FIGURES

Figure 1.1 – Homeostasis of the intestinal epithelium. 17

Figure 1.2 - Intestinal epithelium organization and cell renewal. 23

Figure 1.3 - Schematic representation of the canonical Wnt signaling pathway. 27

Figure 1.4 – Schematic diagram of a polarized epithelial cell. 32

Figure 1.5 - Schematic overview of the intestinal immune system. 42

Figure 1.6 - The NF-κB canonical pathway. 45

Figure 1.7 – Model of intestinal cancer initiation and progression. 60

Figure 1.8 - Schematic structure of the human LKB1, STRAD and Mo25 protein domains. 64

Figure 1.9 - The ASPP family of proteins. 71

Figure 1.10 - Schematic overview of the regulation of p53-dependent apoptosis by the ASPP family members. 75

Figure 1.11 - Loss of cell-cell contacts upon ASPP2 deletion. 81

Figure 3.1 - In duodenum, ASPP2 colocalizes with components of the Apical Polarity Complex. 124

Figure 3.2 - In the colon, ASPP2 colocalizes with components of the Apical Polarity Complex. 125

Figure 3.3 - ASPP2 deficiency leads to epithelial cell disorganization in the duodenum. 128

Figure 3.4 - Loss of ASPP2 results in shortening of the colonic crypts. 129

Figure 3.5 - ASPP2 deficiency does not affect epithelial cell polarity in duodenum. 132

Figure 3.6 - ASPP2 deficiency leads to loss of cell polarity in the colonic epithelium. 133

Figure 3.7 - ASPP2 deficiency leads to mislocalization and decrease in the number of goblet cells, in the duodenum and colon, respectively. 136

Figure 3.8 - Increase and mislocalization of Paneth cell abundance in ASPP2$^{\Delta 3/\Delta 3}$ duodenum. 140

Figure 3.9 - Loss of ASPP2 does not compromise the enteroendocrine and absorptive cell populations. 142

Figure 3.10 - Hes5 is stimulated upon ASPP2 deficiency in the duodenum. 146

Figure 3.11 - Loss of ASPP2 promotes cell proliferation, *in vivo*. 149

Figure 3.12 - Loss of ASPP2 results in an increase of cells undergoing mitosis, *in vivo*. 150

Figure 3.13 - Increased mitotic index in the duodenum and colon from ASPP2$^{\Delta 3/\Delta 3}$ mice. 151

Figure 3.14 – ASPP2$^{\Delta 3/\Delta 3}$ intestinal organoids show an abnormal growth process. 153

Figure 3.15 - Loss of ASPP2 results in an increase in cell proliferation, *ex vivo*. 155

Figure 3.16 - ASPP2 inhibits cell proliferation in *ex vivo* cultures. 156

Figure 3.17 - Increased apoptosis in ASPP2$^{\Delta 3/\Delta 3}$ duodenum. 159

Figure 4.1 - Increase in ASPP2 expression, at the level of tight junctions, upon glucose deprivation. 170

Figure 4.2 - Downregulation of ASPP2 upon suppression of AMPK activation and absence of LKB1. 173

Figure 4.3 - ASPP2 depletion promotes LKB1 cytoplasmic expression and AMPK activation. 177

Figure 4.4 - Deletion of LKB1 compromises ASPP2 cellular location. 180

Figure 4.5 - Mo25 interacts with β-catenin *in vitro* and *in vivo*. 183

Figure 4.6 - ASPP2 interacts with LKB1 and Mo25. 186

Figure 4.7 - Weak ASPP2-PP1 binding under low glucose conditions. 188

Figure 5.1 - Presence of lymphoid follicles in ASPP2$^{\Delta 3/\Delta 3}$ intestine. 195

Figure 5.2 - Evidence of an active immune response in ASPP2$^{\Delta 3/\Delta 3}$ intestine. 197

Figure 5.3 - The inflammatory response is active in ASPP2$^{\Delta 3/\Delta 3}$ intestine. 200

Figure 5.4 - ASPP2$^{loxP/loxP}$; Cre^{+} mice suffer a significant loss of weight and gross bleeding. 204

Figure 5.5 - DSS-challenged ASPP2$^{loxP/loxP}$; Cre^{+} conditional mice score higher in the disease activity index. 206

Figure 5.6 - DSS-induced colitis results in shortening of colon in ASPP2 conditional knockout mice. 207

Figure 5.7 - Loss of ASPP2 increases the susceptibility to DSS-induced colitis. 210

Figure 5.8 - Histological score of DSS-treated ASPP2$^{loxP/loxP}$; Cre^{+} mice. 211

Figure 5.9 - ASPP2 expression is altered in Crohn's colonic tissue. 214

Figure 5.10 - TNF-alpha treatment induces downregulation of ASPP2. 218

Figure 4.11 - Downregulation and mislocalization of ASPP2 under hypoxic conditions. 221

Figure 5.12 - ASPP2 is mislocalized upon *Helicobacter hepaticus* infection. 224

Figure 5.13 - Percentage of weight change during the third cycle of treatment is higher in ASPP2$^{loxP/loxP}$ DSS-fed animals. 227

Figure 5.14 - Loss of ASPP2 increases the susceptibility to chronic DSS-induced colitis. 229

Figure 6.1 - Modulation of intestinal homeostasis by ASPP2. 236

Figure 6.2 - Proposed model of the ASPP2-AMPK-LKB1 on the regulation of tight junctions integrity. 242

LIST OF TABLES

Table 2.1 - Preparation of SDS-Polyacrylamide gels. 97

Table 2.2 - List of primary antibodies. 98

Table 2.3 - List of secondary antibodies. 99

Table 2.4 - List of cell lines and its relevant information. 100

Table 2.5 - List of primers used in RT-PCR experiments. 105

Table 2.6 - List of plasmids and its relevant information. 109

Table 5.1 - Disease activity index (DAI) score. 205

Table 5.2 - Histological score to assess the degree of colonic inflammation. 209

CHAPTER 1 – INTRODUCTION

1.1 – DEVELOPMENT AND HOMEOSTASIS IN THE INTESTINE

1.1.1 – BIOLOGY OF THE INTESTINAL EPITHELIUM

The intestinal tract is composed of three tissue layers. The outer layer contains several sheets of smooth muscle which are responsible for peristalsis, while the middle layer consists of stromal tissue. The inner surface, named the mucosa, is composed of cuboidal epithelial cells. In the mucosa, a single layer of intestinal epithelial cells supports a variety of functions such as digestion, absorption of nutrients and water, and ultimately acts as a barrier against luminal pathogens. The intestinal tube is divided into the colon and small intestine, the latter being subdivided into three parts: the duodenum, jejunum and ileum. The absorptive surface of the small intestine is dramatically increased by finger-shaped luminal protrusions, named villi, and flask-shaped submucosa invaginations called the crypts of Lieberkühn. In contrast, the large intestine has only crypts, and flat surface epithelium replaces the absent villi (Sancho et al., 2004). To accomplish its different biological tasks, the intestinal epithelium relies on two lineages of highly specialized and metabolically active cells: the enterocyte or absorptive lineage; and the secretory lineage, which consists of goblet, Paneth and enteroendocrine cells (Figure 1.1). Enterocytes are the most abundant intestinal epithelial cells. Due to the presence of apically localised microvilli, the enterocytes greatly increase the absorptive surface of the mucosa and the lateral junctions with adjacent cells (Snoeck et al., 2005). Goblet cells secrete the protective mucus which constitutes a barrier against the contents of the intestinal lumen (Specian and Oliver, 1991).

These cells are scattered along the villi and their abundance increases from the duodenum to the colon. Enteroendocrine cells represent a small percentage of the small intestine's epithelial cells, but are considered to be the largest population of hormone-producing cells in the body (Schonhoff et al., 2004). They produce a variety of hormones such as serotonin, secretin and substance P, that help motility in the gastrointestinal tract (Rehfeld, 1998). Finally, Paneth cells are the main source of antimicrobial agents such as cryptdins, defensins and lysozyme, which protect the mucosa against enteropathogens (Ayabe et al., 2000; Porter et al., 2002). The structure of the intestinal epithelium is extraordinarily organized and its maintenance is tightly regulated to ensure tissue homeostasis (Figure 1.1). The intestinal epithelium is dependent on controlled polarization of the epithelial cells to ensure their correct migration (Louvard et al., 1992). Similarly, front-rear polarity determines migration processes during developmental stages and wound healing (Dow and Humbert, 2007). Most importantly, the establishment of cell polarity is essential for the paracellular transit of solutes and nutrients (Matter and Mellman, 1994). The correct maintenance and integrity of epithelial cell polarity is, therefore, important to ensure normal cell physiology and epithelial tissue homeostasis. The intestinal epithelium is often described as one component of a tri-partite communication network that also includes the microflora and the immune system. In fact, for intestinal homeostasis to be ensured, crosstalk between immune cells, the epithelium and enterobacteria must exist (Figure 1.1). Loss of epithelial cell polarity, invasion of the epithelium by opportunistic pathogens or an impaired immune response are all considered to be threats that will compromise the homeostatic balance.

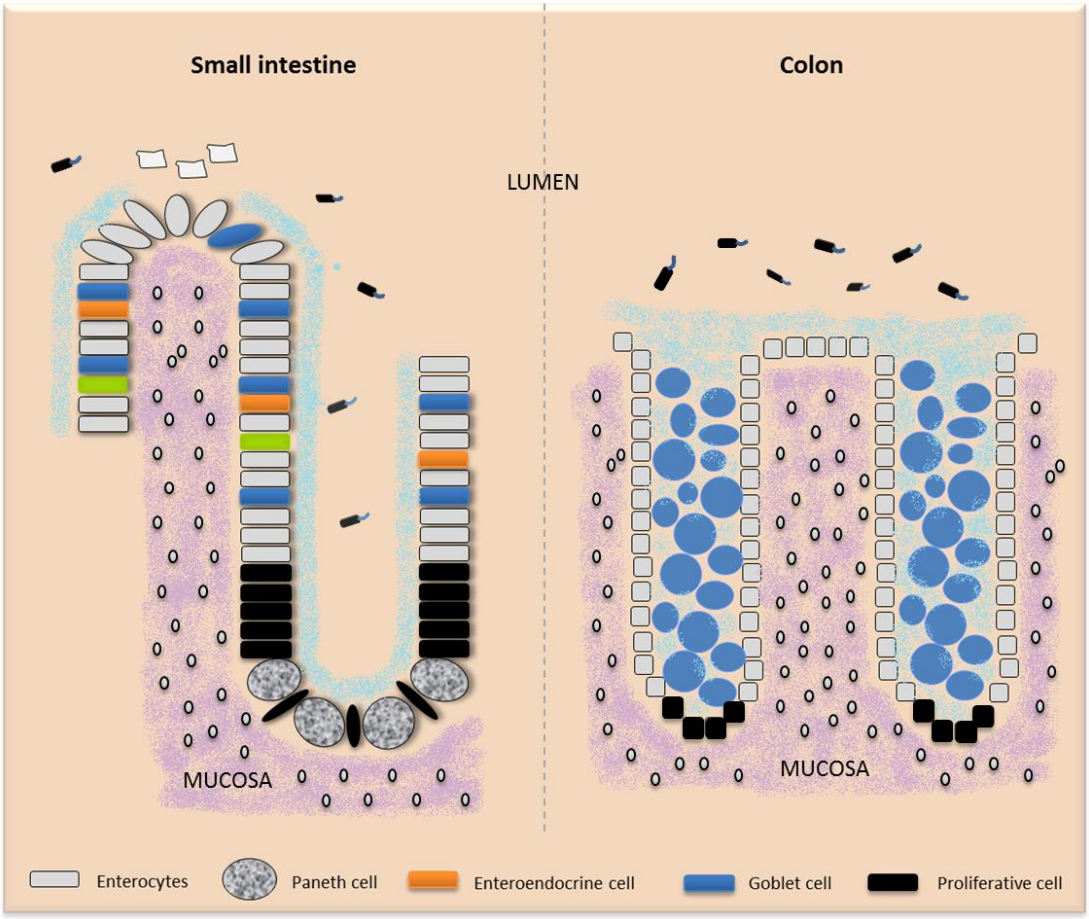


FIGURE 1.1 – Homeostasis of the intestinal epithelium. The small intestine consists of four differentiated cell types. Enterocytes, enteroendocrine and goblet cells are positioned along the villi. Paneth cells are located at the bottom of the crypts. In the colon, only enterocytes and goblet cells are present. Proliferative cells locate at the bottom of the crypts, in both the small intestine and colon. For homeostatic balance to be ensured, tri-partite communication is established between the intestinal epithelium, immune cells present in the mucosa, and the luminal bacteria.

1.1.2 – STEM CELL RENEWAL AND CELL TURNOVER

Homeostasis of the intestinal tissue is maintained by continuous and rapid replacement of differentiated cells, by replication of undifferentiated transit cells located within the crypts. Differentiation in the crypts follows a spatial orientation. With the exception of Paneth cells, which remain at the bottom of the crypts, newly differentiated cells migrate upwards, along the crypt-villus axis, and away from the proliferative zone (van der Flier and Clevers, 2009). Once they have fulfilled their differentiation function, cells at the top of the villus become apoptotic and are sloughed off into the intestinal lumen (Potten et al., 1997). Thus, the tissue has a distinct polarity, with new cells created by mitosis at the base of the crypt and dying cells being shed into the intestinal lumen at the tip of the villi (Creamer et al., 1961; Umar, 2010). Altogether, the crypt is mainly a proliferative compartment, is monoclonal and is maintained by multipotent stem cells, whereas the villus comprises the differentiated compartment and is polyclonal, as it accommodates cells generated in different crypts (Figure 1.2A).

In a healthy adult animal, the rates of cell proliferation and cell death must be balanced and are, therefore, under rigorous surveillance. In fact, situations of decreased proliferation lead to the disruption of epithelial integrity, whereas increased proliferation promotes an increase in the number of cells and possibly to structural alterations of the crypt compartment (Potten, 1997). Much of our current knowledge of intestinal self-renewal is based on classical studies using the adult mouse small intestine as a model system (Potten and Morris, 1988). The driving force of the intestinal renewal program seems to be entirely dependent on a limited number of long-lived multipotent intestinal stem or progenitor cells. These cells are

believed to undergo asymmetric cell division into a new stem cell and a transient amplifying (TA) cell (Figure 1.2A). The latter is capable of undergoing a limited number of cell divisions before terminally differentiating (van der Flier and Clevers, 2009). Morphological criteria do not exist to identify intestinal stem cells (ISCs). For many years, these cells have been characterized by their properties, such as their ability to self-renew during long periods of time and to generate all four intestinal differentiated cell types (Potten and Loeffler, 1990). However, recent studies have identified putative intestinal stem cell markers (Barker and Clevers, 2007). The G protein coupled receptor 5, also known as Lgr5, was found to be only expressed at the base of the intestinal crypts. In particular, the Lgr5 gene was found to be expressed in active cycling crypt base columnar (CBC) cells interspersed between Paneth cells (Barker et al., 2007) (Figure 1.2A). Lineage tracing experiments have provided further evidence that the Lgr5-positive CBC cells constitute multipotent stem cells in both the small intestine and colon (Barker et al., 2007). The discovery that Lgr5-positive single cells can generate a long term culture of crypt-villus differentiated structures *in vitro* supports the hypothesis that intestinal Lgr5 positive cells are, in reality, stem cells (Sato et al., 2009). More intestinal stem cell markers have been identified since then. For instance, Bmi1 has found to be expressed in ISCs *in vivo* (Sangiorgi and Capecchi, 2008). Interestingly, new findings suggest that Lgr5-positive cells are dispensable for intestinal homeostasis, since the ablation of this population is readily compensated by Bmi1-expressing stem cells (Tian et al., 2011). This observation suggests that the two populations of cells can communicate and, in addition, reflects the importance of Bmi1-positive cells as a

reservoir of stem cells that can become useful in case of injury to the intestinal epithelium, or under non-pathological conditions (Figure 1.2A).

1.1.3 – SIGNALING PATHWAYS INVOLVED IN INTESTINAL DEVELOPMENT

Under normal conditions, the equilibrium between cell proliferation and differentiation is critical to maintain the overall homeostasis of the epithelium. Important signaling processes coordinate cell fate decisions in the intestinal epithelium (Sancho et al., 2004). On one hand, specific signaling mediators modulate cell proliferation by interfering with cell cycle progression. On the other hand, different signaling molecules promote cell cycle arrest, thus initiating the differentiation process and gene expression pattern that ultimately leads a single cell towards a specific phenotype (Sancho et al., 2004). The crosstalk between the Notch pathway and Wnt signaling has been widely accepted to be essential for the maintenance of intestinal epithelium homeostasis.

1.1.3.1 – THE NOTCH SIGNALING PATHWAY

The Notch signaling pathway is conserved throughout evolution, being found in a wide variety of organisms from worms to humans (Artavanis-Tsakonas et al., 1999). In mammals, the Notch receptor family comprises four single transmembrane receptors (Notch 1-4) and five single transmembrane ligands: Jagged 1 (Jag1), Jagged 2 (Jag2) and Delta 1 (Dll1), 3 (Dll3) and 4 (Dll4). The activation of the Notch cascade is initiated when ligand-receptor interactions between neighboring cells take place. Following their interaction, proteolytic cleavage by γ-secretase releases

the intracellular domain (NICD) from the receptor, allowing its translocation to the nucleus where it binds the transcription factor CSL (RBPJ-κ in mouse) (Jarriault et al., 1995). Consequently, the expression of Notch-responsive genes is stimulated. The best characterized Notch target genes to date include the basic helix-loop-helix (bHLH) transcription factors of the hairy/enhancer of split (HES) family such as Hes1 and Hes5 (Jarriault et al., 1995).

The Notch pathway is activated at the embryonic level in order to regulate many developmental events and cell fate decisions in a context-dependent manner (Artavanis-Tsakonas et al., 1999). Several reports have also implicated Notch in adult hematopoiesis and skin homeostasis. Notch promotes hematopoietic stem cell (HSC) self-renewal while, in committed progenitor cells, it defines the specific cell phenotype to be adopted (Radtke et al., 2004). In adult skin, Notch inhibits the differentiation of precursor cells. However, it is also involved when a decision on the fate of epidermal and hair cells has to be taken (Yamamoto et al., 2003). In the intestinal epithelium, mRNA encoding Notch ligands, receptors and target genes, such as Hes1 and Hes5, was found to be expressed in proliferating crypt cells (Schroder and Gossler, 2002). Their location reflects the important role of Notch signaling in the self-renewal of stem cells, cell fate determination of progenitor cells, and terminal differentiation of trans-amplifying cells (Katoh, 2007). The first evidence suggesting a role for the Notch pathway in the homeostasis of the intestinal epithelium was obtained following studies in Hes1 knockout mice (Jensen et al., 2000). The deletion of *Hes1* resulted in excessive differentiation of endocrine cells in the small intestine, suggesting that *Hes1* is involved in the repression of the differentiation program towards the endocrine sub-lineage (Jensen et al., 2000).

Subsequent studies have revealed that *Hes1* deficiency stimulates the precocious development of Paneth and Goblet cells in the small intestine, leading to the conclusion that *Hes1* plays an inhibitory role in the differentiation of secretory cells (Suzuki et al., 2005).

Later works have uncovered roles of other Notch target proteins in intestinal homeostasis. For instance, the loss of *Math1*, one of the genes repressed by *Hes1*, compromises the differentiation of goblet, Paneth and enteroendocrine cells without affecting the enterocytes (Yang et al., 2001). Supporting this finding, intestinal cells lacking *Math1* fail to exit the cell cycle, explaining why differentiation does not take place. This specificity suggests that *Math1* is necessary for the establishment of the intestinal secretory lineage: elevated expression of *Hes1* inhibits *Math1* activity leading the cell to an enterocyte phenotype; whereas downregulation of *Hes1* activates Math1 and consequently favors differentiation into a secretory cell lineage (Yang et al., 2001) (Figure 1.2B).

Experiments performed in zebrafish support the hypothesis that the Notch signaling pathway modulates the commitment of progenitor cells to a secretory lineage fate. Indeed, the intestine of DeltaD (Delta 1 in the mouse) mutants exhibits an excess of secretory cells at the cost of absorptive cells (Crosnier et al., 2005). Similarly, in the mouse, Dll1 deficiency induces an increase in the number of goblet cells. However, the complete conversion of progenitor cells to post-mitotic differentiated cells, and the consequent loss of the crypt progenitor compartment, is only achieved when both Dll1 and Dll4 are defective (Pellegrinet et al., 2011). Identical results were obtained by inactivating Notch1 and Notch2 receptors, by conditionally targeting the RBPJ-κ gene or blocking the release of NICD by inhibiting

γ-secretase (Marsh and Clarke, 2007; Riccio et al., 2008; van Es et al., 2005). Thus, the disruption of the Notch signaling pathway results in an exit from the proliferative crypt compartment and commitment to post-mitotic secretory cells (Figure 1.2B).

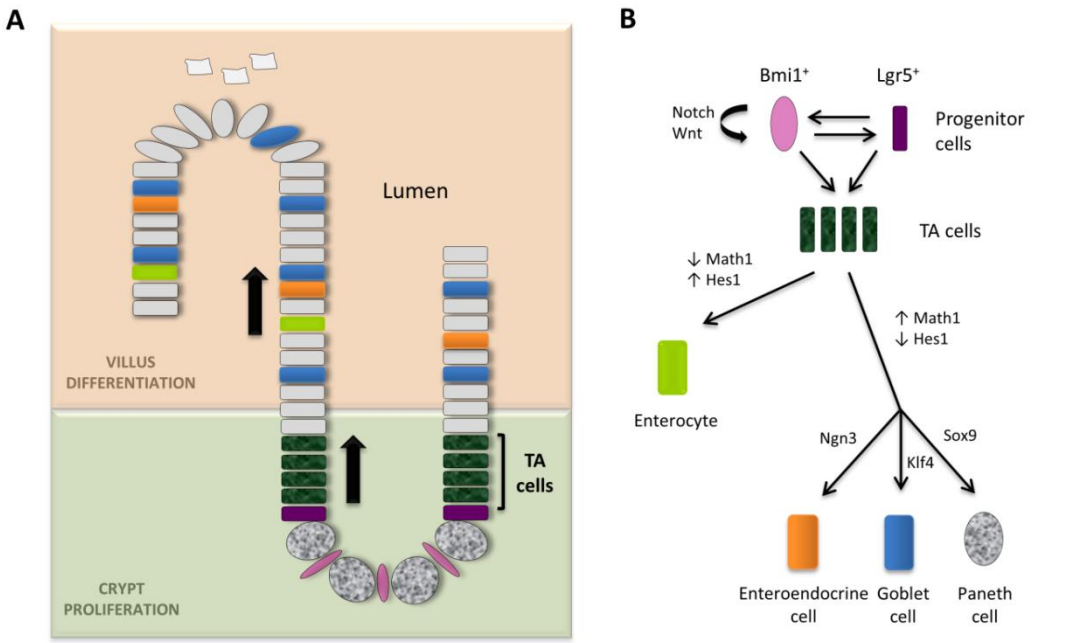


FIGURE 1.2 - Intestinal epithelium organization and cell renewal. (A) Description of epithelial cell turnover in the intestine. Intestinal epithelial cells are located at the bottom of the intestinal crypts together with the Paneth cells. Transient amplifying (TA) cells generate differentiated cells that will be positioned along the intestinal villi. Cells move up towards the lumen where they eventually enter an apoptotic program and are sloughed off. **(B) Schematic overview of epithelial cell lineage commitment in the intestine.** Intestinal stem cells proliferate under the control of the Notch and Wnt pathways, and can originate cells which differentiate into four different types. Math1 is necessary to promote cells to differentiate into the secretory cell lineage, whereas Hes1 promotes the commitment of cells to the absorptive cell lineage. Within the secretory lineage, Sox9 is responsible for differentiation into Paneth cells, kruppel-like factor (Klf4) is necessary for goblet cell differentiation and neurogenin 3 (Ngn3) is required for enteroendocrine cell fate.

1.1.3.2 – THE WNT SIGNALING PATHWAY

The Wnt signaling cascade is conserved in all metazoans, where it is known to regulate important developmental events. The Wnt/wingless genes encode a large family of secreted cysteine-rich proteins, which become biologically active upon palmitoylation of conserved cysteines (Willert et al., 2003). By interacting with the seven-span transmembrane protein Frizzled (Fz), and the single-span transmembrane protein LRP, Wnts activate responding cells and initiate a signaling transduction pathway (Clevers, 2006; Logan and Nusse, 2004) (Figure 1.3). This represents the initial stage in the canonical pathway that ultimately leads to the formation of the nuclear complexes Tcf/β-catenin. The key component of the Wnt signaling pathway is the cytoplasmic protein β-catenin. Intracellular levels of β-catenin are controlled by a multiprotein complex, composed of the scaffolding proteins adenomatous polyposis coli (APC), Axin1, Axin2 and kinases such as glycogen synthase kinase-3β (GSK3β) and casein kinase 1 (CK1) (Clevers, 2006; Logan and Nusse, 2004). In the absence of Wnt signaling, the so-called β-catenin destruction complex binds and phosphorylates β-catenin at serine and threonine residues, thus targeting the protein for ubiquitination and degradation. Under physiological conditions, persistent degradation of β-catenin is interrupted by the interaction of Wnt ligands with the receptors Frizzled and LRP, and their subsequent co-activation. It is believed that the posterior recruitment and docking of Axin to the LRP tail disrupts the destruction complex, thereby releasing β-catenin (Ikeda et al., 1998). The stabilization of β-catenin results in its translocation to the nucleus, where it binds to members of the TCF/LEF family of transcription factors (Daniels and Weis, 2005) (Figure 1.3).

It has been reported that the canonical pathway regulates the 'stemness', proliferation and differentiation of all the so-far defined human adult stem cell niches, including the skin and hair follicles, mammary gland and hematopoietic tissues (Alonso and Fuchs, 2003; Li et al., 2003; Lowry et al., 2005; Reya et al., 2003). In addition, the Wnt signaling pathway has a decisive role in intestinal development, homeostasis and tumourigenesis (Gregorieff et al., 2005).

Various *in vivo* evidence suggest that Wnt signaling is essential for the normal proliferation of transit-amplifying cells, as well as maintenance of the stem cell niche in the intestinal crypts (Pinto et al., 2003). Firstly, it is known that defective Tcf-4 and β-catenin result in the loss of the proliferative cell compartment in adult intestine (Ireland et al., 2004; Korinek et al., 1998b). Similarly, overexpression of the Wnt inhibitor Dickkopf-1 (Dkk-1) significantly inhibits cell proliferation in the small intestine and colon, and affects the architecture of the crypts (Kuhnert et al., 2004). In agreement with these results, mutations in the negative regulator APC, or overexpression of oncogenic mutants of β-catenin, result in a crypt progenitor phenotype characterized by hyper-proliferation of the intestinal epithelium (Andreu et al., 2005; Sansom et al., 2004; van de Wetering et al., 2002). Finally, the expression of nuclear β-catenin at the bottom of the intestinal crypts, where putative stem cells are located, suggests that these cells respond to Wnt activation (van de Wetering et al., 2002). Interestingly, in addition to proliferation, recent results have shown that Wnt signaling is the driving force of the intestinal differentiation program. In fact, blocking the stimulation of the Wnt cascade compromises the goblet, Paneth and enteroendocrine cell sub-lineages, while enterocytes are not affected (Ireland et al., 2004; Korinek et al., 1998b; Pinto et al.,

2003). Supported by these findings, a simplistic view suggests that Wnt signaling is established as a gradient along the crypt-villus axis, which is stronger at the crypt base where cells proliferate and fades away towards the tip of the villus. Accordingly, in the proliferative compartment, transit-amplifying cells respond to intense Wnt stimulation by proliferating and commit themselves to the secretory lineage (Gregorieff et al., 2005). As these immature cells move up the crypt and further away from the Wnt source, the activity of the complex Tcf/β-catenin is inhibited, hence promoting cell cycle arrest and terminal differentiation (Gregorieff et al., 2005).

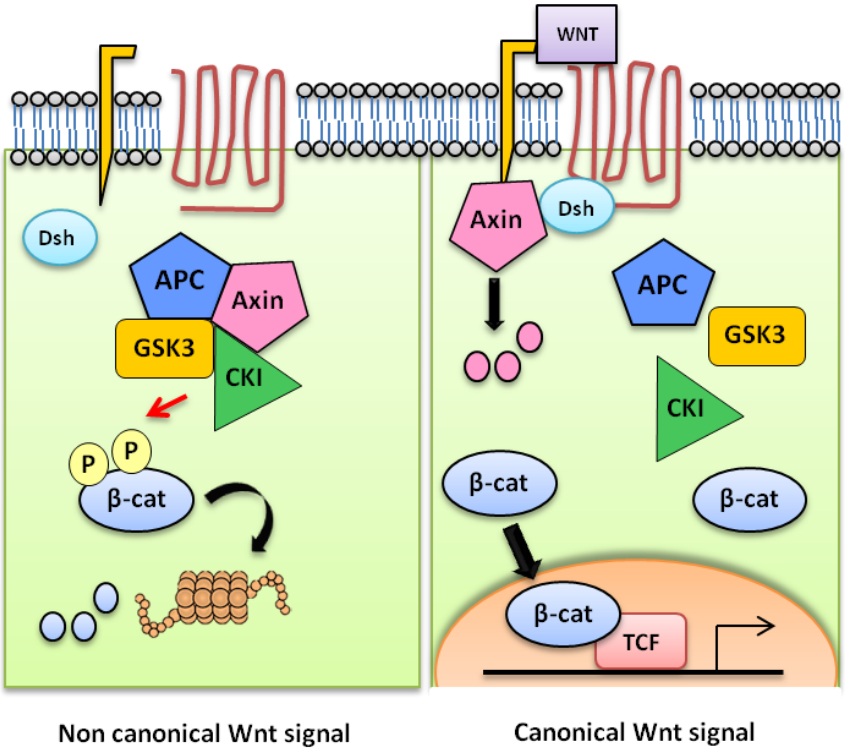


FIGURE 1.3 - **Schematic representation of the canonical Wnt signaling pathway.** In the absence of Wnt stimulation, β-catenin is kept at low levels by the destruction complex, which comprises the adenomatous polyposis coli (APC), axin, casein kinase I (CKI) and glycogen synthase kinase 3 (GSK3). Through phosphorylation, the complex targets β-catenin for proteasome-mediated degradation. When Wnt ligands are present, activation of the Wnt signaling pathway occurs. Wnt ligands bind to the Frizzled receptors and low-density lipoprotein receptor-related protein (LRP) co-receptors. Consequently, the β-catenin destruction complex is inactivated and β-catenin cellular levels increase. β-catenin is translocated to the nucleus where it binds to T cell factor (TCF) transcription factors. A transcriptional complex is activated, leading to the expression of Wnt target genes.

1.2 – EPITHELIAL CELL POLARITY

1.2.1 – EPITHELIAL CELL ARCHITECTURE

The establishment of a cell polarity axis and adhesive cell-cell contacts is an important requisite for the formation of functional epithelial tissues, such as the intestinal epithelium. Cell polarity, fundamental in several aspects of cell biology and development, is determinant in the processes of proliferation, differentiation and morphogenesis. In addition, many cell constituents such as plasma membrane proteins, organelles and cytoskeletal components, depend on a cell polarity axis to be correctly organized within the cell (Muth and Caplan, 2003). The polarization of an epithelial cell results from the regionalization of two plasma membrane domains: the apical surface facing the lumen, and the basolateral domain facing adjacent cells and the connective tissue (Mostov et al., 1992) (Figure 1.4A). The apical domain of the plasma membrane contains anion channels, H^+/K^+ - ATPase, and transporters, whereas the lateral region of the basolateral domain comprises proteins responsible for attachment to adjacent cells and cell-cell communication (Mostov et al., 1992). The basal portion of the basolateral domain accommodates the binding sites for constituents of the basal lamina, as well as receptors for hormones and other signaling molecules (Mostov et al., 1992).

Four types of cell-cell contacts constitute the intercellular junctional complex: tight junctions (TJs), adherens junctions (AJs), desmosomes and gap junctions (Knust and Bossinger, 2002)(Figure 1.4A). TJs are localised at the limit between the apical membrane facing the lumen, and the basolateral surface in contact with the interior of the organism. These specialized intercellular complexes establish barriers

that selectively prevent the leakage of molecules across the intercellular space (Shin et al., 2006). Moreover, TJs behave as fences between the apical and basolateral domain, as they prevent the diffusion of integral proteins and lipids from one domain to the other (Shin et al., 2006). AJs, which are located just below the TJs, are specialized forms of cadherin-based adhesive contacts. These structures are particularly important in cellular organization, but also in transmitting information from the environment to the interior of the cell (Nagafuchi, 2001). Desmosomes are likely to be the most specialized complex of junctional proteins, the constituents of which are indirectly linked to intermediate filaments and microfilaments of the cytoskeleton, therefore regulating the mechanical strength of the tissues (Green et al., 1998; Kouklis et al., 1994). The fourth type of intercellular junction is the gap junction, in which clusters of intercellular pores are tightly packed together, directly connecting the cytoplasm of adjacent cells and allowing the exchange of electrolytes, secondary messengers and metabolites between the cells (Evans and Martin, 2002).

1.2.2 – CROSSTALK BETWEEN CELL POLARITY COMPLEXES

Several proteins that are important for epithelial cell integrity and architecture were first identified and characterized in models like *C. elegans* and *Drosophila melanogaster*. The machinery constructed with these proteins is highly conserved from worm to human. Cell polarity proteins belong to a rich group of protein complexes that play an important role in asymmetric cell division, anterior-posterior polarity in embryogenesis, apical-basal polarity in epithelial cells, and regulation of

junction assembly (Jan and Jan, 1998; Matter et al., 2005; St Johnston and Nusslein-Volhard, 1992; Yeaman et al., 1999). The importance of these proteins has been reflected in a number of studies, which relate cell polarity and epithelial integrity disruption to various human pathologies such as inflammatory disorders, cancer and developmental syndromes (Fish and Molitoris, 1994). Three evolutionarily conserved signaling polarity complexes have been described: the core complex Par3/Par6/aPKC, the apical complex Crumbs/Pals/PATJ and the basolateral complex Scrib/mDlg/mLgl (Assemat et al., 2008; Margolis and Borg, 2005) (Figure 1.4B).

The Par3/Par6/aPKC complex is essential for anterior-posterior polarity in *C. elegans,* and the apical-basal polarity of epithelial cells and neuroblasts in *D. melanogaster* (Hutterer et al., 2004; Tabuse et al., 1998). The complex is localised at the apical region of the TJ, where the two adaptor proteins Par-3 and Par-6 work together with atypical protein kinase C (aPKC) (Ohno, 2001). Par-6 exhibits one PDZ domain, which is necessary for the binding of the amino terminus of Par-3. In agreement, the interaction of Par-3 with aPKC requires the carboxyl terminal region of Par-3 and the catalytic domain of aPKC (Nagai-Tamai et al., 2002). The direct association of Par3 to the protein JAM promotes the tethering of the polarity complex to the TJs, ensuring the proper location of the core complex (Itoh et al., 2001) (Figure 1.4B).

Efficient membrane polarization is achieved by regulated coordination between the core complex and the conserved apical and basolateral complexes (Hurd et al., 2003) (Figure 1.4B). In mammalian cells, the apical complex comprises Crumbs-3, PALS1 and PATJ (Hurd et al., 2003). In MDCK cells, Crumbs-3 binds directly to Par-6, promoting its recruitment via the adapter protein PALS1 and under the regulation

of Cdc42-GTP (Hurd et al., 2003; Lemmers et al., 2004). Besides this interaction, PALS1 is also able to bind PATJ, the mammalian homolog of *Drosophila* Inadl (Roh et al., 2002). Supporting the importance of the coordination between the apical polarity complex and TJs, it has been reported that both ZO-3 and claudin-1 directly interact with PATJ (Roh et al., 2002). PATJ mutants lacking the PDZ domains necessary for these binding interactions have been found to be expressed away from the tight junctions (Lemmers et al., 2002). Interestingly, mislocalization of PALS1, ZO-1 and members of the core complex has also been observed, suggesting that PATJ plays an important role in recruiting core and apical polarity complex members to the tight junctions (Michel et al., 2005).

Coordination between the basolateral polarity and core complexes is mediated by the direct interactions of both aPKC and Par-6 with mLgl (Yamanaka et al., 2003) (Figure 1.4B). Calcium switch assays have shown that, during the initial stages of tight junction assembly, mLgl/aPKC/Par-6 complexes are observed and localised apically at premature cell-cell contact sites (Yamanaka et al., 2003). The establishment of tight junctions is initiated by the phosphorylation and migration of mLgl to the lateral membrane, basal to the TJs (Plant et al., 2003). These findings suggest that the mLgl/aPKC/Par-6 complex has a transient role which could be important in the suppression of TJ assembly depending on the phosphorylation status of mLgl. Once dissociated from mLgl, the aPKC/Par-6 complex is available to bind to Par-3 and assist in the establishment of TJs (Horikoshi et al., 2009). Overall, the selective interaction of aPKC/Par-6, and the phosphorylation of mLgl, contributes to the regulation of epithelial cell polarity and TJ assembly.

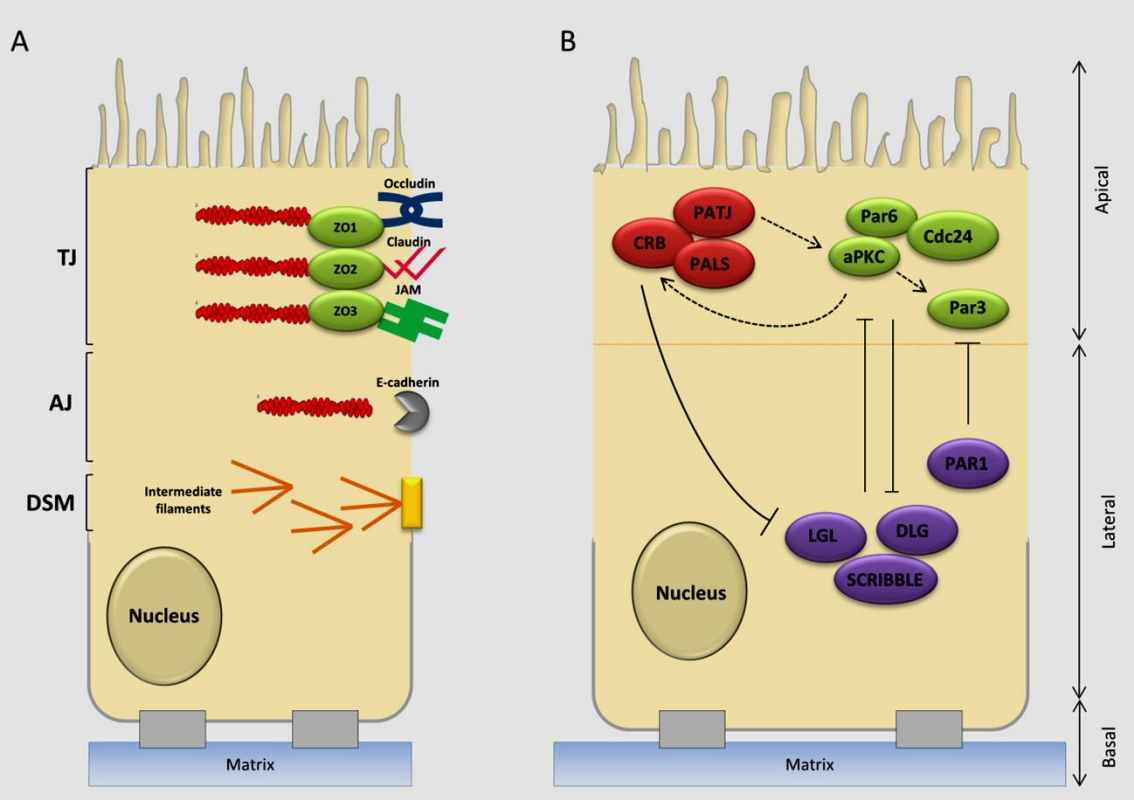


FIGURE 1.4 - Schematic diagram of a polarized epithelial cell. (A) Junction proteins in polarized epithelial cells. Tight junctions (TJs) form a barrier that limits the paracellular permeability of water and nutrients. The proteins Occludin, Claudin, JAM (Junctional adhesion molecules) and ZO (zonula occludens) characterize the TJs. Adherens junctions (AJs) are composed of members of the cadherin family. Both TJs and AJs are linked to the actin cytoskeleton network. Desmosomes (DSM) are connected to intermediate filaments. **(B) Cell polarity complexes in polarized epithelial cells.** Three important polarity complexes participate in the establishment of apical-basal polarity. The Crumbs complex, consisting of the proteins Crb, PALS and PATJ, is necessary for the establishment of the apical membrane. The Par complex comprises the proteins Par3, Par6, aPKC and cell division control Cdc42, and ensures the assembly of the apical lateral membrane. The complex comprising Scribble, Lgl and Dlg defines the basolateral plasma membrane domain. These complexes have opposing interactions and distinct spatiotemporal functions in the regulation of epithelial polarity. Dashed arrows represent translocation to different subcellular locations.

1.2.3 – TIGHT JUNCTIONAL PROTEINS AND THEIR BIOLOGICAL IMPORTANCE

The accepted structural model of epithelial TJs is one of a stable multiprotein complex, which consists of transmembrane and peripheral membrane proteins. Three main families of transmembrane proteins characterize the TJs: occludins, claudins and junctional adhesion molecules (JAMs).

Occludin was described as the first integral membrane protein to be exclusively present at the TJs (Furuse et al., 1993). The localization of occludin at the level of the TJs requires its interaction with adaptor proteins such as ZO-1, ZO-2 and ZO-3 (Furuse et al., 1994; Haskins et al., 1998; Itoh et al., 1999). Furthermore, occludin is able to interact indirectly with the actin cytoskeleton and JAMs (Bazzoni et al., 2000) (Figure 1.4). Occludin has been implicated in regulating the permeability properties of the TJs and, in particular, is involved in the regulation of size-selective particle diffusion (McCarthy et al., 1996). Knock-out studies have suggested that occludin is not essential for the establishment of TJs. In addition, deficient mice are viable and the morphology of TJs does not seem to be affected. Nevertheless, histological abnormalities observed in the gastric epithelium suggest that occludin might be involved in the process of gastric epithelial differentiation (Saitou et al., 1998; Schulzke et al., 2005).

Following on from the studies on occludins, claudins have been classified as important gatekeepers of paracellular transport (Van Itallie and Anderson, 2006). The paracellular ionic selectivity of the TJs is dependent on the distribution and number of charged residues along the extracellular loops of claudins (Colegio et al., 2002). In fact, claudin-2 can form paracellular ion channels, whereas claudin-8 functions as a paracellular ion barrier (Amasheh et al., 2002; Yu et al., 2003) (Figure

1.4). *In vivo* characterization of the claudins is beginning to offer insightful information as to how this family of proteins works. For instance, in mice lacking claudin-11, TJs are absent in the myelin sheaths of oligodendrocytes and Sertoli cells in the testis (Mazaud-Guittot et al., 2010). In addition, claudin-16 mutations, which are often reported in several human diseases, are linked to the impairment of paracellular permeability to calcium and magnesium in kidney epithelial cells (Kausalya et al., 2006). Claudin-5 deficient mice result in the normal development and morphology of blood vessels, but tracer experiments have revealed size-selective loosening of the TJs and the impairment of the blood-brain barrier's functions (Nitta et al., 2003). Furthermore, claudin-1 knockout mice die from dehydration shortly after birth, due to defects in epidermal barrier function (Furuse et al., 2002). Overall, these studies point to an important role of the claudins in maintaining the selectivity and permeability of TJs.

The JAMs constitute the third group of transmembrane proteins that characterize the TJs. These molecules belong to the IgG superfamily of proteins, and are characterized by a single span transmembrane domain, an extracellular domain containing two Ig-like motifs, and a short cytoplasmic C-terminus. This C-terminus contains a PDZ domain, which is likely to be involved in the interaction with TJ scaffolding proteins (Martin-Padura et al., 1998). These scaffolding proteins include ZO-1, calcium/calmodulin-dependent serine protein kinase (CASK/Lin2), membrane-associated guanylate kinase with inverted domain structure 1 (MAGI-1), multi-PDZ domain protein 1 (MUPP1) and partitioning defective 3 (Par3) (Bazzoni et al., 2000; Ebnet et al., 2000; Hamazaki et al., 2002; Hirabayashi et al., 2003; Itoh et al., 2001) (Figure 1.4). To date, 4 members of the JAM family have been identified. JAM-A is

expressed in both endothelial and epithelial cells, where it regulates TJ permeability and facilitates lymphocyte trafficking through the paracellular space (Woodfin et al., 2007). JAM-2 is expressed in endothelial cells, whereas JAM-3 facilitates lymphocyte migration via its expression on T cells (Johnson-Leger et al., 2002; Liang et al., 2002). JAM-4 is localised to the TJs and apical membranes of epithelial cells in the small intestine and renal proximal tubes (Tajima et al., 2003). Inhibition of JAM-A function with a monoclonal antibody is sufficient to decrease trans-epithelial resistance (TER) and promote defects in tight junction assembly (Ebnet et al., 2004). *In vivo* analysis has suggested a role of JAM-A in controlling colon mucosa barrier function, as studies performed with JAM-A deficient mice have revealed normal epithelial architecture but impaired leukocyte infiltration and large lymphoid aggregation in this tissue (Laukoetter et al., 2007).

1.2.3.1 – CELL POLARITY PROTEINS AND PATHOGENS

The apical junctional complex is an important target for microbial pathogens which need to overcome the epithelial barrier in order to colonize the host. Pathogens have evolved in such an intelligent way that they are able to manipulate epithelial cells to survive, proliferate and persist within the host when necessary. Moreover, viruses and bacteria are able to take advantage of the nutrients present in the interstitium, and seek protection from the immune system (Kazmierczak et al., 2001).

The enteropathogen *Escherichia coli* does not interact directly with host adhesion contacts, but instead uses bacterial effectors to disrupt epithelial integrity. In fact, the effector Tir initiates a multistep process that triggers the formation of

actin-based pedestals and, together with other effectors, activates the membrane-associated actin-binding protein ezrin, dephosphorylates occludin and activates myosin II light chain kinase (MLCK) (Goosney et al., 2001; Muza-Moons et al., 2003). *Helicobacter pylori* injects its effector protein CagA into host cells (Amieva et al., 2003). Once injected into stomach cells, CagA undergoes Src-mediated phosphorylation, following which infected cells internalize E-cadherin, become mobile and acquire an elongated morphology that results in the disruption of the epithelial barrier (Selbach et al., 2002). In addition, CagA interacts with ZO-1 and JAM-A, promoting their delocalization from the cell-cell contacts and the formation of ectopic TJs at the bacteria-host interaction sites (Amieva et al., 2003). *Clostridium difficile* secretes toxins that monoglucosylate the small GTPases Rac, Cdc42 and Rho, therefore inhibiting normal cytoskeletal dynamics. In addition, these toxins are also able to dissociate ZO-1, ZO-2 and occludin from the junctional complexes (Voth and Ballard, 2005).

1.2.3.2 – CELL POLARITY PROTEINS AND CANCER

The most convincing evidence presented to date, which suggests a link between cell polarity pathways and tumourigenesis, was generated from studies performed in *Drosophila* (Bilder et al., 2000; Humbert et al., 2003). Mutations of the polarity proteins *little giant larvae* (Lgl), *discs large* (Dlg) and *scribble* (Scrib), which behave as important tumor suppressors in *Drosophila*, result in a loss of apical-basal polarity and tissue structure (Bilder et al., 2000). *Drosophila* Lgl, Dlg and Scrib are unique in that they are the only tumour suppressors, among almost 50 already characterized, in which mutations lead to neoplastic transformation of the imaginal

discs and brain (Bilder et al., 2000). The *scrib*, *lgl* and *dlg* genes are highly conserved between *Drosophila* and mammals (Dow et al., 2003).

Impaired expression of Lgl, Dlg and Scrib has been found in human primary tumors. Scribble was found to be mislocalised and downregulated in human and mice spontaneous tumors including colon adenocarcinoma, endometrial and prostate cancer (Gardiol et al., 2006; Nakagawa et al., 2004; Pearson et al., 2011). In addition, cDNA microarray studies have suggested a decrease in the expression of Dlg homologues in gastric carcinomas, whereas Dlg3 expression is abolished in some oesophageal tumors (Hanada et al., 2000; Liu et al., 2002; Makino et al., 1997). Lgl1 is often associated with more advanced stages of human tumors, lymph node metastasis and poor survival, thereby being used as a marker of poor prognosis (Moreno-Bueno et al., 2008).

Mutations in components of the Par complex of proteins have not been directly associated with tumor formation or progression. However, several studies on this polarity complex indicate that the proteins can serve both tumos suppressive (Par3), as well as oncogenic (aPKC and Par6), functions (Lee and Vasioukhin, 2008). In fact, downregulation of Par3 is often observed in esophageal squamous cell carcinoma cell lines and primary tumors (Zen et al., 2009). On the contrary, overexpression and mislocalization of Par6 and aPKC has been described in poor prognosis human epithelial cancers including breast, lung, pancreas, liver, bladder, ovarian, prostate and colon (Aranda et al., 2008; Nolan et al., 2008; Regala et al., 2005; Viloria-Petit et al., 2009).

1.3 – INFLAMMATION IN THE INTESTINAL EPITHELIUM

1.3.1 – HOST-BACTERIAL RELATIONSHIPS IN THE INTESTINAL EPITHELIUM

Immediately after birth, all mammals are subject to a life-long process of colonization by microorganisms which inhabit most of the environmentally exposed epithelial surfaces such as the skin, mouth, intestinal tract and vagina. These host-bacterial associations have mainly evolved into beneficial relationships, creating conditions for mutualism (Hooper et al., 2001). The mammalian intestine provides a hospitable habitat for bacteria, stable in temperature and rich in nutrients. To the host, commensal bacteria supply important nutrients by digesting luminal contents. They also maintain the appropriate balance between different types of intestinal bacteria, preventing colonization by opportunistic pathogens. Lastly, commensals contribute to the fortification of the epithelial cell architecture (Hooper et al., 2001). The intestinal bacterial environment differs along the length of the gastrointestinal tract, increasing in density from the stomach to the colon (McCarthy et al., 1996). The distal intestine alone harbors a dense and diverse population of bacteria, containing up to 1×10^{14} colony-forming units (CFUs) of bacteria, approximately 10 times the number of host cells (Berg, 1996).

Although the mammalian intestinal epithelium must be sufficiently permeable to allow the absorption of nutrients, it must prevent the entrance of pathogenic bacteria by maintaining a homeostatic balance between its tolerance to commensals and immunity to pathogens.

1.3.2 – KEEPING COMMENSAL BACTERIA UNDER SURVEILLANCE

The mucosal immune system is frequently characterized as 'ignorant' to symbiotic intestinal bacteria. Immunological ignorance refers to the low immune responsiveness to the significant microbial burden in the intestine (Hooper, 2009).

The intestinal mucosa, comprising the intestinal epithelium, connective tissue layer (lamina propria) and gut-associated lymphoid tissues (GALT), has developed intelligent defense mechanisms to control and retain bacterial communities within the lumen and prevent them from breaching the gut mucosal barrier (Kraehenbuhl and Corbett, 2004). Epithelial cells not only provide a strong physical barrier, but are also able to produce mucins and antimicrobial peptides. Paneth cells secrete antimicrobial peptides, such as lysozyme and α-defensins (Figure 1.4), which inhibit both commensal and pathogenic growth and protect the epithelium from microbial adhesion (McCracken and Lorenz, 2001). The goblet cells produce and secrete mucin glycoproteins, which are assembled into a protective gel-like mucus layer (Johansson et al., 2008). This protective layer forms two distinct strata. Bacteria are distributed throughout the outer mucosal layer, whereas the inner layer is resistant to bacterial penetration, thus establishing a sterile zone directly in contact with the epithelial apical surface (Johansson et al., 2008) (Figure 1.5). To enforce the bacterial sequestering mechanism of mucins and antimicrobial peptides, IgA is secreted by B cells located in specialized M cells in the follicular epithelium (Figure 1.5). This immunoglobulin promotes the formation of a bacterial biofilm within the normal gut flora, but also limits the expansion and movement of undesired pathogenic populations (Bollinger et al., 2003).

Specialized lymphoid structures, including Peyer's patches (PPs) and isolated lymphoid follicles (ILFs), cooperate to sample luminal antigens and stimulate the immune system (Wells et al., 2011). In addition to these structures, intestinal dendritic cells (DCs) located in the lamina propria of the small intestine can extend their dendrites between epithelial cell contacts, to directly sample the luminal microenvironment (Coombes and Powrie, 2008) (Figure 1.5). Active sampling of bacteria by dendritic cells induces B cell production of bacteria-specific IgA, which in turn limits bacterial penetration across the epithelium (MacPherson et al., 2004).

This first line of defense, characterized by the mucus barrier, antimicrobial proteins and secretory IgA, can eventually be subverted by intestinal pathogens that use several strategies to gain access to the host's epithelial cells. The closer contact of pathogens with the intestinal epithelial single cell layer triggers a more complex defense response (Kelly et al., 2005). The molecular mechanisms that orchestrate the recognition of commensal microorganisms while maintaining a hypo-responsive immune system are still an area of intense research. Nevertheless, the traditional explanation for the differential immune response to pathogenic versus commensal bacteria relies on the observation that only opportunistic microorganisms have developed mechanisms to invade the epithelial barrier and survive within host tissues. In contrast, commensal bacteria, which lack pathogenicity factors, are not able to disseminate and survive in host cells and therefore fail to trigger the innate and adaptive immune response (Pamer, 2007). In the scenario of bacterial epithelial invasion, specialized cells of the innate immune system located in PPs, lymphoid follicles or the lamina propria are able to recognize pathogenic bacteria ligands due to the presence of pattern-recognition receptors (PRRs) on their surface (Artis,

2008). TLRs and nucleotide-binding oligomerization domain isoforms (NODs) are key examples of receptors necessary for the recognition of these bacteria by the mucosal immune system, reflecting the dynamic communication between the epithelium and lymphoid cells (Kim et al., 2004; Rakoff-Nahoum et al., 2004).

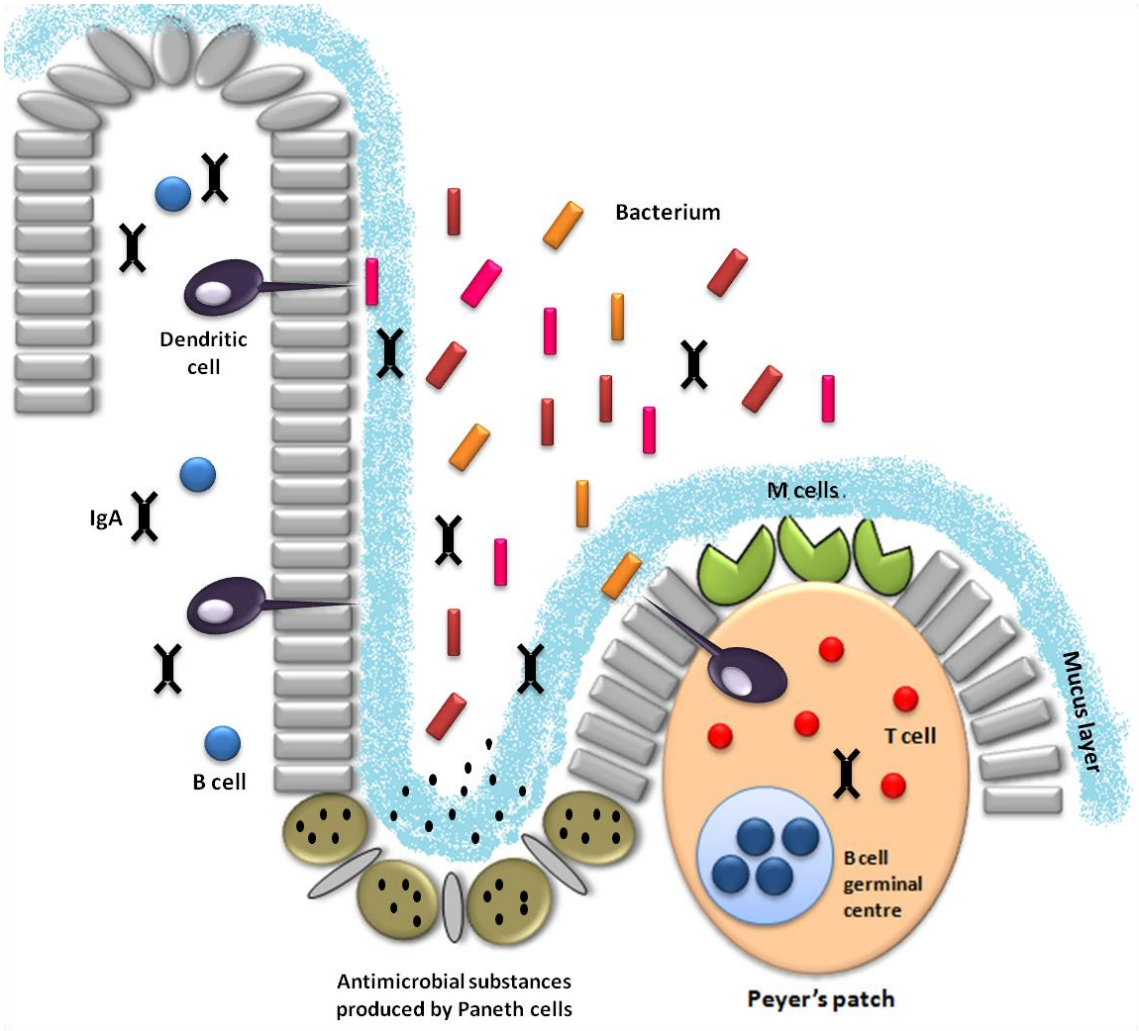


FIGURE 1.5 – Schematic overview of the intestinal immune system. The intestinal immune system has developed numerous tactics to protect the epithelial cells from any pathogenic attempt of invasion. A single layer of epithelial cells characterizes the intestinal epithelium. This epithelium is primarily protected by a thick mucosal layer, antimicrobial substances released by Paneth cells and large amounts of antigen-specific secretory IgA. This primary line of defense is enforced by the presence of T cells, IgA-producing B cells and macrophages which are distributed throughout the lamina propria. Dendritic cells sample bacteria at the epithelial apical surface and carry live bacteria to inductive sites, such as the Peyer's patches, where T and B cells are mainly located and an immune response can be triggered.

1.3.3 – INTESTINAL IMMUNE RESPONSE

Specific components common to a range of bacteria, commonly known as pathogen-associated molecular patterns (PAMPs), are strong activators of the innate immune response. LPS, PGN, lipoprotein and unmethylated DNA with CpG motifs are examples of PAMPs that bind and stimulate the TLRs (Hayashi et al., 2001; Ozinsky et al., 2000; Schwandner et al., 1999). Toll-like receptors are type I integral membrane glycoproteins. More than 10 members of the TLR family have been reported to date, and shown to be expressed differentially among immune and non-immune cells. For instance, TLRs have been reported in immature dendritic cells, vascular endothelial cells, adipocytes, cardiac myocytes and intestinal epithelial cells (Fan et al., 2003; Lee et al., 2006; Muzio et al., 2000). The diversity of TLR members and their different expression patterns suggests that different stimuli may trigger different responses, and hints to cooperation within the family (Ozinsky et al., 2000). In fact, TLR4 is known to recognize LPS, whereas TLR2 and TLR9 are activated by lipoproteins and bacterial CpG DNA, respectively (Bauer et al., 2001; Cario et al., 2000; Lien et al., 2001; Wooten et al., 2002) (Figure 1.5). Toll-like receptors possess a cytoplasmic domain that shares significant homology with the one found in interleukin-1 receptors (IL-1Rs). For this reason, TLRs are often considered to be members of the IL-1R superfamily (O'Neill and Dinarello, 2000). When activated, the conserved cytoplasmic domain, known as Toll/IL-1R (TIR), triggers the recruitment and association of the adaptor myeloid differentiation primary-response protein 88 (MyD88) (Medzhitov et al., 1998). A common MyD88-dependent signaling pathway is, thereby, activated stimulating the phosphorylative functions of members of the IRAK family (Nomura et al., 2000) (Figure 1.6).

Downstream events in this signaling cascade lead to the activation of the NF-κB signaling pathway (Figure 1.6). Briefly, in mammals, the NF-κB family consists of five members, namely RelA/p65, c-Rel, RelB, NF-κB1/p50 and NF-κB2/p52. p50 and p52 are produced by proteolytic processing of their precursors p105 and p100, respectively (Gilmore, 2006; Hoffmann et al., 2002). All members contain a Rel homology domain (RHD), which is necessary for DNA binding, homo- and heterodimerization, nuclear localization and inhibitor (IκB) binding (Baldwin, 1996). NF-κB activation is dependent on its regulation by the IκB family members. The binding of IκBs to NF-κB dimers causes their cytoplasmic retention, thereby inhibiting the transcriptional role of NF-κB. Upon stimulation, IκB proteins are poly-ubiquitinated and subsequently degraded, leaving NF-κB free to translocate to the nucleus where, as a pro-inflammatory transcription factor, it regulates the innate immune response by promoting the expression of antimicrobial and pro-inflammatory genes (Bohuslav et al., 1998). For this reason, the immune response to bacterial ligands activates mammalian macrophages and the production of pro-inflammatory cytokines, such as tumour necrosis factor α (TNFα), IL-1, IL-6 and IL-12. In addition, canonical NF-κB enhances the production of inflammatory effector substances like nitric oxide (NO) and controls the expression of proteins with anti-apoptotic and proliferative characteristics (Wullaert et al., 2011). The cascade of immune reactions generated by TLRs is the first step in the initiation of the adaptive immune response, which is characterized by the activation of T cells and the production of effector cytokines (Iwasaki and Medzhitov, 2004).

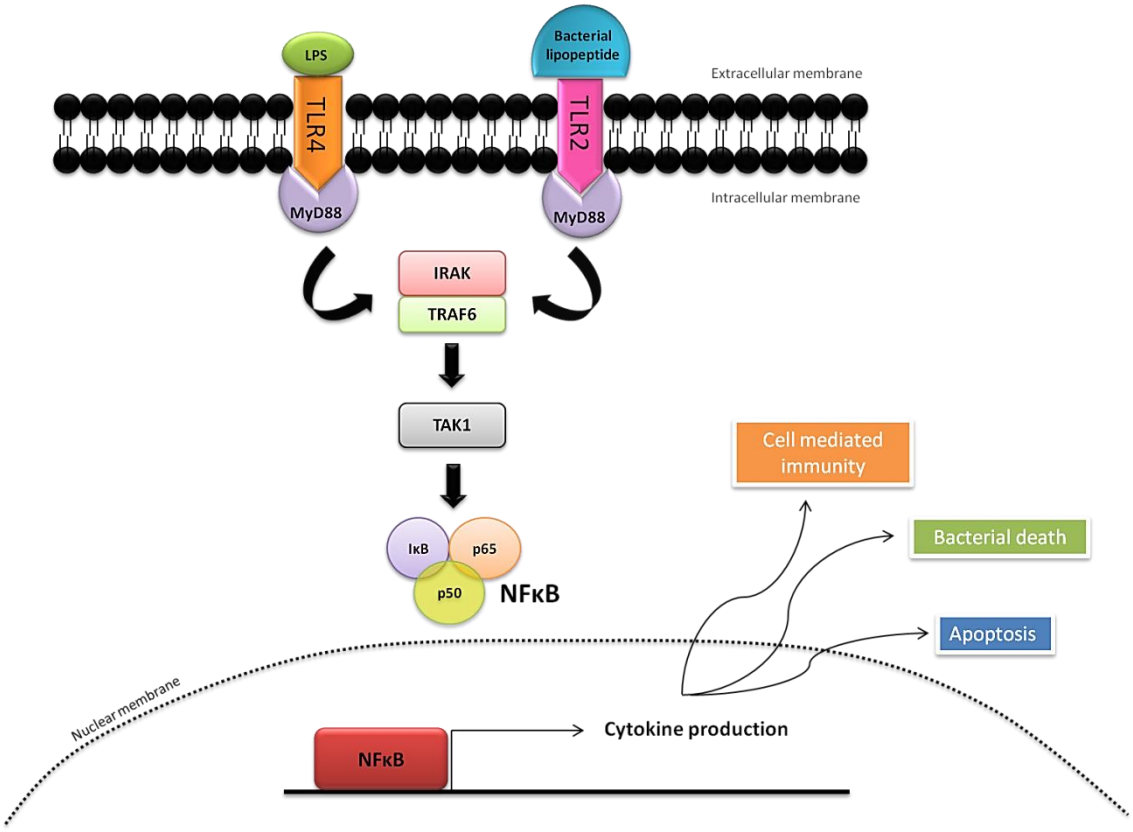


FIGURE 1.6 – The NF-κB canonical pathway. The stimulation of cells with Toll-like receptors (TLRs) by their ligands triggers the activation of the canonical NF-ƙB pathway. The signals transduced by these receptors lead to the MyD88-mediated activation of TRAF proteins, which consequently activate the TAK1 complex. Ubiquitination of IƙB allows the translocation of p65/p50 NFƙB dimers to the nucleus where they activate the transcription of genes. The production of cytokines is one of the most important outcomes of NFƙB activation, playing an essential role in the cell's immune response, bacterial death and apoptosis.

1.3.4 – INFLAMMATION AND EPITHELIAL CELL POLARITY: A VICIOUS CYCLE

Despite being considered a highly efficient mechanism of protection, the innate immune system can also have a dark side. Under conditions of chronic inflammation, the toxicity created by the secretion of cytokines and oxidative species can weaken the epithelium and encourage the entrance of pathogens to occupy niches within the host. Indeed, it is well known that inflammation favors secondary infections. Pro-inflammatory cytokines like interferon-γ (IFN-γ) cause downregulation of ZO-1 and the disassembly of the TJs by triggering the mislocalization of JAM, occludin and claudins (Bruewer et al., 2005; Li et al., 2008). TNF-α is another example of a cytokine that can cause barrier dysfunction (Schmitz et al., 1999). As a consequence of their actions at cell-cell contacts, IFNγ and TNF-α enhance epithelial paracellular permeability both *in vitro* and *in vivo* (Li et al., 2008; Ma et al., 2004). Recent studies have also suggested that interleukins, a large family of cytokines, might also play a role in the regulation of paracellular permeability. In fact, IL-1 and IL-4 are both responsible for increases in cell permeability in colon cell lines such as Caco-2 and T84 but also in the Calu-3 epithelial airway cell line (Al-Sadi and Ma, 2007; Ceponis et al., 2000). In comparison, IL-10 opposes the effect of IFN-γ on the barrier properties of the epithelium (Madsen et al., 1997). These findings suggest that cytokines, including interleukins, modulate TJ components controlling occludin, claudins and ZO-1 protein levels.

1.3.5 – INFLAMMATORY BOWEL DISEASES

An interesting and important feature of the intestinal microbiota is its role in shaping and maintaining normal mucosal immune responses. After birth, the initiation of bacterial colonization promotes significant changes in the intestinal epithelium architecture and the differentiation of cell lineages of the mucosal immune system (Dai and Walker, 1999; Insoft et al., 1996). Due to this early postnatal maturation of the intestinal immune system, which persists throughout life and accounts for the whole body health, the normal physiological response to commensal flora is one of immunological tolerance. Interestingly, it is believed that a reduced exposure to gut bacteria and childhood infections, often postulated as the 'hygiene hypothesis', compromises the mechanisms that regulate T-cell differentiation and affects the susceptibility to immunological tolerance (Hooper, 2004; Wills-Karp et al., 2001). These immunological alterations to the recognition of intestinal antigens are believed to be the trigger to the development of pathological conditions such as inflammatory bowel diseases (IBDs) and food allergies (Bernstein et al., 2006; Guarner et al., 2006; Huibregtse et al., 2007). Supporting this idea is the fact that various mouse models of IBD show an improvement in their health when they are placed in a germ-free environment (Elson et al., 2005).

Ulcerative colitis (UC) and Crohn's disease (CD) are the two major forms of inflammatory bowel disease. IBD represents an inflammatory disorder that mainly affects the intestine, causing diarrhoea, anaemia and fatigue (Podolsky, 1991). In addition, patient with chronic inflammation driven by IBD have an increased susceptibility to develop neoplasias, often known as colitis-associated colorectal cancer (CAC) (Bernstein et al., 2001; Eaden et al., 2001). In IBDs, the persistent

inflammation is characterized by a continuous release of cytokines, growth factors, proteases and reactive oxygen species (ROS). The excessive production of chemokines and cytokines produced by inflammatory cells propagate the inflammatory response and enhance the survival of premalignant cells by activating NF-κB (Schottenfeld and Beebe-Dimmer, 2006). CD can be distinguished from UC in that the inflammation associated with CD is intramural and frequently discontinuous. By contrast, the inflammation caused by UC only affects the superficial mucosal and submucosal layers of the intestinal wall. In addition, CD most commonly affects the ileum and colon although it can affect any region of the gut. However, UC always affects the colon and, in particular, the rectum (Lennard-Jones, 1989).

Various factors compromise intestinal homeostasis and can lead to chronic inflammation. Key examples are the changes in the gut microflora, the alterations in the epithelial barrier functions and a disruption of the innate immune response (Araki et al., 2005; Gitter et al., 2001; Petersson et al., 2011). For instance, JAM-A deficient mice are more prone to dextran sulphate sodium (DSS) induced colitis (Laukoetter et al., 2007). Moreover, abnormal production of the mucin Muc2, the key component of the mucus protective layer, compromises colonic protection and triggers spontaneous colitis in mice (Van der Sluis et al., 2006). Also, studies performed in MyD88 and TLR4-deficient mice have shown defects in LPS-responsive pathways and impaired innate system activation (Araki et al., 2005; Fukata et al., 2005). In agreement, absence of MyD88 and TLR4 increases the susceptibility of mice to develop colitis upon DSS treatment (Araki et al., 2005; Fukata et al., 2005).

Epidemiological studies supported by genome-wide associations (GWA) have provided further information on what genes are supposedly associated with IBDs occurrence. Polymorphisms in genes of the innate system, such as *NOD2* (nucleotide-binding oligomerization domain protein-2) and *ATG16L1* (autophagy related 16-like protein 1) have been found to be linked to CD (Hugot et al., 2001; Massey and Parkes, 2007). In addition, various genes involved in IL23 pathway, including IL23R and STAT3 have been related to both UC and CD (Duerr et al., 2006). Biologically, it has been shown that *NOD2* enhances the production of intestinal anti-microbial peptides (Kobayashi et al., 2005; Ogura et al., 2003). In contrast, *ATG16L1* was reported to play an important role in the formation of Paneth cell granules. *ATG16L1*-deficient mice have a reduced number of Paneth cell granules, significantly increased number of cytoplasmic vesicles and abnormal mitochondrias (Cadwell et al., 2008).

1.4 – TUMORIGENESIS IN THE INTESTINE

1.4.1 – TUMOUR SUPPRESSORS IN COLORECTAL CANCER (CRC)

1.4.1.1 – ADENOMATOUS POLYPOSIS COLI (APC)

Due to its active role in the degradation complex, APC functions as a negative control of the Wnt signaling pathway by controlling the cellular levels of β-catenin. APC, located on chromosome 5q, is mutated in 85% of familial and sporadic CRCs. In humans, germ-line mutations in the APC gene are linked to an inherited autosomal dominant condition named familial adenomatous polyposis (FAP), which is characterized by the development of multiple benign adenomatous polyps in the colorectal epithelium (Bodmer et al., 1987). Almost invariably, some of these will progress to invasiveness and, ultimately, metastasize. Over 300 different disease-associated mutations of APC, including insertions, deletions and nonsense mutations have been reported and it is now commonly accepted that these mutations compromise the destabilization of free β-catenin (Laurent-Puig et al., 1998). Point mutations in the gene encoding β-catenin have been found in the remaining CRCs tumors that retain wild-type (WT) APC. Most of these mutations change one of the four serine/threonine residues in the N terminus of β-catenin preventing its phosphorylation by GSK3 and further degradation (Polakis, 1999; von Kries et al., 2000). APC and β-catenin mutations are mutually exclusive and believed to be functionally distinct. For instance, colon tumors with mutations in APC have a wild-type β-catenin gene, and vice-versa, tumors with mutations in β-catenin gene retain wild-type APC gene. Moreover, despite the fact that both types of mutations having similar consequences on β-catenin stability and TCF transactivation, it has

been shown that small adenomas with β-catenin mutations appear to be less aggressive and invasive since they do not progress to larger adenomas or invasive carcinomas in contrast with adenomas carrying APC mutations (Morin et al., 1997). Occasionally, mutations in the genes encoding axin2/ conductin have also been described (Lammi et al., 2004). Nevertheless, all the mutations found in the components of the Wnt pathway are detected very early in the adenoma-carcinoma sequence of events in colonic mucosa suggesting that functional loss of APC and an accumulation of nuclear β-catenin are early events which probably initiate tumorigenesis in the intestine (Bienz and Clevers, 2000). Researchers are currently interested in understanding how constitutive β-catenin/Tcf transcriptional activity promotes adenoma formation and progression. In the context of homeostasis, Wnt signaling pathway promotes proliferation of progenitor cells being only switched off when cells leave the crypt compartment. Adenomas can be, therefore, characterized as a population of proliferative cells which have adopted a crypt progenitor phenotype (Gregorieff and Clevers, 2005). Consequently, the genes aberrantly activated by constitutive active β-catenin/Tcf reflect the normal genetic program of intestinal progenitor cells. Several effector genes have been identified and found to be involved in biological processes such as cell cycle regulation (c-myc, Cyclin D1), tumor cell migration (MMPs, Nr-CAM), survival (Survivin) and growth (FGF18, Gastrin). Importantly, disrupted β-catenin/Tcf activity further enhances the up regulation of other Wnt signaling components. In fact, in colon cancer cells, Tcf1 and Lef are strongly up-regulated through direct activation of Tcf4 (Roose et al., 1999).

1.4.1.2 – p53

Mutations in p53 are reported to be relatively late events in the development of tumorigenesis in intestine. Nevertheless, p53 gene is mutated in up to 70% of colorectal cancers (Rodrigues et al., 1990). p53 is present at almost undetectable levels in most cells and, perhaps because of this fact, it is not essential for normal growth and development (Donehower et al., 1992). However, various studies uncovered the importance of p53-mediated response to cellular stress signals which can lead to oncogenic alterations. In fact, stresses related to cancer initiation or progression, such as direct DNA damage, chromosomal aberrations, hypoxia, activation of oncogenes, heat and cold shock conditions and inflammation trigger the activation of p53 (Amellem and Pettersen, 1991; Fujita, 1999; Hofseth et al., 2003; Lakin and Jackson, 1999; Lowe, 1999; Takayama et al., 2003). Different types of stress activate enzymes which have the ability to communicate to p53 that the DNA has been affected. This communication is achieved by post-translational modifications such as phosphorylation, acetylation, methylation, ubiquitination or sumoylation of the p53 protein (Appella and Anderson, 2001). It has been suggested that for each type of DNA damage, different enzymes become activated, therefore modifying the p53 protein at different sites (Colman et al., 2000). For instance, gamma radiation activates the ATM kinase and the Chk-2 kinase which can both phosphorylate p53 (Banin et al., 1998; Hirao et al., 2000). In response to UV irradiation, JNK phosphorylates p53 at threonine 81 (Buschmann et al., 2001). In addition, Polo-like kinase 3 activates p53 by phosphorylating serine 20 in response to active oxygen species (Xie et al., 2001).

The activation of p53 consists of a transition from a biologically latent to a functionally active state. This functional state is characterized by an increase in the half-life of the protein, a change in subcellular location as well as an enhancement of the ability of p53 to bind to DNA and modulate gene expression. Overall, p53 acts as a cell protector by controlling damage caused by cellular stress and preventing the expansion of the compromised cell into a large population of malignant cells.

The crucial role of p53 in ensuring cellular homeostasis is only possible due to tight mechanisms of regulation. Loss of function of p53 characterizes tumor progression in most of the epithelial tissues. Therefore, the stability, subcellular localization and transcription activity of p53 must be kept under control (Kruse and Gu, 2009). One of the most important regulators of p53 stability is MDM2, which is also a p53 transcriptional target thus establishing a feedback loop (Wu et al., 1993). In most normally proliferating cells, p53 levels are kept low by ubiquitine-mediated proteasomal degradation. MDM2 functions as a E3 ubiquitin ligase for p53 by interacting with its N-terminal region and allowing it to be recognized and degraded by proteasome (Fang et al., 2000; Haupt et al., 1997; Honda et al., 1997). The role of MDM2 in the turnover mechanism of p53 was further demonstrated with the establishment of a transgenic knockout mouse of MDM2. The loss of this p53 regulator results in the excessive accumulation of cellular p53, which will lead to early embryonic lethality caused by aberrant p53-driven apoptosis. Furthermore, it has been described that amplification of MDM2 is a characteristic of tumors that retain wild-type p53, suggesting that enhanced expression of MDM2 prevent the activation of p53 as a tumor suppressor (Oliner et al., 1992; Ramos et al., 2001; Reifenberger et al., 1993). In general, the activation of p53 upon stress depends on

the inhibition of MDM2 function, which can be achieved by repressing the expression of MDM2, by post-translation modifications on p53, by activation of MDM2 inhibitors or by influencing the localization of p53 (Kubbutat et al., 1997). For instance, it has been suggested that, in a number of tumor types that retain wild-type p53, loss of p53 activity is associated to a failure of the protein to accumulate in the nucleus most likely due to a hyperactive nuclear export driven by an excess of MDM2 activity (Lu et al., 2000).

1.4.2 – SPORADIC COLORECTAL CANCER VS. COLITIS-ASSOCIATED CANCER

Colorectal cancer (CRC) is one of the most deadly cancers in the western world. Only around 20% of CRC cases have a major hereditary component and are associated to well-characterized syndromes, like familial adenomatous polyposis (FAP) (Rustgi, 2007). The largest fraction of CRC is, however, related to environmental causes, rather that genetic susceptibility (Bernstein et al., 2001). Importantly, the main differences between colitis-associated cancer (CAC) and sporadic colorectal cancer (SCC) are the conditions predisposing to cancer, the type of precursor lesion, and the occurrence of mutations in APC and p53, which happen in different stages of the tumorigenesis process (Brentnall et al., 1994; Redston et al., 1995) (Figure 1.7).

SCC is known to arise from a dysplastic precursor lesion referred as an adenomatous polyp, whereas in CAC the patients develop polypoid, flat, localized or multifocal dysplastic lesions (Ullman and Itzkowitz, 2011). Importantly, the progression from early adenoma stage to carcinoma, which characterizes the

sporadic colorectal cancer, occurs differently in colitis-associated cancer. In IBD-driven cancer, the progression consists of an inflammation-dysplasia-carcinoma sequence of events (Figure 1.7). Nevertheless, both subtypes of colorectal cancer involve the accumulation of mutations in tumor suppressor genes (Fearon and Vogelstein, 1990). Sporadic colorectal cancer arises as a result of genomic instability, such as chromosomal instability and microsatellite instability (Pino and Chung, 2010). Loss of chromosomal material, often referred as loss of heterozygosity, results in loss of function of important tumor suppressors, mainly *APC* and *p53* (Nishisho et al., 1991). Loss of *APC* function is widely accepted as an early event in SCC pathogenesis. During the development of the adenoma, in which variation of size, degree of dysplasia and histological changes take place, other genetic changes occur. For instance, intermediate adenoma progression depends on upregulation of K-Ras and is intimately linked to loss of function of tumor suppressor genes on chromosome 18q, in the region of the deleted in colon cancer (DCC). Moreover, loss of *p53* function is a late event in the development of the disease but has been found to greatly increase the transition from dysplastic adenomas to carcinomas (Figure 1.7).

Unlike SCC, in which focal dysplasia is observed, in CAC, multiple areas of the colon are often involved suggesting a broader “field effect”. Moreover, patients suffering from intestinal inflammatory disorders reveal an increased risk to develop CAC, mainly due to the deleterious consequences of a chronic inflammatory response suggesting that chronic inflammation precedes the development of CAC (Bernstein et al., 2001). Importantly, SCC also exhibit inflammatory infiltrated and an active immune response. However, distinctly from CAC, which is characterized by

extrinsic inflammation caused by IBD, inflammation in SCC drives tumorigenesis in an intrinsic manner, since this inflammatory response is triggered by and contained within tumor cells (Terzic et al., 2010). Therefore, in SCC inflammation does not precede tumorigenesis, but instead follows tumor progression.

1.4.2.1 – INFLAMMATION AND CAC INITIATION

Colitis-associated cancer results from successive mutations and epigenetic alterations of cancer-related genes, following the impairment of normal cells growth and tissue homeostasis. Reactive oxygen and nitrogen species released by immune cells is often the trigger for DNA methylation, histone modification and mutations in tumor suppressor genes including *p53* and *APC* (Harpaz et al., 1994; Redston et al., 1995). *APC* loss of function, considered to be one of the earliest events in sporadic colorectal cancer, is much less frequent and usually occurs late during the progression from high-grade dysplasia to carcinoma (Bernstein et al., 2001; Tarmin et al., 1995). In contrast, *p53* is an important player in the development of CAC. *p53* loss of function correlates with malignant progression in this subtype of colorectal cancer. In addition, mutations in *p53* have been detected in non-dysplastic mucosa and in inflamed mucosa from UC patients who did not have cancer, suggesting that p53 mutation is an early molecular change which is driven by chronic inflammation (Hussain et al., 2000).

In addition to reactive oxidative species, several molecules have been described as important players in the link between inflammation and tumorigenesis in colon. The development of animal models has helped uncovering crucial players in inflammation-to-cancer sequence of events. Importantly, several experimental

models of colon cancer have been generated, including the *APC*$^{Min/+}$ and the azoxymethane (AOM) mouse model (Moser et al., 1995; Okayasu et al., 2002; Tanaka et al., 2003).

The role of TLRs is intimately related to colon carcinogenesis. Because of their important role in sensing enterobacteria, toll-like receptors are required for the maintenance of homeostasis in the intestine. In agreement, polymorphisms of TLRs have been reported in UC and CD patients. Interestingly, the deletion of the TLR adaptor MyD88 has been shown to significantly reduce the number and size of tumors in *APC*$^{Min/+}$ mouse model (Fukata et al., 2007; Rakoff-Nahoum and Medzhitov, 2007). Furthermore, the treatment of TLR4-deficient mice with AOM/DSS significantly reduced the number of colonic tumors, when compared to wild type mice. These findings support the hypothesis that colitis-associated cancer is triggered by an immune response, which can only be elicited by an intact TLR signaling pathway (Fukata et al., 2007). The absence of a TLR-dependent inflammatory response is mimicked by the absence of enteric bacteria. In fact, depletion of bacteria in various models of colitis-associated cancer results in the abolishment of dysplasias or tumors (Engle et al., 2002; Sellon et al., 1998).

Proinflammatory citokines have also been implicated in the development of colitis-associated cancer (Figure 1.7). For instance, mice deficient in TNFα or in its receptor TNFR are resistant to skin carcinogenesis (Moore et al., 1999). In addition, blocking TNFα in mice reduces the susceptibility to develop tumors associated to colitis (Popivanova et al., 2008). Expression of TNFα is known to be increased in the mucosa of IBD patients. For this reason, TNFα has been considered a therapeutic target in the treatment of IBD (Rutgeerts et al., 2004). The analysis of samples from

UC and CD patients, in addition to the study of mouse models, has shown that IL-6 has an important role in CAC development. After colitis induction, IL-6 is mainly produced by myeloid cells to promote cell proliferation and survival of malignant intestinal epithelial cells (Becker et al., 2005; Grivennikov et al., 2009; Matsumoto et al., 2010). Taking the advantage of the AOM challenge model, different reports have shown that tumor growth is dependent on the production of IL-6, whereas depletion of IL-6 results in a decrease in size and number of tumors (Becker et al., 2004). Consistent with this idea, it has been reported that IL-6 production is higher in patients suffering from active IBD and in patients who have progressed to CAC, in comparison with control and inactive IBD patients (Reinecker et al., 1993). Not surprisingly, NF-κB is also an important mediator in cancer progression. Given its role in innate immunity, inflammation, cell proliferation and cell survival, NF-κB is described as an initiator and promoter of colitis-associated tumorigenesis. The clearest evidence comes from the study of AOM challenged mice which are deficient in IKKβ/ NF-κB signaling pathway (Greten et al., 2004). Deletion of IKKβ in intestinal epithelial cells results in a decrease of the tumor incidence but does not influence the tumor size. In contrast, deletion of IKKβ in myeloid cells leads to a decrease in the tumor size suggesting that IKKβ/NF-κB complex mediates the formation of tumors through different mechanisms, depending on the intestinal cell type (Greten et al., 2004).

Conversely, the production of IL-10 is often considered to be protective under situations of colitis. In fact, IL-10-deficient mice develop spontaneous colitis (Kuhn et al., 1993). Importantly, these mice develop colitis-associated cancer, which is believed to be due to the IL-6 regulation by IL-10. Since IL-10 has been reported to

suppress IL-6 levels, it is possible that upon deletion of IL-10, cancer progression is driven by uncontrolled production of IL-6 (Fiorentino et al., 1991).

The composition of the intestinal microflora might also play an important role in the development of tumorigenesis in colon. For instance, in some mouse models of IBD commensal bacteria or, in particular, *Helicobacter hepaticus* are necessary to initiate inflammation and develop cancer (Kullberg et al., 1998; Maggio-Price et al., 2006). In fact, IL-10 deficient mice develop spontaneous colitis but this will only occur in the presence of enteric bacteria (Kullberg et al., 1998). In agreement, mice grown under germ-free conditions do not suffer from chronic inflammation and do not develop tumors (Engle et al., 2002). One possible explanation for these observations lies on the fact that microbes influence the balance between protective and aggressive immune response. In addition, their presence might also contribute to dysbiosis, which consists on the change of number, diversity and stability of commensals (Arthur and Jobin, 2011; Zhu et al., 2011).

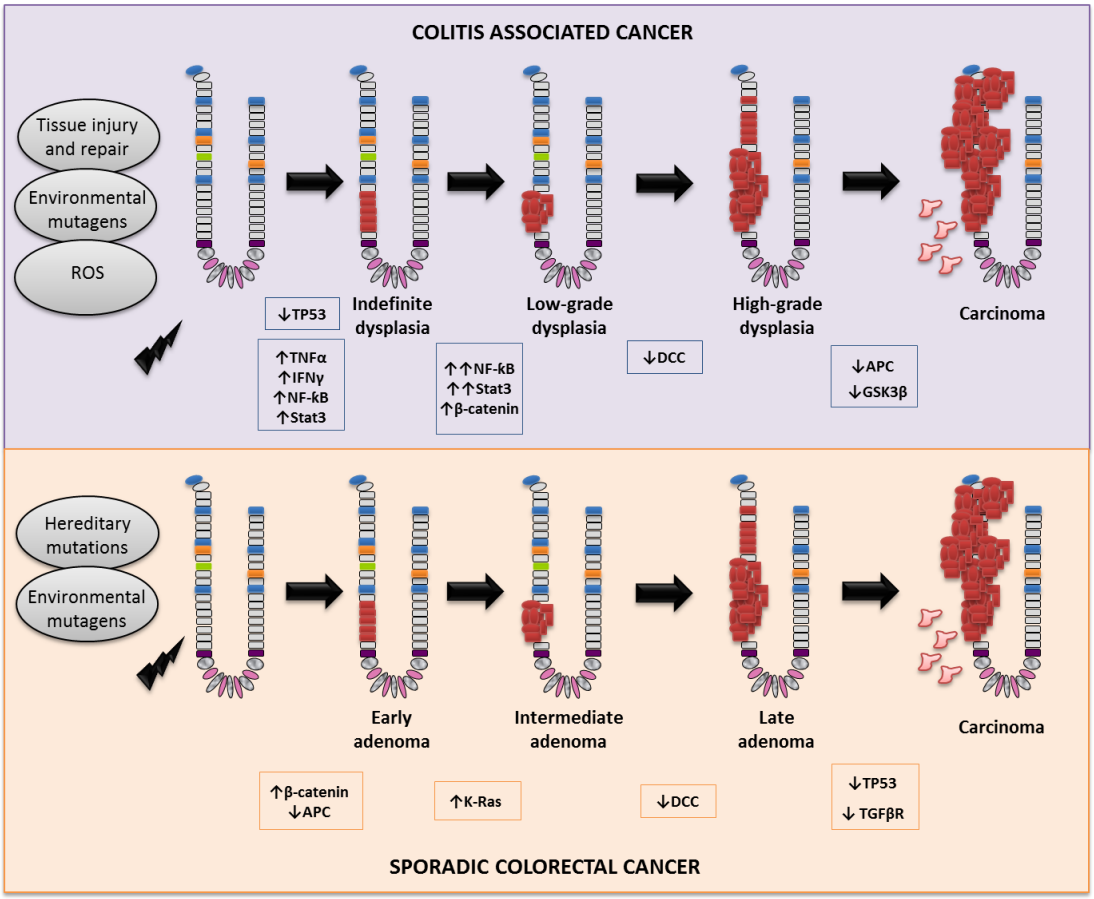


FIGURE 1.7 – Model of intestinal cancer initiation and progression. Colitis associated cancer is characterized by the progressive succession of events from dysplasia to carcinoma. Excess inflammation and the impairment of epithelial regeneration are considered triggers for cancer initiation. Increased production of proinflammatory cytokines and p53's loss of function contribute to the progression of colonic tumorigenesis. Sporadic colorectal cancer is triggered by hereditary mutations such as the loss of adenomatous polyposis coli (APC). Crypt base columnar (CBC) cells (pink) are $Lgr5^{+}$ and suffer transformation upon stress signals. In early adenoma stages, $Lgr5^{+}$-transformed cells generate a β-catenin enriched progeny of cells (red) that forces the Wnt-activated trans-amplifying (TA) cells to move up along the villi. Loss of Kras results in malignant progression. The gradual accumulation of additional mutations affecting *p53* leads to the final transition from advanced adenoma to carcinoma.

1.5 – LKB1 – THE INTESTINAL TUMOR SUPPRESSOR

1.5.1 – LKB1 AND PEUTZ-JEGHERS SYNDROME

In striking contrast to the colon, tumors are rarely generated in the small intestine despite the amount of cells that are replaced daily in this tissue (Lowenfels, 1973). Approximately 10^9 cells are produced in the human small intestine every 20 minutes, yet small intestine malignancies develop at one of the lowest rates of all solid organs (Potten, 1992). Several factors such as increased intestinal motility, increased luminal-fluid volume or reduced bacterial populations have been proposed to explain the lower tumor frequency (Lowenfels, 1973). New insights have come from studies of patients with Peutz-Jeghers syndrome (PJS), who are highly susceptible to the development of benign hamartomatous polyps in the gastrointestinal tract, as well as carcinomas of the small intestine (Jeghers et al., 1949). Germline mutations in the serine/threonine kinase - Liver Kinase B1 (LKB1, also known as STK11), on chromosome 19p13.3, have been shown to result in complete loss of protein product (Hemminki et al., 1998; Wang et al., 1999). Inactivation of the WT LKB1 allele is thought to be the trigger for the formation of hamartomas and tumors in PJS patients (Hemminki et al., 1997). Importantly, somatic mutations in LKB1 have also been found to be related to sporadic cancers including lung and cervical cancer (Sanchez-Cespedes et al., 2002; Wingo et al., 2009). For this reason, LKB1 has been characterized as a recessive tumor suppressor gene.

LKB1 is broadly expressed in adult and fetal tissues. In particular, mRNA expression has been observed in the pancreas, liver, testis and skeletal muscle (Rowan et al., 2000).

LKB1-deficient mice are embryonic lethal, while heterozygous LKB1$^{+/-}$ mice have shown to be viable and prone to severe polyposis recapitulating what is observed in PJS patients (Jishage et al., 2002; Miyoshi et al., 2002). In addition, LKB1 loss has been shown to cause significant defects in cell adhesion, polarity and cell motility in the lung, prostate and pancreas suggesting that LKB1 plays a role in tumor initiation in these epithelial tissues (Hezel et al., 2008; Ji et al., 2007; Pearson et al., 2008).

1.5.2 – STRUCTURE AND REGULATION OF LKB1

Human LKB1 encodes an evolutionarily conserved serine/threonine protein kinase of 433 amino acids. LKB1 homologues include *Drosophila* LKB1, *Xenopus laevis egg* embryonic kinase 1 (XEEK1), *Caenorhabditis elegans* partitioning defective gene 4 (Par-4) and mouse LKB1 (Martin and St Johnston, 2003; Su et al., 1996; Watts et al., 2000). Mouse LKB1 is predominantly nuclear, whereas human LKB1 is expressed both in the nucleus and the cytoplasm (Karuman et al., 2001; Smith et al., 1999). The intracellular distribution of LKB1 is dependent on its interaction with binding partners, such as STE20 related adaptor (STRAD) and the scaffolding protein Mo25, Brahma related gene 1 (Brg1) and the cytoplasmic LKB1 interacting protein (LIP1) (Baas et al., 2003; Marignani et al., 2001; Smith et al., 2001).

Human LKB1 protein consists of a kinase domain (residues 50-319), putative carboxyl-terminal regulatory domain and two potential nuclear localization signals (NLS) which are located at amino acids 38-43 and amino acids 81-84 (Smith et al., 1999; Yoo et al., 2002). The LKB1 protein is rich in posttranslational sites, particularly phosphorylation sites. At least 8 residues have been described to date to be phosphorylated by upstream kinases (Ser31, Ser325, Thr366 and Ser431), such as cAMP-dependent protein kinase A (PKA), p90 ribosomal S6 kinase (RSK) or ataxia-telangeictasia-mutated (ATM), and by autophosphorylation (Thr185, Thr189, Thr336, Ser404) (Alessi et al., 2006; Sapkota et al., 2002) (Figure 1.9). In addition, it has been reported that LKB1's structure has a conserved Cys-Lys-Gln-Gln motif which is likely to be prenylated (Collins et al., 2000) (Figure1.9). In fact, mutations of the Cys residue in the consensus sequence abolish prenylation (Collins et al., 2000).

In mammalian cells, LKB1 is activated in a trimeric complex with STRAD and the scaffold protein Mo25 (Boudeau et al., 2004). STRAD is a pseudokinase that shares homology with the STE20 family of kinases (Baas et al., 2003). Mo25 is a well conserved protein which, in mammals, exists in two closely related isoforms: Mo25α and Mo25β. Mo25α has a structure that is distantly related to armadillo proteins (Boudeau et al., 2003). Both STRAD and Mo25 are necessary for LKB1's catalytic function, stability and cellular localization (Baas et al., 2004; Boudeau et al., 2003). STRAD is directly phosphorylated by LKB1 both *in vitro* and *in vivo*. It has been shown that the interaction of STRAD with LKB1 significantly enhances LKB1 activity (Baas et al., 2003). Accordingly, a SL26 LKB1 mutant fails to bind to STRAD, explaining its exclusive nuclear localization (Baas et al., 2003). Mo25 binds to the C-terminal region of STRAD and is believed to enhance the interaction between

STRAD and LKB1 (Baas et al., 2003) (Figure 1.9). Importantly, complex formation between LKB1, STRAD and Mo25 induces the polarization of single epithelial cells, despite lacking cell-cell contacts (Baas et al., 2004).

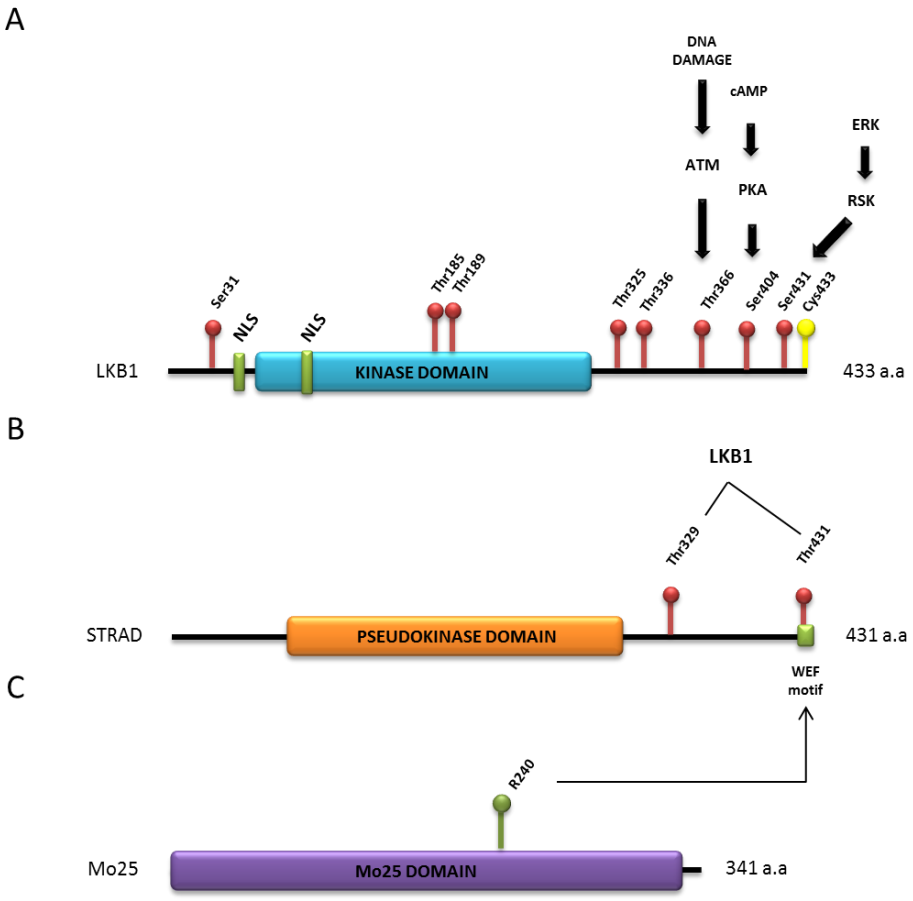


FIGURE 1.8 – Schematic structure of the human LKB1, STRAD and Mo25 protein domains. (A) LKB1 can be phosphorylated by upstream kinases, such as ATM, PKA and RSK, or it can be autophosphorylated. Phosphorylation sites are depicted in red. Farnesylation site (Cys433) is shown in yellow. NLS is a nuclear localization signal. **(B)** STRAD is phosphorylated by LKB1 at the represented sites. The pseudokinase domain interacts with LKB1. The WEF motif (Trp-Glu-Phe residues) mediates its binding to Mo25. **(C)** Mo25 interacts with STRAD through the Arg^{240} site. The Mo25 domain is characterized by α-helical armadillo repeats. Adapted from (Forcet and Billaud, 2007).

1.5.3 – LKB1 AND p53 PARTNERSHIP

Despite its high proliferation rate, the small intestine is rarely affected by tumors, suggesting that this tissue possesses important regulatory mechanisms of protection. *In vivo* studies have provided evidence that LKB1 might play a crucial role in these mechanisms, and suggest that a partnership with p53 is required (Sapkota et al., 2001). One study has shown that impaired expression of LKB1 in human cancer cell lines results in growth suppression (Sapkota et al., 2001). More specifically, in G361 melanoma cells, the growth inhibition is due to a G1 cell cycle arrest (Tiainen et al., 1999). In another study, it was demonstrated that overexpression of LKB1 induces p53-dependent cell death in fibrosarcoma HT1080 cells (Karuman et al., 2001). Importantly, both studies revealed that cell growth suppression and cell death require the kinase activity of LKB1. In fact, the overexpression of the mutants K78M LKB1 and Δ88 LKB1, known to be deficient in kinase activity, fails to suppress cell growth, whereas the overexpression of the kinase domain alone strongly promotes apoptosis (Karuman et al., 2001). In a different study, it was shown that LKB1-induced growth arrest is mediated by cytoplasmic LKB1, suggesting that kinase-deficient LKB1 mutants, known to be located in the nucleus, are not involved in this cellular event (Tiainen et al., 2002).

LKB1 and p53 can physically interact and this association reveals an *in vivo* synergistic cooperation in the acceleration of tumorigenesis (Karuman et al., 2001; Wei et al., 2005). Indeed, a knockout mouse study has revealed that $Lkb1^{+/-}/p53^{+/-}$ mice suffered earlier tumor formation, a dramatic increase in the incidence of various tumors and a shorter life span, when compared to the single mutants $Lkb1^{+/-}$ and $p53^{+/-}$ (Wei et al., 2005). More recently, new evidence has revealed that

LKB1 modulates cell death in response to energetic stress in an AMPK-dependent manner (Shaw et al., 2004b).

1.5.4 – LKB1 AND CELL METABOLISM

Upon activation, LKB1 phosphorylates and activates AMP-activated kinase (AMPKα1 and AMPKα2) and 12 other kinases that are structurally related to AMPK, including NUAK1, NUAK2 and the PAR-1 family of kinases MARK1, MARK2, MARK3 and MARK4 (Lizcano et al., 2004). For this reason, LKB1 is involved in a broad range of cellular events including cell cycle arrest, p53-dependent apoptosis, cell polarity, epithelial integrity, mTOR signaling and energy metabolism (Baas et al., 2004; Karuman et al., 2001; Partanen et al., 2012; Shaw et al., 2004a; Shaw et al., 2004b; Tiainen et al., 1999). The most well characterized LKB1-activated kinase is AMPK, a cellular energy sensor. The first study reporting a link between the two showed that LKB1, by itself, is capable of activating AMPK both *in vivo* and *in vitro* (Shaw et al., 2004b). Genes encoding AMPK are found in essentially all eukaryotes. AMPK and its orthologues exist as a heterotrimeric complex, composed of a catalytic α-subunit and two regulatory subunits (β and γ) (Xiao et al., 2011). Activation of AMPK requires the phosphorylation of Thr172, which is a residue located in the α-catalytic subunit domain (Hawley et al., 1996; Stein et al., 2000). In mammals, the major upstream kinases of AMPK are the LKB1-STRAD-Mo25 complex and the Ca^{2+}/calmodulin-activated protein kinase family, particularly CaMKKβ (Woods et al., 2005; Woods et al., 2003). AMPK senses the intracellular AMP:ATP ratio and is activated by cellular stresses that inhibit the production of ATP, such as glucose starvation and oxygen depletion, as well as energetic stresses that lead to an

excessive consumption of ATP, like muscle contraction (Hayashi et al., 1998; Laderoute et al., 2006). Under energetic stress conditions, AMP or ADP directly bind to the γ regulatory subunit of AMPK, ensuring a conformational change that promotes AMPK phosphorylation. This conformational change also prevents AMPK from being dephosphorylated, thus guaranteeing that it remains activated (Davies et al., 1995). Upon activation, AMPK phosphorylates downstream substrates in an attempt to rescue the AMP:ATP ratio and regulate cell metabolism. AMPK conserves ATP by switching off ATP-consuming pathways, including the biosynthesis of lipids, carbohydrates, proteins and ribosomal RNA. In contrast, it also switches on catabolic processes that will generate ATP, such as mitochondrial biogenesis and glucose uptake (Kemp et al., 1999). AMPK is antagonized by high levels of ATP. Consequently, short-term AMPK-induced effects can be rapidly switched off when the energetic stress is compensated for and levels of ATP have returned to normal.

Recent observations have shown that AMPK not only plays a role in the regulation of cell metabolism, but is also involved in coordinating cell growth and autophagy, and maintaining the integrity of epithelial tissues. In association with LKB1, and in conditions where nutrients are depleted, AMPK inhibits the mammalian target of rapamycin complex 1 (mTORC1), a known player in the mTOR signaling pathway, thus inhibiting cell growth (Shaw et al., 2004a). Moreover, AMPK ensures epithelial integrity by modulating the assembly of tight junctions under energetic stress conditions (Mirouse et al., 2007).

All of the evidence obtained so far has demonstrated that the partnership between LKB1 and AMPK is essential for the regulation of biological processes, such as metabolism, cell growth and cell polarity, which are intimately linked to

tumorigenesis. For this reason, the association between AMPK and LKB1 characterizes a new tumor suppressor pathway which is highly dependent on energetic stress.

1.5.5 – LKB1 AND CELL POLARITY

The first evidence suggesting the existence of a LKB1/AMPK cell polarity signalling pathway was reported in *C.elegans* and *Drosophila* models. In *C.elegans*, PAR-4 controls asymmetry in the zygote by mediating the spatial location of other polarity components such as PAR-3 and PAR-6 (Watts et al., 2000). In *Drosophila*, dLKB1, the homologue of *C.elegans* PAR-4, is required to determine the anterior-posterior (A-P) axis of the oocyte (Martin and St Johnston, 2003). Recently, mammalian LKB1 has also been described as an important player in cell polarity. Activation of LKB1 is only achieved upon its binding to STRAD and Mo25, and is determinant for the activation of downstream kinases (Boudeau et al., 2003; Hawley et al., 2003). The association of LKB1 to cell polarity in a mammalian cell culture came from the remarkable observation that polarization can be induced in individual intestinal epithelial cells, which lack cell-cell contacts, by activation of LKB1 (Baas et al., 2004).

1.6 – THE ASPP FAMILY OF PROTEINS

1.6.1 – DISCOVERY AND CHARACTERIZATION

Nearly 35 years have passed since p53 was first identified, and since then a long list of regulators has been created. Surprisingly, only a few these have been associated with the apoptotic function of p53. The ASPP family members are probably the best described example of such regulators. The ASPP family has three members named ASPP1, ASPP2 and inhibitory ASPP (iASPP). The name 'ASPP' stands for apoptosis stimulating protein of p53, but also reflects the importance of its biological functions by describing the ASPP signature sequence - ankyrin repeats, SH3 and proline-rich domain protein.

ASPP2 was the first member of the family to be discovered (Iwabuchi et al., 1994). The carboxyl terminus of ASPP2 was isolated in a yeast two hybrid screen that used truncated amino-terminal WT mouse p53 (residues 73-390) as bait (Iwabuchi et al., 1994). A p53-interacting protein fragment was subsequently identified and named 53BP2. This protein, containing 529 amino acids, is characterized by one proline-rich sequence, four ankyrin repeats and an SH3 domain (Gorina and Pavletich, 1996). The crystal structure of the p53-53BP2 complex revealed that these regions, which bind to the DNA binding domain of p53, are evolutionarily conserved (Gorina and Pavletich, 1996; Iwabuchi et al., 1994). Most importantly, this binding can only occur in the presence of WT p53. In fact, changes in six of the p53 residues most frequently mutated in human cancers, cause loss of binding to 53BP2 as well as to DNA, suggesting that this protein is likely to regulate the apoptotic function of WT p53 (Iwabuchi et al., 1994; Thukral et al.,

1994). Subsequent characterization of 53BP2 has shown that this protein can also bind BCL-2 (Naumovski and Cleary, 1996), protein phosphatase 1 (PP1) (Helps et al., 1995), RELA/p65 (subunit 3 of nuclear factor κ) (Yang et al., 1999b), adenomatous polyposis coli-like (APCL) (Nakagawa et al., 2000), amyloid-β-precursor protein-binding protein 1 (APPBP1) (Chen et al., 2003) and YES-associated protein 1 (YAP1) (Espanel and Sudol, 2001). Interestingly, in order to establish these interactions, the presence of the ankyrin repeats and SH3 domain of 53BP2 are crucial, suggesting that these regions of the protein are essential for controlling its biological role (Gorina and Pavletich, 1996).

A longer version of 53BP2, containing 1005 amino acids, was later isolated and named Bbp (Bcl-2 binding protein) (Naumovski and Cleary, 1996). In addition to the three functional domains of 53BP2, Bbp contains one α-helical domain at the N-terminus (Naumovski and Cleary, 1996). Further analysis has shown that 53BP2 and Bbp are both truncated variants of ASPP2: 53BP2 is the C-terminal 528 amino acid region of ASPP2 (amino acid residues 600-1128); and Bbp is the C-terminal 1005 amino acid region (residues 123-1128) (Samuels-Lev et al., 2001). However, only ASPP2, the 1128 amino acid full-length protein, is predominant *in vivo* (Samuels-Lev et al., 2001). In order to identify related proteins, the carboxyl-terminus of ASPP2 was used as a signature sequence to screen the human genome. Consequently, ASPP1 and iASPP were found to be closely associated and a new family of proteins was established (Bergamaschi et al., 2003; Samuels-Lev et al., 2001).

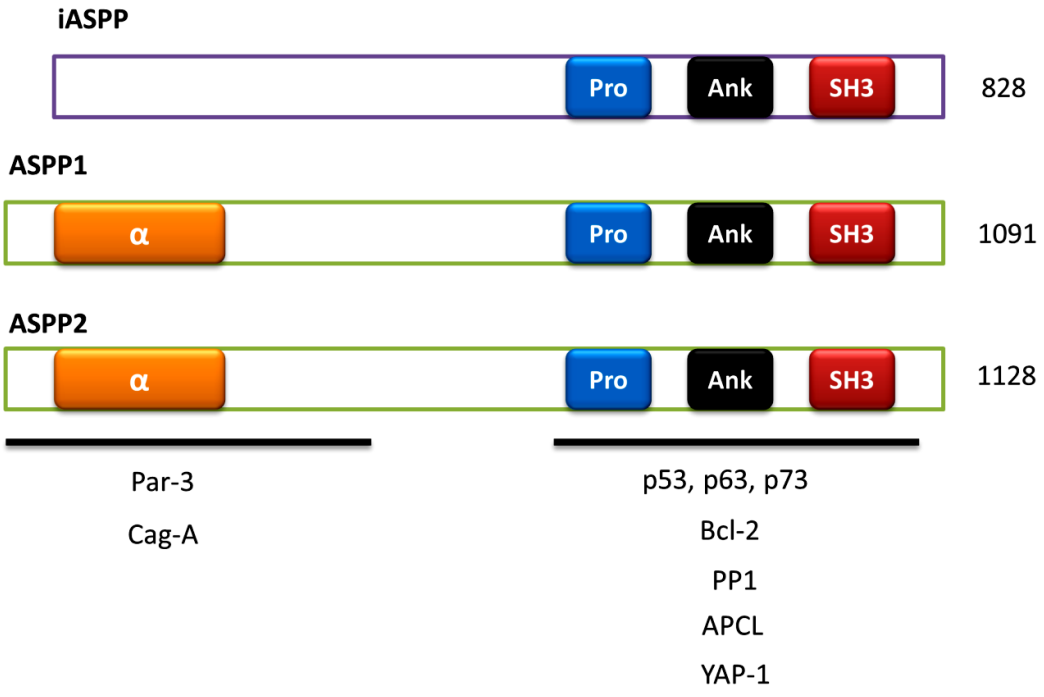


FIGURE 1.9 - The ASPP family of proteins. The three family members iASPP, ASPP1 and ASPP2 are characterized by a common C-terminal domain comprising a proline-rich region (Pro), ankyrin repeats (Ank) and an SH3 domain (SH3). The N-terminal domain of ASPP1 and ASPP2 consists of a α helical domain (α). The best known binding partners of the ASPPs are the members of the p53 family. Bcl-2, PP1, APCL and YAP-1 belong to the list of proteins that bind to the C-terminal domain whereas Par-3 and CagA are known to bind to the N-terminal region. The aminoacid length of each member is indicated on the right and the protein domains highlighted with different colors.

1.6.2 - EXPRESSION AND BIOLOGICAL FUNCTION *IN VIVO*

p53 orthologous proteins have been identified in organisms as distantly related to mammals as *C. elegans* and *D. melanogaster* (Sutcliffe and Brehm, 2004). One could therefore expect to find similar evolutionary conservation in close partners of p53. The ASPP proteins exist in all organisms where p53 orthologues have been identified, and further studies have shown that all of the proteins show significant homology at the C-terminus, where the signature sequence that characterizes these proteins is located. ASPP1 and ASPP2 share 48% sequence identity, and most closely resemble each other at the N- and C-termini. In contrast, the N-terminus of iASPP has no homology with ASPP1 and ASPP2 (Slee et al., 2004). It was considered highly likely that all three family members were capable of interacting with and regulating p53, as they all possess conserved residues in the SH3 and ankyrin repeat regions. (Bergamaschi et al., 2003; Samuels-Lev et al., 2001). These observations suggested that ASPP1 and ASPP2 may have similar biological roles, contrast with those of iASPP.

In vertebrates, the three members of the ASPP family are encoded by three genes located on three different chromosomes. In human chromosomes, ASPP1 is located at 14q32.33, ASPP2 at 1q42.1 and iASPP at 19q13.32-3. Interestingly, however, lower organisms possess only one gene which resembles iASPP (Bergamaschi et al., 2003).

Co-transfection assays revealed that the interaction of the ASPPs with the evolutionarily conserved DNA binding domain of p53 enhanced its apoptotic function, by specifically regulating the transactivation of pro-apoptotic genes like Bax and PIG3 (Samuels-Lev et al., 2001). Interestingly, these genes were often

associated with promoters that had low affinity p53 binding sites, suggesting that the ASPPs might promote a stronger association of p53 to these promoters than would otherwise occur. In contrast, ASPP1 and ASPP2 had little effect on other p53-responsive genes such as $p21^{waf1/cip1}$, Mdm2 and cyclin G which are responsible for the cell cycle arrest properties of p53 (Samuels-Lev et al., 2001). A few years later, it was shown that ASPP1 and ASPP2 are transcriptional targets of E2F, supporting the idea that the ASPP proteins mediate the activation of p53-mediated apoptosis (Fogal et al., 2005). Together with their effects on its gene expression, the ASPP proteins also promote p53-dependent apoptosis in cells. ASPP1 and ASPP2 may therefore act as a second layer of control, additional to p53's functions, that is essential for discrimination between apoptosis and cell cycle arrest and thus decide the cell fate.

The third member of the ASPP family of proteins, iASPP, was originally identified as a 351 amino acid RELA/p65–associated inhibitor (RAI) (Yang et al., 1999a). Further studies later showed that the full-length RAI protein is 828 amino acids long, and that its homologue in *C. elegans* is a 769 amino acid protein characterized by its ability to inhibit p53 (Bergamaschi et al., 2003). The expression of iASPP selectively inhibits the transcriptional activity of p53, particularly when associated with the pro-apoptotic promoters of the Bax and PIG3 genes. In contrast, promoters of cell cycle arrest related genes are not affected, suggesting that iASPP and the other ASPP proteins use a similar but opposing mechanism to regulate p53's apoptotic function (Bergamaschi et al., 2003). When over-expressed, iASPP physically displaces ASPP2 from p53's DNA binding domain, suggesting that the ASPP family members might compete for this domain. By virtue of its ability to

antagonize the activity of tumor suppressors like ASPP1 and ASPP2, and inhibit p53-dependent apoptosis, iASPP has been described as an oncoprotein. Further support for this is given by findings describing the interaction of iASPP with oncogenic Ras, adenovirus E1A and human papilloma virus oncoprotein E7, thus contributing to cell transformation *in vitro* (Bergamaschi et al., 2003). The oncogenic properties of iASPP are notorious when cells expressing this p53 inhibitor become resistant to ultraviolet radiation, and susceptible to the cytotoxic effects of chemotherapeutic drugs such as cisplatin. Moreover, the depletion of iASPP in *C. elegans* and human cells by RNA-mediated interference or antisense RNA, respectively, induces p53-dependent apoptosis, the levels of which are comparable to those observed upon gamma or ultraviolet irradiation (Bergamaschi et al., 2003). Overall, iASPP is believed to be a master inhibitor of p53 and its effects can only be over-ruled by the stimulatory functions of ASPP1 and ASPP2.

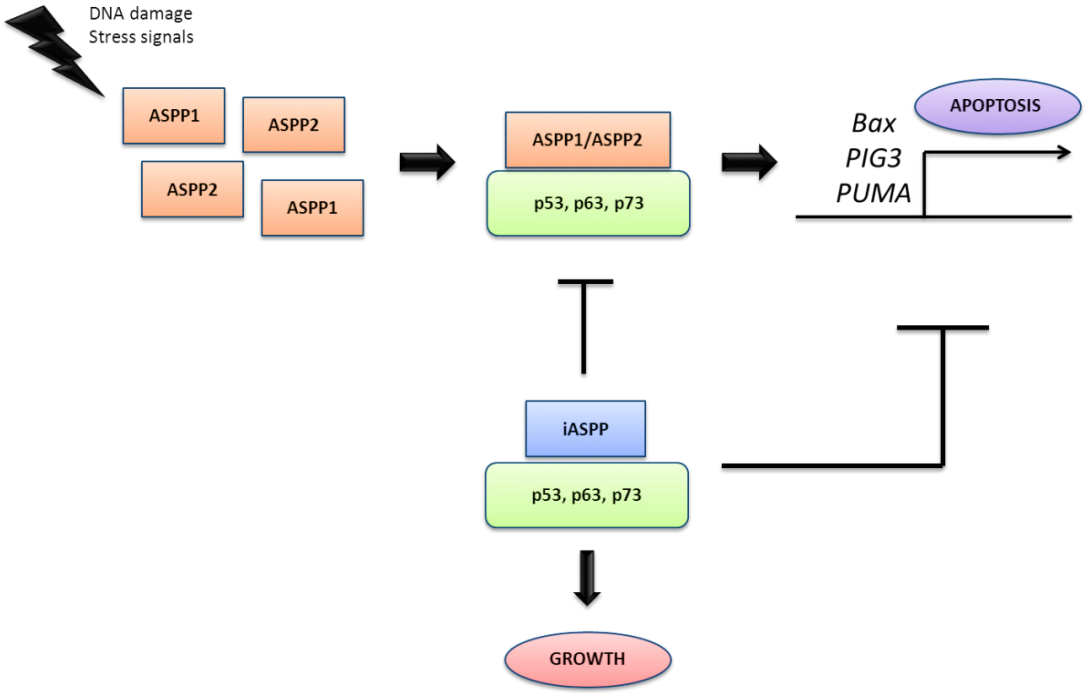


FIGURE 1.10 – Schematic overview of the regulation of p53-dependent apoptosis by the ASPP family members. Stress signals such as DNA damage promote the stabilization and activation of ASPP1 and ASPP2. Their interaction with p53 family members promotes binding to pro-apoptotic promoters like Bax, PIG3 and PUMA leading to apoptosis. In contrast, iASPP prevents apoptosis and stimulates cell proliferation by competing with ASPP1 and ASPP2 and binding to p53 family members.

In order to provide an *in vivo* model system with which to study the biological role of the ASPP family of proteins, ASPP1, ASPP2 and iASPP-deficient mice were generated and characterized. ASPP1-null embryos showed disorganized lymphatic vessels, accompanied by defects in lymphatic vessel development and impaired drainage function (Hirashima et al., 2008). Interestingly, these defects were imperceptible in adult mice. Despite the evidence suggesting that ASPP1 enhances p53's apoptotic function, the same study reported that the lymphatic phenotype observed in ASPP1-deficient mice was not affected by p53 loss or haploinsufficiency. In fact, crossings between ASPP1 mutants and p53 knockout mice did not result in any abnormalities in the lymphatic system, nor was the phenotype of ASPP1 mutant mice enhanced or suppressed by p53 gene dosages (Hirashima et al., 2008).

iASPP-deficient mice were born according to Mendelian segregation but died from sudden death around 6 months of age. Further studies showed that these mice develop focal cardiac necrosis which progresses to a deadly dilated cardiomyopathy (Notari, M. *unpublished data*). Furthermore, these mice suffered from abnormalities in the hair follicles and eye lid closure. Recently, it has been demonstrated that iASPP is involved in epithelial stratification of the skin and esophagus by binding to p63 and inhibiting its transcriptional activity, which is necessary to maintain the self-renewal and proliferative character of the epidermal cells (Notari et al.).

The development and characterization of ASPP2-deficient mice provided the first genetic evidence that ASPP2 is a tumor suppressor. Furthermore, studies performed with these mice have shown, for the first time, that ASPP2 and p53 are genetically

associated and share overlapping functions that are essential for mouse development. The murine ASPP2 gene was inactivated by deleting exon 3 of the gene, which caused a frame shift within the ASPP2 open reading. All heterozygous mice survived and developed normally. In contrast, only 6% of ASPP2-null pups survived birth, which was far below the expected Mendelian frequency of 25% (Vives et al., 2006b). The majority of these mice died within 6 and 30 days, mainly due to a combination of hydrocephalus and heart abnormalities (Sottocornola et al., 2010; Vives et al., 2006b). The potential role of ASPP2 as a tumor suppressor has been further explored through tumor studies using both heterozygous and WT mice. The results obtained over a 3 year period revealed that ASPP2 heterozygous mice were more prone to spontaneously develop tumors when compared to WT littermates, resembling mice deficient for p53 (Donehower et al., 1992; Vives et al., 2006b). B-cell lymphomas, sarcomas and squamous cell carcinomas were frequently found in these animals (Vives et al., 2006b). The work developed by *Vives et al.* suggested that the loss of one allele was sufficient to increase the susceptibility of ASPP2 heterozygous mice to tumorigenesis. Furthermore, the ASPP2 gene was retained in every tumor examined. Altogether, this evidence indicates that ASPP2 behaves as a haploinsufficient tumor suppressor (Santarosa and Ashworth, 2004; Vives et al., 2006b). Interestingly, the haploinsufficiency of ASPP2 accelerates the onset of tumor formation in response to γ-irradiation in a similar way to that observed in p53-heterozygous mice (Kemp et al., 1994). Following studies have gone on to demonstrate that ASPP2 and p53 synergistically cooperate in tumor suppression. ASPP2 and p53-null mutations are synthetic lethal, as all ASPP2/p53 double-homozygote mice appear to die in the first half of gestation (before E11.5),

despite the fact that ASPP2 and p53-null embryos remain viable by E18.5 (Vives et al., 2006a; Vives et al., 2006b). Moreover, data collected with ASPP2-p53 mosaic mice has shown that mice doubly heterozygous for ASPP2 and p53 deletions develop lymphomas earlier than ASPP2 or p53 single heterozygotes.

1.6.3 – ASPP PROTEINS IN CANCER

The ASPP family of proteins plays an important role in determining cell fate by enhancing or inhibiting the p53-dependent apoptotic pathway. Inevitably, it is likely that ASPP1, ASPP2 and iASPP are determinant in human tumorigenesis.

The characterization of the crystal structure of p53's DNA-binding domain bound to the signature sequence of the ASPPs became the first clear evidence of the involvement of the ASPP proteins in human cancer. In fact, all of the amino acids in p53 that are important for ASPP binding, namely 178His, 181Arg, 243Met and 247Arg, are mutated in human cancer (Cho et al., 1994; Gorina and Pavletich, 1996). More interestingly, the two most frequently mutated p53 residues – 248Arg and 273Arg – both contact with DNA and ASPP2. Further analysis has revealed that mutation of the p53-ASPP2 contact residue 181Arg has been observed in human cervical and breast tumor cells (Crook et al., 1998; Ludwig et al., 1996; Samuels-Lev et al., 2001). Interestingly, Arg181Lys and Arg181Leu were classified as part of a new group of p53 mutants that retain full potential to induce cell cycle arrest, but are defective in promoting apoptosis. These mutations prevent ASPP1 and ASPP2 from stimulating the apoptotic function of p53.

The study of human tumor samples has yielded new and significant evidence supporting the importance of the ASPP proteins in tumorigenesis. The analysis of

matched normal and tumor samples from human breast cancer showed downregulation of ASPP1 and ASPP2 in almost 60% of samples expressing WT p53, and about 20% in those expressing mutant p53 (Bergamaschi et al., 2003; Samuels-Lev et al., 2001). Moreover, in the samples in which ASPP1 and ASPP2 expression did not change dramatically, iASPP was found to be overexpressed. The expression of ASPP2 has been associated with breast cancer progression as it has been found to be reduced in metastatic samples when compared with non-metastatic ones in a microarray analysis (Sgroi et al., 1999). Northern Blot analysis has similarly detected low levels of ASPP2 mRNA in some human lung cancer cell lines (Mori et al., 2004). ASPP1 follows a similar trend to ASPP2, being reduced in non-small-cell lung carcinoma and mesothelioma cell lines (Mori et al., 2004). Down-regulation of ASPP1 and ASPP2 has also been described in leukemia cell lines and acute lymphoblastic leukemia (Agirre et al., 2006). In addition, ASPP2 single nucleotide polymorphisms have been shown to be associated with a predisposition to gastric cancer development (Ju et al., 2005).

1.6.4 – ASPP2 AND CELL POLARITY

Over the past few years, several observations have suggested an involvement of ASPP2 in the establishment of cell polarity in epithelial cells (Cong et al., 2010; Sottocornola et al., 2010). The analysis of ASPP2$^{\Delta 3/\Delta 3}$ mice has shown that these mice develop hydrocephalus and dysplasia of the retina, suggesting that ASPP2 plays a role in central nervous system (CNS) development (Sottocornola et al., 2010). Further studies have revealed that an absence of ASPP2 in neuronal cells

leads to the expansion of the neural progenitor cell pool, and loss of organization of the neuronal epithelium. These observations were complemented by the finding that ASPP2 binds to and influences the location of the Par complex components, both *in vitro* and *in vivo.* Sottocornola and colleagues have shown that ASPP2 binds to Par3 and co-localizes with ZO-1, but can only partially co-localize with β-catenin, thus is located at the tight junctions of the neuroepithelium. Since disruption of the neuroepithelium is observed upon ASPP2 deletion, the authors showed that ASPP2 influences the integrity of the tight junctions *in vivo*. Experiments performed in MDCK cells revealed that ASPP2, together with Par-3 and ZO-1, is promptly directed to the cell-cell contacts upon calcium switching (Cong et al., 2010; Sottocornola et al., 2010). This recruitment demonstrates that ASPP2 is necessary for the establishment of tight junctions in epithelial cells. Importantly, it was also discovered that Par-3 binds to ASPP2 through its C-terminal region. Despite the fact that this region, characterized by PDZ domain 3, is also involved in the binding to aPKC and TIAM1, ASPP2 does not affect the assembly of the Par-3/aPKC complex (Sottocornola et al., 2010).

The discovery of this new biological function of ASPP2 brought to light a new mechanism through which ASPP2 might exert its tumor suppressive function. Interestingly, a recent study has shown that Par-3 has a dual role in skin cancer as, depending on the cancer type, loss of Par-3 can predispose to the development of cutaneous tumors named keratoachantomas, or reduce the incidence of Ras-driven papillomas *in vivo* (Iden et al., 2012). The biological importance of ASPP2 as a cell polarity protein was recently reinforced by a study that identified ASPP2 as new target of the gastric *Helicobacter pylori* protein CagA (Buti et al., 2011).

Interestingly, binding between CagA and the N-terminal region of ASPP2 promotes the recruitment and binding of ASPP2 to cytosolic p53, which is then degraded by the proteasome (Buti et al., 2011). It is already known that CagA is able to disrupt epithelial cell integrity by interacting with apical junctional complex proteins, such as ZO-1 and JAM (Amieva et al., 2003). These observations have shown that a pathogen is capable of subverting the tumor suppressive activity of ASPP2. Although further studies are required to understand whether the cell polarity role of ASPP2 is affected, it is possible that other pathogens can act in a similar way, and use ASPP2 as a target to destabilize epithelial cell-cell contacts and invade the host cell.

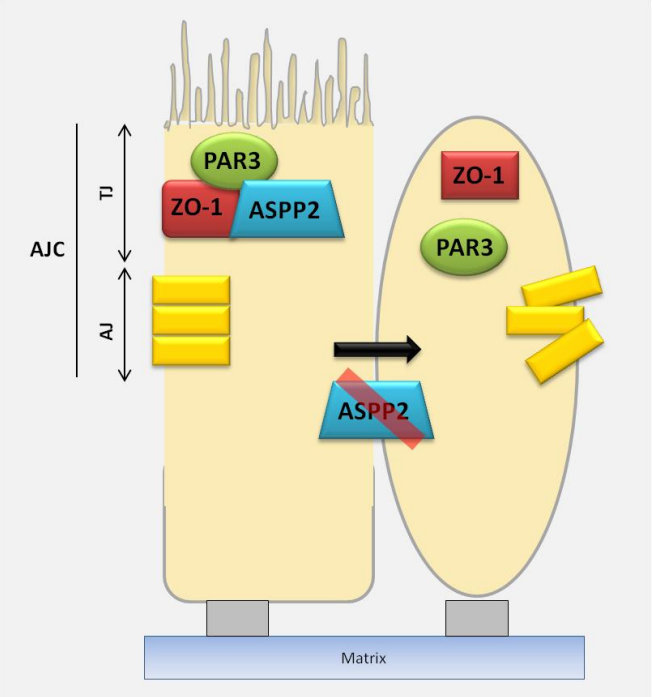


FIGURE 1.11 – Loss of cell-cell contacts upon ASPP2 deletion. ASPP2 colocalizes with ZO-1 and Par-3 at the level of the tight junctions. During the process of cell polarization, ASPP2 ensures the proper location of Par-3 at the apical epithelial surface. ASPP2 deficient cells fail to be polarized since Par-3 and ZO-1 are not located at the tight junctions. ASPP2 is, therefore, important for maintaining the integrity of the cell's architecture.

AIMS OF THE STUDY

The aim of this study is to investigate the role of ASPP2 in cell polarity and homeostasis in the intestine. First, whether or not the homeostasis of the intestinal epithelium is compromised in ASPP2-deficient mice will be investigated, by analyzing different aspects such as cell proliferation, cell death and intestinal epithelial architecture, taking advantage of histological techniques. Secondly, the putative link between ASPP2, LKB1 and AMPK at the level of the tight junctions and cell metabolism will be explored. This study will also investigate whether ASPP2's location and expression as a tight junctional protein can be modulated under energetic stress conditions. Finally, possible signs of colonic inflammation in ASPP2-deficient mice will be analyzed. Our ASPP2 conditional knockout mouse model will be used to determine whether the deletion of ASPP2 is sufficient to increase susceptibility to DSS-induced colitis and tumor formation.

CHAPTER 2 - MATERIALS AND METHODS

2.1 – MATERIALS

2.1.1 – REAGENTS

Unless otherwise stated, reagents were obtained from Sigma or VWR.

All autoradiography films (Hyperfilm) and ECL (Enhanced Chemical Luminescence) reagents were purchased from Amersham Pharmacia Biotech (UK). Nitrocellulose membrane was purchased from Whatman (Germany). All tissue culture dishes and flasks were obtained from Geiner (UK). The QIAGEN Plasmid Maxi Kit and the RNeasy midi kit were purchased from Qiagen (UK). The avidin/biotin-based peroxidase kit and DAB (3, 3'-diaminobenzidine) peroxidase substrate kit were obtained from Vector Labs.

5X Agarose Sample Buffer

50% (w/v)	Sucrose
100mM	EDTA, pH 8.0
0.1% (w/v)	Bromophenol blue
0.1% (w/v)	Xylene cyanol FF

Agarose Gel for DNA Electrophoresis

Agarose powder (Gibco BRL, UK) was weighed and dissolved in 1X TAE buffer at an appropriate percentage (w/v). The mixture was heated in a microwave to dissolve the agarose, and the solution allowed to cool to 40°C. Ethidium bromide was added to a final concentration of 20µg/ml. The agarose solution was poured

into a casting tray with the required comb and was left to solidify at room temperature.

Alcian Blue

1% (w/v) final solution of Alcian Blue 8G was prepared in 3% glacial acetic acid. pH was adjusted to 2.5.

Ammonium Persulfate (APS)

10% (w/v) stock solution was prepared in water and stored at -20°C in single-use aliquots.

Ampicillin Stock Solution

5g of the antibiotic was dissolved in 25ml of sterile distilled water and 25ml of ethanol, making a 100mg/ml stock solution in 50% ethanol. This was stored at -20°C in single-use aliquots.

Blocking Solution

5% (w/v) fat-free milk (Marvel, UK) or 5% (w/v) bovine serum albumin (BSA) was prepared in Tris-buffered saline and Tween 20 (1X TBS-T).

COmplete™ Protein Inhibitor Cocktail

1X COmplete™ protein inhibitor (Boehringer Mannheim, UK) tablet was dissolved in 2.0 ml of sterilized water as a 20x stock solution that is stable at -20°C for 12 weeks.

Citric Acid Buffer

10mM citric acid solution was prepared in water and the pH adjusted to 6.0 with NaOH.

DAPI Staining Solution

1000X stock solution of 10mg/ml was prepared by dissolving 4',6-Diamidino-2-phenylindole (DAPI) dihydrochloride hydrate in water and kept at -20°C.

DNA Marker

100bp and 1kb DNA ladders were purchased from Bioline Reagents Ltd. and were used as size standards for agarose gel electrophoresis.

Dextran Sulphate Sodium

2% and 5% (w/v) dextran sulphate sodium (DSS, mol. wt. 35,000-50,000 Da, MP Biomedicals) was dissolved in 1L of filter-purified and sterilized water.

EDTA Solution

A 0.5M stock solution of ethylenediaminetetraacetic acid (EDTA) was prepared by dissolving 18.6g of EDTA in 70ml distilled water. The pH was adjusted to pH 8.0 with NaOH and the volume made up to 100ml with distilled water.

Ethidium Bromide

A 10mg/ml stock solution was prepared by dissolving 0.2g of ethidium bromide in 20ml of distilled water.

Freezing Medium

50% (v/v)	FBS
45% (v/v)	DMEM
5% (v/v)	DMSO
1% (v/v)	Penicillin-Streptomycin (GIBCO)

Stored at 4°C.

IP Lysis Buffer (NETN)

150mM	NaCl
1mM	EDTA
50mM	Tris, pH 8.0
1% (v/v)	NP40

Stored at room temperature.

Kanamycin Stock Solution

Kanamycin was dissolved at 50mg/ml, filter sterilized and stored at -20°C in aliquots.

Lipotransfection Reagents

Lipotransfections were performed with Fugene 6 (Roche), following the manufacturer's recommendations.

Luria Broth (LB) medium

LB powder was dissolved as recommended by the manufacturer's instructions, autoclaved and stored at room temperature.

LB Agar Plates

LB agar powder was dissolved as recommended by the manufacturer's instructions and autoclaved. The solution was then cooled to 55°C before the addition of 100µg/ml ampicillin or 50µg/ml kanamycin. 20ml of LB agar was then poured into 10cm dishes, allowed to set and the plates stored at 4°C.

Mowiol

6ml of glycerol, 6ml of distilled water and 2.4g of Mowiol 4-88 (Calbiochem) were mixed in a 50ml falcon tube. The mixture was vortexed and then shaken for 2 hours. 12ml of 200mM Tris-HCl, pH 8.5 was added and the solution was incubated at 50°C with occasional mixing until the Mowiol dissolved (approximately 3 hours). The solution was filtered through 0.45µm syringes and stored in aliquots at -20°C. Before each aliquot's use, 2.5% w/v 1,4-diazabicyclo[2.2.2]octane (DABCO) was added and the solution vortexed for 30 minutes, before being left overnight at 4°C for the bubbles to disappear.

Para-formaldehyde (PFA) Fixing Solution

4% (w/v) solution was prepared by first dissolving para-formaldehyde in water in the fume-hood. 10X PBS was added until the final concentration of PBS was 1X. The pH was adjusted to 7.0 with 1M HCl and the solution stored at room temperature.

Permeabilization Solution for Intestinal Organoids

The solution was freshly prepared each time by dissolving 10% (v/v) FBS and 0.5% (v/v) Triton X-100 in PBS. The solution was kept at 4°C until required.

Phosphatase Inhibitor Cocktail

1 PhosSTOP phosphatase inhibitor cocktail (Roche) was dissolved in 10mL cold lysis buffer (RIPA or NETN) before use.

Phosphate Buffered Saline (PBS)

12.5mM	NaCl
1mM	Sodium dihydrogen phosphate, NaH_2PO_4
1.6mM	Disodium dihydrogen phosphate, Na_2HPO_4

The pH was adjusted to 7.0 and autoclaved. The solution was prepared by the Ludwig washroom team.

PBS - Tween-20 (PBS-T)

0.2% Tween-T (v/v) was diluted in PBS.

Ponceau S Staining Solution (10X)

5% (v/v)	Acetic acid
2% (v/v)	Ponceau S (sodium salt)
30% (w/v)	Trichloroacetic acid CCl_3COOH
30% (w/v)	5-sulfosalicyclic acid $C_7H_6O_6S.2H_20$

The solution was dissolved in water to a final concentration of 1X before use.

Primers used in PCR

All primers were synthesized by Operon (Germany). The lyophilized primers were dissolved in sterile water to a stock concentration of 100mM.

Protein G Sepharose

Protein G Sepharose was stored in 20% ethanol at 4°C (Pharmacia Biotech). The beads were washed 3 times with cold PBS and re-suspended in one volume of PBS before use.

Protein Molecular Weight Markers

Pre-stained protein markers were purchased from New England Biolabs (UK) and used as a size standard for SDS-polyacrylamide gel electrophoresis.

RIPA (radioimmunoprecipitation) Lysis Buffer

150mM	NaCl
1% (v/v)	NP40
0.1% (w/v)	SDS
50mM	Tris base

RIPA buffer was stored at room temperature. Complete protease inhibitor cocktail (1:20) was added to the buffer. Depending on the experiment, phosphatase inhibitor cocktail was also added.

SDS Solution

A 10% (w/v) solution of sodium dodecyl sulphate (SDS) was dissolved in water and stored at room temperature.

5X SDS-PAGE loading dye

250nM	Tris-HCl
10% (w/v)	SDS
50% (v/v)	Glycerol
12.5% (v/v)	β-Mercaptoethanol
0.5% (w/v)	Bromophenol blue

10X SDS-PAGE Running Buffer

720g	Glycine
150g	Tris-base
50g	SDS

5L of running buffer were prepared using distilled water.

10X SDS-PAGE Transfer Buffer

725g	Glycine
145g	Tris

5L of transfer buffer were prepared using distilled water. 20% ethanol was added to 1X SDS-PAGE transfer buffer before use.

Stripping Buffer

62.5mM	15.5 ml of 1M Tris-HCl, pH 6.7
100mM	1.75 ml of β-mercaptoethanol
2%	5g SDS

250ml of stripping buffer were prepared with distilled water.

SuperScript® First Stand Synthesis System

Kit for cDNA production from RNA purchased from Invitrogen and stored at -20°C.

Tartrazine-Phloxine B

Phloxine solution was prepared by dissolving 0.5g of Phloxine B and 0.5g of calcium chloride in 100mL of distilled water. Tartrazine solution was prepared by saturating a solution of tartrazine in 2-ethoxyethanol (cellosolve).

50X TAE (Tris-Acetate-EDTA) Buffer

242g	Tris base
57.1ml	Glacial Acetic Acid
100ml	0.5M EDTA, pH 8.0

Distilled water was added up to 1L and the pH was adjusted to 8.5.

TE Buffer

10mM	1.0ml of 1M Tris-HCl, pH 8.0
1mM	0.2ml of 0.5M EDTA, pH 8.0

Distilled water was added up to 100ml.

10X Tris Buffered Saline Tween (TBS-T)

121g	Tris base
36.53g	NaCl
250ml	Tween-20

pH was adjusted to 7.6 with HCl and a total volume of 5L prepared.

Urea Buffer

8M	Urea
1M	Thiourea
0.5%	CHAPS 3(-[(3-cholamidopropyl)-dimethylammonio]-1-propane sulfonate
50mM	DTT (Dithiothreitol)
24mM	Spermine

Water

Nanopure water (Type I) generated from the MilliQ water system was used for all procedures.

2.1.2 – SDS-POLYACRYLAMIDE GELS

All plates were cleaned with water and detergent, dried and assembled in the casting trays (Biorad). The acrylamide content of the gels varied between 6% and 15% depending on the size of the protein of interest. The acrylamide gels were overlaid with 70% isopropanol solution and left to polymerize. After polymerization, the isopropanol was washed away with water and a 4% stacking gel set with the appropriate number and size walls.

	Resolving Gels				Stacking Gel
	6%	8%	10%	12%	4%
Acryl/Bis	2ml	2.7ml	3.3ml	4.0ml	1.3ml
1.5M Tris-HCl pH 8.8	2.5ml	2.5ml	2.5ml	2.5ml	--
1.0M Tris-HCl pH 6.8	--	--	--	--	2.5ml
10% SDS	100µl	100µl	100µl	100µl	100µl
10% APS	100µl	100µl	100µl	100µl	100µl
TEMED	10µl	8µl	5µl	5µl	10µl
Distilled Water	5.3ml	4.6ml	4.0ml	3.3ml	6.1ml
Total Volume	10ml	10ml	10ml	10ml	10ml

TABLE 2.1 – Preparation of SDS-Polyacrylamide gels. All resolving and stacking gels were prepared using 30% acrylamide/bis acrylamide (Acryl/Bis) 29:1 (NBL, UK or BioRad, UK). Values given are per 10ml of gel required. Abbreviations: APS, ammonium persulfate; TEMED, N,N,N',N'-Tetramethylethylenediamine; Tris, Tris(hydroxymethyl)aminomethane; SDS, sodium dodecyl sulphate.

2.1.3 – ANTIBODIES

PRIMARY ANTIBODIES				
Antigen	**Antibody Clone**	**Host/Type**	**Source**	**Application**
Actin	C2	Mouse mAb	Santa Cruz (sc-803)	WB (1:1000)
AMPK	23A3	Rabbit mAb	Cell Signaling	WB (1:1000)
ASPP2	DX54.10	Mouse mAb	Ascite	WB (1:1000), IHC (1:100), IF (1:400)
ASPP2	LX50.13	Mouse mAb	Ascite	IP
ASPP2	S32	Rabbit pAb	Serum	WB (1:1000), IF (1:200)
ASPP2	LX116	Mouse mAb	Ascite	IF (1:200)
ASPP2	BP77	Rabbit pAb	Serum	WB (1:500)
CD45R	RA3-6B2	Rat	BD Biosciences	IF (1:500)
CD3	--	Rabbit pAb	Abcam (ab5690)	IF (1:200)
Chromogranin A	--	Rabbit pAb	Dako	IF (1:1000)
E-cadherin	--	Mouse mAb	BD Transduction	WB (1:100), IF (1:100)
Ezrin	3C12	Mouse mAb	Abcam (ab4069)	IF (1:200)
Flag-tag	F3165	Mouse mAb	Sigma Aldrich	WB (1:500)
Flag-tag	F7425	Rabbit pAb	Sigma Aldrich	WB (1:500)
Hes1	--	Rabbit pAb	Abcam (ab71559)	WB (1:200)
Hes5	--	Rabbit pAb	Abcam (ab107593)	WB (1:200)
Ki67	--	Rabbit pAb	Vector Labs	IF (1:1000)
Ku80	Ab-2	Mouse mAb	Thermo Fisher	WB (1:1000)
LKB1	Ley 37D/G6	Mouse mAb	Santa Cruz	IF (1:200)
LKB1	--	Mouse mAb	Upstate	WB (1:200)
Lysozyme	--	Human	Dako	IHC (1:500), WB (1:1000)
Math1	N-19	Goat pAb	Santa Cruz	WB (1:200)
Mo25	EP1680Y	Rabbit mAb	Epitomics	WB (1:1000)
Muc2	H300	Rabbit pAb	Santa Cruz	IHC (1:1000), IF (1:1000)
Myc-tag	9E10	Mouse mAb	Ascites	WB (1:1000)
Myeloperoxidase		Rabbit pAb	Abcam (ab45977)	IF (1:500)
Par3	--	Rabbit pAb	Upstate	IF (1:400)
Phospho AMPK	40H9	Rabbit mAb	Cell Signaling	WB (1:500)
Phospho Histone 3	--	Rabbit pAb	Upstate	IF (1:200)
STRAD	H-83	Rabbit pAb	Santa Cruz	WB (1:200)
STRAD	--	Rabbit pAb	Abcam (ab64799)	IF (1:100)
V5-tag	SV5-Pk1	Mouse mAb	Serotec	IP, IF (1:500), WB (1:500)
V5-tag	--	Rabbit pAb	Abcam (ab9116)	WB (1:1000)

Villin	R814	Rabbit pAb	Cell Signaling	IF (1:500)
Zo-1	--	Rabbit pAb	Invitrogen	IF (1:500)
β-catenin	--	Mouse mAb	BD Transduction	IF (1:100), WB (1:200)

TABLE 2.2 – List of primary antibodies. Abbreviations – Ab, antibody; mAb, monoclonal antibody; pAb, polyclonal antibody; IHC, Immunohistochemistry; IF, Immunofluorescence; WB, Western blot; IP, Immunoprecipitation.

SECONDARY ANTIBODIES			
Antibody Name	**Host/Type**	**Source**	**Applications**
Alexa Fluor® 488 F(ab')2 fragment Anti-Rabbit	Goat	Invitrogen	IF (1:400)
Alexa Fluor® 488 F(ab')2 fragment Anti-Mouse	Goat	Invitrogen	IF (1:400)
Alexa Fluor® 488 Anti-Mouse IgG (H+L)	Donkey	Invitrogen	IF (1:400)
Alexa Fluor® 647 Anti-Mouse IgG (H+L)	Donkey	Invitrogen	IF (1:400)
Alexa Fluor® 488 Anti-Rabbit IgG (H+L)	Donkey	Invitrogen	IF (1:400)
Alexa Fluor® 647 Anti-Rabbit IgG (H+L)	Donkey	Invitrogen	IF (1:400)
Alexa Fluor® 647 Anti-Rat IgG (H+L)	Goat	Invitrogen	IF (1:400)
Anti-Rabbit Immunoglobulins/HRP	Swine	Dako	WB (1:2000)
Anti-Mouse Immunoglobulins/HRP	Rabbit	Dako	WB (1:2000)
Biotinylated Anti-Mouse IgG	Goat	Vector Labs	IHC (1:250)
Biotinylated Anti-Rabbit IgG	Goat	Vector Labs	IHC (1:250)

TABLE 2.3 – List of secondary antibodies. Abbreviations – HRP, horse-radish peroxidase; IHC, Immunohistochemistry; IF, Immunofluorescence; WB, Western blot.

2.1.4 – CELL LINES

Name	Tissue Type/Origin
Caco-2	Human colon carcinoma, mutant p53 – from Ludwig Institute for Cancer Research (Oxford)
U2OS	Human osteosarcoma, wild type p53 – from Ludwig Institute for Cancer Research (Oxford)

TABLE 2.4 – List of cell lines and relevant information.

2.2 – METHODS

2.2.1 – TISSUE CULTURE

Basic Media

Dulbecco's Modified Eagle Medium (DMEM), Dulbecco's Modified Eagle Medium: Nutrient Mixture F12 (DMEM/F12) and Dulbecco's Modified Eagle Medium without glucose were purchased from Gibco-BRL (UK) and stored at 4°C.

Media Supplements

Fetal calf serum (FCS) was purchased from PAA Laboratories and tested for its ability to support the growth of various cell lines. FCS was heat inactivated for 30 minutes at 55°C and stored at -20°C in 50ml aliquots. L-Glutamine was purchased from Gibco-BRL at a 200mM concentration, stored at -20°C and used at a final concentration of 2mM. Penicillin/Streptomycin was purchased from Gibco-BRL at 10000 units/ml and stored at -20°C. A final concentration of 200 units/ml was used.

Maintenance of Cell Lines

All immortalized cell lines were cultured in complete medium (DMEM, Invitrogen) supplemented with 10% (v/v) FCS, L-glutamine and penicillin/streptomycin. Cells were incubated in flasks or dishes (Falcon), in a Heraeus incubator at 37°C in the presence of 10% CO2. Medium was changed every 2 to 4 days depending on cell line requirements. On reaching confluency, cells were washed with 1X PBS and incubated with 2 to 4ml pre-warmed Trypsin-EDTA (Gibco-BRL) at 37°C until the cells detached from the flasks or dishes. The trypsin was

neutralized by the addition of an appropriate volume of growth medium, and the culture then seeded on to new flasks or dishes at the desired density.

Mouse intestinal organoids were cultured in Advanced DMEM/F12 (ADF) enriched with 25% BSA, 10mM HEPES, glutamine, penicillin/streptomycin, B27 and N2 supplements (Invitrogen). Crypt culture medium was completed by adding 50ng/mL of EGF, 500ng/mL R-spondin and 100ng/mL of Noggin (Prepotech). Primary cells were incubated in 24-well plates in a Heraeus incubator, at 37°C in the presence of 5% CO2. Growth factors were added to the medium every 2 days. All culture media was changed twice per week.

Freezing and Thawing of Cells

To thaw cells from liquid nitrogen stock, vials were placed in a 37°C water bath for 2 minutes. Addition of pre-warmed growth medium and centrifugation for 5 minutes at 1200rpm enabled the removal of the freezing medium. The pellet of cells was then re-suspended in pre-warmed growth medium and transferred to a 6cm or 10cm dish. The cells were kept at 37°C overnight to recover.

For freezing, cells were allowed to grow to about 80% confluency before collection by trypsinization (as described above). Cells were centrifuged for 5 min. at 1200rpm and the supernatant discarded. The cell pellet was re-suspended in the appropriate amount of freezing medium and aliquoted in cryovials (Corning). The vials were labeled and cooled, at the rate of 1°C per minute, in a Nalgen Cryo 1°C freezing container placed in a -80°C freezer for at least 24 hours, before being transferred to a liquid nitrogen tank for long term storage.

2.2.2 – DNA AND RNA TECHNIQUES

Bacterial Strains and Culture

Chemically competent Escherichia coli Alpha-Select™ silver efficiency cells (Bioline) were used as a host for plasmid DNA. Bacteria were cultured in Luria Broth medium containing the appropriate antibiotic (100µg/ml ampicillin or 50µg/ml kanamycin) at 37°C, with shaking at 350rpm.

Transformation

Competent cells were thawed on ice, and the desired plasmid DNA (100ng) added to the vial (50µL). The mixture was kept on ice for 30 minutes. The bacteria then subjected to heat shock by first placing the vial in a 42°C water bath for 45 seconds, before placing it on ice for 2 minutes. 450µL of SOC (super optimal broth containing glucose) medium (Invitrogen) was added to the cells, which were shaken at 37°C for 1 hour before plating on agar plates containing the appropriate antibiotic. Plates were incubated at 37°C overnight to allow colony formation and colony selection the following day.

Small Scale Preparation of Plasmid DNA (QIAprep® Spin Miniprep Kit)

A single bacterial colony was picked and inoculated in 5ml LB medium, containing the appropriate antibiotic, in a sterile test tube. The tube was left shaking at 37°C overnight. Bacteria were collected by centrifugation for 5 minutes at 6000g. The resulting pellet was re-suspended in 250µl of Qiagen Solution 1. 250µl of Qiagen Solution 2 was then added and the tubes inverted 5 times for gentle mixing. 350µl of Qiagen Solution 3 was added and tubes inverted again. The

resultant mixture was centrifuged for 10 minutes at 20000g in a tabletop centrifuge, and the supernatant transferred to a Qiagen Spin column. The spin column was washed once with Qiagen PE buffer containing ethanol and the flow-through discarded. Plasmid DNA was eluted from the column with 30µL of ultrapure distilled water. The concentration was determined using a Nanodrop spectrophotometer (Thermo Scientific).

Large Scale Preparation of Plasmid DNA (QIAfilter® Plasmid Maxi Kit)

A single bacterial colony was picked and inoculated in 200ml of LB medium containing the appropriate antibiotic. The bacterial suspension was left shaking at 37°C overnight. Plasmid DNA extraction was carried out according to the QIAfilter® Plasmid Maxi Kit manufacturer's protocol.

Agarose Gel Electrophoresis

Agarose (Helena) was dissolved in 1X TAE buffer (at the required percentage), boiled until complete dissolution and allowed to cool. Ethidium bromide was added to a final concentration of 20µg/ml. Gels were run in Hoefer running tanks at 100V, and bands visualized in a UV-imaging system (UVP Bio Imaging Systems, Labworks gel analysis software).

DNA samples were mixed with 5X loading buffer to a final concentration of 1X, and run alongside the appropriate-sized DNA ladder (Hyperladder I, Bioline).

RNA Extraction and Reverse Transcription

RNA was extracted from cells and tissues according to the Qiagen RNeasy mini kit protocol, including treatment with DNase I (Qiagen) to eliminate possible genomic

DNA contamination. Up to 5µg of total RNA were used to generate cDNA with the SuperScript® First Stand Synthesis System (Invitrogen) following the manufacturer's protocol.

Real-time Quantitative PCR (RT-qPCR)

Real-time quantitative PCR was performed on the 7500 real time PCR system (Applied Biosystem) using the QuantiTect SYBR Green PCR kit (Qiagen). Each reaction was performed in duplicate using 1µl of cDNA in a final volume of 25µl. The following thermal cycle was used for all the samples

For each experiment, the threshold was set to cross a point at which real-time PCR amplification was linear. Previously published primers were used for all of the genes analyzed (sequences reported in Table 2.6). The expression level of each target gene was analysed based on the ΔΔCt method, with GAPDH as an internal control.

Gene	Primers
HES1	F 5'-GCTTCAGCGAGTGCATGAAC R 5'-GGCGAAGGCTTTGCTGTGT
HES5	F 5'-GCACCAGCCCAACTCAA R 5'-GGCGAAGGCTTTGCTGTGT
IL-17	F 5'-TCTCATCCAGCAAGAGATCC-3' R 5'-AGTTTGGGACCCCTTTACAC-3'
Lysozyme	F 5'-GGTCTACAATCGTTGTGAGTTGG-3' R 5'-CTCCGCAGTTCCGAATATACT-3'
TNF-α	F 5'- GGCAGGTCTACTTTGGAGTCATTGC-3' R 5'- ACATTCGAGGCTCCAGTGAATTCGG-3'

TABLE 2.5 – List of primers used in RT-PCR experiments. Abbreviations – F, forward; R, reverse.

2.2.3 – PROTEIN MANIPULATION

Sample Preparation

Cells growing on plates were washed two times with 1X PBS and lysed in RIPA or NETN buffer (150µL-250µL per 10cm dish). The cells were scraped with a sterile disposable cell scraper (Greiner) and transferred to an eppendorf tube. Samples were kept on ice for 30 minutes before centrifugation at 13200 rpm, 4°C for 20 minutes. The supernatant was collected and used for protein quantification. Mouse tissue was homogenized 2 times for 15 seconds in urea buffer. The resultant lysate was sonicated 3 times for 10 seconds and incubated on ice for 30 minutes. Samples were then centrifuged at 13200rpm, 4°C for 20 minutes, and repeat centrifugations performed until no pellet was obtained. The resulting supernatant was collected and used for protein quantification.

Protein Concentration Determination

The protein concentration of cell and tissue extracts was determined using the BioRad (Bradford) protein assay reagent system. In a 96-well plate, 1µL of cell lysate was dissolved in 200µL of 1x BioRad assay reagent. In the same plate, known concentrations of bovine serum albumin (BSA) were used to establish a standard curve of concentration/absorbance. The plate was read in a spectrophotometer (Anthus Labtech Instrument, using Magellan software) at 595nm, and the concentration of the cell lysate was obtained by extrapolating from the BSA standard curve.

SDS-Polyacrylamide Gel Electrophoresis (PAGE)

Known concentrations of protein were mixed with appropriate volumes of 5x SDS-PAGE loading dye and boiled for 10 minutes. Equal amounts of protein were loaded into the wells of the stacking gel. Gels were run at 130V for 1.5h in 1x running buffer using the Biorad running system. Pre-stained protein markers were purchased from New England Biolabs and used as size standards.

Immunoblotting

When the SDS-PAGE running process was finished, the gel was transferred to a wet transfer cassette unit and the proteins blotted onto nitrocellulose membrane for 2.5h at a constant voltage of 75V, or 30V at 4°C when the transfer was run overnight. The transfer tank was filled with 1x transfer buffer complemented with 20% ethanol. When the transfer process was complete, the membrane was stained with Ponceau S solution (purchased as a 0.1% (w/v) solution in 5% acetic acid) to determine the success of protein transfer and equal loading of the lanes. The membranes were then washed in water and blocked in 5% fat-free milk (Marvel, UK) in 1X TBS-Tween at room temperature for 1h. Primary antibody was added according to the recommended concentration, diluted in 5% milk/TBS-Tween for 3 hr at room temperature or overnight at 4°C. Following incubation with primary antibody, the membranes were washed 3x for 15min with 1x TBS-Tween. The results were visualized by enhanced chemiluminescent detection, ECL (Amersham Biosciences) using X-ray films (Fujifilm). If it was necessary to probe the same membrane with another primary antibody, the membrane was immediately re-probed or incubated with stripping buffer for 30 min at 55°C. Following these steps,

the membrane was re-blocked in 5% milk/TBS-Tween, before being incubated with the new primary antibody.

Immunoprecipitation

Cells growing on plates were washed three times with cold 1x PBS and lysed with NETN buffer containing protease inhibitors and phosphatase inhibitors when necessary. The cells were scraped with a sterile disposable cell scraper (Greiner). The lysate was transferred to an eppendorf and kept on ice for 20 minutes to be later centrifuged at 13200rpm, 4°C for 20 minutes. The resulting supernatant was transferred to a new eppendorf, and protein concentration determined using the BioRad assay system. 80µg of protein was extracted to be used as input. For each immunoprecipitation, 2mg of protein were pre-cleared with 30µL of 70% protein G beads (equilibrated in PBS buffer) for 1hr at 4°C on an eppendorf rotating wheel. Simultaneously, another eppendorf was used to block 70% protein G beads with DMEM containing 5% FBS. The protein lysate was then centrifuged at 13200rpm and the supernatant moved to a new eppendorf, to which the blocked beads and 1µg of purified antibody or 1-5µL ascites/mg lysate were added. The eppendorfs were left rotating overnight at 4°C. Non-specific mouse or rabbit IgG was used as a control. Finally, the beads were washed three times with cold NETN buffer and centrifuged at 13200rpm for 1 minute at 4°C. The supernatant was aspirated and 30µL of SDS-PAGE sample buffer added to the beads. After boiling, the beads were centrifuged once again at 13200rpm for 1 minute at 4°C, and the supernatant analysed by SDS-polyacrylamide gel electrophoresis and western blot.

2.2.4 – CELL-BASED ASSAYS

Cell Transfection

Fugene 6 transfection reagent was used as a DNA-lipid carrier and used according to the manufacturer's protocol. After 24 hours of transfection, cells were used for different experiments.

Plasmid Name	Relevant Information	Source/Reference
pEBG 2T-LKB1	Full length LKB1, GST tagged, in a pEBG plasmid	Dario R. Alessi (Baas et al., 2003)
pCMV5-Mo25	N-terminal Myc tagged full length Mo25, in a pCMV5 plasmid	Dario R. Alessi (Baas et al., 2003)
pCMV5-STRAD	Full length STRAD, FLAG tagged, in a pCMV5 plasmid	Dario R. Alessi (Baas et al., 2003)
LKB1-WT-GFP	Full length LKB1, GFP tagged in pEGFP plasmid	Junying Yuan (Karuman et al., 2001)
LKB1-KM-GFP	Kinase-dead mutant (K78M) LKB1, GFP tagged in pEGFP plasmid	Junying Yuan (Karuman et al., 2001)
ASPP2 (1-360) – V5	ASPP2 fragment (1-360), V5 tagged in pcDNA3.1 plasmid	Xin Lu's lab (Wang et al., 2012)
ASPP2 (360-925) – V5	ASPP2 fragment (360-925), V5 tagged in pcDNA3.1 plasmid	Xin Lu's lab (Wang et al., 2012)
ASPP2 (925-1128) – V5	ASPP2 fragment (925-1128), V5 tagged in pcDNA3.1 plasmid	Xin Lu's lab (Wang et al., 2012)
ASPP2 PP1 mut – V5	Full length ASPP2, PP1 mutant (V922A, F924A), V5 tagged in pcDNA3.1 plasmid	Xin Lu's lab (Llanos et al., 2011)

TABLE 2.6 – List of plasmids and relevant information.

siRNA Experiments

siRNA oligonucleotides (oligos) against ASPP2 and LKB1 were purchased from Dharmacon. siGENOME RISC-free (Dharmacon) was used as a negative control. Cells were transfected with the indicated siRNA oligos at a final concentration of 35nM using Dharmafect 2 reagent (Dharmacon), according to the manufacturer's protocol. 72 hours later, cells were used for different purposes.

Immunofluorescence in Cells

Cells were grown to 70%-80% confluency on coverslips in a 24-well plate. The cells were fixed in 4% PFA solution for 15 minutes after being washed twice with PBS. Cells were permeabilized with 0.1% Triton X solution for 5 minutes. The permeabilization solution was then removed by washing the wells with PBS, and cells were further blocked with 0.2% BSA for 20 minutes. The primary antibody was diluted in 0.2% BSA and incubated at room temperature for 1 hour. Subsequently, the wells were washed 3 times with PBS, each wash lasting for 15 minutes. Cells were then incubated with secondary antibody in 0.2% BSA, for 30 minutes at room temperature. This step was followed by another 3 washes with PBS. Finally, the coverslips were mounted onto microscope slides using mowiol-glycerol based solution. The slides were protected from light and kept at 4°C.

Metabolic Studies

U2OS cells were grown at 70%-80% confluency on top of coverslips. Cells were treated with AICAR 1mM for 4 hours (Cellsignal), Compound C 0,01mM (Millipore) for 4 hours and depleted glucose DMEM for different time points: 30 minutes, 1 hour, 2

hours and 4 hours. Cell lysates were obtained using NET buffer or RIPA buffer, for immunoprecipitation and western blot, respectively. Protease and phosphatase inhibitors were added to cell lysates. For immunofluorescence, cells were fixed and stained as previously described.

TNF-α Treatment

Caco-2 and U2OS cells were grown at 70%-80% confluency on top of coverslips and treated with 10ng/ml TNF-α (Peprotech) for 3hrs, 6hrs, 12hrs, 24hrs and 48hrs. To ensure that cells would be similarly confluent at the end of the experiment, the 48hr time point cells were treated first, and the 3hr time point cells were treated last. Plates were kept at 37°C and at the end of the 48hrs of the experiment, cells were lysed or fixed in 4%PFA, depending on whether Western blotting or immunofluorescence was to be done, respectively (Ma et al., 2004).

2.2.5 – MOUSE WORK

Mouse Colonies

Mice were bred and housed in the British Heart Foundation functional genetics facility in the Henry Wellcome Trust Building of Genomic Medicine (Oxford). They were kept in IVC cages, which have a sealed lid that acts as the second part of a two-barrier system. Procedures were carried out following the Home Office Animals (Scientific Procedures) Act 1986 Act 1986 (PIL: 30/8680, PPL: 30/2862) guidelines.

ASPP2 Δexon3 mutant mice have been previously characterized (Vives et al., 2006). These mice were generated on a mixed C57BL/6Jx129SvJ background and backcrossed in a Balb/c background for 9 generations (Vives et al., 2006).

ASPP2 Δexon3 conditional mice, $ASPP2^{loxP/loxP}$; Cre^{+}, in which exon3 is flanked with LoxP sites, were crossed with R26cre-ER^{T} mice to induce deletion of exon3 by 4-hydroxytamoxifen treatment (Sottocornola et al., 2010).

DNA Extraction from Ear Biopsies

Mice were punched for identification and the resulting ear tissue used for genotyping. Ear tissue was digested overnight at 55°C in 100µl of extraction buffer GNT and 7.8mg/ml of proteinase K (Qiagen). The digested tissue was boiled for 10 minutes at 97°C and 1µl used for polymerase chain reaction (PCR) analysis.

ASPP2$^{\Delta 3/\Delta 3}$ XTV genotyping

DNA extracted from ASPP2$^{\Delta 3/\Delta 3}$ and ASPP2$^{+/+}$ mice was routinely amplified with Promega TAQ polymerase (Promega, UK) using the following primers:

- F4 5'-CGGTTTGGAAGTCAAAGGAA-3'
- B3 5'-TCAATGTGTCCAGCACCCTA-3'
- pGK2 5'-TACCCGCTTCCATTGCTCAG-3'

F4 + B3 produced a 650bp fragment for ASPP2$^{+/+}$ mice and pGK2 + B3 produced a 800bp fragment for ASPP2$^{\Delta 3/\Delta 3}$ mice.

The thermal cycling conditions used were:

1) 94˚C - 3min
2) 94˚C - 40sec
3) 60˚C - 40sec
4) 72˚C - 40sec
5) Back to step 2. → 29 cycles
6) 72˚C - 3min

ASPP2$^{loxP/loxP}$ genotyping

DNA extracted from ASPP2$^{loxP/loxP}$; Cre^{+} and ASPP2$^{wt/wt}$; Cre^{+} mice was routinely amplified with Promega TAQ DNA polymerase (Promega, UK) using the following primers:

- SDL-1 5'-TGGACAGGCTGAGCTGTTAG-3'
- SDL-2 5'-ACACTTTCACCAACCCTAGGTC-3'

SDL-1 + SDL-2 produced a <200bp fragment for ASPP2$^{WT/WT}$ mice, and SDL-1 + SDL-2 produced a >200bp fragment for ASPP2$^{loxP/loxP}$ mice.

The thermal cycling conditions used were:

1) 94˚C 3min
2) 94˚C 40sec
3) 60˚C 40sec
4) 72˚C 40sec
5) Back to step 2. 29 cycles
6) 72˚C 2min

ASPP2$^{\Delta3/\Delta3}$; Cre^{+} genotyping

DNA extracted from ASPP2$^{\Delta3/\Delta3}$; Cre^{+} and ASPP2$^{wt/wt}$; Cre^{+} mice was routinely amplified with Promega TAQ DNA polymerase (Promega, UK) using the following primers:

- F4 5'-CGGTTTGGAAGTCAAAGGAA-3'
- F5 5'-AGTTTGCAGCTCAGCACTCA-3'

The products obtained were 700bp for ASPP2$^{wt/wt}$ mice and 500bp for ASPP2$^{\Delta3/\Delta3}$ mice.

The thermal cycling conditions used were:

1) 94˚C 3min
2) 94˚C 40sec
3) 60˚C 40sec
4) 72˚C 40sec
5) Back to step 2. → 29 cycles
6) 72˚C 2min

Cre genotyping

DNA extracted from ASPP2loxP/loxP and ASPP2wt/wt mice was routinely amplified with Promega TAQ DNA polymerase (Promega, UK) using the following primers:

- Cre-F: 5'-CATTTGGGCCAGCTAAACAT-3'
- Cre-B: 5'-ATTCTCCCACCGTCAGTACG-3'

The product obtained was 308bp.

The thermal cycling conditions used were:

1) 94˚C for 3 min
2) 94˚C for 40 sec
3) 60˚C for 40 sec
4) 72˚C for 40 sec
5) Back to step 2. → 29 cycles
6) 72˚C for 2 min

Generation of Murine Intestinal Organoids

2 month old mice were used in the generation of intestinal organoids (Sato et al., 2009). Small intestines were dissected, opened longitudinally and washed with cold PBS. The isolated tissue was then cut into small pieces and vigorously washed using a 10ml pipette with cold PBS, and supernatants containing the villous fraction discarded after every wash. Tissue fragments were later incubated in 2mM EDTA/0PBS and left rotating for 30 minutes at 4°C. After removal of the EDTA medium with cold PBS, the fragments were mechanically washed with cold PBS 2 to

3 times. The supernatant obtained from these washes was then collected as this contained the crypt fraction. The crypt fraction was diluted in Advanced DMEM/F12 (ADF) and centrifuged for 5 minutes at 1200rpm. The pellet was re-suspended in 15mL ADF and collected in a falcon after passing through a 70µm cell strainer. 2 to 3 centrifugations were performed for 2 minutes at 600 rpm until no single cells were observed in the supernatant. The pellet enriched with crypt cells was the re-suspended in Matrigel at 1000 crypts/mL. 50µL of Matrigel were seeded in a pre-warmed 24-well plate and incubated for 5-10 minutes at 37°C. 500µL of crypt culture media (ADF enriched with growth factors) was added to each well and the plate incubated at 37°C under 5% CO2 conditions (Sato et al., 2009).

Histological Techniques

The small intestines and colons from 2 month old mice were dissected and washed in PBS. The small intestine was further cleaned by gently flushing the lumen with PBS. Tissues were kept in 10% formalin overnight. The tissues were processed for routine paraffin embedding using automated devices and serial 5µm sections were cut. For frozen sections, the tissues were further treated with 20% sucrose overnight, embedded in OCT (frozen tissue matrix) and frozen at -80°C. Serial 15µm sections were obtained.

Hematoxylin and Eosin (H&E) Staining

Slides were de-paraffinized and hydrated in distilled water. The samples were stained with hematoxylin for 2 minutes.

Alcian Blue Staining

Slides were de-paraffinized and hydrated in distilled water. The samples were then stained with alcian blue for 30 minutes and the excess removed by washing the slides under running tap water for 2 minutes. Samples were counterstained with nuclear fast red solution for 5 minutes, following which the excess was washed away with running tap water for 1 minute. The slides were dehydrated in crescent percentages of ethanol and further cleared in histoclear. Slides were the mounted with resinuous mounting media.

Tartrazine-Phloxine B Staining

Slides were de-paraffinized and hydrated through graded alcohols to water. Nuclei were then stained with hematoxylin for 5 minutes and slides washed with water to remove the excess. Following this step, samples were stained with Phloxine solution for 20 minutes. Slides were washed once again with water and allowed to dry for 3 minutes. Staining was concluded by immersing the slides in a solution of tartrazine. The development of the red color in the granules of Paneth cells was controlled microscopically.

Immunohistochemistry

Slides were de-paraffinized and hydrated through graded alcohols to water. Endogenous peroxidases were inactivated by placing slides in 3% H2O2 in methanol. Slides were subsequently immersed in a citric acid buffer and the solution boiled for 10 minutes. Slides were left in the buffer until they were cold enough to handle. Sections were blocked with 5% normal goat serum in PBS for 30 minutes.

Subsequently, sections were incubated in primary antibody diluted in 5% fetal calf serum in PBS overnight at 4°C. The day after, slides were washed in PBS, 3 times for 5 minutes. Biotinylated secondary antibody was diluted in a solution of 5% normal goat serum in PBS. Sections were incubated for 30 minutes at room temperature, following which, slides were washed in PBS 3 times for 5 minutes. Sections were incubated in an avidin/biotin-based peroxidase solution, for 15 minutes at room temperature, and washed in PBS, 3 times for 5 minutes. Subsequently, sections were incubated in a DAB (3, 3'-diaminobenzidine) peroxidase substrate solution for 10 minutes at room temperature. Slides were then rinsed in water and counterstained by immersion in hematoxylin for 15 seconds. Finally, the slides were dehydrated through increasing graded alcohols and immersed in histoclear for 5 minutes before being mounted with coverslips.

Tissue Immunofluorescence (Paraffin Sections)

Slides were de-paraffinized and hydrated through graded alcohols to water. Slides were subsequently immersed in a citric acid buffer, and the solution allowed to boil for 10 minutes. Slides were then left in the buffer until they were cold enough to handle. Sections were blocked with 5% normal goat serum in PBS for 30 minutes. Subsequently, sections were incubated in primary antibody, diluted in 5% fetal calf serum in PBS overnight at 4°C. The day after, slides were washed in PBS 3 times for 5 minutes. Secondary antibody was diluted in a solution of 5% normal goat serum in PBS. Sections were incubated for 45 minutes at room temperature, following which, slides were washed in PBS 3 times for 5 minutes. Finally, coverslips were mounted onto the slides using mowiol-glycerol based solution. The slides

were kept at 4°C, protected from light, until they were observed using a confocal microscope.

Tissue Immunofluorescence (Frozen Sections)

Slides were thawed at room temperature for 10 minutes. Sections were permeabilized with 0.1% Triton in PBS-T for 10 minutes at room temperature. Slides were washed in PBS-T and sections then blocked with 10% normal goat serum in PBS-T for 45 minutes. Subsequently, sections were incubated in primary antibody diluted in 2% BSA diluted in PBS-T overnight at 4°C. The day after, slides were washed in PBS-T, 3 times for 5 minutes. Secondary antibody was diluted in a solution of 2% BSA in PBS-T. Sections were incubated for 45 minutes at room temperature, following which, slides were washed in PBS-T 3 times for 5 minutes. Finally, coverslips were mounted onto the slides using mowiol-glycerol based solution. The slides were kept at 4°C and protected from light, until they were observed using a confocal microscope.

TUNEL Assay

Apoptosis analysis was conducted using an ApopTag® Red in Situ Apoptosis detection kit (Millipore). Paraffin sections were labeled according to the manufacturer's protocol.

Intestinal Organoid Immunofluorescence

Intestinal organoids were grown on cover slips in a 24-well plate for 7 days. The wells were washed 3 times with PBS before being incubated with 4% PFA for 30 minutes at room temperature. After this incubation, the cultures were washed 3

times with PBS for 10 minutes each wash. The cultures were immersed in permeabilization solution for 30 minutes at room temperature. Subsequently, organoids were incubated with primary antibody diluted in permeabilization solution overnight at 4°C. The day after, organoids were washed 6 times, for 10 minutes each, with permeabilization solution. Secondary antibody was diluted in permeabilization solution and the organoids incubation with it for 3 hours at room temperature. Organoids were then washed 6 more times with permeabilization solution, 10 minutes each wash. Cultures were kept in PBS at 4°C until analysis by confocal microscopy.

2.2.6 - DEXTRAN SULPHATE SODIUM-INDUCED COLITIS

2.2.6.1 – Experimental setup

Eight to ten week old ASPP2loxP/loxP; Cre+ mice were injected with 1mg tamoxifen dissolved in sunflower oil at a concentration of 10mg/ml (ASPP2Δ3/Δ3 mice) or sunflower oil (wild type mice) for 4 consecutive days. The experiment was initiated one week after the last tamoxifen injection, to allow the successful deletion of the protein in the organism. During this period, littermates were divided into groups (6 mice in each group that received Dextran Sulphate Sodium (DSS) treatment and 4 mice in each group that received water).

Acute DSS treatment

Freshly prepared autoclaved tap water supplemented with 5% (w/v) DSS salt (36000-50000 Da; MP Biomedicals) was given every two days for eight days (Wirtz et al., 2007)

Chronic DSS treatment

Freshly prepared autoclaved tap water supplemented with 2% (w/v) DSS salt (36000-50000 Da; MP Biomedicals) was given every two days. Mice were submitted to three cycles of 2% DSS (7 days DSS, 14 days water) (Wirtz et al., 2007).

Mouse weight and welfare was evaluated every day during the treatment period. For the acute DSS treatment, all animals were sacrificed after 8 days of the experiment beginning. For the chronic DSS treatment, one animal in each group was sacrificed after three cycles of treatment. The rest of the animals were kept alive until symptoms of colitis were observed.

2.2.6.2 – Histological grading

Histological grading of colonic inflammation was determined as described in (Van der Sluis et al., 2006). The score represents an average of the grading of three different sections, 100µm apart. All scores were obtained in a 'blinded' fashion.

2.2.7 – HUMAN TISSUE SAMPLES

Paraffin-sectioned biopsies of large bowel mucosa of Crohn's disease patients were obtained from the John Radcliffe Hospital, Oxford.

2.2.8 – DATA ANALYSIS

Computer images

All autoradiographs were scanned using the Epson perfection 1660 photo scanner. Adobe photoshop 7.0 and ImageJ software were used to manipulate images (only as a whole for size, brightness and contrast). No signal was modified in relation to the raw image.

Statistical analysis

All statistical analyses for histological characterization were conducted using three different mice (n=3). To measure crypt size, 10 well-oriented sections were chosen and an average was established. To measure mitotic index and evaluate apoptosis, 3 well-oriented sections were chosen. To determine the mitotic index in intestinal organoids, 10 similar sized organoids were isolated for each genotype.

Differences were considered significant at a value of $p \leq 0.05$. The T-test was used to calculate the statistical significance between two measurements.

CHAPTER 3 – ASPP2 DEFICIENCY COMPROMISES THE MORPHOLOGY AND INTEGRITY OF THE INTESTINAL EPITHELIUM

3.1 – INTRODUCTION

The generation of ASPP2 transgenic mice enabled the establishment of *in vivo* studies. Since then, important roles of ASPP2, beyond the regulation of p53-mediated apoptosis, have been identified. The inactivation of the murine *ASPP2* gene was achieved by targeting and replacing *ASPP2* exon3 in 129Sv IT2 embryonic stem (ES) cells with a vector carrying a neomycin resistance gene cassette (Vives et al., 2006b). In C57BL6/6J mice, ASPP2 exon3 homozygous deletion was found to be lethal. In a mixed 129SvxC57BL6 background, only around 6.4% of the ASPP2 mutant pups (out of the 25% according to Mendelian segregation) survived birth, although they all died before weaning (Vives et al., 2006b). Severe defects in the central nervous system, including neural tube closure defects and hydrocephalus, contributed significantly to the premature deaths observed (Sottocornola et al., 2010). In an attempt to obtain viable ASPP2 Δexon3 mice, ASPP2 mutant mice were back-crossed to a Balb/c background to generate a pure strain (Sottocornola et al., 2010). These Balb/c mutant mice were viable, although they did develop hydrocephalus, the severity of which was comparable to that found in mixed background ASPP2 Δexon3 mice. Importantly, despite the presence of hydrocephalus, the mice did not show significant abnormalities in neural tube closure, which had been described as the main cause of lethality of ASPP2 Δexon3 mixed background mice. For this reason, ASPP2 Δexon3 mice in a Balb/c background

were able to survive for up to four months after weaning (Sottocornola et al., 2010). Various studies performed in ASPP2-null and heterozygous mice in the Balb/c background have shown that ASPP2 is at the crossroad of important biological events such as tumorigenesis, cell polarity, and inflammation. For instance, ASPP2 behaves as a haplo-insufficient tumor suppressor *in vivo* (Vives et al., 2006b), and has been identified to be an important regulator in controlling neuronal cell differentiation and cell polarity (Sottocornola et al., 2010). Moreover, *in vitro*, the interaction between ASPP2 and NF-κB suggests that ASPP2 may be the link between inflammation and apoptosis (Yang et al., 1999b).

The maintenance of intestinal homeostasis is dependent on the alliance of signalling pathways involved in cell polarity, tumorigenesis and inflammation. In the intestine, the rapid turnover of epithelial cells results from a well coordinated balance between cell proliferation and cell death (Potten et al., 1997). In addition, the migratory movement of intestinal epithelial cells towards the lumen forces post-mitotic cells to differentiate (van der Flier and Clevers, 2009). Importantly, the polarization of intestinal epithelial cells is a determinant of appropriate cell turnover, and also ensures the accurate traffic and secretion of substances that will contribute to several biological intestinal functions (Matter and Mellman, 1994).

To better understand whether ASPP2 is an important regulator of intestinal homeostasis, we used *ASPP2* Δexon3 mice ($ASPP2^{\Delta 3/\Delta 3}$) in a Balb/c background to analyze the duodenal region of the small intestine, as well as the colon. The morphology of the epithelium, and biological events such as cell proliferation, differentiation and death were studied in detail, to determine whether there were noticeable differences between WT ($ASPP2^{+/+}$) and $ASPP2^{\Delta 3/\Delta 3}$ mice.

3.2 – RESULTS

3.2.1 – ASPP2 IS LOCATED AT THE EPITHELIAL TIGHT JUNCTIONS IN BOTH THE DUODENUM AND COLON

In the intestine, epithelial cell polarity is at the crossroads of important processes occurring in the epithelium. Firstly, the efficiency of cell polarity mechanisms is highly dependent on an accurate synchronization between proliferation and cell death. In fact, an accumulation of cells in the crypts and along the villi, or excessive cell death, can compromise the epithelial cell-cell contacts and the overall intestinal architecture (Watson et al., 2009). Secondly, an impaired differentiation process may result in defective secretory and absorptive cell lineages. Importantly, cell polarity mechanisms are involved in transport and secretion within intestinal epithelial cells, and hence play a crucial role in the homeostasis of the tissue (Matter and Mellman, 1994). Finally, and equally importantly, epithelial cell polarity plays an important role as a barrier against pathogens and components of the apical junctional complex are vulnerable targets of various bacteria in the intestine (Berkes et al., 2003).

In previous studies, ASPP2 was found to be involved in mechanisms of cell polarity by binding to Par3. In the neuroepithelium, ASPP2's colocalization with Par3 in the apical region of epithelial cells controls the integrity of the tight junctions (Sottocornola et al., 2010). In addition, a recent report has shown that ASPP2 binds to, and is targeted for degradation by, *Helicobacter pylori in vitro*, suggesting that ASPP2 might play a role in cell polarity in the gastric glands (Buti et al., 2011). In order to investigate the location of ASPP2 in the intestinal epithelium, sections of

duodenum and colon were analyzed by immunofluorescence. ASPP2 was found to be located at the cell-cell contacts of intestinal epithelial cells. In particular, ASPP2 was found to be apically expressed along the villi in duodenal and colonic crypts (Figures 3.1A and 3.2A). In both the duodenum and colon, the localization of ASPP2 and ZO-1, a known tight junction component, was found to be very similar. Both proteins were expressed at the apical region of intestinal epithelial cells (Figures 3.1B and 3.2B). The specific dot-like staining of ASPP2, and its co-localization with ZO-1, supports the hypothesis that ASPP2 is expressed at the level of the tight junctions in intestinal epithelial cells. In addition, we co-stained ASPP2 and β-catenin in the duodenal and colonic epithelium and observed that ASPP2 was found to be localized apically in relation to β-catenin, and therefore did not colocalize with this adherens junction component (Figure 3.1C and 3.1C). Finally, we performed double staining of ASPP2 and Villin, a well characterized brush border marker. In the duodenum, ASPP2 was found to partially colocalize with villin, denoting the apical location of ASPP2 at the level of the tight junctions (Figure 3.1D).

Our findings revealed that in the intestinal epithelium, ASPP2 is localized at the tight junctions with ZO-1. These observations suggest that, besides the neuroepithelium, the intestinal epithelium is another *in vivo* model where ASPP2 is enriched at the level of tight junctions. It is likely that ASPP2 plays an important role in the maintenance of epithelial integrity. Therefore, we further investigated the morphology of the intestinal epithelium in *ASPP2* Δexon3 mice.

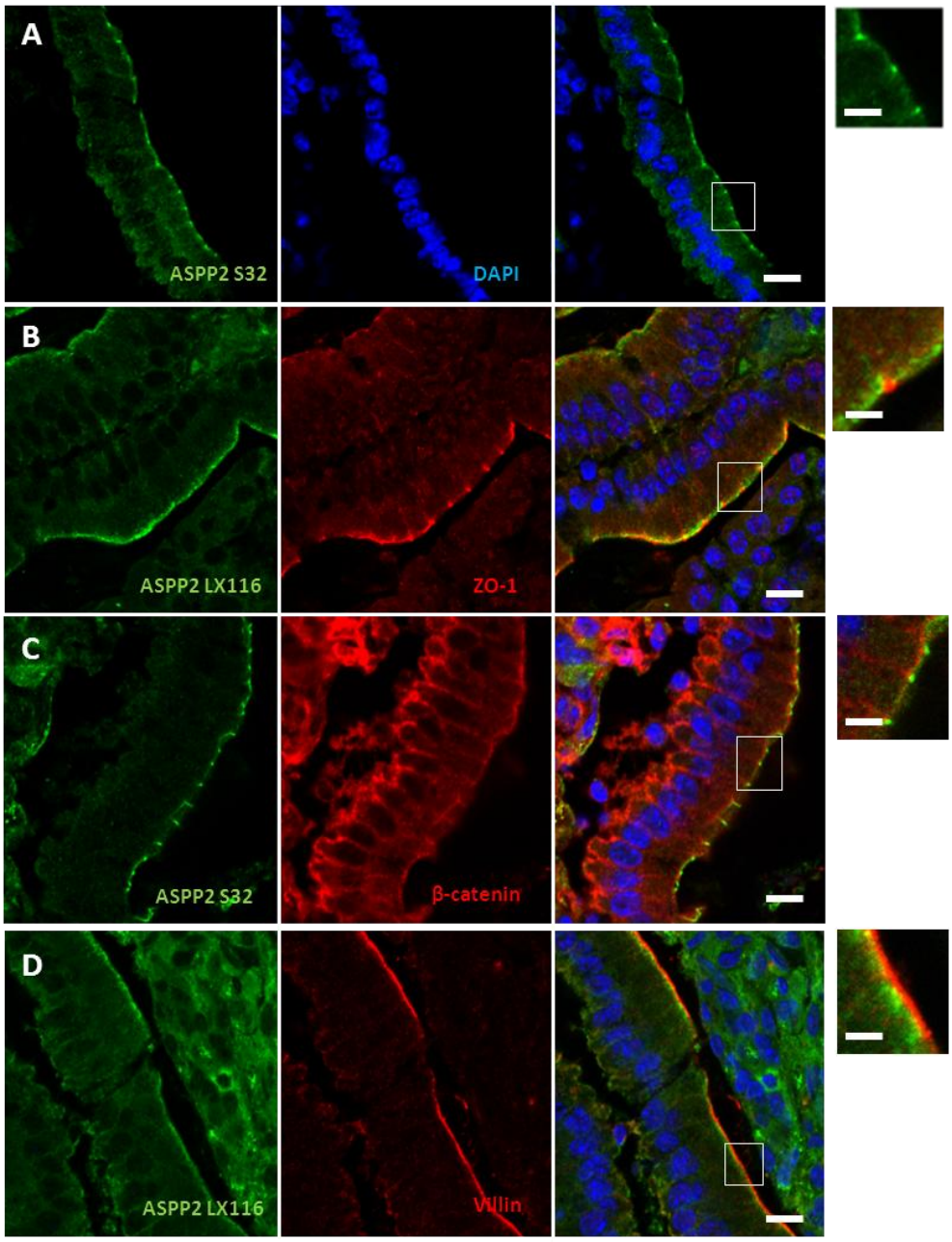


FIGURE 3.1 – In the duodenum, ASPP2 colocalizes with components of the Apical Polarity Complex. Immunofluorescence staining on frozen sections of WT ASPP2 mouse duodenum. Squares show a high magnification view of regions where ASPP2 is expressed. **(A)** ASPP2 (green) immunofluorescence. **(B)** ASPP2 (green) and ZO-1 (red) double immunofluorescence. **(C)** ASPP2 (green) and β-catenin (red) double immunofluorescence. **(D)** ASPP2 (green) and Villin (red) immunofluorescence. Nuclei are counterstained with DAPI. Scale bars – 50µm, 15µm.

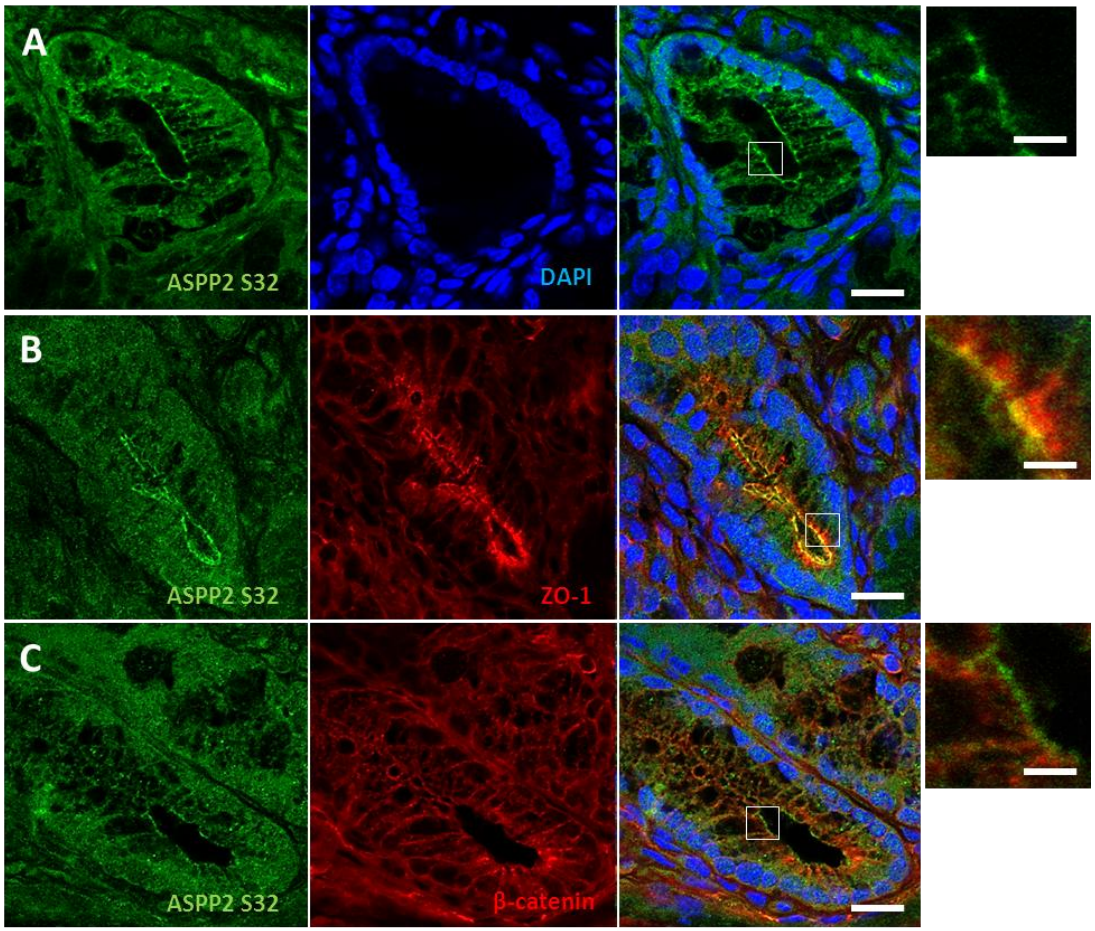


FIGURE 3.2 – In the colon, ASPP2 colocalizes with components of the Apical Polarity Complex. Immunofluorescence staining on frozen sections of WT ASPP2 mouse colon. Squares show a high magnification view of regions where ASPP2 is expressed. **(A)** ASPP2 (green) immunofluorescence. **(B)** ASPP2 (green) and ZO-1 (red) double immunofluorescence. **(C)** ASPP2 (green) and β-catenin (red) double immunofluorescence. Nuclei are counterstained with DAPI. Scale bars – 50µm, 15µm.

3.2.2 – ASPP2 DEFICIENCY LEADS TO CELL DISORGANIZATION AND SHORTENING OF CRYPT STRUCTURES.

The discovery that ASPP2 was involved in the maintenance of cell polarity in the central nervous system brought to light the possibility that ASPP2 has a similar function in tissues that are highly dependent on cell polarization (Sottocornola et al., 2010). In the intestine, epithelial cell polarity is essential to ensure the homeostatic balance in intestine. Defects in cell polarity components, such as claudins and JAM-A, have been shown to greatly compromise the organization of intestinal epithelial cells *in vivo*. The morphological disruption was found to result in epithelial barrier defects that ultimately affect intestinal permeability and cell turnover (Laukoetter et al., 2007; Tamura et al., 2008). In order to determine the biological consequences of ASPP2 deficiency in the intestinal epithelium, the potential existence of morphological abnormalities in the duodenal and colonic epithelium of $ASPP2^{+/+}$ and $ASPP2^{\Delta 3/\Delta 3}$ mice was investigated.

A macroscopic analysis of the length and diameter of both the duodenum and colon did not reveal any significant difference between $ASPP2^{+/+}$ and ASPP2 exon3 deleted mice. However, a more detailed examination of the histology of the duodenum and colon revealed abnormalities in the intestinal epithelium of $ASPP2^{\Delta 3/\Delta 3}$ mice. Overall, the duodenal epithelium of ASPP2-null mice showed significant cell disorganization, which ultimately resulted in general epithelial damage. In $ASPP2^{\Delta 3/\Delta 3}$ duodenums, villi were small and enlarged and revealed cell disorganization, most likely due to the existence of multiple layers of absorptive cells along the villi (Figure 3.3A). A closer look at the proliferative compartment revealed that $ASPP2^{\Delta 3/\Delta 3}$ duodenal crypts were slightly bigger (88.9±11.0) than in

the ASPP2$^{+/+}$ mice (79.5±10.4), but this difference was not significant (p>0,05) (Figure 3.3B). Similarly to that observed in the duodenum, the histological analysis of ASPP2$^{\Delta 3/\Delta 3}$ colonic epithelium revealed morphological abnormalities (Figure 3.4A). In particular, the colonic crypts in ASPP2-deficient mice were significantly smaller (155.7±26.0 vs. 287.8±48.7; p<0,001) (Figure 3.4B). The reduction in the size of the crypt seemed to have affected the number of goblet cells, since the analysis of ASPP2$^{\Delta 3/\Delta 3}$ colonic crypts by H&E showed a reduced number of goblet cells in this epithelium (Figure 3.4A).

Our findings suggest that ASPP2's localization at tight junctions is important for the integrity of the epithelial tissue, since its deficiency results in overall cell disorganization. Furthermore, it is likely that ASPP2's expression contribute to the proper coordination of cell proliferation and differentiation, as ASPP2 deletion compromizes the size of crypt and villi structures in the colon and duodenum.

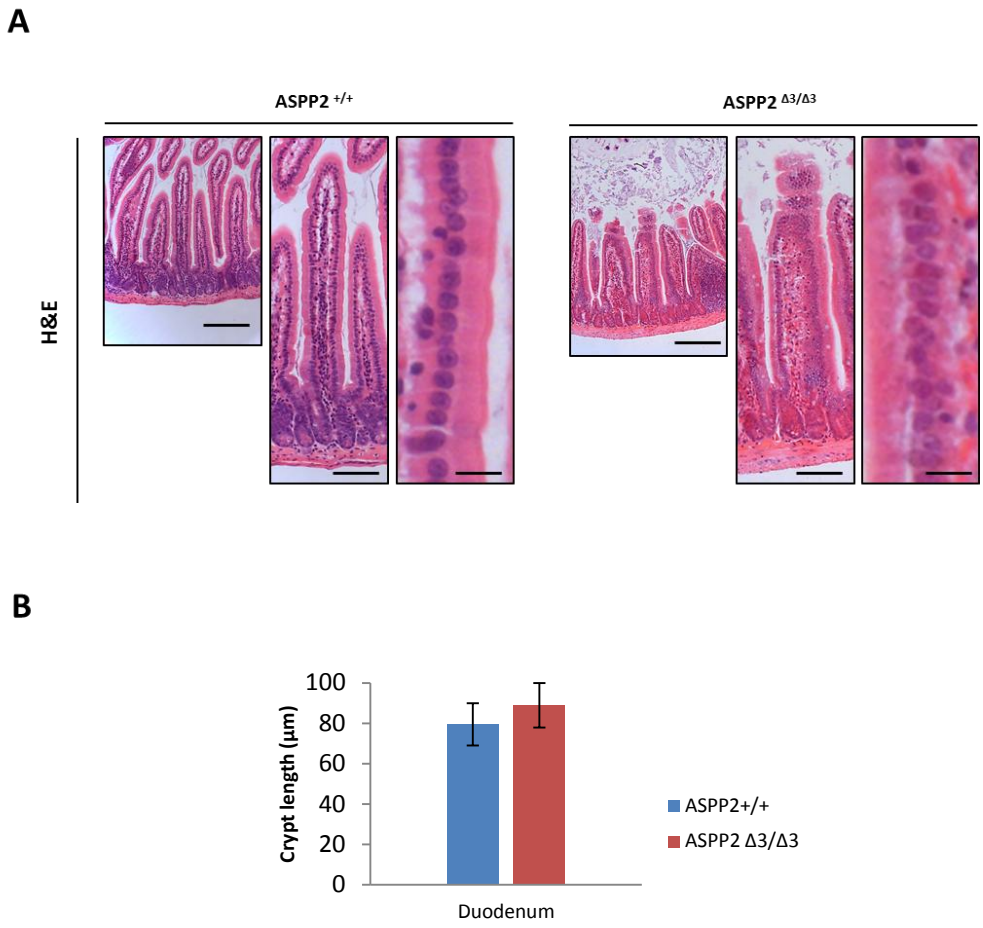


FIGURE 3.3 - ASPP2 deficiency leads to epithelial cell disorganization in the duodenum. (A) Hematoxylin and Eosin (H&E) staining on mouse sections of WT and ASPP2$^{\Delta3/\Delta3}$ duodenal epithelium. Higher magnification figures are shown as evidence of the morphological differences between WT and ASPP2$^{\Delta3/\Delta3}$ epithelia. **(B)** Graphic representation of the crypt length in WT and ASPP2$^{\Delta3/\Delta3}$ duodenum. Scale bars - 300µm, 150µm, 30µm.

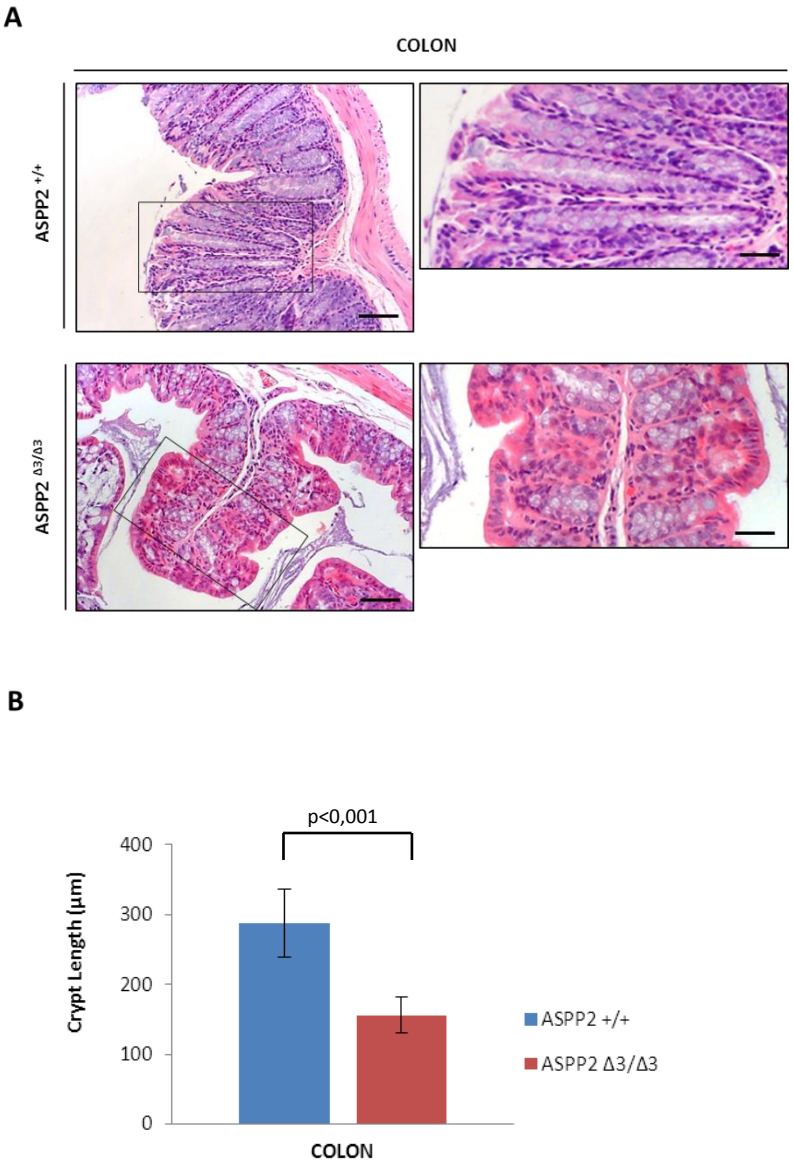


FIGURE 3.4 – Loss of ASPP2 results in shortening of the colonic crypts. (A) Hematoxylin and Eosin (H&E) staining on mouse sections of WT and ASPP2$^{\Delta 3/\Delta 3}$ colonic epithelium. An overview of crypt morphology is shown. Higher magnification figures are shown to illustrate the morphological differences between WT and ASPP2$^{\Delta 3/\Delta 3}$ colonic epithelia. Scale bars - 150µm, 50µm. **(B)** Graphic representation of crypt length in WT and ASPP2$^{\Delta 3/\Delta 3}$ colon.

3.2.3 – AN ABSENCE OF ASPP2 DISRUPTS THE EPITHELIUM IN THE COLON BUT NOT THE DUODENUM

The disruption of tight junctions in the intestinal epithelium compromises its homeostasis by increasing the vulnerability of the tissue to luminal bacteria, interfering with the processes of absorption and secretion in intestinal differentiated cells, contributing to the loss of architecture and affecting intestinal cell turnover (Marchiando et al., 2010). Several studies have claimed the importance of tight junctions in the functioning of the intestinal epithelium. For instance, the loss of JAM-A is known to cause intestinal inflammation, possibly due to an increase in intestinal permeability (Laukoetter et al., 2007). Moreover, mice lacking claudin-15 have problems in glucose absorption, show disruption in the transport of ions across the epithelium and, strikingly, possess a megaintestine, possibly due to an excess of cell proliferation (Tamura et al., 2011). In contrast, a study of occludin-deficient mice concluded that occludin did not seem to be essential for the maintenance and integrity of the intestinal epithelial barrier (Schulzke et al., 2005).

Taken together, the findings reported here suggest that the loss of cell organization is probably the result of a lack of ASPP2 at the level of the tight junctions. In addition, observations obtained from studies of the neuroepithelium of ASPP2$^{\Delta 3/\Delta 3}$ mice have revealed that ASPP2-deficient mice suffer from hydrocephalus, possibly due to the crucial role ASPP2 plays in maintaining the integrity of the neuroepithelial barrier. For these reasons, we were interested in understanding whether the overall cell disorganization observed in *ASPP2* Δexon3 mice is due to the compromised expression of cell polarity components. To address

this question, we analysed frozen sections of duodenal and colonic epithelium from ASPP2$^{+/+}$ and ASPP2$^{\Delta 3/\Delta 3}$ mice, and investigated the expression of important tight and adherens junctional proteins by immunofluorescence.

In the duodenum, a deficiency of ASPP2 does not appear to compromise the expression of the adherens junction component β-catenin, nor the expression of ezrin, a brush border marker (Figure 3.5). However, the expression of ZO-1 in the ASPP2-deficient duodenum was weaker than in the WT tissue, suggesting that ASPP2 deletion specifically disturbed the tight junctions (Figure 3.5). These findings suggest that the cellular disorganization observed in the duodenal epithelia of ASPP2$^{\Delta 3/\Delta 3}$ mice does not entirely result from an abnormal architecture in the tissue. In contrast to that observed in the duodenum, ASPP2 deficiency in the colon resulted in significant epithelial defects. The expression of E-cadherin and β-catenin was significantly disrupted in ASPP2$^{\Delta 3/\Delta 3}$ mice, possibly explaining the epithelial disorganization observed in the colon (Figure 3.6). More severely, ezrin expression in the apical domain of the colonic epithelial cells was lost in ASPP2-deficient tissue (Figure 3.6). The analysis of the duodenum and colon has shown that a lack of ASPP2 at the level of tight junctions results in severe colonic defects. In the duodenum, however, only ZO-1 was affected and no disruption of adherens junctions or the brush border was observed. For this reason, we believe that other causes may explain the disorganization observed in ASPP2-deficient duodenum. However, in the colon, the loss of ezrin and the disruption of adherens junctions might be sufficient to cause the cellular disorganization observed.

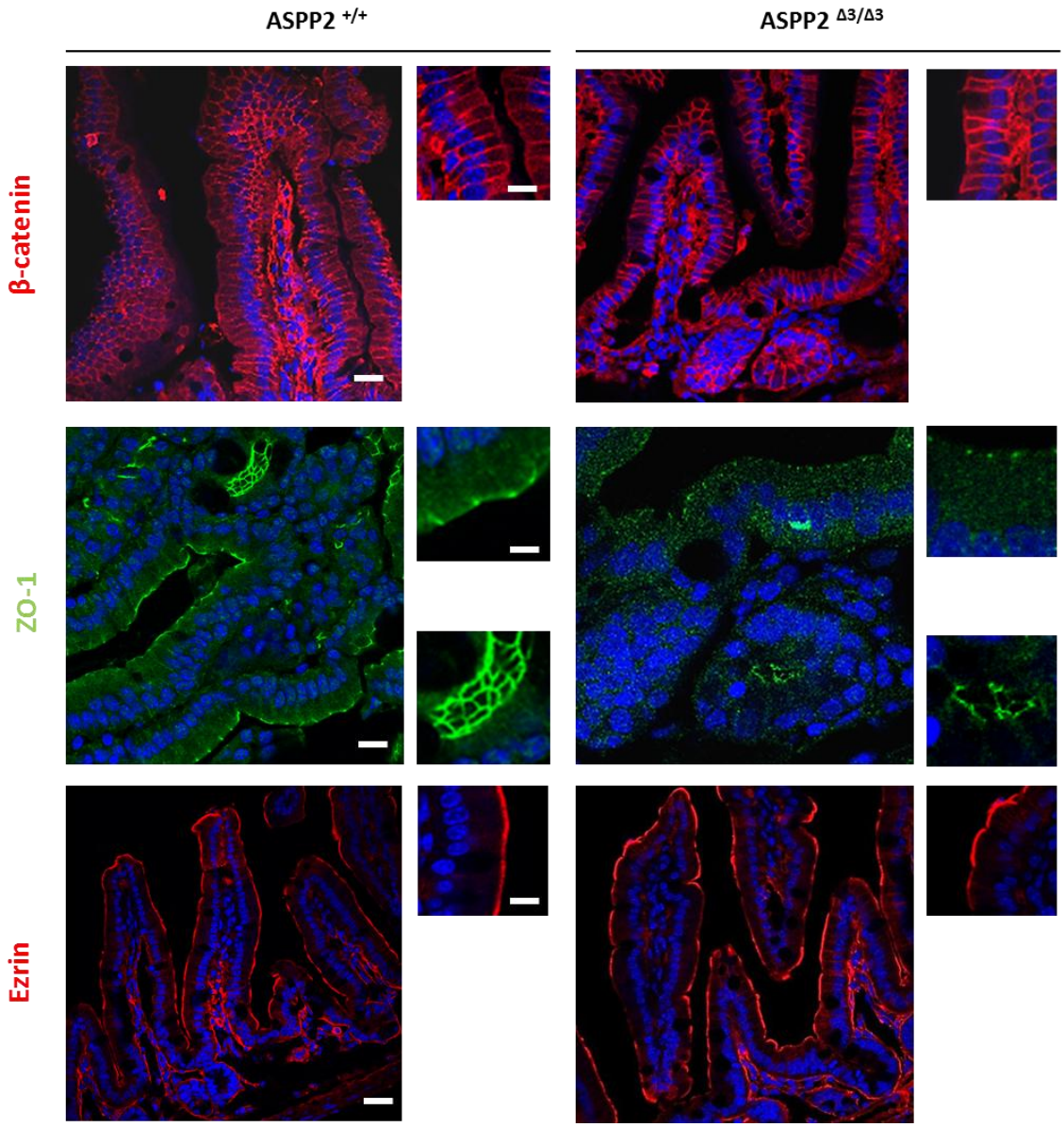


FIGURE 3.5 – ASPP2 deficiency does not affect epithelial cell polarity in the duodenum. Immunofluorescence staining of β-catenin (upper panel), ZO-1 (middle panel) and Ezrin (lower panel) on sections of WT and ASPP2$^{\Delta 3/\Delta 3}$ mouse duodenum. High magnification images are shown to illustrate detailed regions. Nuclei are counterstained with DAPI. Scale bars – 130µm, 100µm, 20µm.

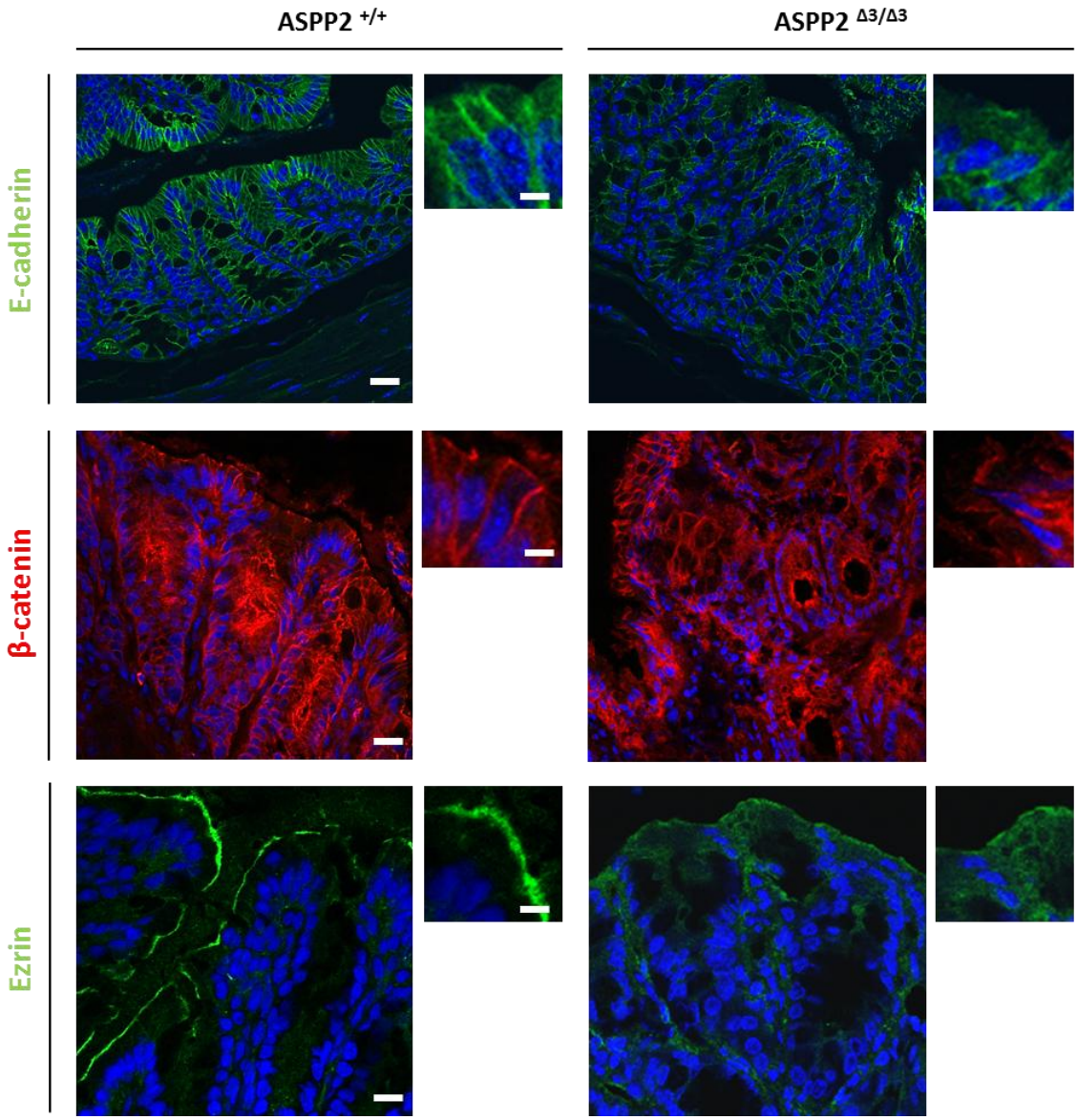


FIGURE 3.6 - ASPP2 deficiency leads to loss of cell polarity in the colonic epithelium. Immunofluorescence staining of E-cadherin (upper panel), β-catenin (middle panel) and Ezrin (lower panel) on sections of WT and ASPP2$^{\Delta 3/\Delta 3}$ mouse colon. High magnification images are shown to illustrate detailed regions. Nuclei are counterstained with DAPI. Scale bars – 130µm, 100µm, 80µm, 20µm.

3.2.4 – GOBLET CELL LINEAGE IS IMPAIRED IN ASPP2$^{\Delta 3/\Delta 3}$ INTESTINE

In addition to cell disorganization, histological H&E analysis of the ASPP2$^{\Delta 3/\Delta 3}$ colon suggested that the goblet cell lineage was altered. Goblet cells are differentiated intestinal cells that are responsible for the production and secretion of high molecular weight glycoproteins named mucins (Specian and Oliver, 1991). These large glycoproteins form a very thick gel that covers the epithelial monolayer of cells, and functions as a surface for protection against luminal pathogens, lubrication and transport between luminal substances and intestinal epithelial cells (IECs) (Deplancke and Gaskins, 2001). Remarkably, the composition of the intestinal mucus is adjustable depending on the gut microflora and the nutritional diet (Fukushima and Mukai, 1999; Montagne et al., 2004). Mucin 2 (Muc2) is considered the main component of the mucosal layer in the intestine. Mutations in this protein, or impairment in its secretion, compromise the homeostasis of the intestinal epithelium. In fact, Muc2$^{-/-}$ mice lack recognizable goblet cells and show signs of significant intestinal inflammation, being prone to spontaneously develop colitis (Van der Sluis et al., 2006).

To more specifically address the impact of ASPP2 deficiency on the maturation and function of goblet cells, Muc2 and alcian blue stainings, a histological technique frequently used to stain mucous substances, were performed. In the duodenum, the total number of goblet cells did not seem to be affected when ASPP2$^{\Delta 3/\Delta 3}$ and ASPP2$^{+/+}$ tissues were compared. However, the localization of the goblet cells along the crypt-villi axis seemed compromised (Figure 3.7A). In WT duodenum, alcian blue positive cells were observed along the villi and in the upper region of the crypts. In contrast, ASPP2$^{\Delta 3/\Delta 3}$ duodenum revealed a reduction of goblet cells along the villi

but enriched alcian blue staining was observed in the duodenal crypts, particularly in the lower part of the crypts where only mature Paneth cells are known to be localized (Figure 3.7A). The stainings performed in ASPP2$^{\Delta 3/\Delta 3}$ colonic tissue confirmed the initial H&E analysis (Figure 3.2). The size of the colonic crypts was indicative of a reduced number of goblet cells. Nevertheless, the staining of alcian blue and Muc2, performed in ASPP2$^{\Delta 3/\Delta 3}$ colon, confirmed the decrease in goblet cells, but also suggested a decrease in Muc2 production in ASPP2$^{\Delta 3/\Delta 3}$ colon (Figure 3.7B).

Taken together, these observations suggest that ASPP2 deletion compromises the number and localization of goblet cells. Interestingly, ASPP2 seems to play different roles in the duodenum and colon. In the duodenum, ASPP2 is required to ensure the proper localization of goblet cells along the villi and the upper region of the crypts, whereas in the colon it influences the size of the crypts and, therefore, the number of goblet cells within the crypt compartment. Thus, it is possible that ASPP2 is involved in the regulation of mucus production, by influencing the number of colonic goblet cells.

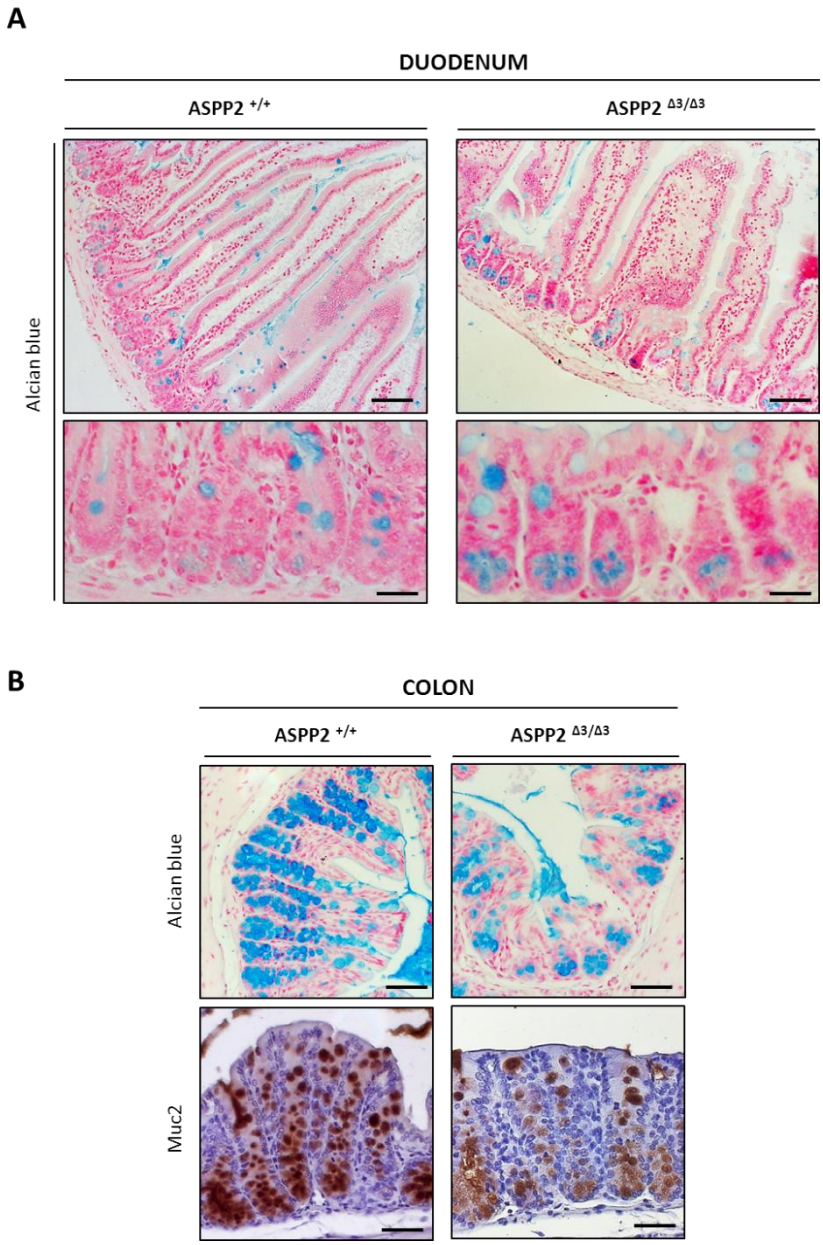


FIGURE 3.7 – ASPP2 deficiency leads to mislocalization and decrease in the number of goblet cells in the duodenum and colon, respectively. (A) Overview of the goblet cell lineage in duodenal epithelium. Alcian blue staining on paraffin sections of ASPP2$^{+/+}$ and ASPP2$^{\Delta3/\Delta3}$ mouse duodenum. Detailed images are shown to depict the presence of goblet cells in the crypt compartment. Scale bars - 150µm, 50µm. **(B)** Overview of the goblet cell lineage in colonic epithelium. *Upper panel:* Alcian blue staining on paraffin sections of ASPP2$^{+/+}$ and ASPP2$^{\Delta3/\Delta3}$ mouse colon. Scale bar - 180µm. *Lower panel:* Mucin 2 (Muc2) immunohistochemistry staining on paraffin sections of WT and ASPP2$^{\Delta3/\Delta3}$ mouse duodenum. Scale bar - 150µm.

3.2.5 – PANETH CELL NUMBER IS INCREASED IN ASPP2-DEFICIENT MICE

The intestine is characterized by two different cell lineages: the secretory cell lineage, comprised of goblet, Paneth and enteroendocrine cells; and the absorptive cell lineage, which consists of enterocytes. The work reported here shows that ASPP2 plays a role in the maturation and localization of goblet cells. In addition, in the duodenum of ASPP2$^{\Delta 3/\Delta 3}$ mice, Paneth cells were stained for alcian blue which is usually used to identify goblet cells. This finding suggests that the maturation decision between Paneth and goblet cells might be compromised, resulting in intermediate forms of differentiated cells.

Since ASPP2-deficient mice show defects in goblet cell maturation, we were interested to know whether a lack of ASPP2 compromises the maturation of secretory cells in general. To answer this question, we investigated the presence and location of Paneth cells in both ASPP2$^{+/+}$ and ASPP2$^{\Delta 3/\Delta 3}$ duodenum. In healthy individuals, Paneth cells are specialized differentiated cells usually present in the small intestine. However, abnormal localization of Paneth cells in the colon and oesophagus is triggered in some stages of chronic inflammatory disorders and tumorigenesis (Cunliffe et al., 2001; Schreiber et al., 1978). Paneth cells are important regulators in the process of secretion of antimicrobial peptides, such as lysozyme and α-defensins, which act as modulators of the host defense and play a homeostatic role in establishing and maintaining the intestinal microflora (Bevins and Salzman, 2011). Despite of this important protective role, the loss of Paneth cells *per se* is not sufficient to induce intestinal inflammation (Garabedian et al., 1997). The role of Paneth cells in the maintenance of the stem cells has also been extensively investigated, since it was found that Paneth cells are responsible for the

secretion of essential trophic factors for their neighbor stem cells (Sato et al., 2011). In fact, EGF, TGF-α and Wnt3, which are known examples of factors involved in the maintenance of cell stemness, were found to be secreted by Paneth cells in culture. Moreover, the genetic removal of Paneth cells *in vivo* results in the loss of Lgr5 stem cells, suggesting that these secretory cells provide a protective niche for the proliferative stem cells (Sato et al., 2011).

In order to identify Paneth cells in duodenal epithelia we used Tartrazine-Phloxine, a histochemical staining agent frequently used to detect Paneth cell granules. The presence of Paneth cells was confirmed in both WT and ASPP2-deficient duodenal crypts. In ASPP2$^{\Delta 3/\Delta 3}$ duodenum, however, the crypts were enriched with Paneth cell granules and misplaced tartrazine-phloxine positive granules were observed at the crypt-villi junction (*upper panel* Figure 3.8A). In order to understand whether these granules were constituents of mature Paneth cells, lysozyme staining was performed in both ASPP2$^{+/+}$ and ASPP2$^{\Delta 3/\Delta 3}$ duodenal sections (*lower panel* Figure 3.8A). The staining revealed that ASPP2$^{\Delta 3/\Delta 3}$ duodenum had lysozyme enriched crypts, as well as misplaced Paneth cells outside the proliferative compartment where they are known to be located, confirming the result obtained with Tartrazine-Phloxine staining (*lower panel* Figure 3.8A). The quantification of the number of Paneth cells in both WT and ASPP2$^{\Delta 3/\Delta 3}$ duodenums revealed that, for every 100 duodenal crypts, ASPP2-deficient tissue has a higher percentage of lysozyme positive cells than the WT (78.8±6.8 vs. 39.8±1.9; $p<0.05$)(Figure 3.8B).

Our observations suggest that ASPP2 controls the number and localisation of Paneth cells. Similarly to the results obtained from the analysis of goblet cells, analysis of ASPP2$^{\Delta 3/\Delta 3}$ duodenums revealed the existence of intermediate forms of

Paneth cells, which express lysozyme but are wrongly placed in the upper region of the crypt compartment. The enrichment of duodenal crypts with Paneth cells also suggests that an absence of ASPP2 stimulates the commitment of cells towards Paneth cell differentiation.

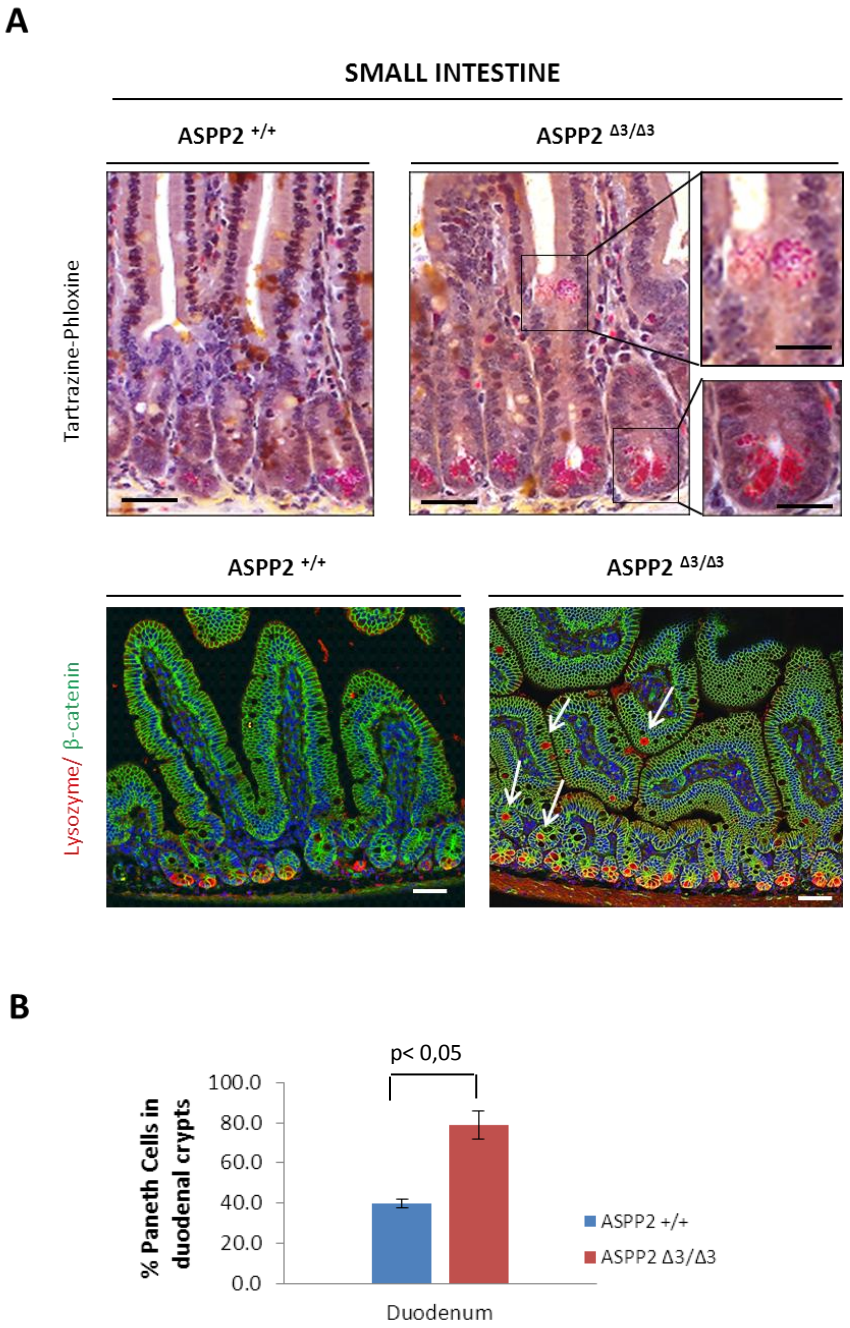


FIGURE 3.8 – Increase and mislocalization of Paneth cell abundance in ASPP2$^{\Delta3/\Delta3}$ duodenum. (A) *Upper panel:* Tartrazine-Phloxine staining of Paneth cells on paraffin sections of WT and ASPP2$^{\Delta3/\Delta3}$ mouse duodenum. High magnification figures are depicted to illustrate details of the Paneth cells. Scale bars - 100µm, 30µm. *Lower panel*: Immunofluorescence staining of lysozyme on paraffin sections of WT and ASPP2$^{\Delta3/\Delta3}$ mouse duodenum. White arrows point to the mislocalization of lysozyme staining. Scale bars - 200µm. **(B)** Graphic representation of the percentage of crypts containing Paneth cells in the duodenum of WT and ASPP2$^{\Delta3/\Delta3}$ mice.

3.2.6 – ASPP2 DEFICIENCY DOES NOT AFFECT ENTEROENDOCRINE AND ABSORPTIVE CELL LINEAGES

The findings obtained from histological analyses of the duodenum and colon of ASPP2$^{\Delta 3/\Delta 3}$ mice suggests that ASPP2 is involved in the maturation of goblet and Paneth cells. The intestinal secretory cell lineage also comprises the terminally differentiated enteroendocrine cells, which are found at a very low frequency in the intestinal mucosa. Enteroendocrine cells regulate intestinal function through the production of specific hormones, such as secretin and serotonin (van der Flier and Clevers, 2009). Neurogenin 3 (Ngn3) is required for the specification of this cell lineage and, for this reason, ngn3-deficient mice fail to specifically generate an enteroendocrine cell lineage, not only in the small intestine, but also in the pancreas (Jenny et al., 2002).

Taken together, the observations reported here suggest that the goblet cells and Paneth cells are compromized. However, we do not know whether this morphological abnormality applies to the enteroendocrine cell lineage. Therefore, to further understand whether ASPP2 deficiency affects the maturation of intestinal cells into secretory cells, we investigated whether the enteroendocrine cell population was disrupted. The expression of chromogranin A, a known marker of enteroendocrine cells, was analyzed in duodenal sections from ASPP2$^{+/+}$ and ASPP2$^{\Delta 3/\Delta 3}$ mice. Enteroendocrine cells represented less than 1% of the total number of differentiated cells in the intestinal epithelium. Therefore, as expected, only a few chromogranin A-positive cells were observed along the ASPP2$^{+/+}$ villi. The number of chromogranin A-positive enteroendocrine cells in ASPP2$^{\Delta 3/\Delta 3}$ duodenum

was comparable to that found in WT tissue, suggesting that this cell population was not affected by ASPP2 deficiency (Figure 3.9A).

In addition to the differentiated secretory cells, the intestinal epithelium is also characterized by the existence of absorptive cells known as enterocytes. These highly polarized columnar cells play an important role in the absorption and transport of nutrients across the epithelium (van der Flier and Clevers, 2009). In the ASPP2-deficient mouse, the intestinal secretory cell lineage was partially compromised with abnormalities in the goblet and Paneth cell population, but not in the enteroendocrine cell population. In order to clarify whether a lack of ASPP2 would also affect the absorptive cell lineage, the expression of alkaline phosphatase, a known brush border marker of enterocytes, was investigated. Alkaline phosphatase was observed at the apical surface of absorptive cells, in both WT and mutant intestine. Moreover, in the WT duodenum, alkaline phosphatase was also expressed at the basolateral region of the enterocytes (Figure 3.9B). Overall, there was no significant difference in the staining of alkaline phosphatase on WT and ASPP2-deficient duodenal tissue, suggesting that ASPP2 deficiency does not affect the commitment of cells to the absorptive lineage.

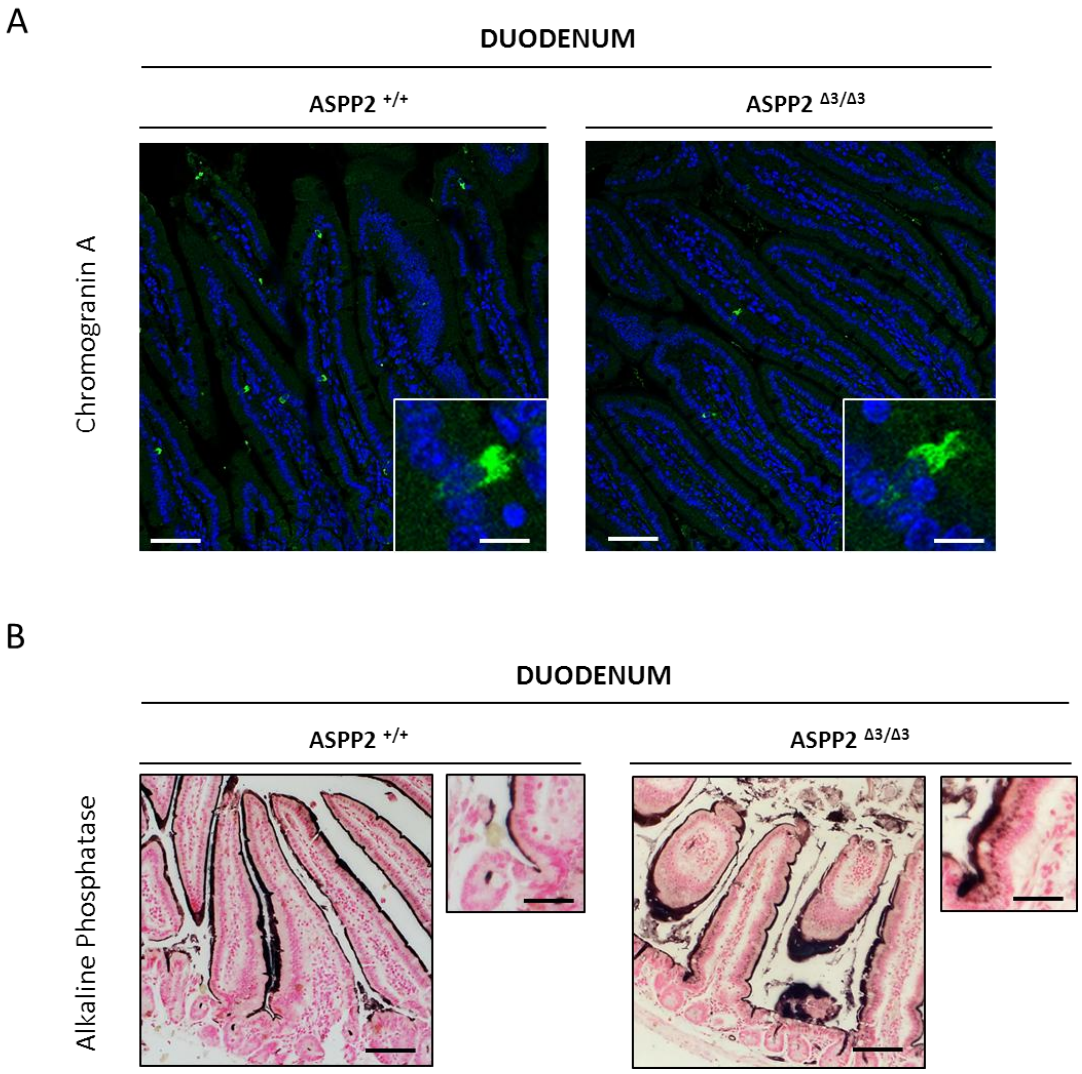


FIGURE 3.9 – Loss of ASPP2 does not compromise the enteroendocrine and absorptive cell populations. (A) Immunofluorescence staining of chromogranin A on sections of WT and ASPP2$^{\Delta 3/\Delta 3}$ mouse duodenum. Higher magnification images are shown to illustrate details of chromogranin A staining. Scale bars - 150µm, 15µm. **(B)** Alkaline phosphatase staining on sections of WT and ASPP2$^{\Delta 3/\Delta 3}$ mouse duodenum. Higher magnification figures are depicted to illustrate details of the alkaline phosphatase staining. Scale bars - 200µm, 130µm.

3.2.7 – NOTCH TARGET GENE HES5 IS UPREGULATED IN ASPP2$^{\Delta 3/\Delta 3}$ DUODENUM

In the intestine, the Notch signaling pathway plays an important role in the self-renewal of stem cells, cell fate determination of progenitor cells, and terminal differentiation of proliferating cells (Fre et al., 2005). Various *in vivo* studies have shown that Notch signaling promotes the commitment of the cells towards an absorptive phenotype. Indeed, the combined deletion of Notch1 and Notch2, inhibition of RBPJk, and pharmacological inhibition of γ-secretase, all lead to loss of cell proliferation, premature cell differentiation and an excessive generation of secretory cells (Riccio et al., 2008; van Es et al., 2005). Similarly, depletion of *Hes1*, a known Notch target gene, results in an excess of secretory cells *in vivo*, possibly at the expense of absorptive cells (Jensen et al., 2000; Suzuki et al., 2005). In addition, *Math1*-deficient mice lack goblet, Paneth and enteroendocrine cells but their absorptive cell lineage is not affected (Yang et al., 2001).

Previous studies have revealed that the expansion of the neural progenitor cell pool is associated with the deregulation of some Notch target genes, such as *Hes1* and *Hes5*, in ASPP2$^{\Delta 3/\Delta 3}$ brains (R. Sottocornola, personal communication). In addition, *in vitro* studies performed in our lab have shown that ASPP2 can bind to MAML-1 and RBP-jκ, the two main components of the Notch transcriptional machinery (L. Tordella, personal communication). Taken together, it appears that ASPP2 can modulate the Notch signaling pathway *in vivo* and *in vitro*, and can therefore play a role in the commitment of cell differentiation towards a specific cell lineage in the intestine. ASPP2-deficient mice show an increase in the number of Paneth cells, and mislocalization of both goblet and Paneth cells in the duodenum. Importantly, the Hes1/Hes3/Hes5 conditional knockout possesses

misplaced Paneth cells, similarly to ASPP2 Δexon3 mice, suggesting that the Notch signaling pathway might be compromised in ASPP2-null mice (Ueo et al., 2012). Taking this into account, we were interested to understand whether Notch signaling was impaired in the duodenum of ASPP2-deficient mice. To address this question, the protein and mRNA levels of Notch target genes such as Hes1 and Hes5, which are known to determine the specification of the cell lineage phenotype, were analyzed (Fre et al., 2005). In addition, we investigated Math1, which is a well characterized cell fate modulator in the gut and a determinant in cells committing to a secretory phenotype (Yang et al., 2001).

We performed a western blot with lysates of $ASPP2^{+/+}$ and $ASPP2^{\Delta3/\Delta3}$ mouse duodenum. Hes5 and Math1 protein levels were upregulated in $ASPP2^{\Delta3/\Delta3}$ duodenum, whereas Hes1 was slightly increased in the $ASPP2^{\Delta3/\Delta3}$ sample and a second, upper band was noticed (Figure 3.10A). Previous works have shown that Hes1 and Hes5 are mainly expressed in the proliferative compartment of the intestinal crypts (Schroder and Gossler, 2002). In order to accurately quantify the mRNA levels of *Hes1* and *Hes5,* we obtained an enriched duodenal crypt fraction by isolating crypt cells from the dissected intestinal tissue (Sato, 2009). An upregulation of *Hes1* transcripts was observed in the $ASPP2^{\Delta3/\Delta3}$-enriched crypt fraction (1.81±0.60) in comparison with the $ASPP2^{+/+}$ sample (1.00±0.36) ($p>0,05$). In addition, significant upregulation of the *Hes5* transcript was observed in the $ASPP2^{\Delta3/\Delta3}$ fraction (2.87±0.78), when compared with the $ASPP2^{+/+}$ sample (1.00±0.28) ($p<0,05$) (Figure 3.10B).

Our results show that the Notch signaling targets *Hes1* and *Hes5* are upregulated in the duodenum of $ASPP2^{\Delta3/\Delta3}$ mice. The activation of Hes5 in $ASPP2^{\Delta3/\Delta3}$

duodenum suggests that the commitment of cells to differentiate into secretory cells is stimulated. This observation is supported by the finding that Math1 is similarly upregulated in ASPP2$^{\Delta 3/\Delta 3}$ duodenum. However, the relative upregulation of Hes1 demonstrates that the stimulation of the secretory lineage does not happen at the expenses of the absorptive lineage.

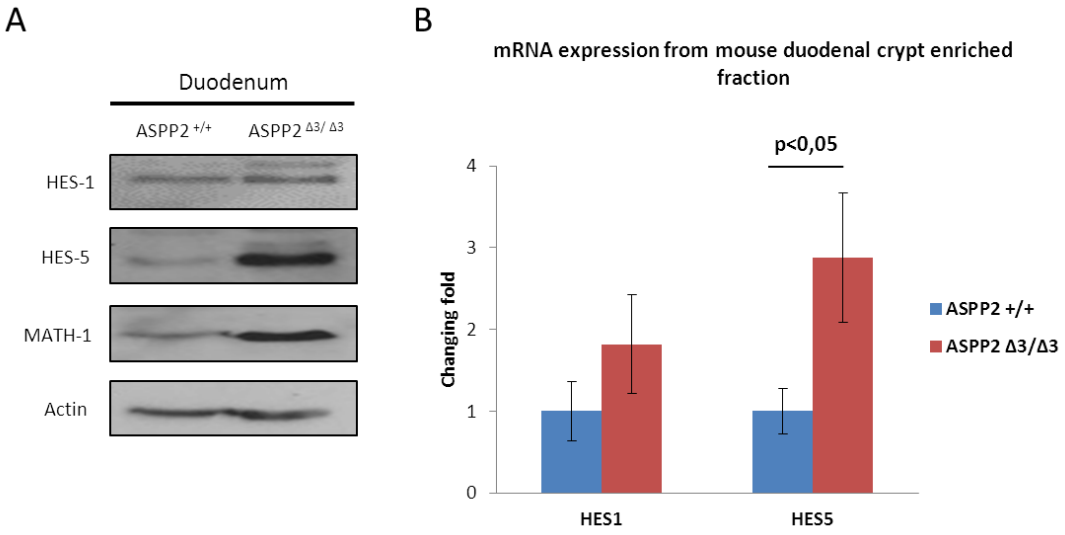


FIGURE 3.10 – Hes5 is stimulated upon ASPP2 deficiency in the duodenum. (A) Western blots on lysates prepared from WT and ASPP2$^{\Delta 3/\Delta 3}$ duodenal tissue. The expression of HES-1, HES-5 and MATH1 was studied by loading 80µg of protein, and using actin as a loading control. **(B)** Relative expression of HES-5 and HES-1 mRNA by quantitative RT-PCR in murine crypt cells.

3.2.8 – ASPP2 DEFICIENCY RESULTS IN INCREASED PROLIFERATION OF THE INTESTINAL EPITHELIUM *IN VIVO*

The simultaneous upregulation of Hes5, and to a less extent Hes1, observed in ASPP2$^{\Delta 3/\Delta 3}$ duodenum suggests that other factors repress the Notch lateral inhibition mechanism in this tissue, favoring both the absorptive and secretory cell lineages. It has become widely accepted that crosstalk between Notch and Wnt is required for continuous cell proliferation and commitment to differentiation. Differentiation takes place in some cells when Notch signaling is switched off and Math1 is upregulated (Nakamura et al., 2007). In this case, Wnt signals may still be required since complete impairment of the Wnt cascade blocks the generation of secretory cells (Pinto et al., 2003). However, if Wnt signals are lost in proliferating cells, differentiation towards the absorptive lineage occurs. A fine balance between proliferation and differentiation is, therefore, crucial to ensure the continuous renewal of the intestinal tissue. Deregulation of one of these processes compromises the epithelial architecture and, subsequently, the homeostasis of the intestinal epithelium. In order to further characterize the intestinal phenotype presented by ASPP2$^{\Delta 3/\Delta 3}$, we investigated whether cell proliferation in the duodenum and colon is deregulated.

ASPP2 has been extensively characterized as a tumor suppressor, by enhancing the apoptotic activity of p53. The loss of one allele in ASPP2 heterozygous mice is sufficient to induce the spontaneous development of tumors. However, these tumors have been found to be located in the head and neck region (Luca Tordella, personal communication, 2012) (Vives et al., 2006b). The histological analysis of ASPP2$^{\Delta 3/\Delta 3}$ intestinal epithelium did not reveal the presence of tumors or dysplasias.

Nevertheless, it is likely that the absence of ASPP2 compromizes the proliferation rate of intestinal epithelial cells. In fact, it has been shown that, in the central nervous system, ASPP2 inhibits neural progenitor proliferation leading to deregulated neuroepithelial growth (Sottocornola et al., 2010).

$ASPP2^{\Delta 3/\Delta 3}$ intestinal proliferation was assessed by performing immunofluorescence staining of Ki67 and phospho-Histone 3 (pH3). In $ASPP2^{+/+}$ mice, duodenal Ki-67 positive cells were localized below the crypt-villi transition, whereas the lower region of the crypt contained Ki-67 positive cells in the colon (Figure 3.11). A significant difference was observed in the $ASPP2^{\Delta 3/\Delta 3}$ duodenum. In this tissue, not only were the crypts enriched with proliferative Ki-67- positive cells, but Ki-67- positive cells were also observed in the villi, immediately above the crypt-villi transition. In $ASPP2^{\Delta 3/\Delta 3}$ colons, Ki-67 positive cells occupied half of the crypt compartment (Figure 3.11). The proportion of cells in mitosis, stained with an anti-pH3 antibody, was found to be higher in $ASPP2^{\Delta 3/\Delta 3}$ duodenum and colon (Figure 3.12). In fact, in contrast with that observed in $ASPP2^{+/+}$ tissue, an accumulation of pH3 immunofluorescence staining was observed in $ASPP2^{\Delta 3/\Delta 3}$ duodenal crypts, suggesting that each ASPP2-deficient crypt had more cells undergoing mitosis than $ASPP2^{+/+}$ crypts (Figure 3.12). A similar difference in the number of pH3-positive cells was observed between the $ASPP2^{+/+}$ and ASPP2-deficient colon. Taken together, these observations suggest that ASPP2 inhibits cell proliferation in duodenal and colonic epithelium.

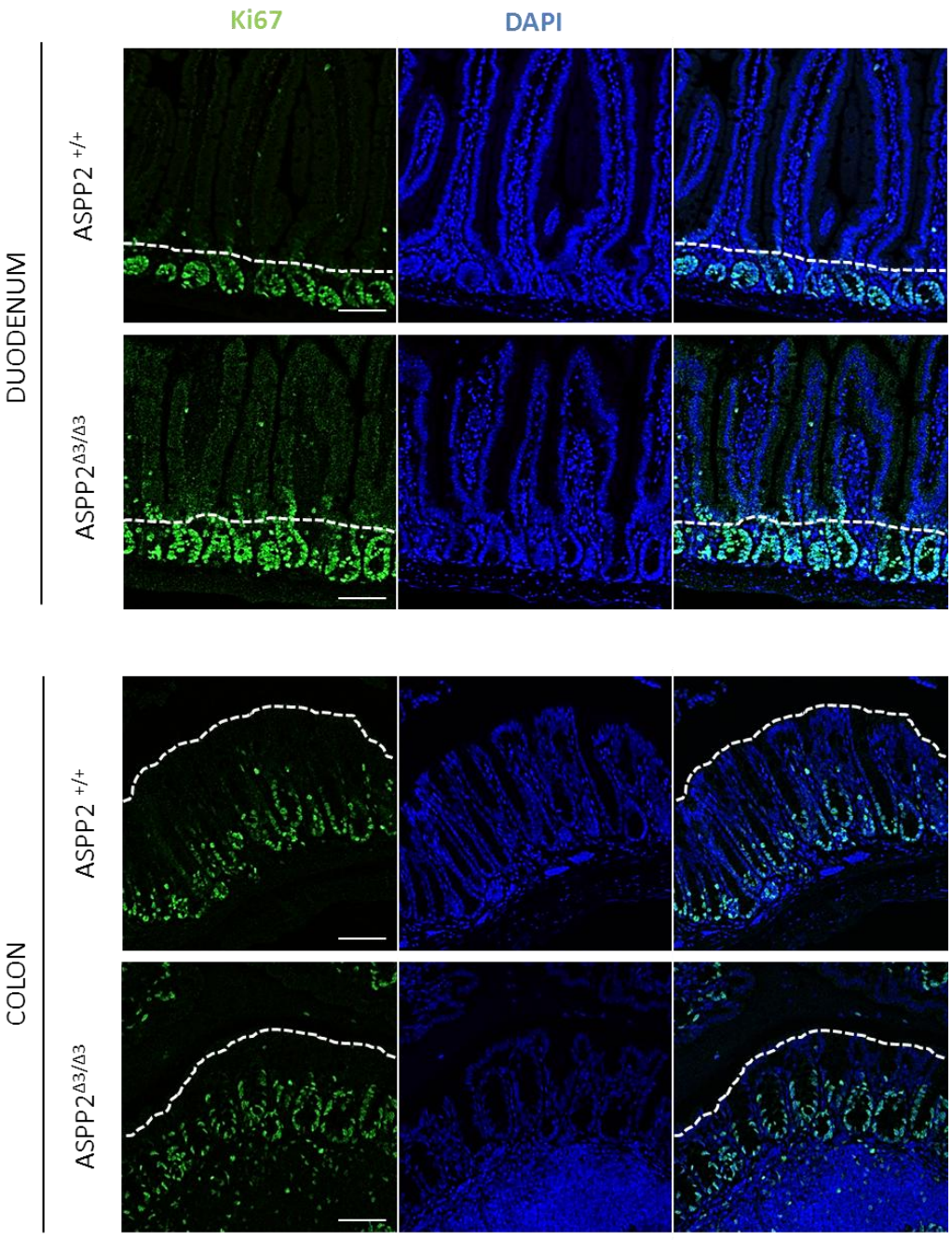


FIGURE 3.11 – Loss of ASPP2 promotes cell proliferation *in vivo*. Immunofluorescence staining of paraffin sections of WT and ASPP2$^{\Delta 3/\Delta 3}$ duodenum and colon. *Upper canvas*: Ki67 (green) immunofluorescence on duodenal sections of WT and ASPP2$^{\Delta 3/\Delta 3}$ mice. White lines establish the transition between the duodenal crypt and villi. *Lower canvas*: Ki67 (green) immunofluorescence on colon sections of WT and ASPP2$^{\Delta 3/\Delta 3}$ mice. White lines establish the apical surface of colonic crypts. Nuclei are counterstained with DAPI. Scale bars – 150µm.

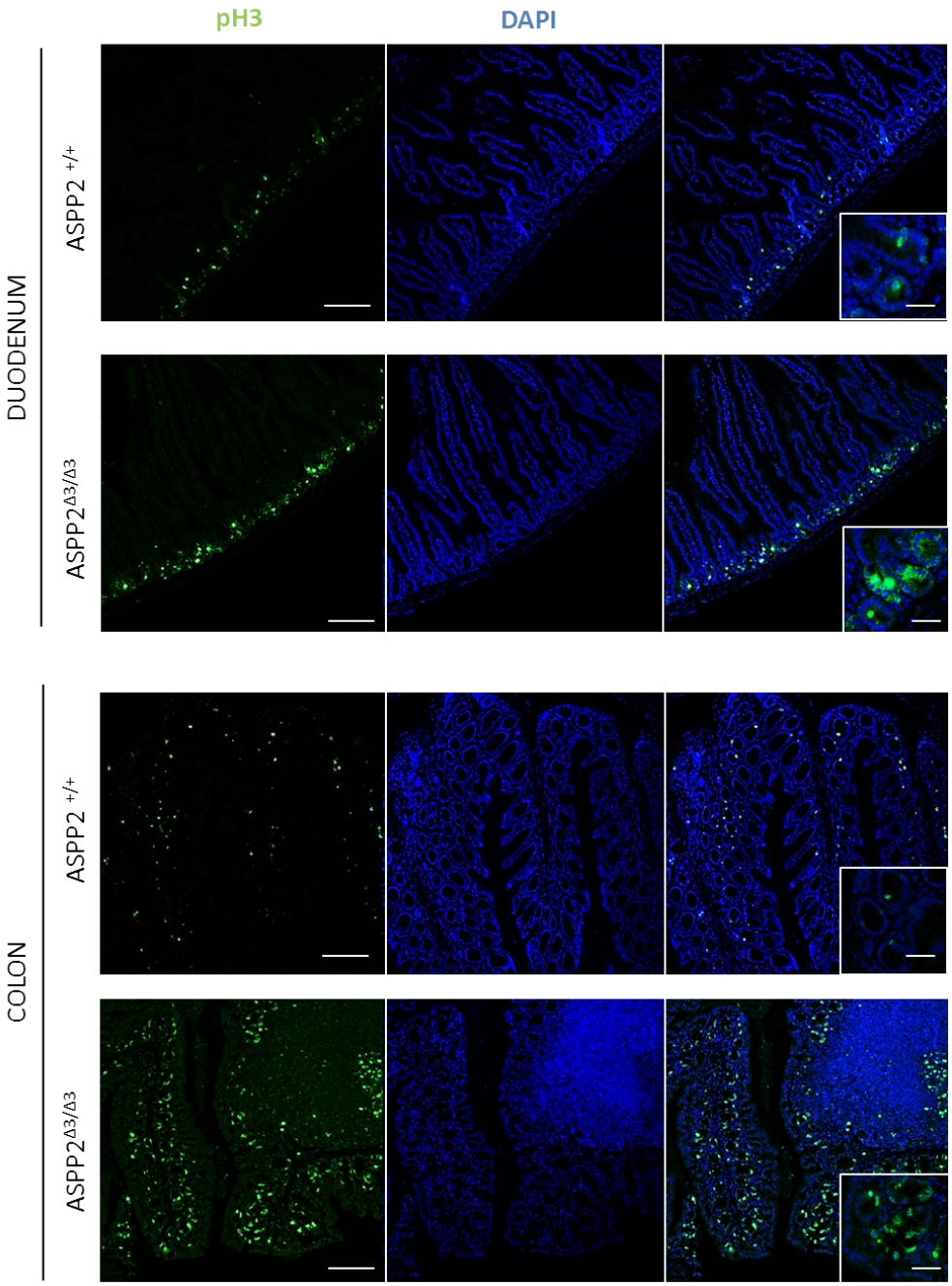


FIGURE 3.12 - Loss of ASPP2 results in an increase of cells undergoing mitosis *in vivo*. Immunofluorescence staining of pH3 on paraffin sections of WT and ASPP2$^{\Delta 3/\Delta 3}$ duodenum and colon. Squares show a high magnification view of pH3 staining. *Upper canvas*: phosphor-histone 3 (pH3) (green) immunofluorescence on duodenal sections of WT and ASPP2$^{\Delta 3/\Delta 3}$ mice. *Lower canvas*: phosphor-histone 3 (pH3) (green) immunofluorescence on colon sections of WT and ASPP2$^{\Delta 3/\Delta 3}$ mice. Nuclei are counterstained with DAPI. Scale bars – 200µm, 150µm.

In order to confirm the significant difference in the number of pH3 positive cells between WT and ASPP2-deficient intestinal epithelia, the mitotic index for both the duodenum and colon was determined (Figure 3.13). For every crypt where pH3 staining was observed, the total number of crypt cells was counted. In both tissues, the mitotic index was significantly higher in ASPP2$^{\Delta 3/\Delta 3}$ mice, when compared to ASPP2$^{+/+}$ littermates (in duodenum: 9.6±2.64 vs. 5.7±2.21 and p<0,001; in colon: 12.9±2.81 vs. 8.5±3.97 and p<0.05). This result confirmed our previous observations, which suggested that the ASPP2$^{\Delta 3/\Delta 3}$ intestine had more cells undergoing mitosis (Figure 3.13). Our findings revealed that, in addition to an upregulation of Notch signaling, cell proliferation is also stimulated, most likely due to active Wnt signaling.

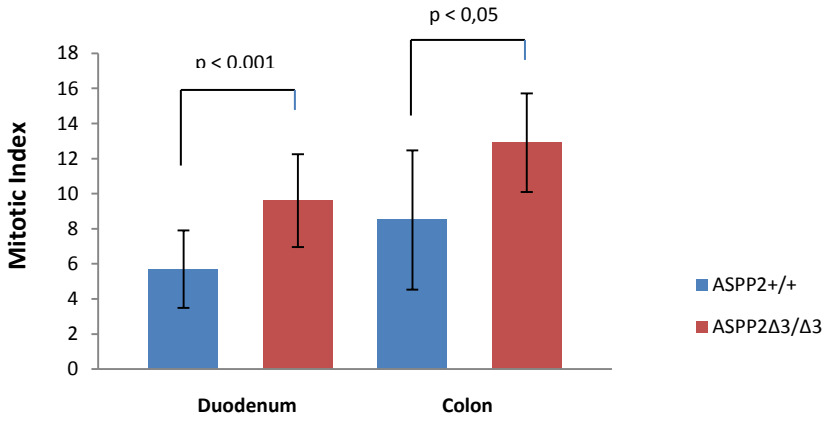


FIGURE 3.13 – Increased mitotic index in the duodenum and colon from ASPP2$^{\Delta 3/\Delta 3}$ mice. Graphic representation of the mitotic index defined as the ratio of phospho-Histone3 (pH3)-positive cells to total cell number in the intestinal epithelium, duodenum or colon (n=3).

3.2.9 – ASPP2 DEFICIENCY PROMOTES THE PROLIFERATION OF *EX VIVO* INTESTINAL ORGANOID CULTURES

Recently, a robust long-term culture system was established to realistically mimic what is observed in the intestinal epithelium (Sato et al., 2009). In this system, the crypt villus physiology is maintained, thus processes such as multi-lineage differentiation and proliferation can be studied in detail and in real time. A crypt organoid generated from small intestinal crypts is characterized by a central lumen lined by an epithelial layer, similar to that observed in the villi, and surrounded by several crypt-like structures (Sato et al., 2009).

Following on from the *in vivo* observations outlined above, suggesting that ASPP2 deficiency promotes cell proliferation in the duodenum, we were interested to understand whether the generation of organoids using ASPP2$^{\Delta 3/\Delta 3}$ single cells would recapitulate what we noticed *in vivo*. We, therefore, grew ASPP2$^{+/+}$ and ASPP2$^{\Delta 3/\Delta 3}$ intestinal organoids, after isolating single cells from duodenal crypts (Sato et al., 2009). After six days of growth, both ASPP2$^{+/+}$ and ASPP2$^{\Delta 3/\Delta 3}$ single cells formed complex organoids. However, during the first two days of culture, we observed that ASPP2$^{\Delta 3/\Delta 3}$ organoids grew faster than ASPP2$^{+/+}$ organoids (Figure 3.14). Over the following days, the growth rate of ASPP2$^{\Delta 3/\Delta 3}$ organoids decreased, and the ASPP2$^{+/+}$ organoids were similar in size and in shape to ASPP2-deficient organoids. Importantly, apoptosis was observed in ASPP2$^{\Delta 3/\Delta 3}$ organoids, and after eight days of culture the majority of the cells within the organoids died (Figure 3.14).

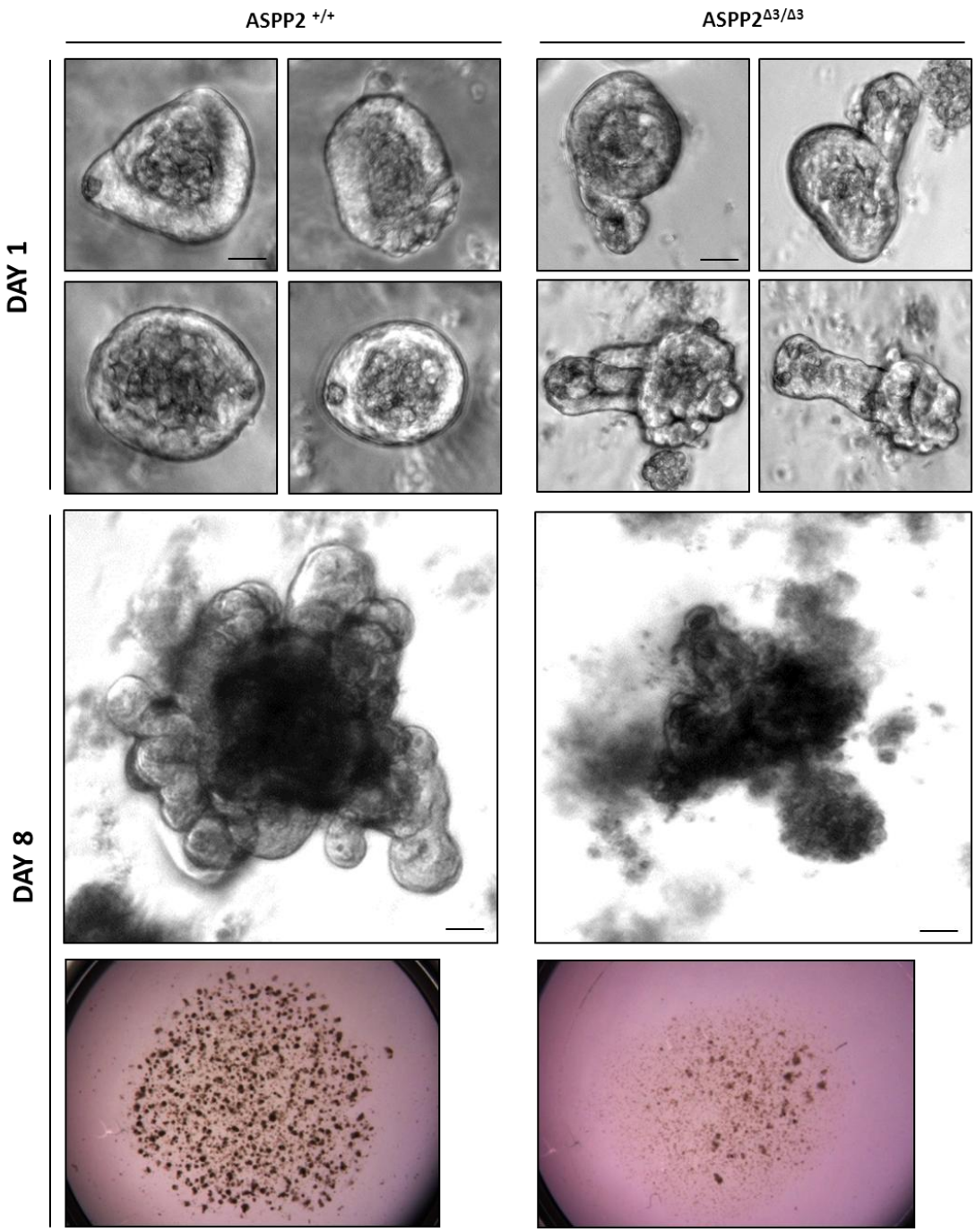


FIGURE 3.14 – ASPP2$^{\Delta3/\Delta3}$ intestinal organoids show an abnormal growth process. Contrast images of early stages (day 1) (x20) and differentiated stages (day 8) (x10) of intestinal WT and ASPP2$^{\Delta3/\Delta3}$ organoids. A wide field image of the number of surviving organoids by day 8 is depicted.

In order to study cell proliferation in this culture system, we waited six days so that both ASPP2$^{+/+}$ and ASPP2$^{\Delta 3/\Delta 3}$ organoids were well developed and still viable. No morphological differences were observed between WT and ASPP2-deficient organoids, as confirmed by β-catenin immunofluorescence staining (Figure 3.15A). Ki-67 immunofluorescence staining worked in both ASPP2$^{+/+}$ and ASPP2$^{\Delta 3/\Delta 3}$ organoids. Similarly to that observed *in vivo*, the analysis of ASPP2$^{+/+}$ organoids revealed Ki-67 staining to be limited to the crypt-like regions, where the proliferative compartment is located (Figure 3.15A). In these organoids, the villi-like domain was not stained for Ki-67. Conversely, Ki-67 staining in ASPP2$^{\Delta 3/\Delta 3}$ organoids was scattered throughout the epithelial structure, and not solely limited to the crypt-like region (Figure 3.15A). To further confirm our *in vivo* observations, we investigated the expression of phopho-Histone 3 in the duodenal organoids. Both ASPP2$^{+/+}$ and ASPP2$^{\Delta 3/\Delta 3}$ organoids revealed pH3-positive cells, although the number of was apparently higher in ASPP2$^{\Delta 3/\Delta 3}$ organoids than in ASPP2$^{+/+}$ similarly sized organoids (Figure 3.15B). To compare the number of pH3-positive cells in both ASPP2$^{+/+}$ and ASPP2$^{\Delta 3/\Delta 3}$ organoids, the total number of DAPI-positive nuclei was considered and a ratio of mitotic cells (pH3) to total cell number established (mitotic index). It was revealed that, at the same time point of six days, ASPP2$^{\Delta 3/\Delta 3}$ organoids contained an average of three times more nuclei than the WT, despite appearing similar in volume (data not shown). Determination of the mitotic index in ASPP2$^{+/+}$ and ASPP2$^{\Delta 3/\Delta 3}$ mice revealed that the ration of positive pH3 cells out of the total number of cells was significantly higher in ASPP2$^{\Delta 3/\Delta 3}$ when compared to the WT (12,29±5.06 vs. 3.73±2.11; p=0.007) (Figure 3.17).

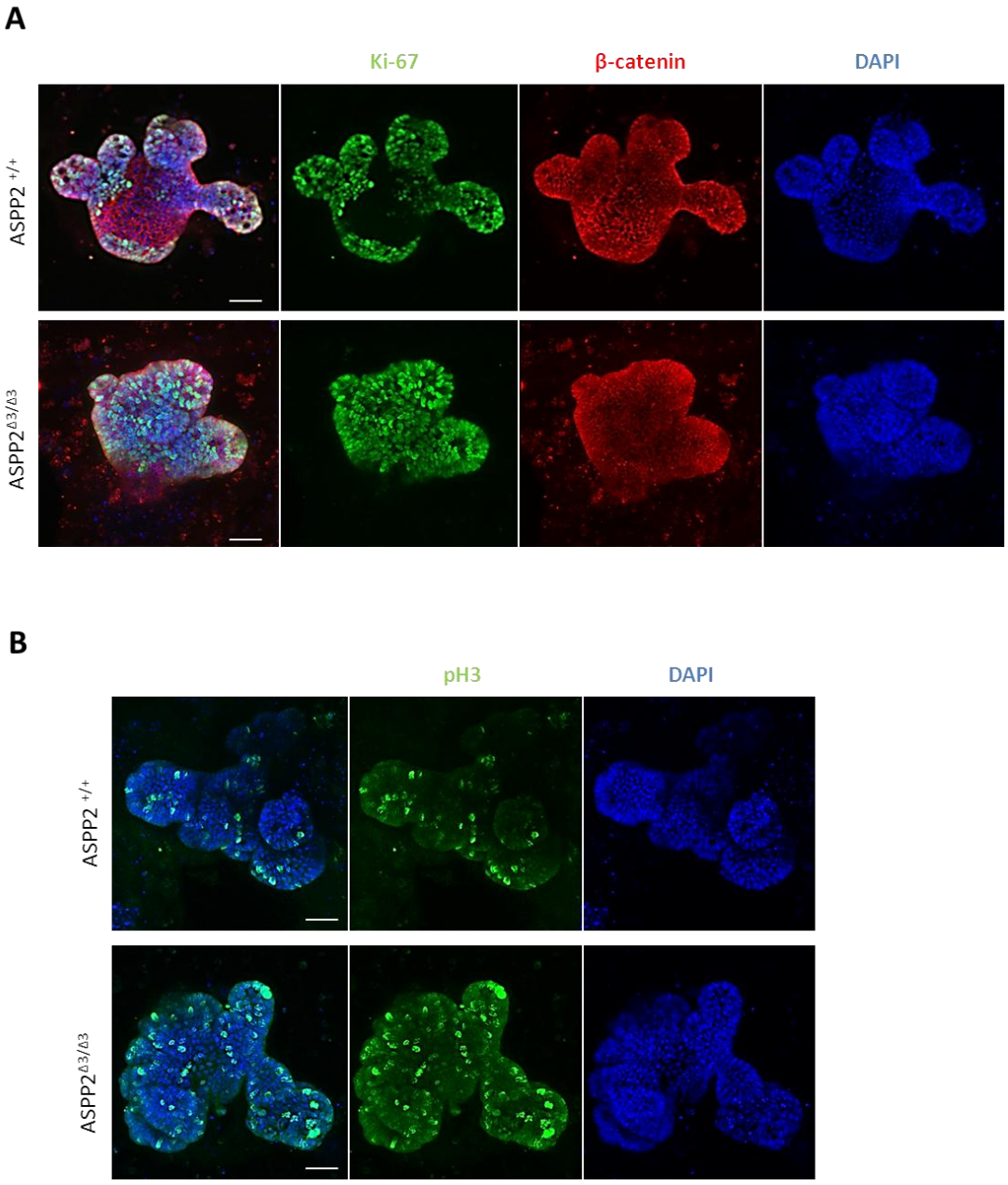


FIGURE 3.15 - Loss of ASPP2 results in an increase in cell proliferation *ex vivo*. (A) Ki-67 (green) and β-catenin (red) immunofluorescence staining of WT and ASPP2$^{\Delta 3/\Delta 3}$ duodenal organoids. **(B)** Phospho-histone 3 (pH3) (green) immunofluorescence staining on WT and ASPP2$^{\Delta 3/\Delta 3}$ duodenal organoids. Nuclei are counterstained with DAPI. Scale bars – 150µm.

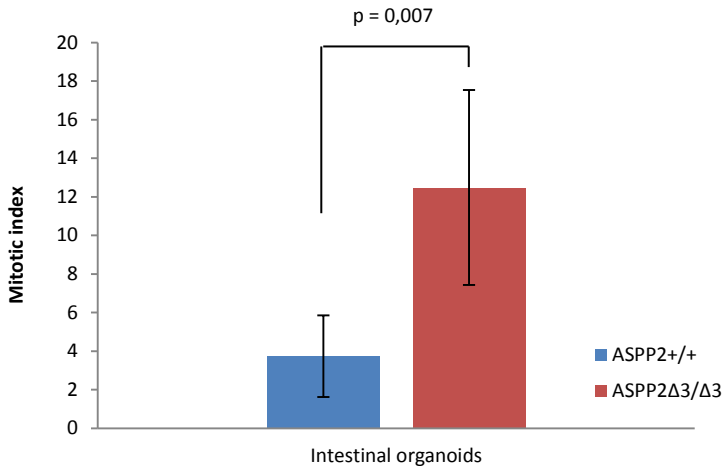


Figure 3.16 - ASPP2 inhibits cell proliferation in *ex vivo* cultures. Graphic representation of the mitotic index, defined as the ratio of phospho-Histone3 (pH3)-positive cells to total cell number in intestinal organoids (n=10).

3.2.10 – ASPP2-DEFICIENT MICE SHOW INCREASED APOPTOSIS IN THE DUODENAL EPITHELIUM

The adult intestinal epithelium is characterized by rapidly proliferating cells located in crypts, from which cells differentiate and migrate along the villi towards the lumen. To ensure that the number of epithelial cells is kept constant and that epithelial architecture is not lost, a balance between proliferative and apoptotic cells must be tightly regulated (Edelblum et al., 2006). Under healthy conditions, apoptotic cells are observed at the villi tips, as well as in the duodenal crypts. Inflammatory stimuli, environmental factors such as the gut microflora, and transforming growth factor-β (TGFβ) have all been reported to be important modulators of cellular apoptosis in the intestine (Dunker et al., 2002; Kim et al., 1998; Ramachandran et al., 2000). In coeliac disease and chronic inflammatory disorders, apoptosis is greatly increased, probably due to the excessive production of inflammatory cytokines in the mucosa (Ramachandran et al., 2000).

Since a significant increase in the number of proliferative cells in ASPP2$^{\Delta 3/\Delta 3}$ had been observed, both *in vivo* and *ex vivo*, we were interested in investigating whether this increase in proliferation was compensated for by an increase in apoptosis. To address this question, a TUNEL assay was performed using duodenal and colonic tissue from ASPP2$^{+/+}$ and ASPP2$^{\Delta 3/\Delta 3}$ mice (Figure 3.17). In ASPP2$^{+/+}$ duodenums, apoptotic cells were observed at the tips of the villi, similarly to reports from previous studies. In contrast, in the ASPP2$^{\Delta 3/\Delta 3}$ duodenal epithelium we noticed the existence of several apoptotic cells at the tips of the villi, as well as along the villi and in their lamina propria (Figure 3.17). Interestingly, this significant

difference was not observed in the colonic epithelium. In fact, the number of apoptotic cells in ASPP2$^{+/+}$ and ASPP2$^{\Delta 3/\Delta 3}$ colons was similar (Figure 3.17).

Intestinal cell turnover is characterized by a balance between proliferation and cell death. Our observations, therefore, suggest that in the ASPP2$^{\Delta 3/\Delta 3}$ duodenum there is a balance between proliferation and apoptosis, since both processes are frequent in the tissue. However, we believe that the balance between proliferation and cell death is compromised in the colons of ASPP2$^{\Delta 3/\Delta 3}$ mice. In fact, the excessive proliferation observed in this epithelium did not appear to be counterbalanced with the reduced level of apoptosis observed, which is similar to WT tissue.

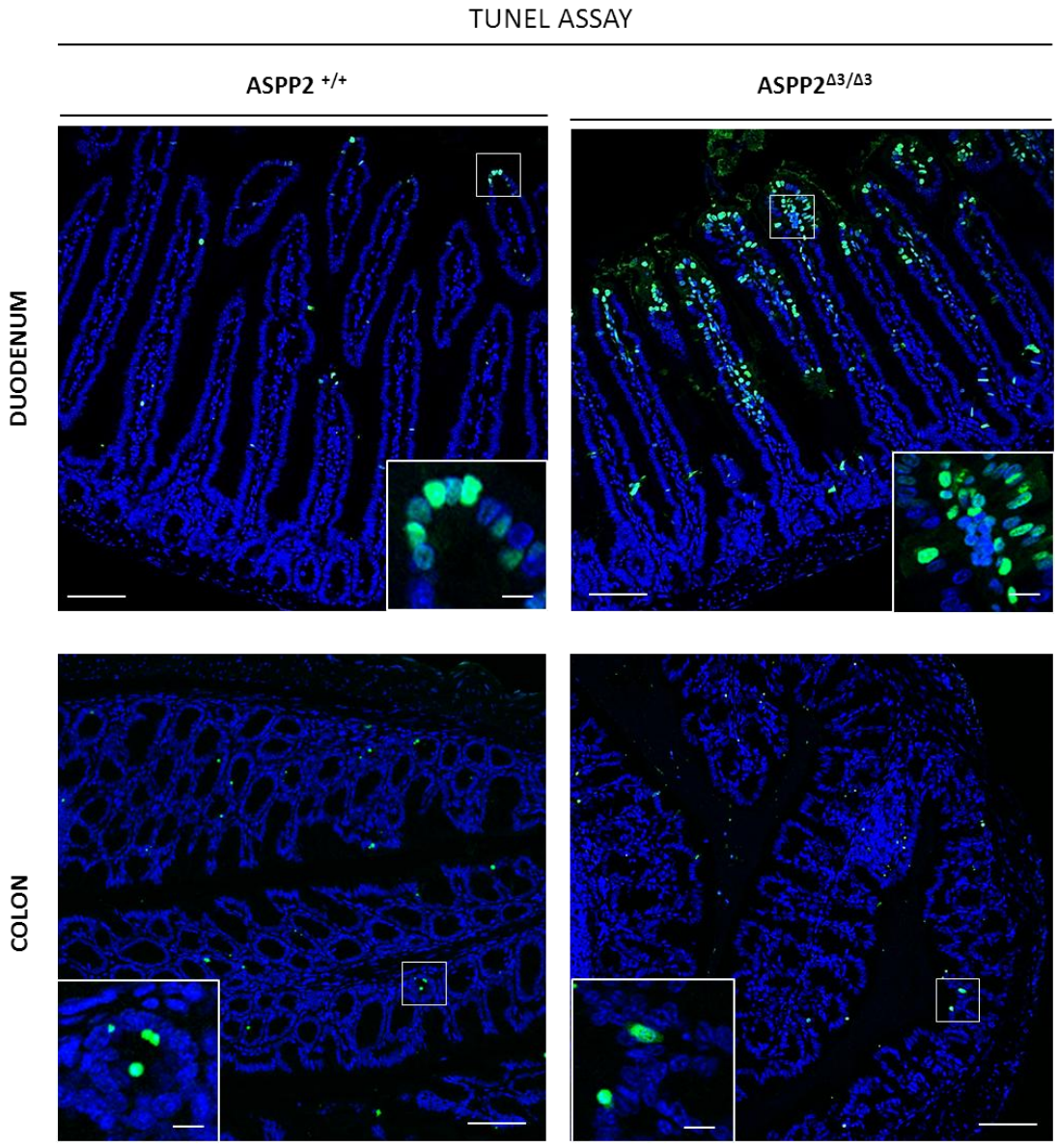


FIGURE 3.17 – Increased apoptosis in ASPP2$^{\Delta3/\Delta3}$ duodenum. Immunofluorescence TUNEL staining (green) of the apoptotic cells on paraffin sections of WT and ASPP2$^{\Delta3/\Delta3}$ duodenum and colon. Higher magnification images are shown to reveal details of the apoptotic cell staining. Scale bars: 150µm, 15µm.

3.3 – SUMMARY AND BRIEF DISCUSSION

The intestinal epithelium is highly dependent on cell polarity to exert its secretory, absorptive and barrier functions. For this reason, we were interested in understanding whether ASPP2, a known tumor suppressor and epithelial cell polarity guardian, is involved in the regulation of intestinal homeostasis.

In our approach to characterize the intestines of $ASPP2^{+/+}$ and $ASPP2^{\Delta 3/\Delta 3}$ mice, we analyzed the histology of the tissue and investigated whether the main processes that characterize the intestinal epithelium, such as cell polarity, differentiation and proliferation, were compromized by the loss of ASPP2. ASPP2-deficient mice do not present clinical evidence of tumorigenesis or intestinal inflammatory disorders, and a broader examination of the duodenum and colon did not show any relevant difference in length and diameter between $ASPP2^{+/+}$ and $ASPP2^{\Delta 3/\Delta 3}$. Importantly, this work showed that, in addition to the neuroepithelium, the intestinal epithelium is a good model with which to study ASPP2 *in vivo,* since this protein is expressed at the tight junctions in both the colon and duodenum. Histological analysis of $ASPP2^{+/+}$ and $ASPP2^{\Delta 3/\Delta 3}$ sections revealed an increase in cell disorganization in $ASPP2^{\Delta 3/\Delta 3}$ intestinal epithelia. For instance, in the duodenum, ASPP2-deficient villi were shorter and larger than the WT ones, whereas the crypts were slightly bigger. In the $ASPP2^{\Delta 3/\Delta 3}$ colon, crypts were significantly shorter than those observed in the $ASPP2^{+/+}$ mouse. Cell disorganization in the intestinal epithelium can be due to defects in cell polarity, abnormalities in cell differentiation and impaired cell proliferation. Importantly, loss of ASPP2 compromised epithelial organization in the colon, but not in the duodenum. Our observations suggest that ASPP2 plays an important role in maintaining cell polarity in the colon. Interestingly,

the duodenum of ASPP2-deficient mice shows significant cell disorganization. However, even though ZO-1 is disrupted, intact adherens junctions and brush borders might compensate for the loss of tight junction integrity. We believe that cell disorganization in the duodenum can result from altered processes, such as proliferation and differentiation. In the colon, tight junctions play a crucial role in the establishment of an epithelial barrier. It is possible that ASPP2 has a more important role as a tight junction component in the colon and that, for this reason, the tissue is dramatically affected by ASPP2 deficiency.

Further studies have revealed that the goblet and paneth cell populations were impaired in ASPP2$^{\Delta 3/\Delta 3}$ mice. In particular, in the duodenum, goblet cells were found to be less scattered along the villi and abnormally present in the bottom of the crypts, whereas less goblet cells were observed in the colon. Paneth cells, only present in the duodenal crypts, were found to be increased and misplaced in ASPP2$^{\Delta 3/\Delta 3}$ mice. In contrast, the enteroendocrine and absorptive cells were able to mature normally. Our observations suggest that the secretory cell lineage, particularly the goblet and Paneth cells, is impaired in the intestinal epithelium. Various transcription factors control the maturation of cells into distinct differentiated cells. For this reason, it is likely that loss of ASPP2 compromizes the expression of factors related to the differentiation of goblet and Paneth cells, but not enteroendocrine cells. In addition, most of the studies performed have shown that the generation of secretory cells occurs at the expenses of absorptive cells. Since we did not observe any impairment of enterocyte maturation, it is possible that other mechanisms prevent the loss of absorptive cells.

Notch is considered to be the master regulator of cell differentiation in the intestine and, together with Wnt, ensures the maintenance of stemness in its the proliferative compartment. It was, therefore, investigated whether Notch signaling was disrupted by the loss of ASPP2. Our findings revealed that, at the protein level, Hes5 and Math1 were significantly increased in the ASPP2$^{\Delta 3/\Delta 3}$ duodenum. The mRNA levels of Hes5 confirmed the protein levels, and are likely to explain the phenotypic increase and mislocation of Paneth and goblet cells. However, Hes1 mRNA levels were also found to be upregulated, suggesting that the absorptive lineage was also stimulated. Since there is a crosstalk between the Notch and Wnt signaling pathways, and abnormalities in Notch signaling were observed at the level of cell differentiation, we were interested to understand whether cell proliferation is altered in the intestine of ASPP2$^{\Delta 3/\Delta 3}$ mice. This question was addressed by analyzing the expression of Ki67 and pH3, in both the duodenum and colon. Cell proliferation was found to be increased in the intestinal epithelium, upon loss of ASPP2. In particular, the mitotic index determined by pH3 staining was significantly higher in ASPP2$^{\Delta 3/\Delta 3}$ mice.

To understand whether there is an increase in cell death in ASPP2$^{\Delta 3/\Delta 3}$ intestinal epithelia, we performed TUNEL a assay using ASPP2$^{+/+}$ and ASPP2$^{\Delta 3/\Delta 3}$ duodenal and colonic samples. We observed that cell death in the duodenum of ASPP2$^{\Delta 3/\Delta 3}$ mice was high, whereas the levels were comparable to ASPP2$^{+/+}$ mice in the colon. Our observations support the ones obtained with duodenal organoids, and suggest that cell turnover in the duodenum is more rapid than in ASPP2$^{+/+}$.

Taking advantage of new culture systems to study the dynamics of the intestinal epithelium, we studied cell proliferation in duodenal organoids. Interestingly, we observed a significantly increased proliferation rate in ASPP2$^{\Delta 3/\Delta 3}$ organoids, which was followed by abrupt cell death. In fact, it was very difficult to maintain ASPP2$^{\Delta 3/\Delta 3}$ organoids for more than 8 days, whereas ASPP2$^{+/+}$ organoids were able to last longer. Our observations suggest that cell turnover in ASPP2$^{\Delta 3/\Delta 3}$ organoids was faster than in ASPP2$^{+/+}$. In addition, the death of the ASPP2$^{\Delta 3/\Delta 3}$ cultures suggests the existence of a protective mechanism to compensate for the excessive rate of proliferation.

These findings show, for the first time, that ASPP2 can be expressed at the tight junctions in epithelial tissues other than the neuroepithelium. In addition to being involved in the maintenance of epithelial cell polarity, we believe that ASPP2 represses cell proliferation and modulates differentiation by regulating the crosstalk between Notch and Wnt activity.

CHAPTER 4 – ASPP2 IS AFFECTED BY GLUCOSE STARVATION: A LINK TO LKB1

4.1 – INTRODUCTION

The existence of tumor suppressors playing crucial roles in cell polarity has been discovered via studies on ASPP2 and, more recently, on PAR-3 (Iden et al., 2012; Sottocornola et al., 2010). Observations from previous work performed in our lab suggest that ASPP2 might contribute to the suppression of tumorigenesis in a p53-independent manner, by playing a role in epithelial cell polarity. Interestingly, the duodenal phenotype presented by ASPP2$^{\Delta 3/\Delta 3}$ resembles the phenotype of LKB1 conditional knockout mice (Shorning et al., 2009). For instance, loss of LKB1 results in changes in the secretory cells, and misplacement of goblet and Paneth cells (Shorning et al., 2009). Moreover, Hes5 expression is significantly upregulated in the small intestine of LKB1-deficient mice, whereas no significant differences were observed in Hes1 expression (Shorning et al., 2009). In addition, both ASPP2 and LKB1 can bind to p53 and mediate p53-dependent cell death (Karuman et al., 2001). Interestingly, they have also been linked to the establishment of cell polarity in epithelial cells, and have both been described as tumor suppressors. In particular, LKB1 has been described as the master tumor suppressor in small intestine (Yoo et al., 2002). For these reasons, it is important to determine whether ASPP2 and LKB1 have overlapping functions in the duodenum. The majority of the studies conducted on LKB1 to date have been performed *in vitro*. The LKB1$^{-/-}$ mouse is lethal, and the only studies available have been performed using a conditional LKB1 model. Anti-

LKB1 antibodies also work significantly better *in vitro*, limiting their use in *in vivo* studies. The possible link between ASPP2 and LKB1 has, therefore, been analysed *in vitro* in this study.

LKB1 has also been described as a master upstream kinase due to the fact that it phosphorylates a group of protein kinases named AMPK-related kinases, which are homologous to the AMP-activated protein kinase (Lizcano et al., 2004). It is believed that the wide range of biological functions played by LKB1 relies on these downstream kinases. For instance, the MARK kinase, also known as PAR-1, has been related to cell polarity regulation, whereas AMPK is considered to be a sensor of cellular energy (Bohm et al., 1997; Hardie et al., 2006). It is therefore possible that benign and malignant tumors in Peutz-Jeghers patients arise from abnormalities in the regulatory mechanisms that cells use to modulate cell polarity and metabolism (Forcet et al., 2005). In fact, the integrity of the C-terminal of LKB1, which is frequently mutated in Peutz-Jeghers syndrome, is essential for the activation and regulation of AMPK, as well as for LKB1's polarity functions (Forcet et al., 2005). AMPK is a LKB1-dependent metabolic checkpoint, which restores ATP levels and ensures energy homeostasis in cells by sensing the AMP/ATP ratio (Shaw et al., 2004b). Further studies in *Drosophila* have revealed that AMPK-null mutants are lethal, mostly due to dramatic polarity defects (Lee et al., 2007). Curiously, AMPK-null mutants and LKB1-null mutants display similar phenotypes, suggesting that these kinases work together in the same signalling pathway to establish cell polarity. Confirmation of this hypothesis through further studies has defined a new signalling pathway in cell polarity. Importantly, the LKB1/AMPK partnership establishes a link between cell polarity and cell metabolism, disruptions of which

are considered to be important hallmarks in tumorigenesis. We have previously shown that ASPP2 is an important component of the tight junctions in the duodenum. In addition, the similarities between the roles of ASPP2 and LKB1 in the duodenum suggest that these two proteins play roles in the same molecular pathways. For this reason, the crosstalk between LKB1 and ASPP2 at the level of cell polarity, and the involvement of AMPK in its regulation *in vitro*, are investigated in this chapter.

4.2 – RESULTS

4.2.1 – ASPP2 EXPRESSION IS ALTERED UNDER GLUCOSE DEPRIVATION CONDITIONS

AMPK functions as a sensor of cellular energy by responding to elevated levels of AMP upon energetic stress. It has been reported that the assembly of tight junctions and the maintenance of epithelial cell polarity are among the cellular responses triggered by AMPK's activation (Mirouse et al., 2007; Zhang et al., 2006). For example, studies in MDCK cells have revealed that the activation of AMPK leads to an increase in trans-epithelial resistance (TER), and a decrease in cellular permeability. The prompt relocation of ZO-1 to the tight junctions suggests that the activation of AMPK facilitates the assembly of tight junctions in this cell line (Zhang et al., 2006). Interestingly, the expression of the AMPK KD mutant (D157A) significantly attenuates the effects observed in TER and paracellular permeability, supporting the hypothesis that AMPK modulates the formation of functional tight junctions (Zheng and Cantley, 2007). In addition, studies performed in *Drosophila melanogaster* have shown that *ampkα* mutant cells show a complete loss of polarity, characterized by the downregulation and mislocalization of aPKC and Crumbs under energetic starvation conditions (Mirouse et al., 2007). More dramatically, some of the mutant cells lose their epithelial organization and acquire a round-shape structure.

ASPP2 is an important element in the tight junction polarity complex, playing an important role in maintaining the integrity of the neuroepithelium (Sottocornola et

al., 2010). Little is known about whether ASPP2's expression and location are affected upon energetic stress. However, the important role that ASPP2 plays in the tight junctions lead us to hypothesize that ASPP2 can be involved in AMPK-dependent tight junction assembly, under starvation conditions.

The human osteosarcoma-derived cell line U2OS was used in this study as we had observed, in previous experiments, that the junctional location of ASPP2 is less significant than in other polarized cell lines, such as MDCK and Caco-2. The use of U2OS cells would therefore allow us to better observe whether the localization of ASPP2 to junctions is enhanced under energetic stress. Based on published work, AMPK is activated when cells are incubated in low glucose medium (Mirouse et al., 2007; Okoshi et al., 2008). For this reason, we decided to trigger energetic stress in cells by depriving them of glucose. The activation of AMPK can be further stimulated by treating the cells with 5-Aminoimidazole-4-carboxyamide ribonucleoside (AICAR) (Corton et al., 1995). AICAR is quickly transported into cells and phosphorylated to 5-aminoimidazole-4-carboxyamideribonucleoside monophosphate (ZMP), a similar form of AMP. Therefore, AICAR mimics the action of AMP on AMPK activation. In this study, U2OS were treated with low glucose medium for 4 hours, and 1mM AICAR used to further stimulate AMPK activation. AMPK activation in U2OS cells was confirmed by the phosphorylation of Thr172. The levels of phosphorylation are low under normal conditions. However, an increase is observed when cells are deprived of glucose. Importantly, the phosphorylation state of AMPK is attenuated when cells are treated with AICAR only, possibly because the levels of AMP generated by glucose deprivation are better sensed by AMPK. For this reason, the effect of glucose deprivation in addition to AICAR

treatment on AMPK phosphorylation was similar to that of glucose deprivation alone (Figure 4.1A).

These experiments also revealed that an increase in ASPP2 protein levels occurs under energetic stress conditions (Figure 4.1A). This expression was significantly increased when cells were deprived of glucose, in addition to being treated with AICAR. However, in contrast to that observed with AMPK phosphorylation, ASPP2 expression was slightly stimulated after treatment with AICAR only (Figure 4.1A). The effect of glucose starvation on ASPP2 was further investigated via analysis of its cellular location. Immunofluorescence staining suggested that ASPP2 expression at tight junctions significantly increased, in a glucose starvation-dependent way. In fact, after 2 hours of glucose starvation, ASPP2 was strongly localized at the tight junctions when compared to the control (Figure 5.1B). This effect was observable after 30 minutes, and lasted for up to 4 hours, suggesting that a lack of glucose promptly triggers the movement of ASPP2 to cell-cell contacts (Figure 4.1B).

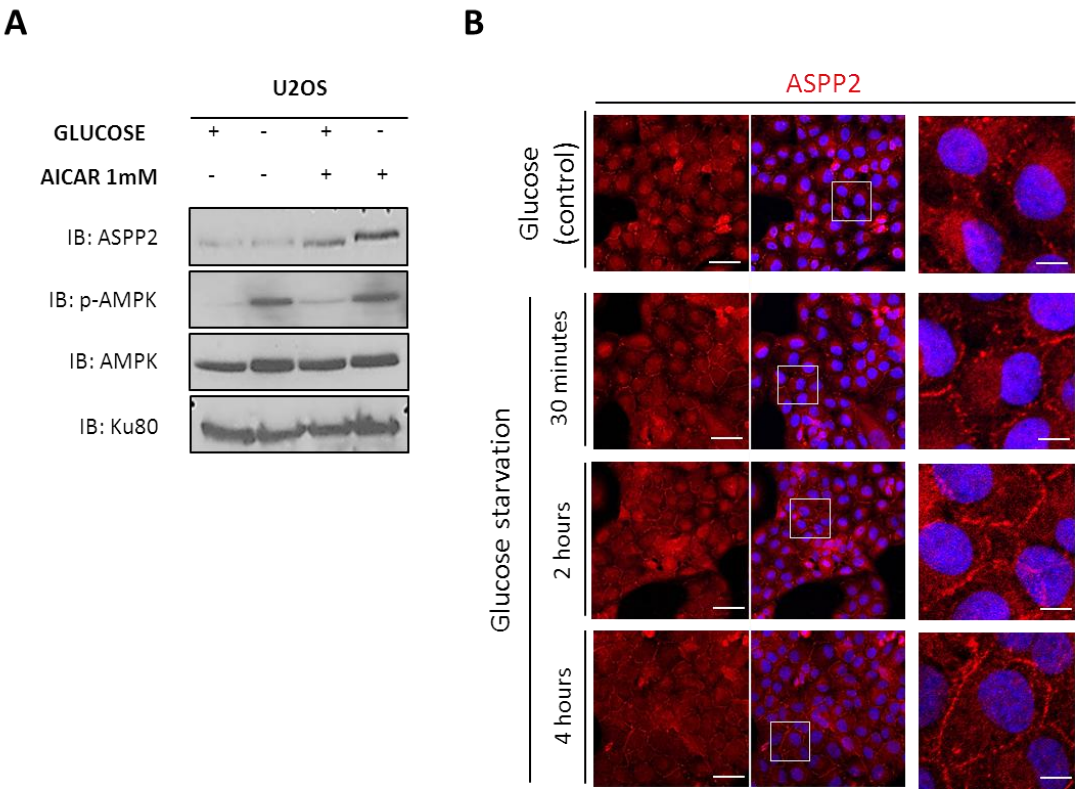


FIGURE 4.1 – Increase in ASPP2 expression, at the level of tight junctions, upon glucose deprivation. (A) Western blot analysis using 80µg of protein lysate from U2OS cells. Cells were kept under high glucose conditions (+), glucose starvation (-), AICAR 1mM stimulation (+) and absence of AICAR, for 4 hours, and ASPP2, p-AMPK and AMPK protein levels analysed. Actin protein levels were used as a loading control. (B) Immunofluorescence staining of ASPP2 (red) in fixed U2OS cells, after 30 minutes, 2 hours and 4 hours of glucose starvation. Cells growing under normal glucose conditions were used as a control. Nuclei were counterstained with DAPI. Scale bars: 50µm, 10µm.

4.2.2 – UNDER GLUCOSE DEPRIVATION CONDITIONS, THE EXPRESSION OF ASPP2 IS DEPENDENT ON AMPK ACTIVATION

Several works have recently suggested that AMPK might be an intermediary player through which LKB1 modulates epithelial cell integrity (Martin and St Johnston, 2003; Watts et al., 2000; Zheng and Cantley, 2007). In agreement with this, AMPK has been implicated in the polarization of LS174T, a human colorectal cell line (Lee et al., 2007). In addition, it has been shown that the stable expression of a LKB1 kinase-dead mutant in MDCK cells attenuated AMPK activation, and prevented the assembly of tight junctions upon calcium switching (Zheng and Cantley, 2007). Taken together, these findings suggest that the alliance of LKB1 and AMPK ensures the polarization of epithelial cells, even when energetic stresses threaten their homeostasis.

Our observations suggest that ASPP2 is upregulated upon glucose starvation. In addition, its localization at cell-cell contacts is intensified. However, it is not yet known whether this effect is a direct consequence of AMPK activation, or whether LKB1 is the upstream regulator of the ASPP2 modulation observed. To understand the causes of such an increase in ASPP2 protein level, we first analysed the effect of Compound C, a specific inhibitor of AMPK activation, on the expression of ASPP2. To address this question, we treated U2OS cells with and without glucose, in addition to AICAR and Compound C.

Under normal glucose conditions, the phosphorylation of AMPK was inhibited when Compound C treatment was initiated (Figure 4.2A). However, this suppression was attenuated when AICAR was used, probably due to an increase in the levels of cellular AMPK (Figure 4.2A). In fact, an increase in total AMPK was observed every

time cells were treated with AICAR. The depletion of glucose greatly induced AMPK activation, as expected. This effect was promptly inhibited upon treatment with Compound C (Figure 4.2A). Co-treatment with AICAR and low glucose medium did not significantly change AMPK phosphorylation levels suggesting, once again, that AICAR does not simulate AMPK activation in U2OS cells as significantly as glucose depletion (Figure 4.2A). Taken together, our observations show that Compound C successfully inhibited AMPK activation. Under rich glucose conditions, ASPP2 expression is slightly increased upon treatment with AICAR. However, these levels decrease when 0.01mM Compound C is used. Under glucose starvation conditions, and upon treatment with Compound C, the decrease in ASPP2 expression levels was more significant when compared to normal conditions (Figure 4.2A). The decrease in ASPP2 protein levels follows the observed decrease in AMPK activation, suggesting that inhibition of AMPK function prevents the stabilization of tight junction components, such as ASPP2 (Figure 4.2A).

Our findings propose that ASPP2 protein levels are affected by glucose starvation, possibly due to AMPK activation, but it remains unclear whether this stabilization of AMPK is dependent on LKB1.

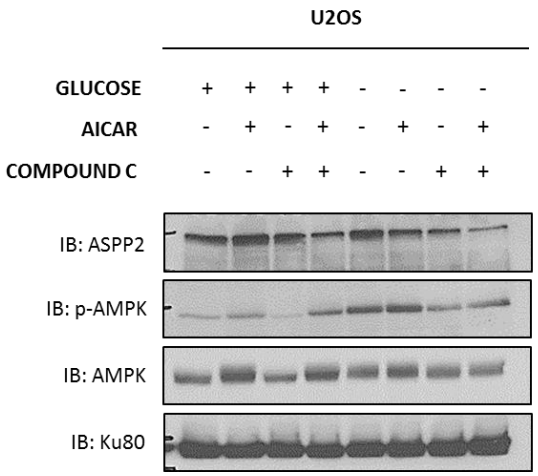


FIGURE 4.2 - Downregulation of ASPP2 upon suppression of AMPK activation and absence of LKB1. (A) Western blot performed using protein lysates from U2OS cells. Cells were treated with different combinations of Glucose, AICAR (1mM) and Compound C (0,01mM), for 4 hours. ASPP2, p-AMPK and AMPK expression levels were studied. Ku80 was used as a loading control.

4.2.3 – DELETION OF ASPP2 INFLUENCES LKB1 CELLULAR LOCATION AND AMPK ACTIVATION

LKB1 is an important regulator of cell polarity in many systems, such as *C. elegans*, *Drosophila* and mammals. The first evidence suggesting a role of LKB1 in cell polarity was obtained from studies in *C. elegans* and *D. melanogaster*. Importantly, both *C. elegans* Par-4 mutants and *Drosophila* LKB1 mutants display abnormal polarity and disrupted anterior-posterior patterning (Martin and St Johnston, 2003; Watts et al., 2000). In epithelial cells, the polarizing function of LKB1 is mediated through PAR-1/MARK, which regulates the activity of various proteins involved in morphogenesis. A LKB1 knockout mouse model has not been extensively studied, however, the generation of a β-napthoflavone-induced Cre system has allowed the study of LKB1 deletion in the intestinal tract, using LoxP flanked LKB1 mice (Shorning et al., 2009). This approach has revealed that a loss of LKB1 changes secretory cell morphology in the intestine. In particular, goblet cell size was dramatically affected and intermediate cells (between the goblet and Paneth cells) were observed (Shorning et al., 2009). In addition, the expression of Notch transcription factors was impaired. Overall, LKB1-null mice show defects in the intestinal secretory lineage (Shorning et al., 2009).

Interestingly, ASPP2 is also a tumor suppressor and an important cell polarity component. Previous studies have shown that ASPP2 is essential for maintaining the integrity of neuroepithelial polarity (Sottocornola et al., 2010). Nevertheless, our studies suggest that these findings can be extended to the intestinal epithelium. Noticeably, ASPP2-null and LKB1-null mice have similar phenotypes in the intestine, which has led us to speculate that both proteins may lie in the same signalling

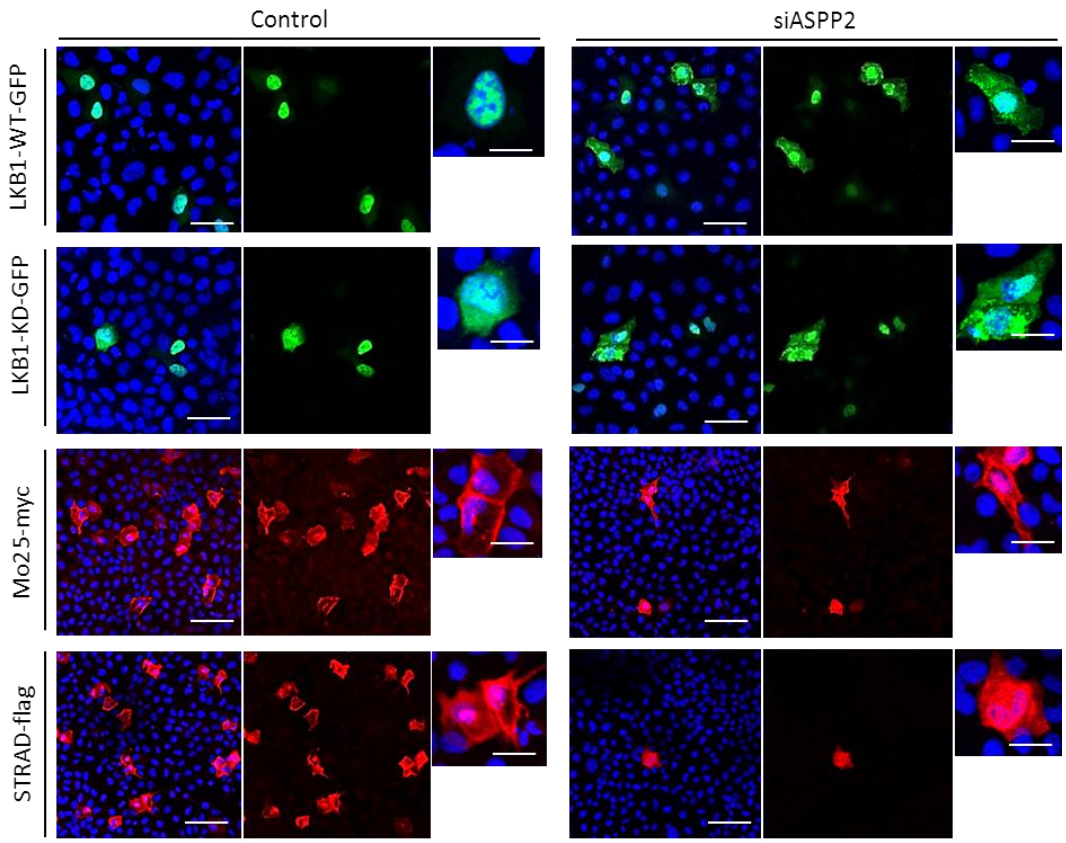
pathway. This idea is supported by our observation that ASPP2 expression is modulated by AMPK under glucose starvation.

To better understand whether the function of ASPP2 and LKB1 are related, the location and expression levels of LKB1, STRAD and Mo25 upon ASPP2 silencing *in vitro* were investigated. To address this question, we used U2OS cells and deleted ASPP2 using siRNA. The location of transfected LKB1, LKB1-KD, Mo25-myc, and STRAD-Flag was analysed in both control and siASPP2 cells (Figure 4.3A). As expected, transfected LKB1 is nuclear in control cells. However, in siASPP2 cells, LKB1-GFP was observed in the cytoplasm and nucleus of transfected cells. In control cells, LKB1-KD protein was found to be expressed in both the cytoplasm and nucleus, and remained at these locations when ASPP2 was depleted. Moreover, the cytoplasmic expression of Mo25 and STRAD did not change upon deletion of ASPP2 (Figure 4.3A). Our preliminary observations suggest that LKB1's location might be influenced by ASPP2 deletion *in vitro*. To further investigate this result, we analysed the expression of endogenous LKB1, STRAD and Mo25 in both control and ASPP2-depleted U2OS cells (Figure 4.3B). Upon ASPP2 deletion, we observed that the protein levels of LKB1, STRAD and Mo25 were not significantly affected by the deletion of ASPP2 (Figure 4.3B). Our observations suggest that a loss of ASPP2 alters the location of LKB1 but not its expression level. None of the other trimeric complex components, STRAD and Mo25, were changed upon depletion of ASPP2.

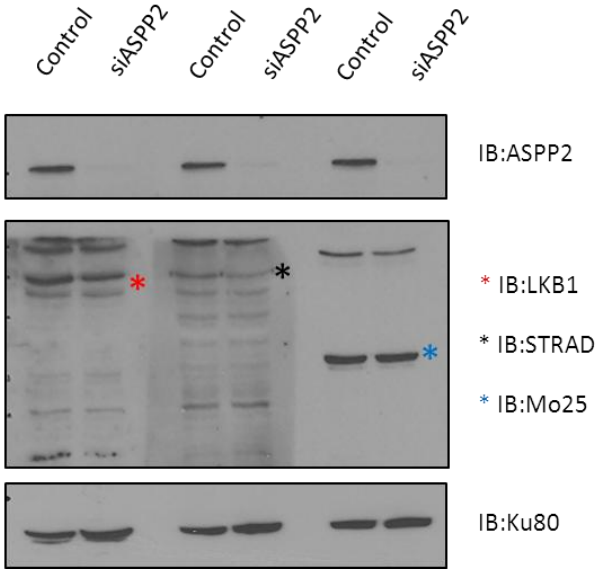
It has been reported that nuclear LKB1 is functionally inactive, whereas cytoplasmic LKB1 is fully active. STRAD is required to establish the subcellular location of LKB1 and anchor it to the cytoplasm, where it can perform its biological functions (Baas et al., 2003). As a consequence, the translocation of LKB1 to the

cytoplasm suggests that LKB1 can phosphorylate downstream kinases upon cellular stress. Although it is still unclear why ASPP2 deletion triggers the translocation of LKB1 to the cytoplasm, it is possible that this change promotes the phosphorylation of kinases such as AMPK. In order to confirm that LKB1 is, indeed, enriched in the cytoplasm upon ASPP2 deletion, we investigated the expression levels of phospho-AMPK. U2OS cells were depleted for ASPP2 using siRNA. In addition, cells were treated with or without AICAR, to modulate the expression of AMPK (Figure 4.3C). The deletion of ASPP2 in U20S cells was successful. The protein levels of ASPP2 were slightly enriched upon treatment with AICAR. An increase in p-AMPK expression level was observed by depleting ASPP2 in cells, or by treating cells with AICAR, in similar proportions. Importantly, the combination of siASPP2 and AICAR worked in synergy, significantly increasing the phosphorylation levels of AMPK (Figure 5.3C). These observations suggest that the deletion of ASPP2 affects the levels of phospho-AMPK, possibly due to an increase in cytoplasmic LKB1. Importantly, the combination of ASPP2 depletion and AICAR significantly increases the phosphorylation of AMPK, suggesting that these two triggers act on different AMPK-activating pathways. It is important to note that the activation of AMPK by AICAR is known to occur in a LKB1-independent manner (Sun et al., 2007).

A


Control
siASPP2
LKB1-WT-GFP
LKB1-KD-GFP
Mo25-myc
STRAD-flag

B


Control
siASPP2
Control
siASPP2
Control
siASPP2
IB:ASPP2
* IB:LKB1
* IB:STRAD
* IB:Mo25
IB:Ku80

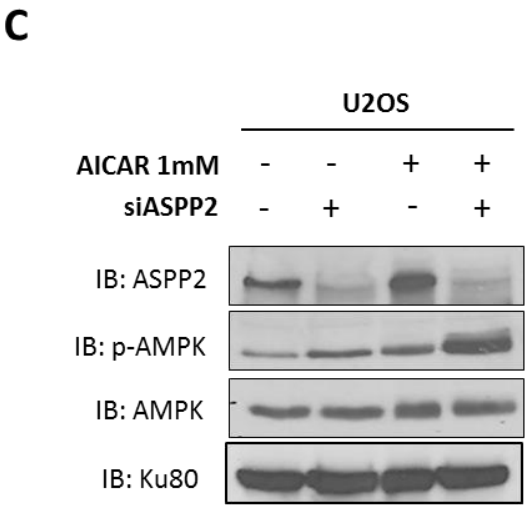


FIGURE 4.3 – ASPP2 depletion promotes LKB1 cytoplasmic expression and AMPK activation. (A) Immunofluorescence of LKB1-GFP, LKB1-KD-GFP, Mo25-MYC and STRAD-FLAG in U2OS cells with normal levels of ASPP2 or depleted ASPP2 (siASPP2). Nuclei were counterstained with DAPI. Scale bars: 50µm, 15µm. (B) Western blot performed with 80µg of protein lysates obtained from U2OS cells in which ASPP2 was depleted (siASPP2). U2OS cells with normal endogenous levels of ASPP2 were used as controls. The protein levels of LKB1, STRAD and Mo25 were determined. Ku80 protein level was used as a loading control. (C) Western blot performed with 80µg of protein lysates obtained from U2OS cells. Cells with normal endogenous levels of ASPP2 (+) and cells in which ASPP2 was depleted (-), were treated with 1mM AICAR for 4 hours (+) or kept under normal conditions (-).

4.2.4 – LKB1 EXPRESSION INTERFERES WITH ASPP2's LOCATION

Recent *in vitro* works have shown that an absence of AMPK, or its inability to become phosphorylated, disrupts the location of cell polarity components (Zhang et al., 2006; Zheng and Cantley, 2007). Despite the evidence suggesting that AMPK is directly regulated by LKB1, little is known about how LKB1 regulates the formation and maintenance of tight junctions. The first report revealing the endogenous location of LKB1 in polarized epithelial cells has shown that LKB1 is mainly localised at adherens junctions, together with E-cadherin (Sebbagh et al., 2009). Interestingly, suppression of LKB1 was followed by downregulation of E-cadherin and villin. Similarly, the location of LKB1 at the membrane was also affected by downregulation of E-cadherin (Sebbagh et al., 2009). Although the authors did not find a direct interaction between E-cadherin and LKB1, they do not exclude the possibility that LKB1 binding partners exist at the level of the adherens junctions.

We were keen to investigate the implications of both deletion and overexpression of LKB1 on the subcellular localization of ASPP2. Silencing of LKB1 in Caco-2 cells resulted in a slight decrease in ASPP2 at the level of tight junctions and a possible translocation of ASPP2 to the nucleus, in comparison with control cells (Figure 4.4A). When LKB1-GFP was overexpressed in U2OS cells, it was observed that ASPP2's location was attenuated at the level of tight junctions, suggesting that LKB1 nuclear expression might prevent tight junction formation or promote tight junction disassembly (Figure 4.4B). In both experiments, endogenous levels of STRAD and Mo25 were not considered and, for this reason, it is unclear whether they have an important role in mediating ASPP2's subcellular localization.

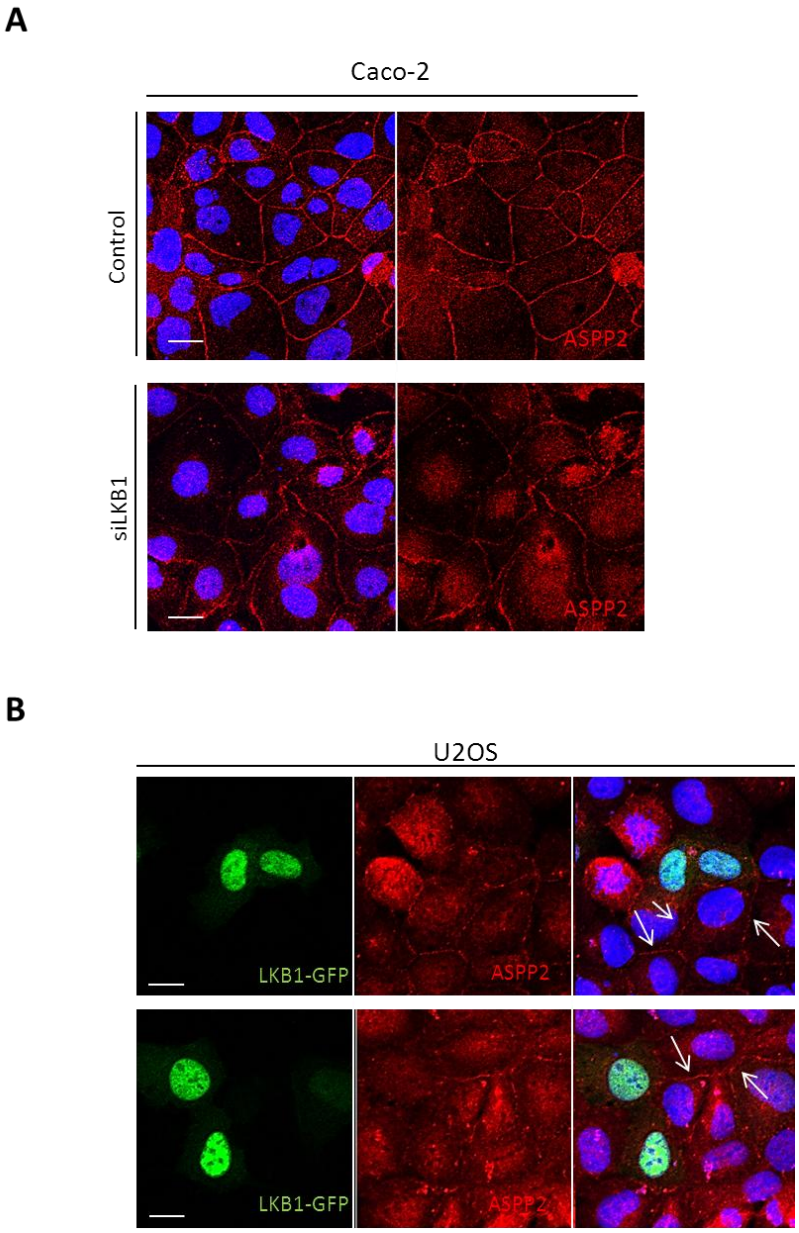


FIGURE 4.4 – Deletion of LKB1 compromises ASPP2 cellular location. (A) Immunofluorescence of ASPP2 on fixed Caco-2 cells with normal endogenous levels of LKB1 (upper panel), and depleted levels of LKB1 (lower panel). Nuclei were counterstained with DAPI. (B) Two examples of double immunofluorescence of transfected LKB1-GFP tagged and endogenous levels of ASPP2 in fixed U2OS cells. White arrows show ASPP2 expression at the level of the tight junctions. Nuclei were counterstained with DAPI. Scale bars: 15μm.

4.2.5 – ASPP2 INTERACTS WITH THE LKB1 COMPLEX

The *in vivo* subcellular location of LKB1, Mo25 and STRAD has not been extensively studied. The only report describing LKB1 expression in the small intestine to date has revealed that LKB1 is expressed in both the nucleus and cytoplasm of small intestinal epithelial cells. In addition, the expression pattern of LKB1 in the cytoplasm shows a gradient characterized by a progressive increase in LKB1 expression along the villus towards the lumen, leading the authors to conclude that LKB1 is expressed in older intestinal epithelial cells, referring to apoptotic cells (Karuman et al., 2001). Recently, one report has suggested that Ezrin and Mst4, known brush border markers in the intestine, are activated and translocated to the subapical region of epithelial cells by the active complex LKB1/Mo25/STRAD (ten Klooster et al., 2009). Importantly, this report claims that Mo25's interaction with Mst4 is a decisive player in triggering LKB1/STRAD-induced brush border formation (ten Klooster et al., 2009). In addition, phosphorylation of Ezrin is dependent on the LKB1/STRAD/Mo25 complex. However, this phosphorylation is not observed upon Mo25 silencing *in vitro* (ten Klooster et al., 2009).

The crystal structure of Mo25 has shown that Mo25 is a helical-repeat protein with significant similarity to the Armadillo family of repeat proteins (Milburn et al., 2004). This family includes the β-catenin and importin-α, known to be involved in nuclear transport and, more recently, shown to be blocked by STRAD upon LKB1 translocation to the cytoplasm (Dorfman and Macara, 2008; Milburn et al., 2004).

ASPP2 has previously been described as a binding partner of β-catenin, both *in vivo* and *in vitro* (Sottocornola et al., 2010). This interaction is not reversible and is weaker than the one found between ASPP2 and PAR-3. It is possible, for this reason,

that ASPP2 strongly localizes at tight junctions instead of adherens junctions. Nevertheless, we hypothesized that ASPP2 can bind to Mo25 due to its similarities with β-catenin, and that the effects that LKB1 had on ASPP2 could be due to Mo25.

To address this question, we first investigated the expression of Mo25 *in vivo*. The specificity of the antibody against Mo25 was confirmed by silencing Mo25. As the expression of Mo25 was completely downregulated (data not shown), we used the antibody to detect Mo25 by immunofluorescence *in vivo*. The expression of Mo25 in the small intestine was analysed via co-localization with β-catenin, (Figure 5.5A). We noticed that there was significant co-localization between Mo25 and β-catenin in small intestinal epithelial cells, suggesting that Mo25 might be involved in epithelial polarity, as already described *in vitro* (Figure 4.5A). The interesting observation that Mo25 and β-catenin co-localize *in vivo* led us to investigate the possible interaction between both proteins in Caco-2 cells, which are known for being a good model with which to study epithelial polarity *in vitro*. The two proteins were found to interact in Caco-2 cells (Figure 4.5B). However, the binding appeared to be established between Mo25 and a lower molecular weight form of β-catenin. It is possible that β-catenin is expressed in cells presenting various post-translational modifications. Therefore, its interaction with Mo25 may be dependent on β-catenin bearing specific modifications.

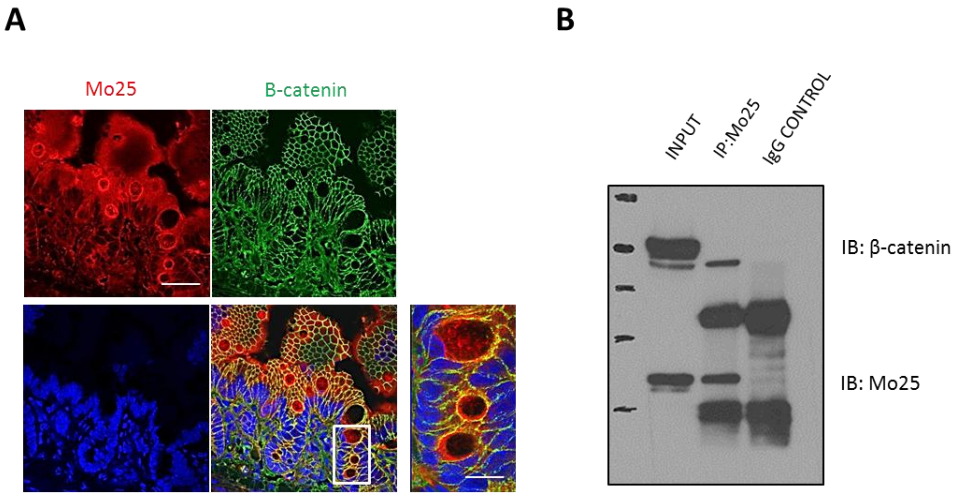


FIGURE 4.5 – Mo25 interacts with β-catenin *in vitro* and *in vivo*. (A) Double immunofluorescence of Mo25 (red) and β-catenin (green) on paraffin section of WT duodenum. A high magnification view is shown to note the co-localization between Mo25 and β-catenin. Nuclei were counterstained with DAPI. Scale bars: 100µm, 20µm. (B) Immunoprecipitation (IP) of β-catenin by pulling down Mo25. 2mg of protein lysate were used to perform the IP. 80µg of protein were used for the Input. IgG produced in the same host as the anti-Mo25 antibody was used as a control.

Taken together, recently published reports and the observations outlined in this report suggest that Mo25 plays a role in epithelial cell polarity in the intestine. We still do not know how ASPP2 and the LKB1/Mo25/STRAD complex are related. However, the evidence suggests that an interaction between β-catenin and Mo25 could be the missing link, since ASPP2 is known to bind to β-catenin. We, therefore, investigated the possible interactions between ASPP2 and Mo25, as well as ASPP2 and LKB1 (Figure 4.6A). Importantly, we observed that ASPP2 is able to physically interact with both Mo25 and LKB1 in U2OS cells, by pulling down ASPP2 (Figure 4.6A). However, we assume that these bindings are not strong as reversible binding was never observed (data not shown). To further characterize the binding between ASPP2 and Mo25, we decided to map the interaction and find out which region of ASPP2 binds to Mo25.

The C-terminal region of ASPP2, characterized by ankyrin repeats and SH3 domains, is involved in several interactions with binding partners. Most of these interactions are believed to be related to ASPP2's apoptotic function (Rotem et al., 2007). Recently, however, new interactions have been found to involve the N-terminal region of ASPP2, including its binding to CagA and Par-3, suggesting that the N-terminal region is involved in ASPP2's polarity functions (Buti et al., 2011; Sottocornola et al., 2010). We took advantage of several v5-tagged plasmids of ASPP2 fragments designed and characterized in our lab, and analysed the binding of Mo25 to these fragments. One fragment consisted of the first 360 residues of human ASPP2, the second spanned the middle region of ASPP2 (360-925) and the third represented its C-terminus (925-1128). In addition, we used the full-length human ASPP2 plasmid as a control. We also included a plasmid containing a

phosphatase PP1-mutant site in full length ASPP2 in the experiment. All plasmids were successfully transfected and expressed in U2OS cells. With the exception of full-length ASPP2 and the ASPP2 360-925 fragment, all other plasmids were well expressed *in vitro* (Figure 4.6B). Moreover, endogenous levels of Mo25 were observed in U2OS cells. Importantly, the pulldown levels of all fragments, with the exception of the ASPP2 C-terminal (fragment 925-1128), were successfully detected (Figure 4.6B). These results revealed that Mo25 and the ASPP2 360-925 fragment were able to immunoprecipitate, suggesting that Mo25 can interact with the middle region of ASPP2. Interestingly, the PP1 mutation (ASPP2 V922A, F924A), which lies in this region, prevents the binding of Mo25 to ASPP2 (Llanos et al., 2011). Considering our findings, we believe that ASPP2 is able to bind to Mo25 through its 360-925 region. Further investigations are necessary to understand whether this binding is modulated by PP1.

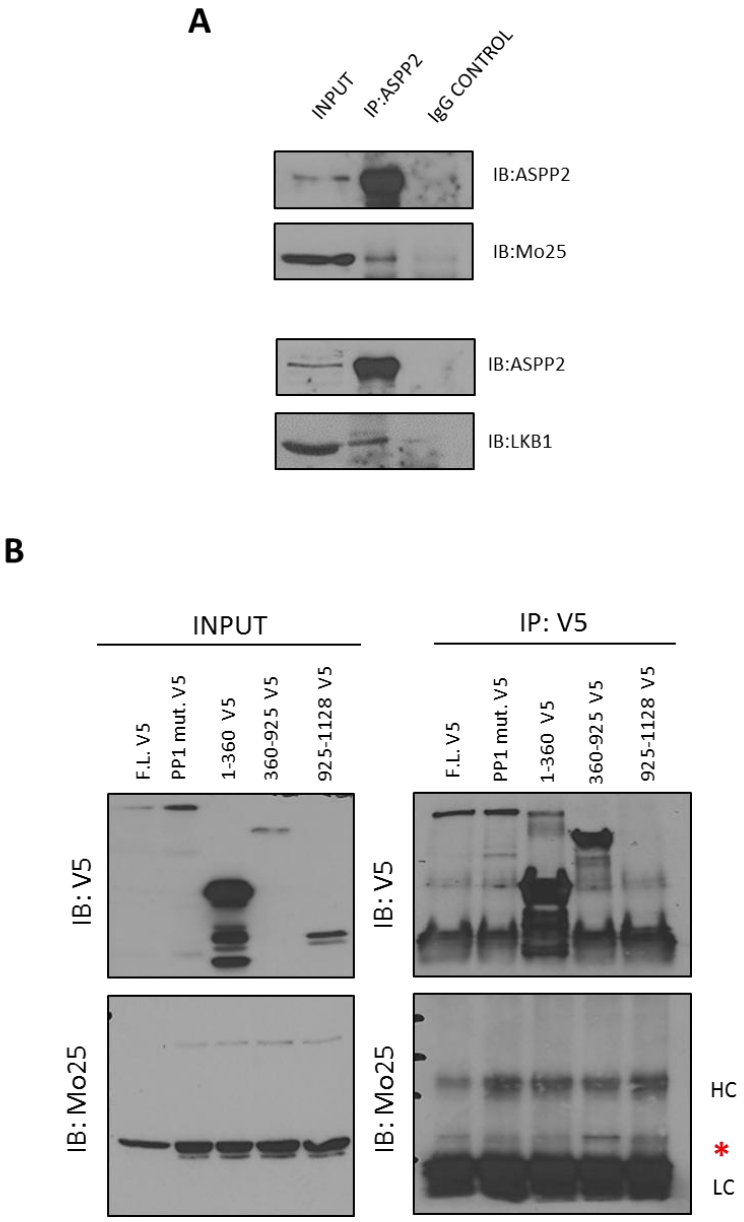


FIGURE 4.6 – ASPP2 interacts with LKB1 and Mo25. (A) Immunoprecipitation of Mo25 and LKB1 by pulling down ASPP2 in U2OS cells. 2mg of protein were used per immunoprecipitation experiment. 80µg of protein were used for the input. IgG, produced in the same host as the anti-ASPP2 antibody, was used as a control in the experiment. (B) Immunoprecipitation of Mo25 by pulling down different ASPP2 transfected V5 tagged fragments. 3mg of protein were used per immunoprecipitation experiment. 80µg of protein were used for the input. Red asterisk shows Mo25 molecular weight band. Abbreviations: Immunoprecipitation, IP; Immunoblot, IB; Heavy chain, HC; Light chain, LC

4.2.6 – THE INTERACTION BETWEEN ASPP2 AND PP1 IS WEAKER UPON GLUCOSE STARVATION

Protein Ser/Thr phosphatase-1 (PP1) mediates the majority of dephosphorylation reactions in biological events. Interestingly, the mammalian genome encodes approximately 400 Ser/Thr kinases, whereas the number of Ser/Thr phosphatases is less than 100 (Bollen et al., 2010). Several reports have suggested that this discrepancy between the number of kinases and phosphatases is overcome by diversity in affinity to the substrate. In fact, the substrate selectivity of PP1 is largely conferred by its specific regulatory subunits, which are extremely varied. The associations between PP1's different regulatory and catalytic subunits accounts for more than 100 different PP1 holoenzymes, which have their own regulatory mechanisms (Bollen et al., 2010).

ASPP2 is among the PP1 regulatory subunits capable of binding PP1 through a RVXF motif (Llanos et al., 2011). In response to nutrient availability, AMPK is promptly phosphorylated by LKB1 or CaMKKβ. However, the phosphorylation of the Thr172 residue is reversible when energetic stress is overcome. The phosphatases PP1, PP2A and PP2Cα are all known to efficiently dephosphorylate AMPK's Thr172 residue in cell-free assays (Hardie et al., 2011). Furthermore, in MIN6 cells, it has been shown that PP1 and its regulatory subunit R6 are involved in the regulation of AMPK by glucose. Little is known about the functional role of the interaction between ASPP2 and PP1, nor about the modulation of this interaction. However, our group has evidence that ASPP2's expression and subcellular location is mediated by the LKB1-AMPK axis, which is highly dependent on reversible phosphorylation. It was, therefore, hypothesized that the interaction between

ASPP2 and PP1 could play a role in this mediation. We investigated whether the binding between ASPP2 and PP1 is affected under glucose starvation conditions. To address this question, we performed an immunoprecipitation using ASPP2 to pull-down PP1, under two different conditions: high concentration and depletion of glucose. Interaction between ASPP2 and PP1 was observed in both cases (Figure 4.7). However, for the same amount of pulled down ASPP2, its binding to PP1 was slightly lowered under glucose starvation (Figure 4.7). This result is preliminary, but suggests that glucose concentration and energetic stress might modulate the post-translational modification of ASPP2.

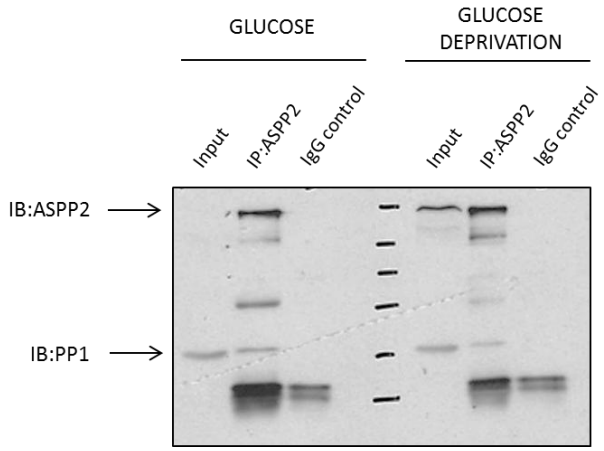


FIGURE 4.7 – Weak ASPP2-PP1 binding under low glucose conditions. Immunoprecipitation of PP1 by pulling down ASPP2 under different glucose conditions. Glucose starvation lasted 4 hours. 2mg of protein lysate was used per immunoprecipitation experiment. 80µg of protein lysate were used for the input. IgG, raised in the same host as the anti-ASPP2 antibody, was used as a control.

4.3 – SUMMARY AND BRIEF DISCUSSION

In this chapter, the implications of AMPK-energetic stress regulation on the expression and subcellular localization of ASPP2 *in vitro* have been analysed. In addition, the link between AMPK-regulatory complex LKB1/Mo25/STRAD and ASPP2 has been investigated. The possible interactions between ASPP2 and Mo25, and ASPP2 and LKB1, have also been considered.

The results presented here show that the expression and subcellular localization of ASPP2 are altered upon glucose depletion. In particular, an increase in ASPP2 was observed at the level of cell-cell contacts. It is therefore concluded that the changes in ASPP2 are mediated by AMPK, since its specific inhibition with Compound C was sufficient to rescue the expression level of ASPP2. This result was particularly significant under glucose starvation conditions. Furthermore, it has been demonstrated that the deletion of ASPP2 promotes the translocation of LKB1 to the cytoplasm, possibly resulting in the phosphorylation of AMPK. These results are not, however, supported by a corresponding reduction of LKB1, Mo25 and STRAD protein levels. This suggests that ASPP2 deletion has no impact on the expression of these proteins, and acts instead by activating the complex by enriching LKB1 cytoplasmic levels. Our preliminary observations have revealed that LKB1 deletion, or nuclear localization, compromise the location of ASPP2 at the membrane. Further experiments are therefore needed to better understand how LKB1 modulates ASPP2's localization. Finally, the possibility of an interaction between ASPP2 and the trimeric LKB1/Mo25/STRAD complex has been explored, and it has been discovered that ASPP2 binds not only to Mo25, but also to LKB1. It has also

been shown that Mo25 can bind to β-catenin, possibly establishing a link to ASPP2. Further analysis of the interaction between ASPP2 and Mo25 has revealed that Mo25 binds to the middle region of ASPP2, which contains the PP1 binding motif. This result not only excludes the usual C-terminal region of ASPP2 as the responsible binding region, but also suggests that PP1 might play an important role in mediating this binding, since a mutation in the PP1 site prevents the interaction between ASPP2 and Mo25. In a separate experiment, it was observed that ASPP2's binding to PP1 might be affected by glucose starvation, supporting the hypothesis that ASPP2 stabilization is modulated upon energetic stress and might depend its ability to complex with other binding partners.

Taken together, the observations reported in this chapter suggest that crosstalk exists between ASPP2 and LKB1. This association is likely to occur upon metabolic stress, and under the regulation of AMPK. Moreover, these findings imply that a loss of ASPP2 from tight junctions triggers a signal that promotes LKB1's activation, possibly due to the phosphorylation of AMPK. We did not investigate the crosstalk between ASPP2 and LKB1 in the duodenal epithelium. However, we believe that a deficiency of ASPP2 in the duodenum could elicit the activation of LKB1. Importantly, the possibility that ASPP2-deficient mice present defects at the level of paracellular transport of ions and glucose absorption cannot be discounted. Loss of ASPP2 *in vivo* can, therefore, lead to a situation of metabolic stress, which results in activation of AMPK and stimulates the protective role of LKB1 as a tumor suppressor.

CHAPTER 5 – ASPP2 DEFICIENCY INCREASES SUSCEPTIBILITY TO COLONIC INFLAMMATION

5.1 – INTRODUCTION

Under healthy conditions, tight junctions exert a barrier function that regulates the trafficking of macromolecules between the lumen and epithelial cells. Most importantly, they establish an interface for the crosstalk between intestinal luminal bacteria and the immune system. For this reason, tight junctions ensure the balance between surveillance and immunological hyporesponse between the host and gut flora (Artis, 2008; Goto and Kiyono, 2012). Upon the loss of cell polarity components, the intestinal epithelial cells become easier targets for opportunistic pathogens, while the immunological tolerance of the host to commensals is compromised (McCracken and Lorenz, 2001). As a consequence, a rapid and appropriate immune response, followed by a pathogen-specific adaptive response, is required to contain the harmful effects of pathogenic infection. The gut microenvironment is one of the least sterile in the human body. For this reason, the immune system is often considered to be in a no-win situation since it has the difficult task of protecting the host by eliciting immune responses on the one hand, while needing to control its own actions by preventing a vigorous and uncontrolled immune reaction against pathogens on the other (McCracken and Lorenz, 2001).

When an exacerbated innate immune response occurs, the proper regeneration of the intestinal epithelial tissue is compromised, thus affecting the establishment

of the barrier function. Consequently, the time of exposure to microbial toxic products is amplified and, ultimately, the inflammation is prolonged (Kinnebrew and Pamer, 2012). Cancer risk increases in situations of chronic inflammation, depending on the site, extension and duration of the inflammation (Rhodes and Campbell, 2002).

The analysis of ASPP2$^{\Delta 3/\Delta 3}$ mice has revealed overall morphological disruption of the colon. Interestingly, cell polarity defects were also observed suggesting that the homeostasis of the intestinal epithelium is compromised in ASPP2-deficient mice. For these reasons, whether or not the deficiency of ASPP2 has any repercussions on the susceptibility of the mice to develop inflammation is investigated here, by examining evidence of colonic inflammation in ASPP2$^{\Delta 3/\Delta 3}$ mice. In addition, the response of ASPP2 Δexon3 conditional knockout mice to DSS-induced colitis is analyzed to determine whether these mice are prone to develop the disease.

5.2 - RESULTS

5.2.1 – ASPP2-DEFICIENT MICE SHOW EVIDENCE OF INTESTINAL INFLAMMATION

The epithelium is an important member of a tripartite functional relationship, together with the gut microflora and the intestinal immune system. The success of this relationship ensures immunological tolerance towards the microbes living in the intestine and, hence, the homeostasis of the tissue (Goto and Kiyono, 2012). Importantly, data from both human patients and mouse experimental models has shown that disruption of tight junctions is not sufficient to cause disease, but can increase paracellular permeability, active mucosal immune responses and, therefore, enhance disease progression (Ding et al., 2011; Laukoetter et al., 2007; Su et al., 2009). Unsurprisingly, loss of epithelial tight junctions is considered a risk factor in the development of intestinal inflammatory diseases (Turner, 2009).

The observations outlined in this report suggest that the loss of ASPP2 compromises the integrity of tight junctions in the intestinal epithelium, particularly in the colon. It was therefore hypothesized that, in the ASPP2$^{\Delta 3/\Delta 3}$ intestinal epithelium, the barrier function is impaired. The disruption of this epithelial line of defense is considered an open door for opportunistic pathogens that can easily invade the host. As a consequence, the intestinal innate immune system is triggered and acute inflammation occurs (Medzhitov, 2008).

In this study, it was expected signs of mucosal inflammation in ASPP2$^{\Delta 3/\Delta 3}$ colons would be observed. Therefore, in order to understand whether ASPP2 plays a role as a regulatory tight junctional protein in the process of intestinal inflammation, the

intestines of ASPP2$^{\Delta 3/\Delta 3}$ mice were observed and the possible signs of inflammation in the colonic epithelium investigated.

Macroscopically, ASPP2$^{\Delta 3/\Delta 3}$ colons did not show signs that indicated intestinal pathology. For instance, stool consistency was normal and bleeding was never observed. In agreement with other studies, the absence of ASPP2 in colonic tissue did not seem to be sufficient to trigger inflammatory disease. However, microscopic analysis revealed significant differences between ASPP2$^{+/+}$ and ASPP2$^{\Delta 3/\Delta 3}$ colonic epithelia. In the ASPP2-deficient mouse, a higher number of inflammatory cells in the colonic mucosa was observed. In addition, the existence of isolated lymphoid follicles (ILFs) was noticed, the sizes of which were significantly greater than the ones found in WT tissue (Figure 5.1). It has been reported that there is a close link between inflammatory conditions and the number, size and density of ILFs. In fact, dramatic loss of architecture leads to an increase in the number of mucosal ILFs (Sipos and Muzes, 2011). Our observations are, therefore, indicative of an active immune response in ASPP2$^{\Delta 3/\Delta 3}$ colons (Figure 5.1). The isolated lymphoid follicles observed in ASPP2$^{\Delta 3/\Delta 3}$ colons were distributed in the mucosal and submucosal region, in contrast to those found in ASPP2$^{+/+}$ mice, which were only found in the mucosa (Figure 5.1).

ILFs are composed of large germinal centers that consist of B cell-enriched regions with intervening T cell areas, and an overlying follicle-associated epithelium (FAE) containing M cells. The composition of ILFs suggests that they function as inductive sites for the mucosal immune response (Lorenz and Newberry, 2004).

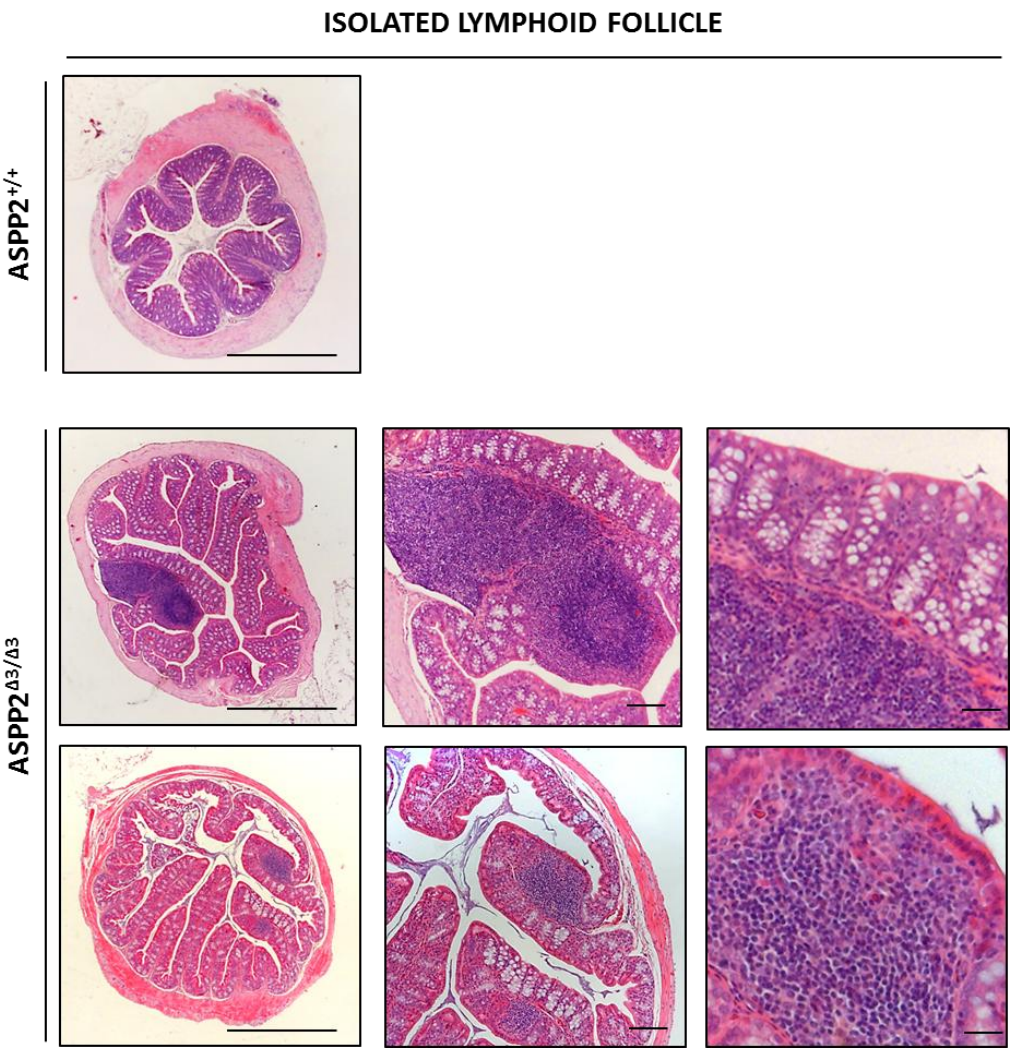


FIGURE 5.1 – Presence of lymphoid follicles in ASPP2$^{\Delta 3/\Delta 3}$ intestine. H&E staining was performed on paraffin sections of WT and ASPP2$^{\Delta 3/\Delta 3}$ colon. High magnification images are shown to reveal details of the histology of the lymphoid aggregate. Scale bars: 1mm, 300µm, 100µm.

Similarly to the results described in several previous reports, immunofluorescence experiments using samples from ASPP2$^{\Delta 3/\Delta 3}$ colons showed that the ILFs were enriched with B cells which were interspersed with T cells, as shown by CD45R and CD3 markers, respectively (Figure 5.2A). Neutrophils, also known as polymorphonuclear leukocytes (PMN) are essential components of the innate immune response, protecting the host against pathogens while minimizing the dangerous consequences of dying and injured cells (Fournier and Parkos, 2012). These cells are responsible for the production of reactive oxidant intermediates, antimicrobial molecules, myeloperoxidase and hydrolytic enzymes. Neutrophils are a key player in the innate immune system and constitute one of the most important effectors in sites of inflammation (Fournier and Parkos, 2012).

Evidence reported here suggests that the immune system's response in ASPP2$^{\Delta 3/\Delta 3}$ colonic tissue is significantly more active when compared to WT tissue. To further analyze the extent of the inflammation in ASPP2$^{\Delta 3/\Delta 3}$ colons, the presence of neutrophils infiltrating the mucosa was investigated by studying the expression of myeloperoxidase (MPO), a lysosomal protein produced by neutrophils, by immunofluorescence (Figure 5.2B). In the mucosa of ASPP2$^{\Delta 3/\Delta 3}$ colons, MPO expression was considerably higher than in WT tissue, suggesting increased infiltration of PMN in ASPP2$^{\Delta 3/\Delta 3}$ colonic mucosa (Figure 5.2B).

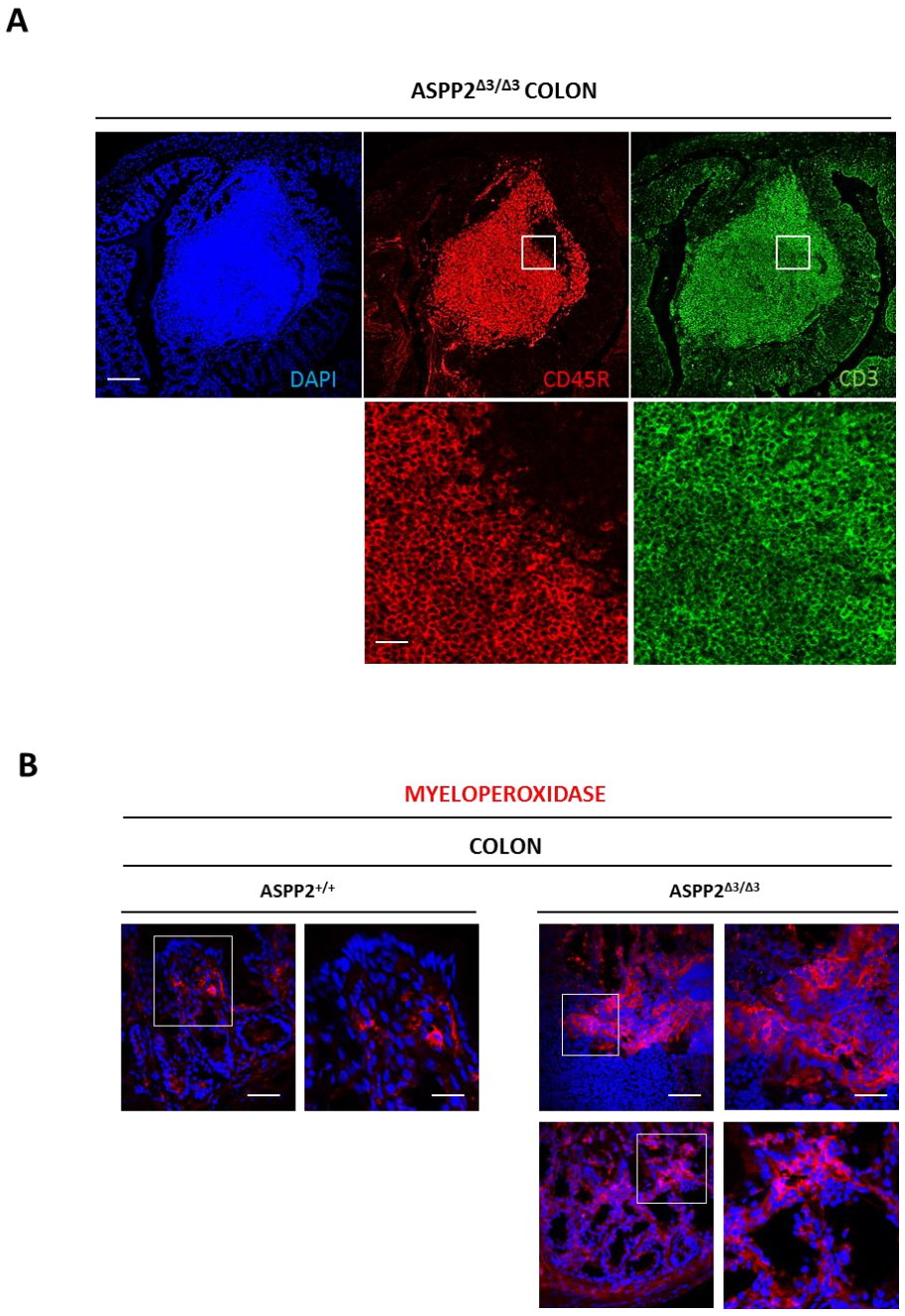


FIGURE 5.2 – Evidence of an active immune response in ASPP2$^{\Delta 3/\Delta 3}$ intestine. (A) Immunofluorescence staining of sections of WT and ASPP2$^{\Delta 3/\Delta 3}$ colons with CD45R (red) and CD3 (green). White squares show high magnification images of the lymphoid aggregate, and CD45R and CD3 stainings. Scale bars: 200µm, 50µm **(B)** Immunofluorescence staining of myeloperoxidase (red) on sections of WT and ASPP2$^{\Delta 3/\Delta 3}$ colons. Nuclei are counterstained with DAPI. Scale bars: 100µm, 30µm.

In sites of inflammation, the regulated production of antimicrobial peptides and cytokines by intestinal epithelial cells and inflammatory cells such as neutrophils, macrophages and T cells is beneficial for the host. On one hand, these molecules can prevent the deleterious consequences of a microbial pathogen invasion. On the other, cytokines exist in a balance of pro-inflammatory and anti-inflammatory molecules and can, therefore, minimize the effects of an inflammatory response while recruiting new inflammatory cells to the site of inflammation (Sanchez-Munoz et al., 2008).

The results reported here suggest that ASPP2$^{\Delta 3/\Delta 3}$ mice have a prominent inflammatory response in the colon. For this reason, the inflammatory response in ASPP2$^{\Delta 3/\Delta 3}$ mice was further characterized by investigating the production of antimicrobial peptides and cytokines. As inflammation in ASPP2$^{\Delta 3/\Delta 3}$ mice seemed to be more significant in the colon than the duodenum, the expression of lysozyme in duodenal tissue was analyzed (Figure 5.3A). The quantification of the protein by western analysis revealed a slight increase in antimicrobial lysozyme in the duodenum of ASPP2$^{\Delta 3/\Delta 3}$ mice (Figures 5.3A). To prevent contamination of our samples with villi epithelial cells and muscle cells, which could compromise the quantification of lysozymal RNA, we first obtained an enriched fraction of duodenal crypts and then extracted RNA from these cells to perform RT-PCR. The lysozymal mRNA levels in the ASPP2$^{\Delta 3/\Delta 3}$ crypt-enriched fraction was significantly higher than in ASPP2$^{+/+}$ cells (6,91±2,84 vs. 0,73±0,38, respectively; $p<0,05$) (Figures 5.3B). These observations suggest that the ASPP2$^{\Delta 3/\Delta 3}$ duodenum produces more antimicrobial peptides than ASPP2$^{+/+}$ tissue.

The production of TNF-α and IL-17 in both ASPP2$^{+/+}$ and ASPP2$^{\Delta 3/\Delta 3}$ colonic tissue was also investigated. TNF-α and IL-17 are known pro-inflammatory cytokines and, therefore, play an important role in modulating the immune response. Various studies have reported evidence that TNF-α and IL-17 are crucial components in intestinal inflammation, and their deregulation is known to be linked to the development of inflammatory bowel diseases such as Crohn's disease. Colonic tissue was therefore used here from both ASPP2$^{+/+}$ and ASPP2$^{\Delta 3/\Delta 3}$ mice, to quantify the mRNA levels of TNF-α and IL-17. In ASPP2$^{\Delta 3/\Delta 3}$ mice, these cytokines were both upregulated when compared to the levels in ASPP2$^{+/+}$ tissue (4,74±3,03 fold change for TNF-α and 8,16±5,85 fold change for IL-17; $p<0,05$) (Figure 5.3C). In agreement with our previous observations, these results support the idea that ASPP2$^{\Delta 3/\Delta 3}$ colonic mucosa show signs of acute inflammation.

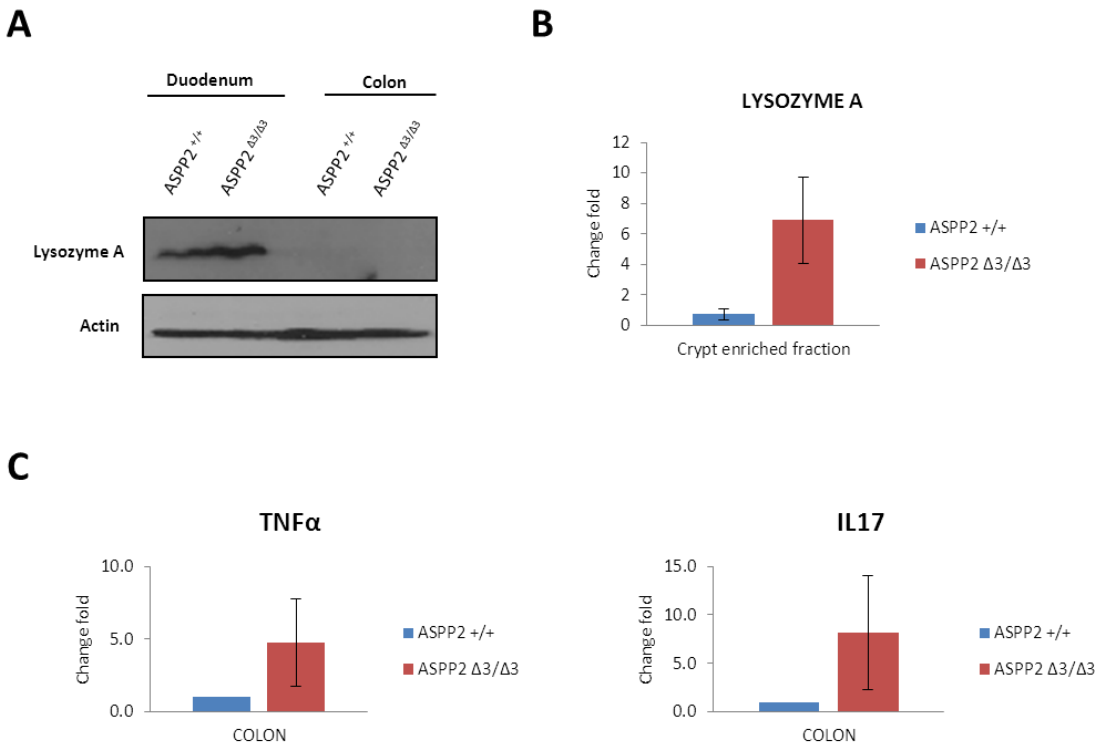


FIGURE 5.3 – The inflammatory response is active in ASPP2$^{\Delta 3/\Delta 3}$ intestine. (A) Western blot of lysates prepared from WT and ASPP2$^{\Delta 3/\Delta 3}$ duodenal tissue. The expression of lysozyme A was studied by loading 80µg of protein and using actin as a loading control. **(B)** Relative expression of lysozyme A mRNA by quantitative RT-PCR using an enriched fraction of murine crypt cells of WT and ASPP2$^{\Delta 3/\Delta 3}$ duodenum. **(C)** Relative expression of TNF-α and IL-17 mRNA by quantitative RT-PCR using colonic tissue.

5.2.2 – ASPP2$^{loxP/loxP}$; Cre^{+}ER MICE ARE MORE SUSCEPTIBLE TO DEVELOPING DSS-INDUCED COLITIS

Tight junctions are often described as the biological door to intestinal inflammation (Fasano, 2011). In fact, the epithelial barrier that exists in the intestine, together with an active immune system response, is an important component of the first line of defense against commensal and pathogenic bacteria (Goto and Kiyono, 2012). The importance of ASPP2 in maintaining the integrity of cell polarity in neuroepithelial cells led us to hypothesize that ASPP2 might be a player in the establishment of a proper intestinal epithelial barrier. Several reports have shown a link between the disruption of epithelial tight junctions and defects in mucosal barrier function in intestinal diseases (Turner, 2009). However, our knowledge of intestinal inflammation in mice lacking tight junction components is still very limited, with occludin and JAM-A-deficient mice remaining the best characterized models (Laukoetter et al., 2007; Schulzke et al., 2005).

ASPP2-deficient mice do not spontaneously develop colitis, despite the evidence suggesting acute inflammation in the colon. In fact, ASPP2$^{\Delta 3/\Delta 3}$ mice appeared to have increased B cell-rich lymphoid aggregates and increased levels of antimicrobial substances and cytokines, even though there was no clinical evidence that they suffered from colitis. Interestingly, the acute immune response observed in ASPP2-deficient mice resembled the one observed in the JAM-A knockout mouse (Laukoetter et al., 2007). Based on these observations, whether or not the absence of ASPP2 was sufficient to predispose ASPP2-deficient mice to an experimentally induced acute colitis was investigated. Oral administration of DSS to mice induces acute or chronic colitis, depending on the time of the treatment and dosage

(Okayasu et al., 1990). Physiologically, the treatment results in the chemical destruction of intestinal epithelial cells, increasing the permeability to commensal bacteria.

To perform this experiment, ASPP2 conditional mice previously generated in our lab were used. The use of these transgenic mice enabled the use of adult mice (3 months old), thus avoiding the premature death of ASPP2$^{\Delta 3/\Delta 3}$ mice by hydrocephalus. In addition, bigger cohorts could be used in the experiments since ASPP2 conditional mice are born according to the Mendelian ratio, in contrast to ASPP2$^{\Delta 3/\Delta 3}$. ASPP2 was confirmed to be expressed in the colon in ASPP2 conditional mice, and its deletion by tamoxifen treatment was successful.

In this experiment, 5% DSS was given to tamoxifen-injected ASPP2 Δexon3 conditional knockout mice, (these mice will be referred to as ASPP2$^{loxP/loxP}$; Cre^{+}ER) on a daily basis for eight days. One control group was established with oil-injected ASPP2$^{loxP/loxP}$ mice and will be referred to heanceforth as wild type (WT). Another control group was given water instead of DSS. The physical condition of all mice was followed every day during the treatment period, and their weight measured to estimate daily weight loss. At the end of the treatment period all mice had survived, even though some of the ASPP2$^{loxP/loxP}$; Cre^{+} mice were very close to the end point as a result of their loss of weight. Anal bleeding was observed in all DSS-treated animals, being more severe in ASPP2$^{loxP/loxP}$; Cre^{+}ER animals when compared to the control littermates (Figure 5.4A). In contrast to the WT animals, which started to suffer bleeding around day 6, ASPP2$^{loxP/loxP}$; Cre^{+} mice suffered from bleeding earlier at around day 4 (data not shown).

Weight loss was noticed at day 3 and was more significant in ASPP2 conditional knockout mice treated with DSS (Figure 5.4 B). Until the last day of treatment, all of the animals treated with 5% DSS lost weight progressively. However, ASPP2 conditional knockout mice lost weight more dramatically and, by day 8, the difference in the percentage of weight lost between wild type and $ASPP2^{loxP/loxP}$; $Cre^{+}ER$ mice was significant (91.7±2.9 vs. 82.8±3.6; p<0,05) (Figure 5.4.B).

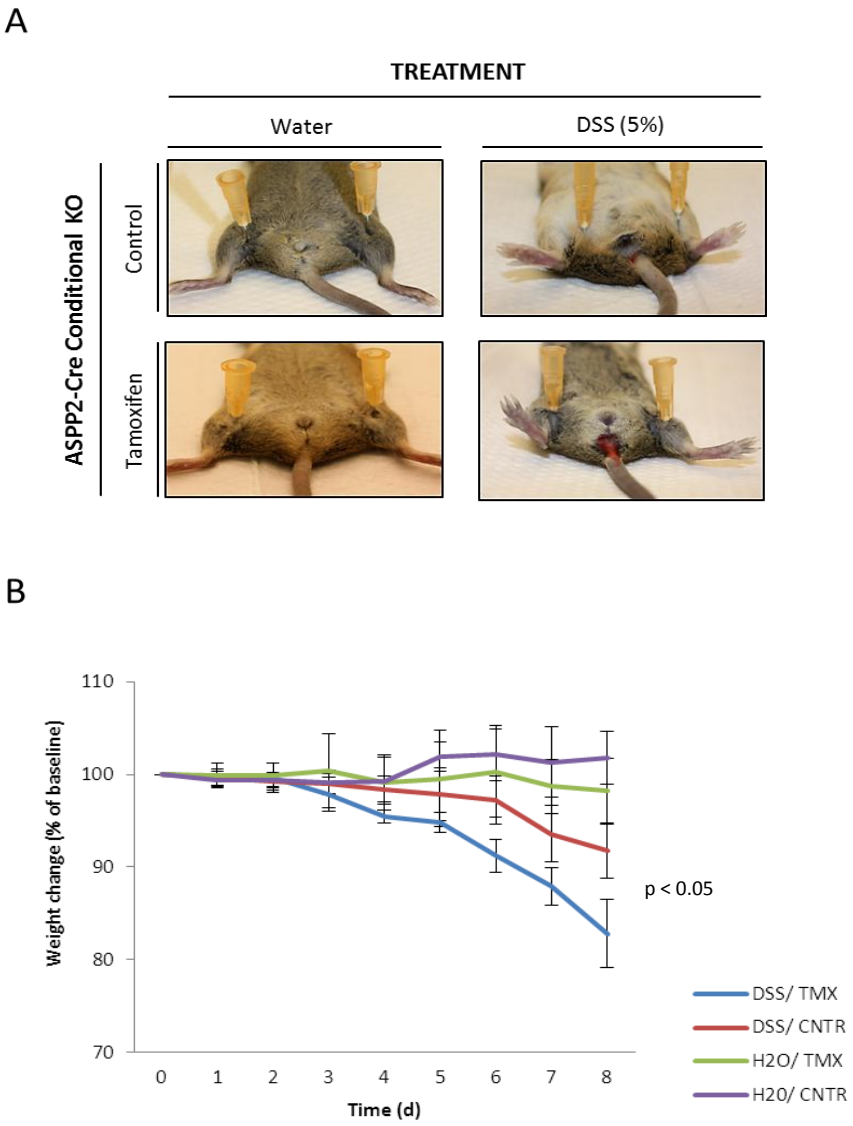


FIGURE 5.4 – ASPP2$^{loxP/loxP}$; Cre^{+}ER mice suffer significant loss of weight and gross bleeding. (A) Observation of gross bleeding in control and ASPP2$^{loxP/loxP}$; Cre^{+}ER mice treated with 5% DSS or water, for 8 days. **(B)** Graphic representation of the mice's weight change throughout 8 days of DSS (n=6) or water treatment (n=4). Baseline is defined as the initial weight of the mouse in the beginning of the experiment (day 0). H_2O, water treatment; DSS, dextran sodium sulphate; TMX, tamoxifen; CNTR, control.

All of the animals in this experiment were monitored on a daily basis. Various clinical parameters, analogous to the ones observed in human IBD such as weight loss, stool consistency, blood loss and appearance, were recorded (Cooper et al., 1993) (Table 5.1).

DISEASE ACTIVITY INDEX				
Score	**% Weight loss**	**Stool consistency**	**Blood loss**	**Appearance**
0	None	Normal stool	None	Lively/normal
1	0-10	Loose stool	Hemoccult positive	Hunched
2	10-20	Diarrhea	Gross bleeding	Starey coat
3	>20			Lethargic

TABLE 5.1 – Disease activity index (DAI) score. Adapted from (Van der Sluis et al., 2006).

Scores were given to each clinical parameter on a daily basis. By averaging these scores, the disease activity index (DAI) was established for every day of the DSS treatment. Similar to that observed with the percentage of weight loss, the disease activity index was higher in mice treated with 5% DSS, when compared to control mice. However, when ASPP2$^{loxP/loxP}$; Cre^{+}ER and WT mice were compared, the former had a significantly higher DAI (Figure 5.5). This difference was mainly due to the fact that ASPP2$^{loxP/loxP}$; Cre^{+}ER mice showed, earlier and more dramatic signs of weight loss, gross bleeding and lethargic appearance, when compared to the control animals. The overall severity of colitis, at day 8, was 8.0±0.5 in the ASPP2$^{loxP/loxP}$; Cre^{+}ER /DSS group vs. 6.17±0.75 in the WT/DSS group (Figure 5.5).

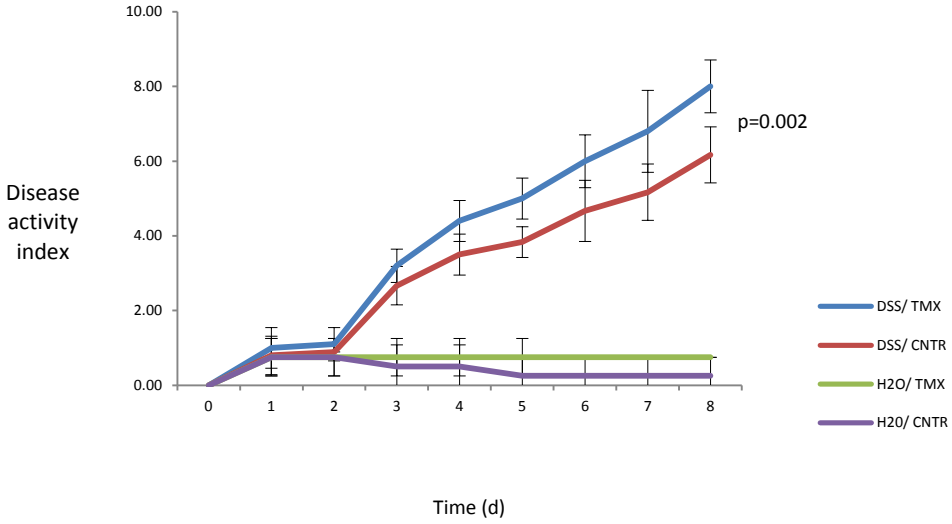


FIGURE 5.5 – DSS-challenged ASPP2$^{loxP/loxP}$; Cre^{+}ER conditional mice score higher in the disease activity index. Disease activity index is defined as the sum of scores obtained for 4 different aspects of DSS treatment: weight loss, stool consistency, blood loss and mouse appearance. The scores were determined every day, for 8 days of treatment. H_2O, water treatment; DSS, dextran sodium sulphate; TMX, tamoxifen; CNTR, control.

Colon length is often taken into consideration as a marker of inflammation. To further investigate the severity of the DSS-induced colitis in ASPP2 conditional knockout mice, we measured the colon length of non-DSS-treated and DSS-treated mice in both WT and ASPP2$^{loxP/loxP}$; Cre^{+}ER mice.

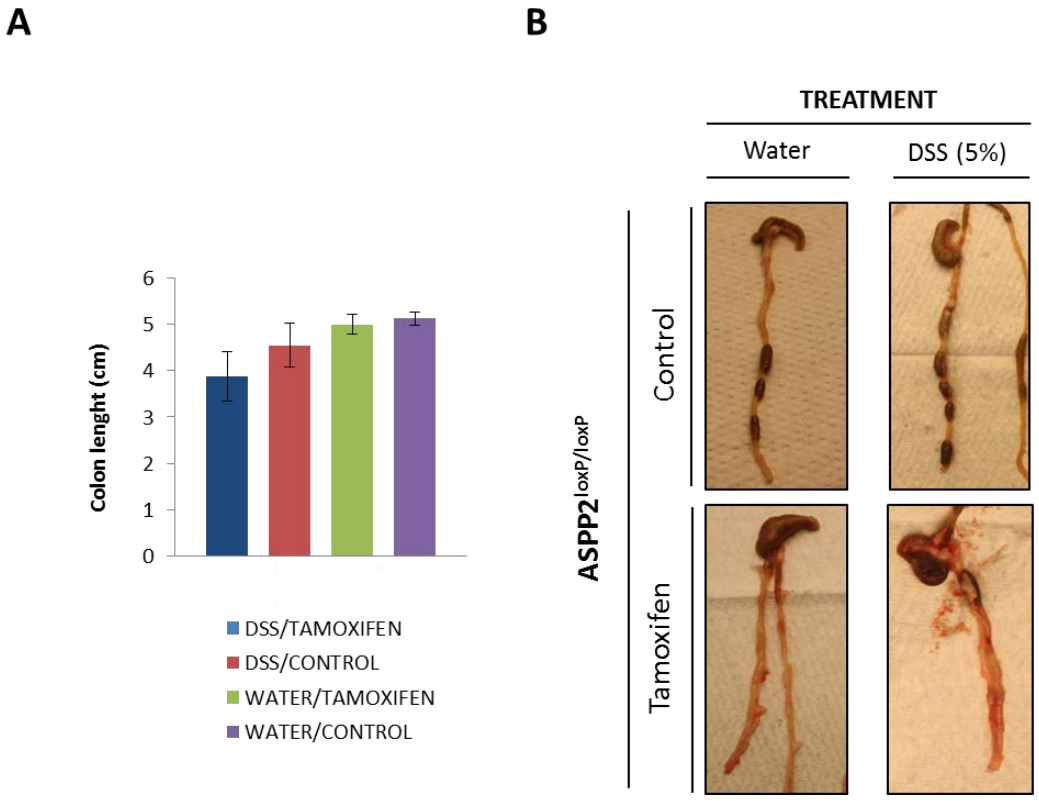


FIGURE 5.6 – DSS-induced colitis results in shortening of the colon in ASPP2 conditional knockout mice. (A) Graphic representation of average colon length in centimetres, for all animal groups studied (p>0,05). **(B)** Overview of the representative colon structure for all four animal groups.

Shortening of the colon was observed in all animals treated with 5% DSS (Figure 5.6A). Despite no significant difference being observed (p>0,05) between DSS-fed ASPP2$^{loxP/loxP}$; Cre^{+}ER mice and the DSS-fed control group, the colon length of ASPP2$^{loxP/loxP}$; Cre^{+} mice animals was shorter (3.88±0.54) than in the WT group of mice (4.55±0.48) (Figure 5.6A). At the time of death, 5% DSS-treated mice were suffering from anal bleeding and no stools were found in the colon, which was shorter and thicker than the control (Figure 5.6B).

The study of DSS-induced colitis has, so far, shown that the conditional loss of ASPP2 increases the physical suffering of animals treated with DSS. One of the hallmarks of DSS-induced colitis is dramatic inflammation and tissue destruction in the colon. Loss of architecture is characterized by crypt destruction, mucosal ulceration, crypt abscesses enriched with neutrophils, and mucosal infiltration by macrophages and lymphocytes (Cooper et al., 1993).

In order to evaluate the extent of colonic inflammation in ASPP2 conditional knockout mice, histological analysis of the colons of non-DSS treated and DSS-treated animals was performed, in both WT and ASPP2$^{loxP/loxP}$; Cre^{+}ER animals. Several histological aspects that characterize the severity of colitis were considered (Van der Sluis et al., 2006) (Table 5.2). The scoring was performed blind, and an average of the scores for each experimental group calculated to represent the overall histological score.

	HISTOLOGICAL SCORE				
	0	**1**	**2**	**3**	**4**
Goblet cells	-	↓	↓↓	↓↓↓	↓↓↓
Mucosal thickening	-	↑	↑↑	↑↑↑	↑↑↑
Inflammatory cells	-	↑	↑↑	↑↑↑	↑↑↑
Submucosa cell infiltration	-	-	↑	↑↑	↑↑↑
Destruction of architecture	-	-	-	↑	↑↑
Ulcers (epithelial cell surface)	0%	0-25%	25%-50%	50-75%	75-100%
Crypt abscesses	None	1-3	4-6	7-9	>10

TABLE 5.2 – Histological score to assess the degree of colonic inflammation. Adapted from (Van der Sluis et al., 2006).

Histological analyses such as H&E and alcian blue staining were used to evaluate the extent of inflammation in the colon. In agreement with previous studies, the colons of DSS-fed control animals were found to show a significant loss of crypts and goblet cells, as suggested by alcian blue staining. Crypt abscesses were found in the colonic tissue. Moreover, a massive infiltration of inflammatory cells was observed in the tissue mucosa. Strikingly, DSS-treated ASPP2$^{loxP/loxP}$; Cre^{+}ER animals revealed a dramatic loss of tissue architecture characterized by the depletion of crypts and goblet cells, as shown by alcian blue staining (Figure 5.7). The thickening of the mucosa was observed in all DSS-treated mice. However, the number of inflammatory cells and the extent of the cell infiltration in the mucosal and submucosal regions was particularly severe in ASPP2-conditionally deleted animals. Epithelial destruction was visible in both groups of animals treated with DSS, control and ASPP2$^{loxP/loxP}$; Cre^{+}ER animals. However, the loss of colonic structures was

particularly evident in ASPP2$^{loxP/loxP}$; Cre^{+}ER animals. For this reason, crypt abscesses were rarely found due to the significant loss of architecture (Figure 5.7).

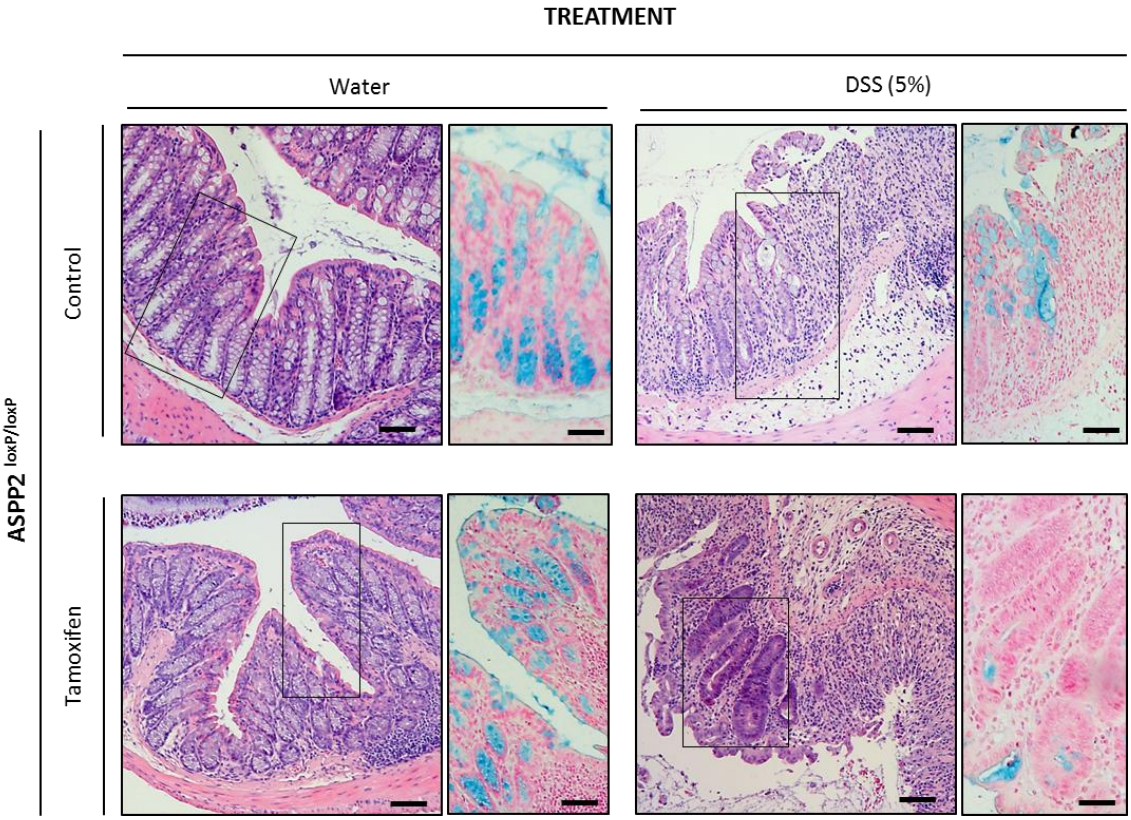


FIGURE 5.7 – Loss of ASPP2 increases susceptibility to DSS-induced colitis. H&E staining on paraffin sections of colon from ASPP2$^{loxP/loxP}$; Cre^{+} and WT animals, fed with water or DSS (5%), after 8 days of treatment. Squares represent higher magnifications of the alcian blue staining of colonic crypts. Scale bars: 150µm, 100µm.

All of the histological parameters observed and described previously (Figure 5.7) were considered to establish a histological score (Figure 5.8). The histological score was considerably higher in DSS-treated animals. However, the histological signs of inflammation were prominent in ASPP2$^{loxP/loxP}$; Cre^{+}ER animals in comparison with DSS-treated WT mice. Histological scores of 21.2±2.3 and 15.2±4.0 were observed in DSS-treated ASPP2$^{loxP/loxP}$; Cre^{+}ER and DSS-treated WT mice, respectively ($p<0,05$) (Figure 5.8).

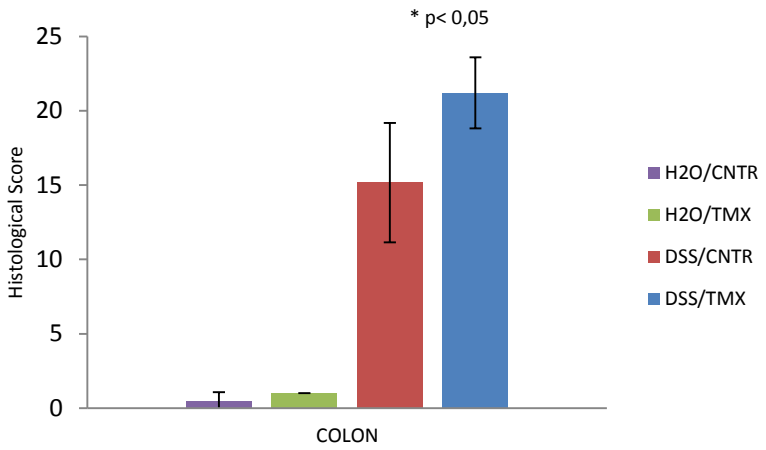


FIGURE 5.8 – Histological score of DSS-treated ASPP2$^{loxP/loxP}$; Cre^{+}ER mice. Graphic representation of the histological score following DSS-induced acute colitis. Histological score is defined as the sum of scores obtained for 7 different aspects of DSS treatment: loss of goblet cells, mucosal thickening, the presence of inflammatory cells, submucosal cell infiltration, loss of epithelial architecture, epithelial ulcerations and crypt abcesses. The scores were determined by histological analysis. H_2O, water treatment; DSS, dextran sodium sulphate; TMX, tamoxifen; CNTR, control.

5.2.3 – ASPP2 IS DOWNREGULATED IN THE COLONIC EPITHELIA OF CROHN'S PATIENTS

Crohn's Disease (CD) and ulcerative colitis (UC), commonly referred to as inflammatory bowel diseases (IBDs), are examples of chronic intestinal disorders. In patients suffering from CD, any part of the gastrointestinal tract can be affected, whereas in UC the disease is limited to the colon (Podolsky, 1991). Although the precise cause of IBD remains to be found, it has been widely accepted that genetic predisposition, immune cell deregulation and environmental factors, such as the gut microbiota, are all important contributors to the disease's pathogenesis (Fiocchi, 1998). IBDs are characterized by recurrent inflammation, exacerbation and latent periods. At the peak of the disease, PMNs transmigrate across the epithelial monolayer, via a paracellular route, inducing inflammation at the intestinal surface and generating crypt abscesses (Kucharzik et al., 2001). The process of transmigration is facilitated by an increase in intestinal permeability, which results from a downregulation of tight junctional components. This observation is supported by the fact that patients with IBD suffer from relapsing diarrhea, which is often associated with impaired paracellular permeability in the inflamed intestinal epithelium (Mankertz and Schulzke, 2007). Evidence that IBD patients suffer from increased intestinal paracellular permeability was first reported more than 25 years ago and, since then, it has been widely accepted that the intestinal barrier function of these patients is compromized (Hollander et al., 1986; May et al., 1993). The dysfunction of the epithelial barrier can be a contributor in the multi-factorial range of causes for the development of IBD. However, different mouse models have shown that disruption of the epithelial tight junctions *per se* is not sufficient to

cause disease, and have implied that a subtle crosstalk between epithelial cell integrity and immune cells must exist to prevent more dramatic phenotypes than the ones observed (Laukoetter et al., 2007; Su et al., 2009). For instance, increased activity of intestinal epithelial myosin light chain kinase (MLCK) is known to be associated with tumor necrosis factor-induced barrier dysfunction, and is a hallmark of human IBD. However, a study of transgenic mice expressing constitutively active MLCK revealed that, despite increased intestinal paracellular permeability, the mice did not show any symptoms or histological features of colitis (Su et al., 2009). In a $JAM^{-/-}$ mouse model, epithelial barrier permeability was increased but this did not increase the susceptibility of the mice to developing spontaneous colitis (Laukoetter et al., 2007). Remarkably, although it remains unclear whether abnormal epithelial barrier function precedes or is a consequence of active inflammation, recent studies have shown that unaffected first degree relatives of IBD patients suffer from increased intestinal permeability as well (Katz et al., 1989). Several studies have analyzed the expression and location of tight junction proteins, such as JAM-A, claudin-1 and ZO-1, in mucosal tissue from patients with chronic active ulcerative disease. In agreement with the hypothesis stated before, the expression levels of tight junctions are downregulated or are misplaced at sites of active intestinal inflammation when compared to control biopsies (Das et al., 2012; Kucharzik et al., 2001; Vetrano et al., 2008). Taking into consideration all of the studies described previously, and the data obtained from ASPP2 knockout mice presented thus far, it was hypothesized that ASPP2' role in the maintenance of tight junctions is disrupted in CD patients. To investigate whether the expression of ASPP2 was affected, paraffin sections from CD patients were obtained, as well as biopsies that were

used as positive controls. In order to understand whether ASPP2 expression was compromized in Crohn's colonic epithelium, immunohistochemical analysis was performed (Figure 5.9). ASPP2 staining was never consistent within the samples. In healthy human colonic tissue, ASPP2 was found to be expressed in the cytoplasm, nucleus or both subcellular locations (n=7) (Figure 4.9). In contrast, the analysis of Crohn's sections revealed that ASPP2 expression was predominantly cytoplasmic, but significantly downregulated when compared with healthy colonic tissue (n=7) (Figure 5.9).

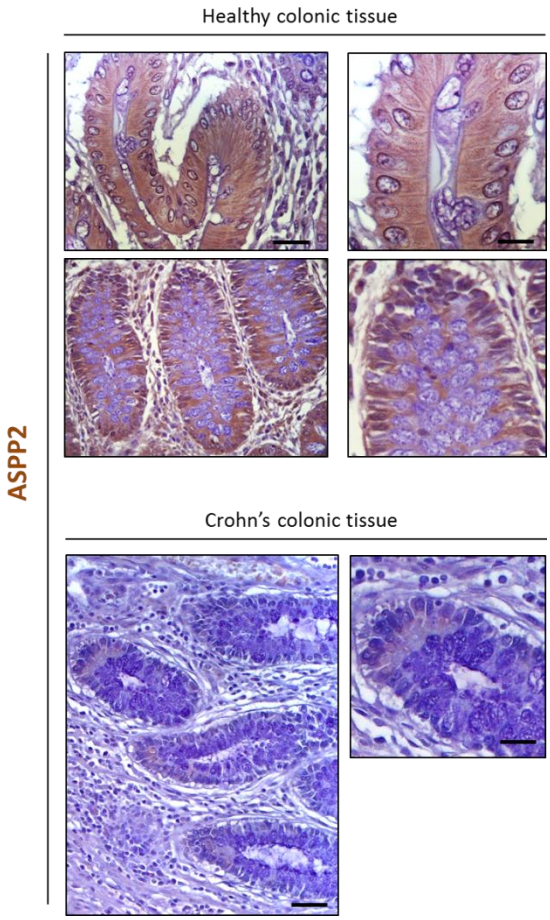


FIGURE 5.9 – ASPP2 expression is altered in Crohn's colonic tissue. Immunohistochemical staining of ASPP2 on paraffin sections of human healthy and Crohn's disease colonic mucosa. Scale bars: 75µm, 25µm.

5.2.4 – ASPP2 EXPRESSION AND CELLULAR LOCALIZATION ARE MODULATED BY TNF-α PRODUCTION AND HYPOXIC CONDITIONS.

What drives the downregulation of ASPP2 in chronic inflammatory disorders such as CD is unclear. However, it is possible that the synergy of different biological and environmental factors, together with the breakdown of tight junctions, can trigger the disease. Several studies have considered inflammatory cytokines, oxidative species and enteropathogens as the center of IBDs, being putative enemies of the intestinal homeostasis when dyregulated (Mankertz and Schulzke, 2007). It is well established that in patients suffering from IBD, levels of pro-inflammatory cytokines are significantly higher than in healthy individuals. In particular, CD patients produce elevated amounts of tumor necrosis factor alpha (TNF-α) and interferon-gamma (IFN-γ), characteristic of a Th1-mediated inflammatory response (Sawa et al., 2003). In animal mouse models, neutralization of TNF-α has been shown to dramatically reduce the inflammatory response in DSS-induced colitis (Kojouharoff et al., 1997). In agreement, the deleterious role of TNF-α and IFN-γ in CD progression has been considered for many years. For the past 15 years, the application of anti-TNF-α and anti-IFN-γ treatments has benefitted many CD patients, by downregulating these inflammatory cytokines in the inflamed intestinal mucosa (Agnholt and Kaltoft, 2001; van Dullemen et al., 1995).

Various *in vitro* works have reinforced the perspective that inflammatory cytokines regulate the stability of tight junctions and, consequently, modulate the paracellular permeability of epithelial cells. The increase in permeability observed in cells upon treatment with TNF-α and IFN-γ, is characterized by a decrease in transepithelial resistance (TER) and increased paracellular flux of solutes. In

particular, TNF-α was shown to downregulate the levels of occludin mRNA in HT-29 cells, whereas IFN-γ was found to affect barrier function in T84 cells by downregulating ZO-1 mRNA and protein levels (Mankertz et al., 2000; Youakim and Ahdieh, 1999). In addition, upon treatment with TNF-α and IFN-γ, ZO-1 and occludin were found to be mislocalized from the site of cell-cell contact, mimicking that was observed in patients with CD (Oshitani et al., 2005).

Considering the results presented here, it is possible that ASPP2 might play an important role in protecting intestinal epithelial cells from the harmful effects of an inflammatory response. On one hand, ASPP2-deficient mice show signs of exarcebated inflammation and are more susceptible to developing DSS-induced colitis. On the other, ASPP2 can be downregulated in CD inflamed mucosa. It is therefore hypothesized that the downregulation of ASPP2, in agreement with that observed for other tight junctional proteins, may be due to the effect that an overproduction of pro-inflammatory cytokines has on barrier function in CD patients. For this reason, the expression levels of ASPP2 in both U2OS and Caco-2 cell lines upon treatment with TNF-α were investigated. Different time points of TNF-α treatment were considered, but only a single concentration of 10ng/ml was used (He, 2012). In both cell lines, the administration of TNF-α resulted in a time-dependent downregulation of ASPP2, becoming significant around 12 hours of TNF-α treatment (Figure 5.10A). Interestingly, it has been shown that ZO-1 is downregulated after 6 hours of treatment, whereas occludin is disrupted later, after around 24 hours of treatment (He et al., 2012). Importantly, the downregulation of ASPP2 was apparently more significant in U2OS cells than in Caco-2 (Figure 5.10A). To further understand the effect of TNF-α on the cellular localisation of ASPP2,

immunofluorescence staining was performed on cells that had been treated with the pro-inflammatory cytokine. This experiment revealed that, in a time-dependent response, ASPP2 was dislocated from the tight junctions upon treatment with TNF-α (Figure 5.10B). This mislocalization of ASPP2 became noticeable after 12 hours of treatment, as a significant fraction of tight junctions looked disrupted. After 48 hours, ASPP2 could hardly be perceived at the level of tight junctions (Figure 5.10B). These observations suggest that ASPP2's protein levels and cellular localization can indeed be affected by the pro-inflammatory cytokine TNF-α. It is therefore possible that, together with other tight junction proteins such as ZO-1 and occludin, ASPP2 plays a role in the establishment of the epithelial barrier in the intestine and consequently becomes a target under acute and chronic inflammatory conditions.

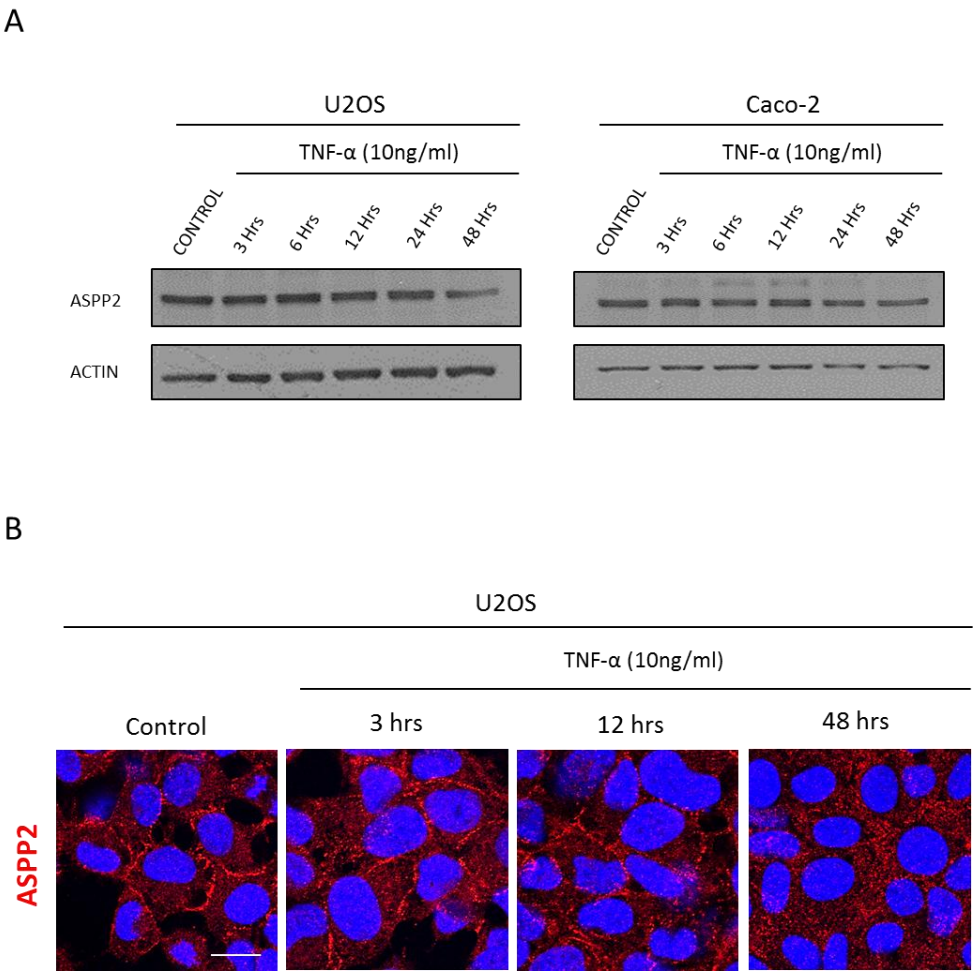


FIGURE 5.10 – TNF-alpha treatment induces downregulation of ASPP2. (A) Western blot analysis using 80µg of protein lysate from U2OS and Caco-2 cells. Cells were kept at 37˚C during the experimental procedure. 10ng/ml TNF-α was administered to the cells for a duration of 3, 6, 12, 24 and 48 hours. Protein levels of ASPP2 were analyzed. Actin protein levels were used as a loading control. Control lysate was obtained from cells that were not treated with 10ng/ml TNF-α. **(B)** Immunofluorescence staining of ASPP2 in U2OS cells to which 10ng/ml TNF-α was administered for 3, 12 and 48 hours. Control cells were not treated with 10ng/ml TNF-α. Nuclei were counterstained with DAPI. Scale bars: 15µm.

Another factor that can contribute to the disruption of tight junctions, although less explored than the influence of cytokines, is the production of oxidative species and the hypoxic environment generated under inflammatory conditions. In fact, overexpression of HIF-1α has been described in surgical specimens of active CD patients (Giatromanolaki et al., 2003).

IBDs result from the amplification of an uncontrolled and sustained immune reaction by the host (Duchmann et al., 1995). The immune response is, therefore, characterized as a two-edged sword since its beneficial contributions to prevent inflammation can become, whenever they are dysregulated, deleterious to the host. The hyperactivation of numerous neutrophils at the inflammatory sites results in a powerful oxidative burst which forces the intestinal tissue to be exposed to a harmful arsenal of toxic and damaging substances, such as reactive oxygen metabolites, for a prolonged time (Kruidenier and Verspaget, 2002). This presence of oxidative species contributes to the creation of a hypoxic environment in the region affected by inflammation. As a consequence, hypoxia activates the NF-κB pathway by increasing the expression and signaling of TLRs, which then stimulate the production of antimicrobial substances, phagocytosis and leukocyte recruitment (Eltzschig and Carmeliet, 2011). The association between ROS and epithelial barrier dysfunction remains unclear. However, important studies have suggested that the increase in epithelial permeability observed in cells treated with TNF-α and IFN-γ is accompanied by an increase in the production of inducible nitric oxide synthase (iNOS), explaining the increase in NO· observed in these studies (Chavez et al., 1999a; Chavez et al., 1999b; Unno et al., 1995). Further investigations have revealed that the production of NO· can indeed alter the permeability of the intestinal

epithelial barrier (Salzman, 1995). In particular, it has been shown that NO· directly affects the expression of ZO-1, as well as the cellular localization of ZO-1, occludin and claudin-1 in Caco-2 cells (Han et al., 2003). The increase in permeability can be blocked by inhibiting iNOS expression in Caco-2, following incubation with pro-inflammatory cytokines, namely IFN-γ and TNF-α (Unno et al., 1995).

To determine whether ASPP2's expression could be altered upon hypoxic conditions, which resemble the ones found in inflamed tissues, U2OS cells were grown under hypoxic conditions (1% O_2) and the expression and cellular location of ASPP2 analyzed (Figure 5.11). Similarly to that observed when the cells were treated with TNF-α, ASPP2 was downregulated under hypoxic conditions. However, time-dependent downregulation was not observed in the first 4 hours of treatment (Figure 5.11A). In fact, ASPP2's expression was momentarily upregulated and only started to decrease after 4 hours of hypoxia. Importantly, around the same time point, upregulation of hypoxia-inducible factor 1 alpha (HIF-1α) was observed, suggesting that the downregulation of ASPP2 and upregulation of HIF-1α are associated (Figure 5.11A). In agreement with these observations, the cellular localization of ASPP2 was altered under hypoxic conditions. In the first four hours of hypoxia, ASPP2 was strongly expressed at the level of the tight junctions (Figure 5.11). In contrast, after being under hypoxic conditions for 8 hours, ASPP2 levels were decreased and its cellular location altered, being less expressed at the cell-cell contacts (Figure 5.11B). These preliminary results reveal that ASPP2's expression and location are modulated by hypoxic conditions, and thus constitute a starting point from which we can better understand what happens in inflamed mucosal tissue in the intestine.

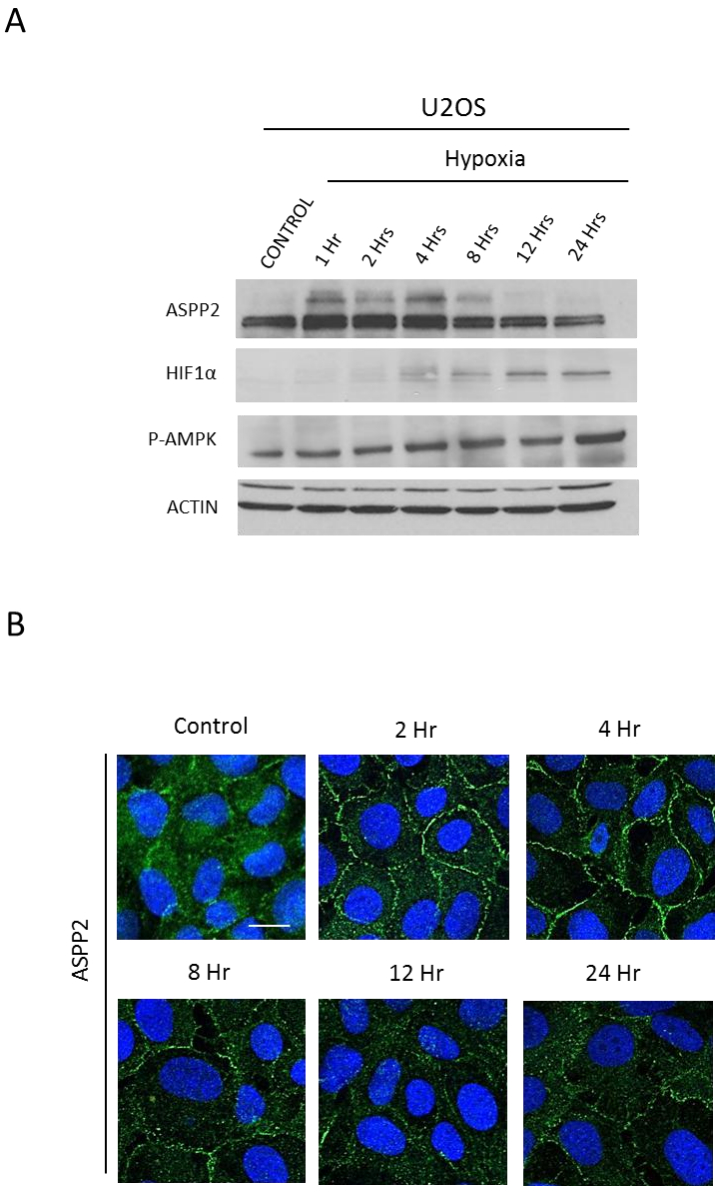


FIGURE 5.11 – Downregulation and mislocalization of ASPP2 under hypoxic conditions. (A) Western blot analysis using 80µg of protein lysate from U2OS cells. Cells were kept under hypoxic conditions (1% O_2) for 1, 2, 4, 8, 12 and 24 hours. Protein levels of ASPP2, HIF1α and p-AMPK were analyzed. Actin protein levels were used as a loading control. Control lysate was obtained from cells kept under normoxia (10% O_2). **(B)** Immunofluorescence staining of ASPP2 in U2OS cells which underwent hypoxic treatment (1% O_2) for 2, 4, 8, 12 and 24 hours. Control cells were kept under normoxia (10% O_2). Nuclei were counterstained with DAPI. Scale bar: 20 µm.

5.2.5 – NORMAL LOCALIZATION OF ASPP2 IS DISRUPTED IN THE COLON OF *HELICOBACTER HEPATICUS* INFECTED MICE

Despite the scarcity of information concerning the modulation of tight junctions by the immune system, it is widely accepted that the weakening of tight junctions leaves a door open for many environmental threats, such as the gut microbiota. On one hand, enteropathogens promote mislocalization of the tight junctional proteins whereas, on the other hand, they behave opportunistically by invading the host through disrupted paracellular spaces (Guttman and Finlay, 2009). From both perspectives, however, tight juctions play a crucial role in the protective mechanisms acquired by the host.

Several studies have reported examples of how bacteria can subvert the host through its epithelial cell polarity. However, there is currently no evidence to suggest that the subcellular localization of ASPP2 can be affected by colonic pathogens. The recently described interaction between ASPP2 and the *Helicobacter pylori* effector protein CagA, shows that opportunistic pathogens can subvert the function of ASPP2 enable their invasion of the host (Buti et al., 2011). We, therefore, decided to investigate the *in vivo* expression of ASPP2 in colonic samples of mice experimentally infected with *Helicobacter hepaticus.* Persistent infection with *H. hepaticus* does not induce colitis in most WT mouse strains (Fox et al., 2011). However, it has been reported that T-cell deficient recombination activation gene 2-deficient ($Rag2^{-/-}$) mice are susceptible to *H. hepaticus* infection and are, therefore, used as experimental models of colitis (Izcue et al., 2006). We obtained colonic samples of $Rag2^{-/-}$ *H. hepaticus*-infected mice and performed immunofluorescence staining of ASPP2 (Figure 5.12). In healthy non-infected tissue,

ASPP2 was expressed in intestinal epithelial cells and located at the tight junctions (Figure 5.12A). However, in colonic samples of *H. hepaticus*-infected animals, ASPP2 was mislocalized from the tight junctions, and instead located at the basal domain of epithelial cells (Figure 5.12B). To understand whether other tight junctional proteins are affected by *H. hepaticus* infection the location of ZO-1, a known binding partner of ASPP2 located at the tight junctions in intestinal epithelial cells, was investigated. Interestingly, upon infection, the subcellular location of ZO-1 is normal, suggesting that the mislocalization of ASPP2 is not dependent on disruption of ZO-1's localization (Figure 5.12C). The basal location of ASPP2 was further confirmed with β-catenin immunofluorescence staining. β-catenin is expressed in *H. hepaticus*-infected samples, and does not co-localize with ASPP2 at the lateral domain of intestinal epithelial cells (Figure 5.12D). Our observations revealed that ASPP2's location is disrupted upon intestinal infection with *H. hepaticus*, suggesting that ASPP2's downregulation at inflamed sites may be due to the deleterious consequences of enteropathogen infection of mucosal tissue. Importantly, we were able to show that ASPP2 expression can be modulated by pro-inflammatory cytokines, hypoxia and pathogens, which are together considered hallmarks of chronic inflammatory disorders.

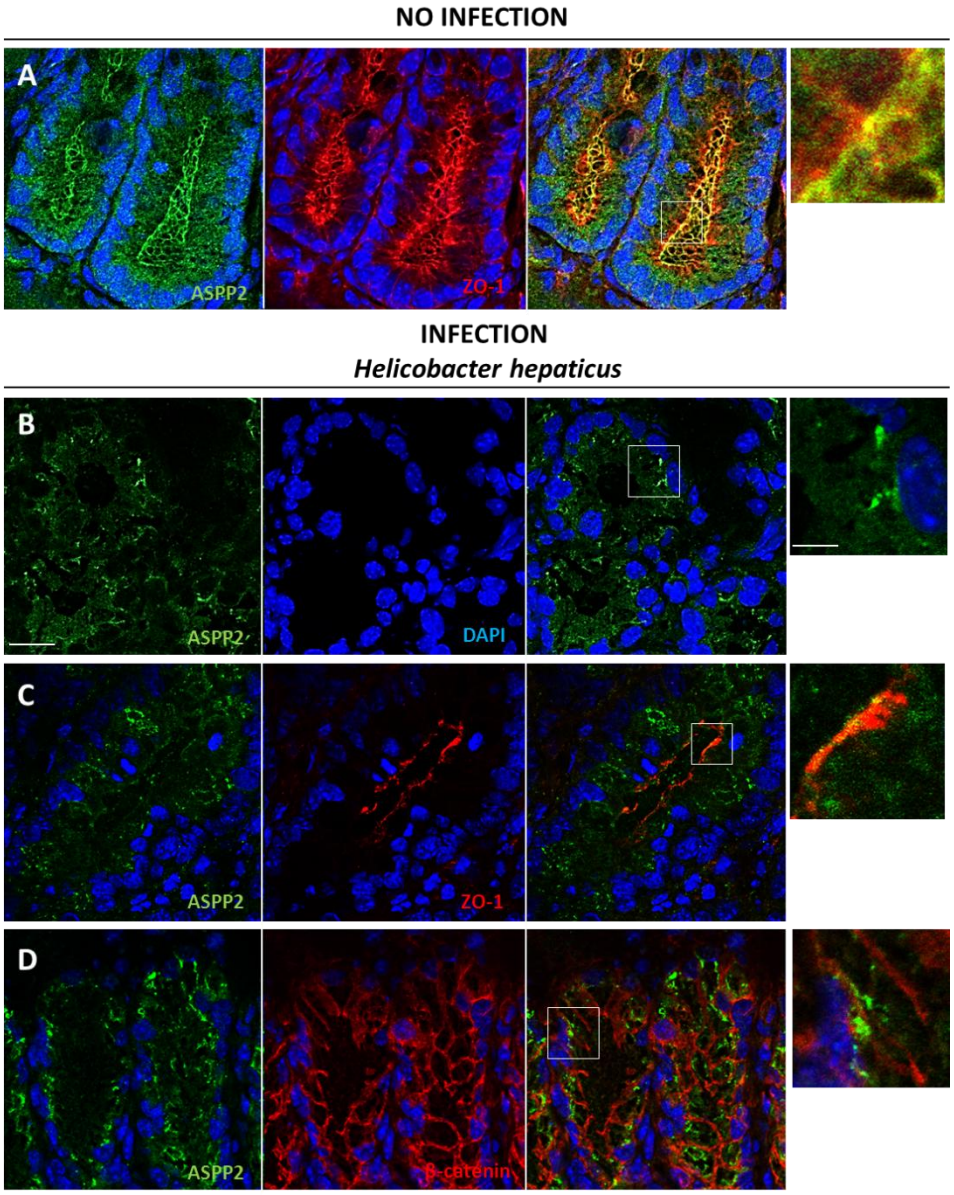


FIGURE 5.12 – ASPP2 is mislocalized upon *H. hepaticus* infection. (A) Immunofluorescence staining of ASPP2 (green) and ZO-1 (red) on frozen sections of WT colonic tissue. **(B)** Immunofluorescence staining of ASPP2 (green) on frozen sections of *H. hepaticus*-infected colon. **(C)** Double immunofluorescence staining of ASPP2 (green) and ZO-1 (red) on frozen sections of *H. hepaticus*-infected colon. **(D)** Double immunofluorescence staining of ASPP2 (green) and β-catenin (red) on frozen sections of *H. hepaticus*-infected colon. High magnification images are depicted to show the location of ASPP2 in detail. Nuclei are counterstained with DAPI. Scale bars: 70µm, 10µm.

5.2.6 – ASPP2-DEFICIENT MICE ARE SUSCEPTIBLE TO CHRONIC DSS-INDUCED COLITIS

Chronic intestinal inflammation is widely accepted as one of the risk factors for colorectal cancer. Genetic mouse models have been generated to study the mechanisms underlying colitis and colitis-associated cancer (CAC). Cyclic administration of DSS in drinking water triggers colitis in mice which, depending on the duration and extension of the resulting inflammation, can result in the development of colorectal dysplasias (Sussman et al., 2012). The pathological characteristics of these tumors mimic those found in human CACs, reflecting the importance of these mouse models in the study of IBDs and tumorigenesis.

The results presented here suggest that ASPP2-deficient mice are susceptible to DSS-induced acute colitis. In addition, it has been described that ASPP2 heterozygosity confers susceptibility to tumour formation *in vivo* (Vives et al., 2006b). However, colorectal tumors have never been observed in ASPP2-deficient or heterozygous mice. Whether ASPP2-deficient mice could develop colorectal cancer after treatment with DSS to induce chronic colitis was, therefore, of interest. The development of DSS-induced colonic neoplasias has been reported in $p53^{-/-}$ mice which, under normal circumstances, do not spontaneously develop colorectal tumors (Fujii et al., 2004). In this mouse model, the colonic neoplasias were triggered by DSS treatment alone. However, the incidence of neoplasias and its progression to cancer can be driven dramatically by the administration of DSS in association with known colonic carcinogens, such as azoxymethane (AOM) (Rosenberg et al., 2009). In contrast with these studies, the decision was taken not to administer a combination of DSS with a colonic carcinogen in this study, the main

reason being that we wanted to understand whether the conditional deletion of ASPP2 was sufficient to induce colonic tumorigenesis in DSS-treated animals. However, it was also hypothesized that ASPP2-deleted colonic tissue does not regenerate as quickly as control tissue, since its epithelial cell integrity is disrupted. Thus, by not using a colonic carcinogenic together with DSS treatment, it would be possible to evaluate the extension of epithelial regeneration after the cycles of treatment, and correlate it to ASPP2 deficiency only.

In our experimental procedure, 2% DSS or water was given to ASPP2$^{loxP/loxP}$; Cre^{+}ER mice on a daily basis, for three cycles. One cycle was defined as 8 days of DSS treatment, followed by 14 days of distilled water. One control group was established with oil-injected ASPP2$^{loxP/loxP}$; Cre^{+} mice. Another control group was given water instead of DSS. By the end of the treatment period, all mice had survived. However, by the end of the second cycle of treatment, severe anal bleeding was observed in ASPP2$^{loxP/loxP}$; Cre^{+}ER mice, which continued for one week post-treatment and gradually became insignificant. The weight of all animals was evaluated daily and the percentage of weight change assessed, based on the initial weight at day 0, for each cycle (Figure 5.13). Weight loss was noticed at day 1 and was more significant in ASPP2$^{loxP/loxP}$; Cre^{+}ER mice treated with DSS (Figure 5.13). Until the last day of treatment, all animals treated with 2% DSS lost weight progressively. However, ASPP2$^{loxP/loxP}$; Cre^{+}ER mice lost weight more dramatically. Although the difference between ASPP2$^{loxP/loxP}$; Cre^{+}ER and the control mice was not significant ($p>0.05$), we observed that ASPP2$^{loxP/loxP}$; Cre^{+}ER mice lost more weight than the controls (94.5±3.5 vs. 96.5±2.2) (Figure 5.13).

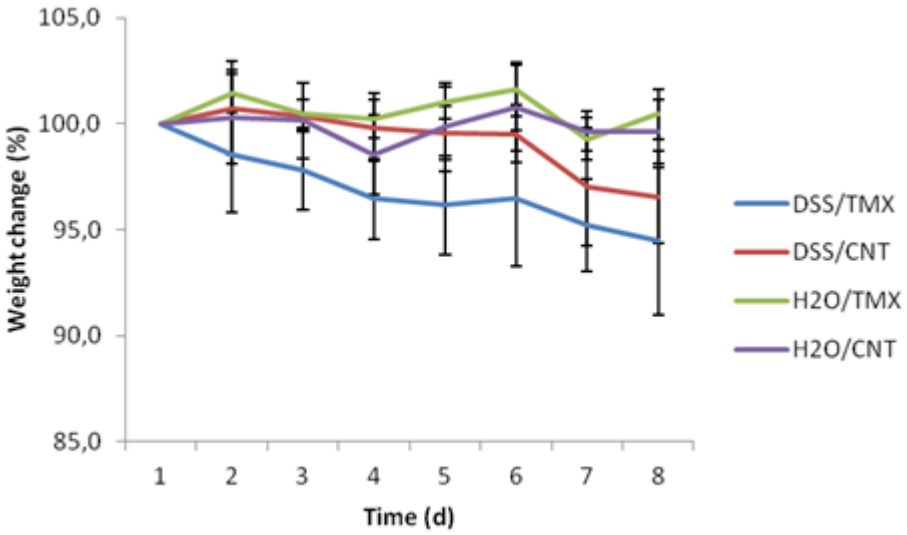


FIGURE 5.13 – Percentage of weight change during the third cycle of treatment is higher in ASPP2$^{loxP/loxP}$; Cre^{+}ER DSS-fed animals. Graphic representation of mouse weight change throughout 8 days of the third cycle of DSS-induced chronic colitis. Baseline is defined as the initial weight of the mice in the beginning of the cycle (day 0). Abbreviations: H_2O, water; DSS, dextran sodium sulphate; TMX, tamoxifen; CNTR, control.

To evaluate the success of the experiment and understand whether the ASPP2$^{loxP/loxP}$; Cre^{+}ER mice were affected by DSS-induced colitis, we culled one mouse of each experimental group and analyzed similar regions of the colon by H&E staining. The histological study revealed that both control and ASPP2$^{loxP/loxP}$; Cre^{+}ER mice were significantly affected by the DSS treatment (Figure 5.14). In both animals, we observed mucosal and submucosal infiltration of inflammatory cells, as well as thickening of the mucosa. However, the loss of architecture was more dramatic in

the ASPP2$^{loxP/loxP}$; Cre^{+}ER mouse. In fact, only a few crypts were detected and, importantly, were depleted of goblet cells (Figure 5.14). It was possible to observe that the control mice treated with 2% DSS still showed crypt structures containing goblet cells after three cycles of treatment, suggesting that the colonic tissue in control mice was less affected by the chemical treatment with DSS, or was able to regenerate its epithelium quicker than the ASPP2$^{loxP/loxP}$; Cre^{+}ER mice (Figure 5.14).

Taken together, the results presented here suggest that ASPP2 plays a role in the integrity of intestinal epithelial cells, possibly by being important for the epithelial barrier function. For this reason, ASPP2 seems to be necessary to protect the animals from the deleterious effects of both acute and chronic DSS-induced colitis. The appearance of colorectal tumors in ASPP2$^{loxP/loxP}$; Cre^{+}ER mice is still under investigation, however, as the decision has been taken not to cull the mice until any symptoms become apparent.

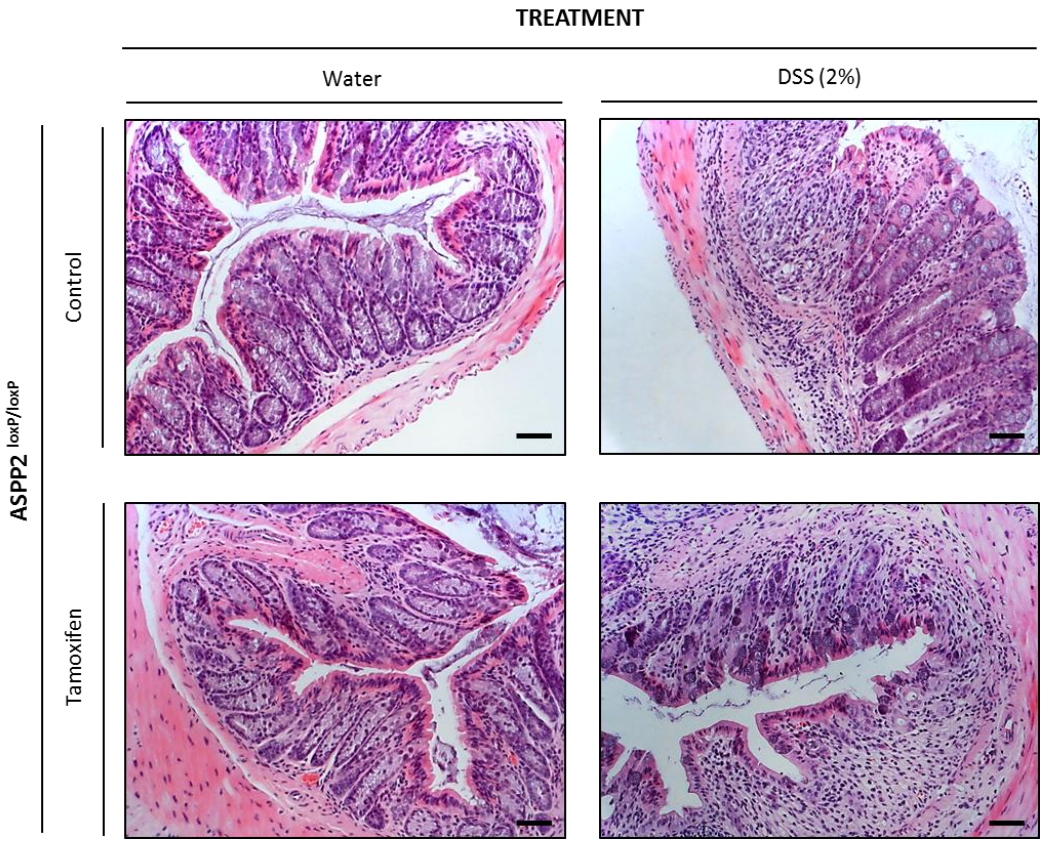


FIGURE 5.14 - Loss of ASPP2 increases susceptibility to chronic DSS-induced colitis. H&E staining on paraffin sections of colon from control and ASPP2$^{loxP/loxP}$; Cre^{+}ER mice, fed with water or DSS (2%), after 3 cycles of treatment. Scale bars: 150µm.

5.3 – SUMMARY AND BRIEF DISCUSSION

In this chapter, signs of intestinal inflammation in ASPP2$^{\Delta 3/\Delta 3}$ colonic epithelia have been examined. In addition, the deleterious effects of inflammatory cytokines, oxygen depletion and *H. hepaticus* infection on the expression and location of ASPP2 have been investigated. Finally, the consequences of ASPP2 deficiency on susceptibility to acute and chronic intestinal inflammation have been analyzed *in vivo*.

Taken together, the results outlined above reveal that ASPP2-deficient mice suffer from mild colonic inflammation, characterized by hyperplasia of individual lymphoid follicles enriched with T and B cells, an overproduction of myeloperoxidase as a result of the neutrophil recruitment, and the overexpression of pro-inflammatory cytokines such as TNF-α and IL-17. Although signs of inflammation in the small intestine were never observed, the levels of lysozyme revealed an upregulation of this antimicrobial substance in the duodenal tissue. Importantly, the signs of intestinal inflammation present in the ASPP2$^{\Delta 3/\Delta 3}$ mouse were not sufficient to trigger disease in the animal, since no evidence of spontaneous colitis was observed. ASPP2's expression and localization was shown to be negatively modulated by the action of pro-inflammatory cytokines, such as TNF-α, hypoxic conditions and enteropathogens like *Helicobacter hepaticus*. Essentially, these observations suggest that ASPP2 plays an important role in protecting the host's epithelial barrier, as it can be subverted by inside mechanisms of uncontrolled immunity as well as by outside environmental threats. The absence of a colitis phenotype in the mice, but the clear evidence that ASPP2's expression prevents intestinal inflammation, led us to investigate whether ASPP2 conditional

knockout mice would be more susceptible to DSS-induced colitis and, ultimately, develop intestinal tumors. These are unfinished experiments, and conclusive evidence on tumorigenesis predisposition has not been obtained. Nevertheless, it has been demonstrated that ASPP2-deficienct mice are more prone to develop acute DSS-induced colitis, and are responsive to chronic DSS-induced colitis, after being administered with DSS when compared to control mice. These results further support the idea that tight junctions are important contributors, although not the only ones, to the tri-partite crosstalk between the epithelial barrier, gut microflora and immune system. Thus, they reinforce the hypothesis that the disruption of tight junctions disrupts cell permeability and increases susceptibility to inflammation, but is not sufficient to trigger colitis and colitis-associated cancer.

CHAPTER 6 – DISCUSSION AND FUTURE PLANS

6.1 – ASPP2, NOTCH and WNT signaling: crosstalk *in vivo*

In this study, evidence has been presented that intestinal cell proliferation and differentiation is abnormal in ASPP2-null mice. Morphologically, the absence of ASPP2 resulted in cell disorganization, enlargement of the villi and variations in the size of the crypts, particularly in the colon. In addition, a significant expansion of proliferative cells was observed upon ASPP2 deletion, in both the duodenum and colon. These observations were further supported by the generation of ASPP2-null organoid cultures. Moreover, the secretory cell lineage was compromised in *ASPP2* Δexon3 duodenum. First, we observed an increase in the number of Paneth cells. Secondly, we noticed the existence of lysozyme-positive cells present at the crypt-villus junction. Finally, we detected an accumulation of goblet cells at the bottom of the proliferative crypts. Importantly, these observations were further supported by the upregulation of *Math1*, *Hes5* and, to a less extent, Hes1. In contrast, the colon of *ASPP2* Δexon3 mice revealed abnormalities in the secretion of mucin, possibly due to a reduction in the number of goblet cells. Taken together, these results provide evidence that epithelial cell maturation and turnover are compromised in ASPP2 Δexon3 intestinal epithelia.

In the intestinal epithelium, the molecular pathways controlling cell positioning, proliferation, death and differentiation are intimately associated and controlled by the crosstalk between the Notch and Wnt signaling cascades. We believe that the

loss of ASPP2 compromises the communication between these pathways, a hypothesis that is supported by previous results obtained by our lab. Firstly, ASPP2 co-localizes and interacts with MAML and RBPJκ, thereby modulating Notch's function *in vitro* (data not published). In addition, ASPP2 partially binds to β-catenin at cell-cell contacts and, for this reason, most likely regulates the decision of β-catenin to choose between adhesion and transcription (Harris and Peifer, 2005; Sottocornola et al., 2010).

Notch plays an essential role in modulating the fate of proliferative intestinal stem cells. Various studies have shown that Notch stimulates cell differentiation towards the absorptive lineage, by laterally inhibiting differentiation towards the secretory lineage *in vivo* (Noah and Shroyer, 2012). In this model, *Hes1* activation drives the cells towards an absorptive phenotype, while repressing the activity of the secretory cell fate determinant *Math1* (Yang et al., 2001). The Wnt signaling cascade provides the driving force for stem cell renewal by maintaining the proliferative state of intestinal crypt progenitor cells, and repressing the differentiation of cells (Fre et al., 2005; Korinek et al., 1998a). *In vivo* studies have revealed that β-catenin and Tcf4 are the main players in this process, since their inhibition results in the complete abrogation of intestinal crypt structures (Fevr et al., 2007; Korinek et al., 1998a). Based on previous reports in the literature, it is surprising to observe a simultaneous upregulation of *Hes1* and *Math1*. Nevertheless, considering our findings, one would expect that the loss of ASPP2 results in a significant increase in differentiated cells, including secretory and absorptive cells. However, the study of ASPP2-null intestine did not reveal a

significant increase in absorptive or secretory number (Figure 6.1). In agreement, an increase in the main markers of differentiated cells was not detected. On the one hand, it is possible that the excessive cell death observed in ASPP2-deficient duodenum balances the increased number of cells migrating along the villi. On the other, despite the observed increases in *HES1* and *Math1*, no evidence was obtained to suggest that downstream transcription factors, which are required to generate different cell lineages, are also upregulated. Therefore, it is possible that the transcription of Klf4, Ngn3 and Sox9 is not significantly enhanced in ASPP2-deficient mice, hence counteracting the effects of *Hes1* and *Math1* action (Figure 6.1).

Remarkably, it was noticed that cell organization and bilateral migration of differentiated cells along the crypt/villi axis was compromised upon the loss of ASPP2 (Figure 6.1). In particular, goblet cells were found in the bottom of proliferative crypts, and the positioning of Paneth cells in the transition between the crypt and the villus was detected (Figure 6.1). This increase in cell disorganization may be due to an excess of proliferating cells creating pressure on cells to migrate towards the lumen. However, the mislocalization of goblet and Paneth cells suggests that, despite the existence of a driving force stimulating cells to migrate, the mechanisms regulating the positioning of the cells are compromised in ASPP2-deficient mice.

Differentiated cells are positioned along the villi according to gradients established by the receptors EphB2/EphB3, and the ligand EphrinB1 (Batlle et al., 2002). Importantly, several reports have shown that Wnt and Notch signaling regulate the expression of these receptors and ligand (Batlle et al., 2002). In fact,

these gradients have been shown to be disturbed in various mouse models, such as Fdz5 KO, EphB2/EphB3 KO, Hes1/Hes3/Hes5 KO and overexpression of Dickkopf-1 (Batlle et al., 2002; de Lau et al., 2007; Deschenes et al., 2001; Ueo et al., 2012). Two reports have shown that EphrinB1 interacts with Par-6 and claudins. In addition, the integrity of epithelial cell-cell contacts might be determinant for the activity of EphrinB1 (Lee et al., 2008; Tanaka et al., 2005). Therefore, the phenotype observed in this study in ASPP2-deficient mice suggests that ASPP2 might be an important player in the regulation of EphB/EphrinB complexes by Notch signaling. Loss of ASPP2 disrupts the Par complex and it might, consequently, affect the association of EphrinB to cell polarity proteins. Deficiency of ASPP2 can, therefore, destabilize the expression gradient EphrinB1, prevent its binding to the receptors EphB2 and EphB3 and, ultimately, lead to the wrong positioning of cells along the villi.

In the future, we would like to better understand whether the loss of ASPP2 compromizes the stability and gradient of EphrinB1 *in vitro* and *in vivo*, and the intestinal organoid culture system may be a powerful tool with which to investigate the dynamics of intestinal cell turnover. This system will be used to further explore the implications of ASPP2's deletion on the regulation of the Notch and Wnt signaling pathways. By taking advantage of well described Notch and Wnt inhibitors, such as γ-secretase and Dickkopf-1, we will be able to modulate these key signaling pathways and better understand their roles in ASPP2-null cells.

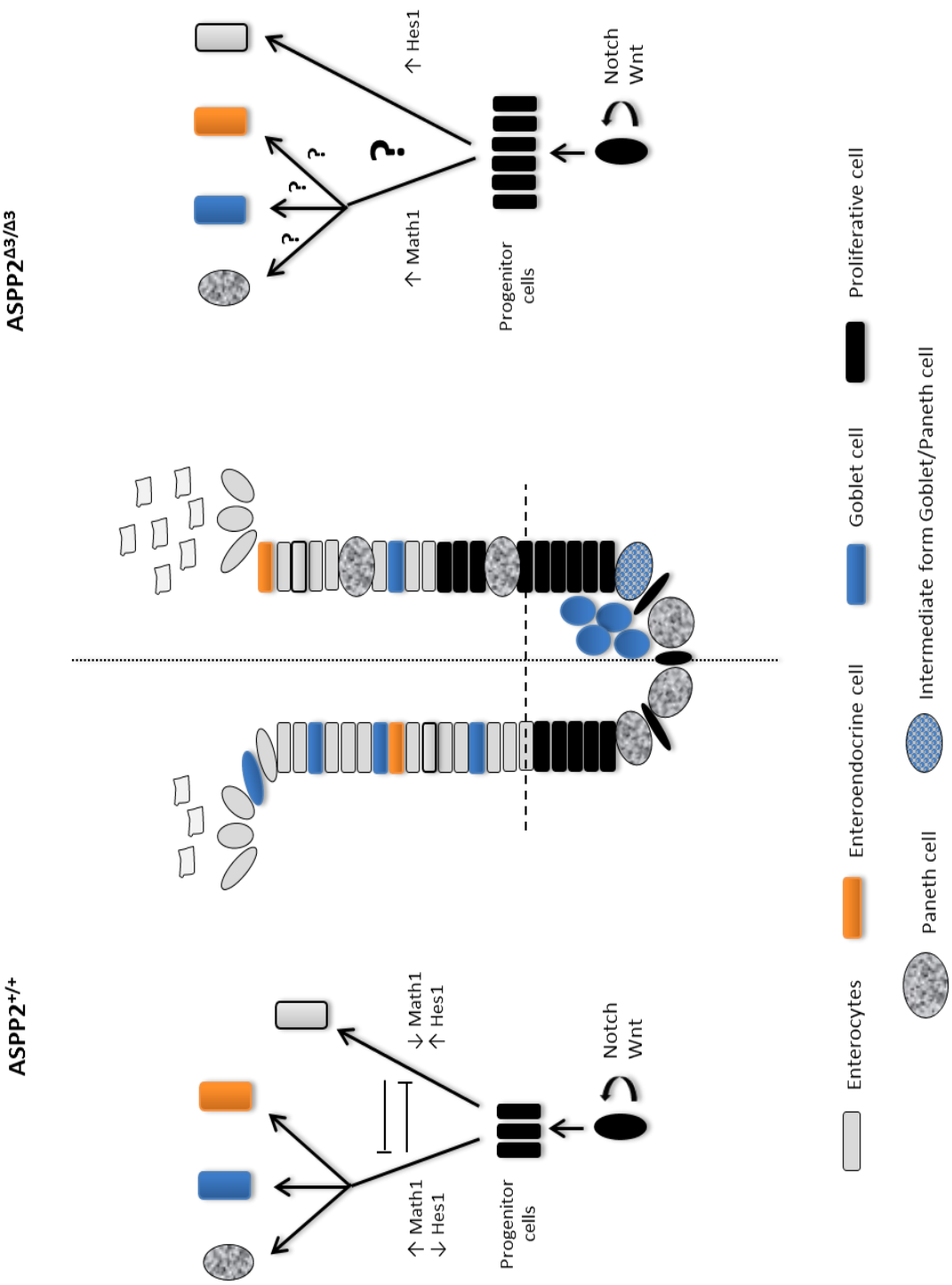


FIGURE 6.1 – Modulation of intestinal homeostasis by ASPP2. Increased cell death, proliferation and misplacement of goblet and Paneth cells are observed in ASPP2$^{\Delta3/\Delta3}$ mice. The phenotype of ASPP2$^{\Delta3/\Delta3}$ mice may be due to abnormalities in the Notch and Wnt signaling pathways: lateral inhibition by Notch is compromised in ASPP2$^{\Delta3/\Delta3}$ mice, and Wnt signaling is more active. Bilateral migration of Paneth and goblet cells is inversed in ASPP2$^{\Delta3/\Delta3}$ mice.

6.2 – ASPP2 and the intestinal epithelium: one role, different outcomes

This study has revealed that ASPP2 is located at the tight junctions in both duodenal and colonic epithelia. In the colon and, to a lesser extent, the duodenum, the expression of cell polarity components was compromised in ASPP2 Δexon3 mice. One fact that surprised us was the realization that the phenotypes in the duodenum and colon are very distinct. Clearly, ASPP2 has different roles in these organs. Most of the studies of tight junctions in the small intestine to date have focused on metabolism, whereas in the colon the link between tight junctions and inflammation has been widely investigated.

Interestingly, analysis of a gene array performed using duodenal and colonic tissue from $ASPP2^{+/+}$ and $ASPP2^{\Delta 3/\Delta 3}$ mice revealed that the genes most significantly affected by ASPP2 deletion are related to metabolism and cell polarity, respectively (data not shown). It is possible that the importance of ASPP2 as a cell polarity protein is tissue-dependent. For instance, it is known that the expression of claudins modulates ion selectivity by altering paracellular permeability, hence its study in the context of metabolism. However, little is known about the role of claudins in the prevention of intestinal inflammation. Conversely, the protective role of JAM-A against colonic inflammation has been widely accepted, but nothing is known about its contribution in the duodenal epithelium. This study has shown that is possible for one cell polarity regulator, such as ASPP2, to have different biological roles depending on the epithelial context where is expressed, and on the events that take place in the tissue. For this reason, the following discussion will consider the putative role of ASPP2 in the duodenum and colon separately.

6.3 – ASPP2: a putative link between cell polarity and metabolism

The *in vitro* work reported here shows that ASPP2 is modulated by the levels of glucose. In the first hours of glucose deprivation, ASPP2 is upregulated and promptly recruited to cell-cell contacts in U2OS cells. In this cell line, ASPP2 is not particularly polarized at the tight junctions, therefore, changes in the localization of ASPP2 are easily noticed when the formation of tight junctions is stimulated. Interestingly, the combination of AICAR with glucose deprivation resulted in a synergistic effect on ASPP2 expression. Furthermore, it was observed that Compound C (a specific chemical inhibitor of AMPK) downregulated ASPP2, and that ASPP2 deletion resulted in the phosphorylation of AMPK when combined with glucose deprivation. Interestingly, ASPP2 depletion promoted the translocation of LKB1 to the cytoplasm. In investigating the putative interaction between ASPP2, Mo25 and LKB1, it was found that ASPP2 binds to Mo25 and LKB1 *in vitro*. However, ASPP2 deletion did not affect LKB1/STRAD/Mo25 complex expression levels. The co-localization of ASPP2 and Mo25 was further supported by studies *in vivo*.

Several studies have reported that the assembly of cell-cell contacts, particularly the tight junctions, is intrinsically related to the levels of intracellular AMPK (Zhang et al., 2006; Zheng and Cantley, 2007). Therefore, it is believed that the establishment and maintenance of tight junctions can be modulated by the levels of ATP and, consequently, any energetic stress could lead to the disruption of cell-cell contacts (Zhang et al., 2006; Zheng and Cantley, 2007). Disruption of cell polarity is a hallmark of cancer, therefore, there is increasing acceptance that the alliance

between cell polarity and energy metabolism can function as a protective mechanism to prevent tumorigenesis. Interestingly, many of the features that characterize LKB1 are common to ASPP2. In particular, the analysis of LKB1 and ASPP2 transgenic knockout mice revealed similarities between both phenotypes – although the intestinal phenotype in ASPP2-null mice was less severe – suggesting that these two proteins might have overlapping functions in the same molecular pathways.

Evidence reported here suggests that ASPP2's localization and expression are regulated by AMPK under energetic stress. In addition, it appears that LKB1 is necessary for the AMPK-dependent regulation of ASPP2.

Under energetic stress, such as glucose deprivation, the integrity of the cell-cell contacts is essential to help the cell overcome the stress. In this situation, AMPK is likely to promote the recruitment of cell polarity proteins to the membrane. Not surprisingly, the deletion of a cell polarity regulator like ASPP2 increases the vulnerability of the epithelial cells when they are submitted to glucose deprivation. Therefore, we believe that the loss of ASPP2 triggers a signal to the cell alerting for increased vulnerability, which is translated in the significant phosphorylation of AMPK. Since ASPP2 plays a role as a tumor suppressor, it is possible that the activation of AMPK beyond its threshold levels is required to activate protective molecular pathways that would otherwise be inactive. No evidence was obtained during this study to suggest that other cell polarity proteins are recruited to the cell membrane in a compensatory manner. Nevertheless, it is known that the cytoplasmic translocation of LKB1 results in its activation, and it is well documented

that LKB1 phosphorylates Par1, which promotes the assembly of tight junctions by recruiting Par3 to the cell-cell contacts. Our model suggests that the loss of ASPP2 results in the activation of LKB1, which will then phosphorylate AMPK and Par1. We believe that, in healthy situations, ASPP2's localization at the cell-cell contacts negatively regulates LKB1's activation. By binding to Mo25 and β-catenin, possibly simultaneously, ASPP2 ensures the integrity of tight junctions and stabilization of the adherens junctions. However, under a stressful event that disrupts ASPP2's localization, Mo25 becomes available to bind to other partners including LKB1, which is recruited to the cytoplasm in the meantime. The formation of the complex LKB1/Mo25/STRAD and consequent activation of LKB1 results in the phosphorylation of AMPK and the activation of signaling pathways, which will protect the cell or, as last alternative, cause its p53-dependent death.

To further support our model, it is necessary for us to understand whether ASPP2 glucose starvation-driven enrichment at the tight junctions is impaired upon AMPK or LKB1 depletion. We first thought of using a silencing strategy to delete LKB1 and AMPK in U2OS cells. However, we have found that the combination of gene silencing and energetic stress is lethal to the cells. For this reason, we now plan to work with LKB1-null cell lines such as A549, and verify what happens to ASPP2 when glucose deprivation is triggered. Another question that needs to be considered is whether ASPP2 modulation is specific to AICAR, or is also observed when other AMPK stimulators (such as metformin, sucrose and H_2O_2) are used. Whether the loss of ASPP2 from the cell-cell contacts is compensated for by the recruitment of other cell polarity components will also be investigated. In order to

address this question we will explore the Par1 signaling pathway *in vitro* upon ASPP2 deletion.

We further plan to map the interaction between ASPP2 and LKB1 and determine which region of ASPP2 is necessary for the binding. Conversely, we intend to discover which regions of LKB1 and Mo25 are required for binding to ASPP2. It will be very important to determine whether the nuclear localization signal or kinase domain present in LKB1 is essential for binding. Finally, we will study the role of PP1 in the modulation of ASPP2 by AMPK, since PP1 has been shown to be a binding partner of AMPK and ASPP2. We will study the putative phosphorylation of ASPP2 by AMPK and the dephosphorylation of AMPK and ASPP2 by PP1, when cellular stresses are overcome.

While the work outlined here was performed *in vitro,* we should not exclude the possibility that the model previously described exists in the context of an epithelial tissue. LKB1 is a duodenal tumor suppressor, thus, it is possible that the mild phenotype that we observed in the duodenum is due to the protective role of LKB1 in this tissue. To address this question, we plan to support our *in vitro* data by investigating the association ASPP2/LKB1 *in vivo*. We will analyze the expression levels of LKB1, Mo25 and STRAD in ASPP2$^{\Delta 3/\Delta 3}$ and WT duodenum. Moreover, we will also determine whether ASPP2-deficient mice show metabolic defects, and the consequences of the resulting energetic stress on LKB1 expression.

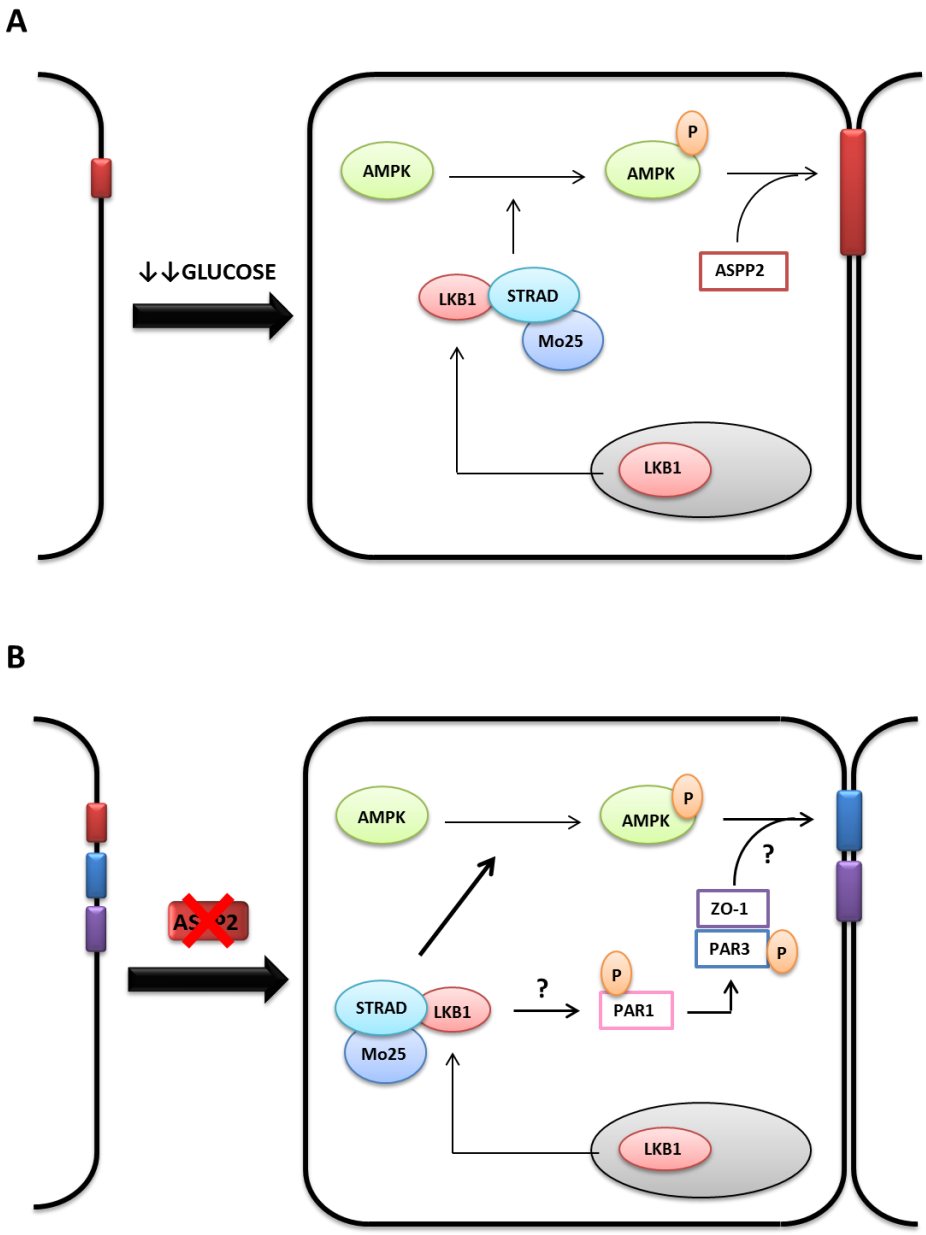


FIGURE 6.2 – Proposed model of the ASPP2-AMPK-LKB1 interaction on the regulation of tight junction integrity. (A) ASPP2 regulation under glucose deprivation. The reduction of glucose concentration promotes an increase of ASPP2 at the level of the tight junctions. This increase is due to the phosphorylation of AMPK, which is triggered by the translocation of LKB1 to the cytoplasm. **(B) Stimulation of tight junction formation upon the loss of ASPP2.** In the absence of ASPP2, LKB1 is translocated to the cytoplasm and the formation of the LKB1/Mo25/STRAD complex activates LKB1, leading to AMPK phosphorylation. As a result, Par3 might be phosphorylated and tight junction assembly is enhanced to compensate for the loss of ASPP2.

6.4 – ASPP2: the gatekeeper in cell polarity and intestinal inflammation

Our work has provided evidence that ASPP2 plays a role in the defense of the epithelium. Loss of ASPP2 results in the disruption of the colonic tight junctions. The histological study of ASPP2 Δexon3 intestines revealed signs of inflammation in the colon, which were translated in hyperplasia of isolated lymphoid centers, increased production of myeloperoxidase and secretion of pro-inflammatory cytokines such as TNFα and IL-17. *In vivo* and *in vitro*, we found that ASPP2's location and expression can be modulated by bacteria and by the deleterious immune response, particularly by proinflammatory cytokines and hypoxia. *In vivo*, the deficiency of ASPP2 in ASPP2 Δexon3 mice increases their susceptibility to intestinal inflammation. Our observations suggest that the loss of ASPP2 predisposes the animals to develop DSS-induced colitis, when considering DSS-treated WT littermates as controls. Thus far, signs of suffering, colitis or tumorigenesis have not been noticed in our tamoxifen-treated $ASPP^{loxP/loxP}$ mice, suggesting that the conditional deletion of ASPP2 is not sufficient to drive the formation of colonic tumors under conditions of chronic inflammation. Taken together, our findings suggest that ASPP2 is a first-line defense protein, since it maintains the integrity of tight junctions whilst keeping the door closed to intestinal inflammation. However, the loss of this tumour suppressor is, apparently, not sufficient to trigger colitis-associated cancer in ASPP2-deficient mice.

Epithelial cell-cell contacts can be used opportunistically by enteropathogens to invade the intestinal mucosa. In agreement, various studies have shown the

involvement of tight junction components in the development of intestinal inflammation *in vivo* (Ding et al., 2012; Laukoetter et al., 2007; Poritz et al., 2011).

In this study, we have obtained evidence that a loss of ASPP2 weakens the epithelial line of defense in the colon. On one hand, ASPP2-null mice suffer from colonic inflammation. On the other, ASPP2's expression can be disturbed by hypoxic conditions, proinflammatory cytokines and enterobacteria like *H. hepaticus*. Importantly, despite the signs of intestinal inflammation in ASPP2$^{\Delta 3/\Delta 3}$ mice, spontaneous colitis was never observed. Interestingly, all transgenic mice lacking tight junctional components such as JAM-A, claudins and occludin suffer from colonic inflammation, but do not present any clinical evidence of colitis (Amasheh et al., 2011; Laukoetter et al., 2007; Schulzke et al., 2005). Therefore, we hypothesize that ASPP2 loss, by itself, is not enough to trigger colitis in mice, but is sufficient to increase vulnerability to inflammation in these animals. Inflammation in the intestine can be explored from three perspectives: the epithelial cells, inflammatory cells and luminal agents. Taking into consideration the location of ASPP2, at the level of the tight junctions, we believed that studying inflammation from the epithelial cell point of view was the most straightforward approach. However, tight junctions, immune cells and the luminal content might weigh differently in the balance of intestinal homeostasis. Therefore, it is likely that ASPP2 plays a role in the biological function of the immune cells. This hypothesis is supported by the existing literature, which states that cell polarity components such as occludin, JAM-A, and E-cadherin are expressed in immune cells, including T-lymphocytes and leukocytes (Alexander et al., 1998; Cepek et al., 1994; Woodfin et al., 2007). In particular, JAM-A is required for the transendothelial migration of

leukocytes, whereas E-cadherin interacts with integrins to mediate T-lymphocyte migration (Cepek et al., 1994; Woodfin et al., 2007). Interestingly, the results obtained from a gene array performed using mRNA extracted from ASPP2 Δexon3 colonic tissue revealed that Tiam1 is upregulated (data not shown). Tiam1 was recently described as an important regulator of T-cell trafficking and transendothelial migration, supporting the hypothesis that ASPP2's expression can influence the action of immune cells (Gerard et al., 2009).

The induction of acute colitis, by challenging mice with DSS, is used as a tool to investigate the susceptibility of the animal to develop intestinal inflammation. We took advantage of this experimental procedure to understand whether the conditional deletion of ASPP2 was sufficient to generate an acute inflammatory response. Importantly, from this experiment, we concluded that the deletion of ASPP2 and the immediate DSS-challenge was sufficient to induce colitis in ASPP2 conditional deleted mice. This crucial observation further supports our hypothesis that ASPP2 establishes a first line of defense by acting as a gatekeeper in colonic cell polarity. The induction of chronic colitis by challenging ASPP2-conditionally deleted mice did not result in the generation of colitis-associated cancer, up to four months post-treatment. This experiment was performed in order to understand whether the deletion of ASPP2 was sufficient to drive tumorigenesis in the colon, following DSS-induced colitis. If this was found to be the case, we could then conclude that ASPP2 is not only a cell-cell contact protector, but also a colonic tumor suppressor. However, this study has yielded no evidence that the loss of ASPP2 is sufficient to induce tumors in the colon.

In the future, we plan to evaluate the epithelial barrier function of ASPP2 Δexon3 mice. To address this question, we will investigate the absorption of fluorescein isothiocyanate (FITC) dextran in the intestine of ASPP2 Δexon3 mice. To further support this study, we plan to investigate the expression of claudins in ASPP2 Δexon3 intestine, and determine whether polarized ASPP2-depleted cell line, such as Caco-2 have impaired transepithelial resistance. In order to determine whether the ASPP2 deletion has any deleterious effects beyond the disruption of epithelial cell integrity, we will study the expression of ASPP2 in immune cells and determine whether ASPP2's depletion compromises the functionality of these cells. We are also interested in studying the composition of the intestinal microbiome in ASPP2 Δexon3 mice, as intestinal dysbiosis is often related to gastrointestinal disorders (Tamboli et al., 2004). It is likely that differences in the composition of the intestinal microbiota between WT and ASPP2-null mice can account for the differences in epithelial permeability and susceptibility to inflammation.

Finally, we plan to optimize the protocol for acute and chronic DSS-challenge. We are interested in studying different DSS dose responses in ASPP2 conditional deleted mice. Moreover, we want to investigate whether tumorigenesis is triggered by using a carcinogenic agent, such as AOM, or by infecting the mice with an enteropathogen like *H. hepaticus*.

The statistical analysis performed in this work considered the results obtained from three pairs of animals, $ASPP2^{+/+}$ and $ASPP2^{\Delta 3/\Delta 3}$. Due to differences in the severity of ASPP2-deficient mice's phenotype it is important that variation within the intestinal tissue analysed is considered. The increase in the number of studied

samples would be a way of counterbalance this fact. In addition, it would contribute to an increase in the statistical significance of the findings here reported. Furthermore, different ways of analysing the samples will also be explored so that the interpretation of the results is more accurate. For instance, longitudinal sections of the tissue should be done and studied as opposed to transversal sections. Moreover, the technique of "swiss roll" will be used in the future since it allows the study of a larger area of the tissue in a single section.

The existence of hydrocephalus in ASPP2$^{\Delta 3/\Delta 3}$ mice, as well as their premature death, is an important disadvantage for the study of the intestinal epithelium in ASPP2-deficient mice. For this reason, an inducible knockout system will be used more frequently in the future. On one hand, it is essential to determine the extension of ASPP2 deletion in this system as it is still unknown whether ASPP2 is conditionally deleted in the epithelial cells, immune cells or in both. On the other hand, it will be important to establish a new system ASPP2-Villin-Cre in which the deletion of ASPP2 would be specific to the villin positive cells in the intestine. This way, the deletion of ASPP2 would be ensured in the intestinal epithelial cells, therefore making the study of ASPP2's role in the epithelial barrier possible and more accurate.

BIBLIOGRAPHY

Agirre, X., Roman-Gomez, J., Jimenez-Velasco, A., Garate, L., Montiel-Duarte, C., Navarro, G., Vazquez, I., Zalacain, M., Calasanz, M.J., Heiniger, A.*, et al.* (2006). ASPP1, a common activator of TP53, is inactivated by aberrant methylation of its promoter in acute lymphoblastic leukemia. Oncogene *25*, 1862-1870.

Agnholt, J., and Kaltoft, K. (2001). Infliximab downregulates interferon-gamma production in activated gut T-lymphocytes from patients with Crohn's disease. Cytokine *15*, 212-222.

Al-Sadi, R.M., and Ma, T.Y. (2007). IL-1beta causes an increase in intestinal epithelial tight junction permeability. J Immunol *178*, 4641-4649.

Alessi, D.R., Sakamoto, K., and Bayascas, J.R. (2006). LKB1-dependent signaling pathways. Annual review of biochemistry *75*, 137-163.

Alexander, J.S., Dayton, T., Davis, C., Hill, S., Jackson, T.H., Blaschuk, O., Symonds, M., Okayama, N., Kevil, C.G., Laroux, F.S.*, et al.* (1998). Activated T-lymphocytes express occludin, a component of tight junctions. Inflammation *22*, 573-582.

Alonso, L., and Fuchs, E. (2003). Stem cells in the skin: waste not, Wnt not. Genes Dev *17*, 1189-1200.

Amasheh, S., Fromm, M., and Gunzel, D. (2011). Claudins of intestine and nephron - a correlation of molecular tight junction structure and barrier function. Acta Physiol (Oxf) *201*, 133-140.

Amasheh, S., Meiri, N., Gitter, A.H., Schoneberg, T., Mankertz, J., Schulzke, J.D., and Fromm, M. (2002). Claudin-2 expression induces cation-selective channels in tight junctions of epithelial cells. Journal of cell science *115*, 4969-4976.

Amellem, O., and Pettersen, E.O. (1991). Cell inactivation and cell cycle inhibition as induced by extreme hypoxia: the possible role of cell cycle arrest as a protection against hypoxia-induced lethal damage. Cell proliferation *24*, 127-141.

Amieva, M.R., Vogelmann, R., Covacci, A., Tompkins, L.S., Nelson, W.J., and Falkow, S. (2003). Disruption of the epithelial apical-junctional complex by Helicobacter pylori CagA. Science *300*, 1430-1434.

Andreu, P., Colnot, S., Godard, C., Gad, S., Chafey, P., Niwa-Kawakita, M., Laurent-Puig, P., Kahn, A., Robine, S., Perret, C.*, et al.* (2005). Crypt-restricted proliferation and commitment to the Paneth cell lineage following Apc loss in the mouse intestine. Development *132*, 1443-1451.

Appella, E., and Anderson, C.W. (2001). Post-translational modifications and activation of p53 by genotoxic stresses. European journal of biochemistry / FEBS *268*, 2764-2772.

Araki, A., Kanai, T., Ishikura, T., Makita, S., Uraushihara, K., Iiyama, R., Totsuka, T., Takeda, K., Akira, S., and Watanabe, M. (2005). MyD88-deficient mice develop severe intestinal inflammation in dextran sodium sulfate colitis. Journal of gastroenterology *40*, 16-23.

Aranda, V., Nolan, M.E., and Muthuswamy, S.K. (2008). Par complex in cancer: a regulator of normal cell polarity joins the dark side. Oncogene *27*, 6878-6887.

Artavanis-Tsakonas, S., Rand, M.D., and Lake, R.J. (1999). Notch signaling: cell fate control and signal integration in development. Science *284*, 770-776.

Arthur, J.C., and Jobin, C. (2011). The struggle within: microbial influences on colorectal cancer. Inflammatory bowel diseases *17*, 396-409.

Artis, D. (2008). Epithelial-cell recognition of commensal bacteria and maintenance of immune homeostasis in the gut. Nature reviews Immunology *8*, 411-420.

Assemat, E., Bazellieres, E., Pallesi-Pocachard, E., Le Bivic, A., and Massey-Harroche, D. (2008). Polarity complex proteins. Biochimica et biophysica acta *1778*, 614-630.

Ayabe, T., Satchell, D.P., Wilson, C.L., Parks, W.C., Selsted, M.E., and Ouellette, A.J. (2000). Secretion of microbicidal alpha-defensins by intestinal Paneth cells in response to bacteria. Nature immunology *1*, 113-118.

Baas, A.F., Boudeau, J., Sapkota, G.P., Smit, L., Medema, R., Morrice, N.A., Alessi, D.R., and Clevers, H.C. (2003). Activation of the tumour suppressor kinase LKB1 by the STE20-like pseudokinase STRAD. The EMBO journal *22*, 3062-3072.

Baas, A.F., Kuipers, J., van der Wel, N.N., Batlle, E., Koerten, H.K., Peters, P.J., and Clevers, H.C. (2004). Complete polarization of single intestinal epithelial cells upon activation of LKB1 by STRAD. Cell *116*, 457-466.

Baldwin, A.S., Jr. (1996). The NF-kappa B and I kappa B proteins: new discoveries and insights. Annual review of immunology *14*, 649-683.

Banin, S., Moyal, L., Shieh, S., Taya, Y., Anderson, C.W., Chessa, L., Smorodinsky, N.I., Prives, C., Reiss, Y., Shiloh, Y.*, et al.* (1998). Enhanced phosphorylation of p53 by ATM in response to DNA damage. Science *281*, 1674-1677.

Barker, N., and Clevers, H. (2007). Tracking down the stem cells of the intestine: strategies to identify adult stem cells. Gastroenterology *133*, 1755-1760.

Barker, N., van Es, J.H., Kuipers, J., Kujala, P., van den Born, M., Cozijnsen, M., Haegebarth, A., Korving, J., Begthel, H., Peters, P.J.*, et al.* (2007). Identification of stem cells in small intestine and colon by marker gene Lgr5. Nature *449*, 1003-1007.

Batlle, E., Henderson, J.T., Beghtel, H., van den Born, M.M., Sancho, E., Huls, G., Meeldijk, J., Robertson, J., van de Wetering, M., Pawson, T.*, et al.* (2002). Beta-catenin and TCF mediate cell positioning in the intestinal epithelium by controlling the expression of EphB/ephrinB. Cell *111*, 251-263.

Bauer, S., Kirschning, C.J., Hacker, H., Redecke, V., Hausmann, S., Akira, S., Wagner, H., and Lipford, G.B. (2001). Human TLR9 confers responsiveness to bacterial DNA via species-specific CpG motif recognition. Proceedings of the National Academy of Sciences of the United States of America *98*, 9237-9242.

Bazzoni, G., Martinez-Estrada, O.M., Orsenigo, F., Cordenonsi, M., Citi, S., and Dejana, E. (2000). Interaction of junctional adhesion molecule with the tight junction components ZO-1, cingulin, and occludin. The Journal of biological chemistry *275*, 20520-20526.

Becker, C., Fantini, M.C., Schramm, C., Lehr, H.A., Wirtz, S., Nikolaev, A., Burg, J., Strand, S., Kiesslich, R., Huber, S.*, et al.* (2004). TGF-beta suppresses tumor progression in colon cancer by inhibition of IL-6 trans-signaling. Immunity *21*, 491-501.

Becker, C., Fantini, M.C., Wirtz, S., Nikolaev, A., Lehr, H.A., Galle, P.R., Rose-John, S., and Neurath, M.F. (2005). IL-6 signaling promotes tumor growth in colorectal cancer. Cell Cycle *4*, 217-220.

Berg, R.D. (1996). The indigenous gastrointestinal microflora. Trends in microbiology *4*, 430-435.

Bergamaschi, D., Samuels, Y., O'Neil, N.J., Trigiante, G., Crook, T., Hsieh, J.K., O'Connor, D.J., Zhong, S., Campargue, I., Tomlinson, M.L.*, et al.* (2003). iASPP oncoprotein is a key inhibitor of p53 conserved from worm to human. Nature genetics *33*, 162-167.

Berkes, J., Viswanathan, V.K., Savkovic, S.D., and Hecht, G. (2003). Intestinal epithelial responses to enteric pathogens: effects on the tight junction barrier, ion transport, and inflammation. Gut *52*, 439-451.

Bernstein, C.N., Blanchard, J.F., Kliewer, E., and Wajda, A. (2001). Cancer risk in patients with inflammatory bowel disease: a population-based study. Cancer *91*, 854-862.

Bernstein, C.N., Rawsthorne, P., Cheang, M., and Blanchard, J.F. (2006). A population-based case control study of potential risk factors for IBD. The American journal of gastroenterology *101*, 993-1002.

Bevins, C.L., and Salzman, N.H. (2011). Paneth cells, antimicrobial peptides and maintenance of intestinal homeostasis. Nature reviews Microbiology *9*, 356-368.

Bienz, M., and Clevers, H. (2000). Linking colorectal cancer to Wnt signaling. Cell *103*, 311-320.

Bilder, D., Li, M., and Perrimon, N. (2000). Cooperative regulation of cell polarity and growth by Drosophila tumor suppressors. Science *289*, 113-116.

Bodmer, W.F., Bailey, C.J., Bodmer, J., Bussey, H.J., Ellis, A., Gorman, P., Lucibello, F.C., Murday, V.A., Rider, S.H., Scambler, P.*, et al.* (1987). Localization of the gene for familial adenomatous polyposis on chromosome 5. Nature *328*, 614-616.

Bohm, H., Brinkmann, V., Drab, M., Henske, A., and Kurzchalia, T.V. (1997). Mammalian homologues of C. elegans PAR-1 are asymmetrically localized in epithelial cells and may influence their polarity. Current biology : CB *7*, 603-606.

Bohuslav, J., Kravchenko, V.V., Parry, G.C., Erlich, J.H., Gerondakis, S., Mackman, N., and Ulevitch, R.J. (1998). Regulation of an essential innate immune response by the p50 subunit of NF-kappaB. The Journal of clinical investigation *102*, 1645-1652.

Bollen, M., Peti, W., Ragusa, M.J., and Beullens, M. (2010). The extended PP1 toolkit: designed to create specificity. Trends in biochemical sciences *35*, 450-458.

Bollinger, R.R., Everett, M.L., Palestrant, D., Love, S.D., Lin, S.S., and Parker, W. (2003). Human secretory immunoglobulin A may contribute to biofilm formation in the gut. Immunology *109*, 580-587.

Boudeau, J., Baas, A.F., Deak, M., Morrice, N.A., Kieloch, A., Schutkowski, M., Prescott, A.R., Clevers, H.C., and Alessi, D.R. (2003). MO25alpha/beta interact with STRADalpha/beta enhancing their ability to bind, activate and localize LKB1 in the cytoplasm. The EMBO journal *22*, 5102-5114.

Boudeau, J., Scott, J.W., Resta, N., Deak, M., Kieloch, A., Komander, D., Hardie, D.G., Prescott, A.R., van Aalten, D.M., and Alessi, D.R. (2004). Analysis of the LKB1-STRAD-MO25 complex. Journal of cell science *117*, 6365-6375.

Brentnall, T.A., Crispin, D.A., Rabinovitch, P.S., Haggitt, R.C., Rubin, C.E., Stevens, A.C., and Burmer, G.C. (1994). Mutations in the p53 gene: an early marker of neoplastic progression in ulcerative colitis. Gastroenterology *107*, 369-378.

Bruewer, M., Utech, M., Ivanov, A.I., Hopkins, A.M., Parkos, C.A., and Nusrat, A. (2005). Interferon-gamma induces internalization of epithelial tight junction proteins via a macropinocytosis-like process. FASEB journal : official publication of the Federation of American Societies for Experimental Biology *19*, 923-933.

Buschmann, T., Potapova, O., Bar-Shira, A., Ivanov, V.N., Fuchs, S.Y., Henderson, S., Fried, V.A., Minamoto, T., Alarcon-Vargas, D., Pincus, M.R*., et al.* (2001). Jun NH2-terminal kinase phosphorylation of p53 on Thr-81 is important for p53 stabilization and transcriptional activities in response to stress. Molecular and cellular biology *21*, 2743-2754.

Buti, L., Spooner, E., Van der Veen, A.G., Rappuoli, R., Covacci, A., and Ploegh, H.L. (2011). Helicobacter pylori cytotoxin-associated gene A (CagA) subverts the apoptosis-stimulating protein of p53 (ASPP2) tumor suppressor pathway of the host. Proceedings of the National Academy of Sciences of the United States of America *108*, 9238-9243.

Cadwell, K., Liu, J.Y., Brown, S.L., Miyoshi, H., Loh, J., Lennerz, J.K., Kishi, C., Kc, W., Carrero, J.A., Hunt, S*., et al.* (2008). A key role for autophagy and the autophagy gene Atg16l1 in mouse and human intestinal Paneth cells. Nature *456*, 259-263.

Cario, E., Rosenberg, I.M., Brandwein, S.L., Beck, P.L., Reinecker, H.C., and Podolsky, D.K. (2000). Lipopolysaccharide activates distinct signaling pathways in intestinal epithelial cell lines expressing Toll-like receptors. J Immunol *164*, 966-972.

Cepek, K.L., Shaw, S.K., Parker, C.M., Russell, G.J., Morrow, J.S., Rimm, D.L., and Brenner, M.B. (1994). Adhesion between epithelial cells and T lymphocytes mediated by E-cadherin and the alpha E beta 7 integrin. Nature *372*, 190-193.

Ceponis, P.J., Botelho, F., Richards, C.D., and McKay, D.M. (2000). Interleukins 4 and 13 increase intestinal epithelial permeability by a phosphatidylinositol 3-kinase pathway. Lack of evidence for STAT 6 involvement. The Journal of biological chemistry *275*, 29132-29137.

Chavez, A.M., Menconi, M.J., Hodin, R.A., and Fink, M.P. (1999a). Cytokine-induced intestinal epithelial hyperpermeability: role of nitric oxide. Critical care medicine *27*, 2246-2251.

Chavez, A.M., Morin, M.J., Unno, N., Fink, M.P., and Hodin, R.A. (1999b). Acquired interferon gamma responsiveness during Caco-2 cell differentiation: effects on iNOS gene expression. Gut *44*, 659-665.

Chen, Y., Liu, W., Naumovski, L., and Neve, R.L. (2003). ASPP2 inhibits APP-BP1-mediated NEDD8 conjugation to cullin-1 and decreases APP-BP1-induced cell proliferation and neuronal apoptosis. Journal of neurochemistry *85*, 801-809.

Cho, Y., Gorina, S., Jeffrey, P.D., and Pavletich, N.P. (1994). Crystal structure of a p53 tumor suppressor-DNA complex: understanding tumorigenic mutations. Science *265*, 346-355.

Clevers, H. (2006). Wnt/beta-catenin signaling in development and disease. Cell *127*, 469-480.

Colegio, O.R., Van Itallie, C.M., McCrea, H.J., Rahner, C., and Anderson, J.M. (2002). Claudins create charge-selective channels in the paracellular pathway between epithelial cells. American journal of physiology Cell physiology *283*, C142-147.

Collins, S.P., Reoma, J.L., Gamm, D.M., and Uhler, M.D. (2000). LKB1, a novel serine/threonine protein kinase and potential tumour suppressor, is phosphorylated by cAMP-dependent protein kinase (PKA) and prenylated in vivo. The Biochemical journal *345 Pt 3*, 673-680.

Colman, M.S., Afshari, C.A., and Barrett, J.C. (2000). Regulation of p53 stability and activity in response to genotoxic stress. Mutation research *462*, 179-188.

Cong, W., Hirose, T., Harita, Y., Yamashita, A., Mizuno, K., Hirano, H., and Ohno, S. (2010). ASPP2 regulates epithelial cell polarity through the PAR complex. Current biology : CB *20*, 1408-1414.

Coombes, J.L., and Powrie, F. (2008). Dendritic cells in intestinal immune regulation. Nature reviews Immunology *8*, 435-446.

Cooper, H.S., Murthy, S.N., Shah, R.S., and Sedergran, D.J. (1993). Clinicopathologic study of dextran sulfate sodium experimental murine colitis. Laboratory investigation; a journal of technical methods and pathology *69*, 238-249.

Corton, J.M., Gillespie, J.G., Hawley, S.A., and Hardie, D.G. (1995). 5-aminoimidazole-4-carboxamide ribonucleoside. A specific method for activating AMP-activated protein kinase in intact cells? European journal of biochemistry / FEBS *229*, 558-565.

Creamer, B., Shorter, R.G., and Bamforth, J. (1961). The turnover and shedding of epithelial cells. I. The turnover in the gastro-intestinal tract. Gut *2*, 110-118.

Crook, T., Brooks, L.A., Crossland, S., Osin, P., Barker, K.T., Waller, J., Philp, E., Smith, P.D., Yulug, I., Peto, J*., et al.* (1998). p53 mutation with frequent novel condons but not a mutator phenotype in BRCA1- and BRCA2-associated breast tumours. Oncogene *17*, 1681-1689.

Crosnier, C., Vargesson, N., Gschmeissner, S., Ariza-McNaughton, L., Morrison, A., and Lewis, J. (2005). Delta-Notch signalling controls commitment to a secretory fate in the zebrafish intestine. Development *132*, 1093-1104.

Cunliffe, R.N., Rose, F.R., Keyte, J., Abberley, L., Chan, W.C., and Mahida, Y.R. (2001). Human defensin 5 is stored in precursor form in normal Paneth cells and is expressed by some villous epithelial cells and by metaplastic Paneth cells in the colon in inflammatory bowel disease. Gut *48*, 176-185.

Dai, D., and Walker, W.A. (1999). Protective nutrients and bacterial colonization in the immature human gut. Advances in pediatrics *46*, 353-382.

Daniels, D.L., and Weis, W.I. (2005). Beta-catenin directly displaces Groucho/TLE repressors from Tcf/Lef in Wnt-mediated transcription activation. Nature structural & molecular biology *12*, 364-371.

Das, P., Goswami, P., Das, T.K., Nag, T., Sreenivas, V., Ahuja, V., Panda, S.K., Gupta, S.D., and Makharia, G.K. (2012). Comparative tight junction protein expressions in colonic Crohn's disease, ulcerative colitis, and tuberculosis: a new perspective. Virchows Archiv : an international journal of pathology *460*, 261-270.

Davies, S.P., Helps, N.R., Cohen, P.T., and Hardie, D.G. (1995). 5'-AMP inhibits dephosphorylation, as well as promoting phosphorylation, of the AMP-activated protein kinase. Studies using bacterially expressed human protein phosphatase-2C alpha and native bovine protein phosphatase-2AC. FEBS letters *377*, 421-425.

de Lau, W., Barker, N., and Clevers, H. (2007). WNT signaling in the normal intestine and colorectal cancer. Frontiers in bioscience : a journal and virtual library *12*, 471-491.

Deplancke, B., and Gaskins, H.R. (2001). Microbial modulation of innate defense: goblet cells and the intestinal mucus layer. The American journal of clinical nutrition *73*, 1131S-1141S.

Deschenes, C., Vezina, A., Beaulieu, J.F., and Rivard, N. (2001). Role of p27(Kip1) in human intestinal cell differentiation. Gastroenterology *120*, 423-438.

Ding, L., Lu, Z., Foreman, O., Tatum, R., Lu, Q., Renegar, R., Cao, J., and Chen, Y.H. (2012). Inflammation and disruption of the mucosal architecture in claudin-7-deficient mice. Gastroenterology *142*, 305-315.

Ding, L., Zhang, Y., Tatum, R., and Chen, Y.H. (2011). Detection of tight junction barrier function in vivo by biotin. Methods Mol Biol *762*, 91-100.

Donehower, L.A., Harvey, M., Slagle, B.L., McArthur, M.J., Montgomery, C.A., Jr., Butel, J.S., and Bradley, A. (1992). Mice deficient for p53 are developmentally normal but susceptible to spontaneous tumours. Nature *356*, 215-221.

Dorfman, J., and Macara, I.G. (2008). STRADalpha regulates LKB1 localization by blocking access to importin-alpha, and by association with Crm1 and exportin-7. Molecular biology of the cell *19*, 1614-1626.

Dow, L.E., Brumby, A.M., Muratore, R., Coombe, M.L., Sedelies, K.A., Trapani, J.A., Russell, S.M., Richardson, H.E., and Humbert, P.O. (2003). hScrib is a functional homologue of the Drosophila tumour suppressor Scribble. Oncogene *22*, 9225-9230.

Dow, L.E., and Humbert, P.O. (2007). Polarity regulators and the control of epithelial architecture, cell migration, and tumorigenesis. International review of cytology *262*, 253-302.

Duchmann, R., Kaiser, I., Hermann, E., Mayet, W., Ewe, K., and Meyer zum Buschenfelde, K.H. (1995). Tolerance exists towards resident intestinal flora but is broken in active inflammatory bowel disease (IBD). Clinical and experimental immunology *102*, 448-455.

Duerr, R.H., Taylor, K.D., Brant, S.R., Rioux, J.D., Silverberg, M.S., Daly, M.J., Steinhart, A.H., Abraham, C., Regueiro, M., Griffiths, A*., et al.* (2006). A genome-wide association study identifies IL23R as an inflammatory bowel disease gene. Science *314*, 1461-1463.

Dunker, N., Schmitt, K., Schuster, N., and Krieglstein, K. (2002). The role of transforming growth factor beta-2, beta-3 in mediating apoptosis in the murine intestinal mucosa. Gastroenterology *122*, 1364-1375.

Eaden, J.A., Abrams, K.R., and Mayberry, J.F. (2001). The risk of colorectal cancer in ulcerative colitis: a meta-analysis. Gut *48*, 526-535.

Ebnet, K., Schulz, C.U., Meyer Zu Brickwedde, M.K., Pendl, G.G., and Vestweber, D. (2000). Junctional adhesion molecule interacts with the PDZ domain-containing proteins AF-6 and ZO-1. The Journal of biological chemistry *275*, 27979-27988.

Ebnet, K., Suzuki, A., Ohno, S., and Vestweber, D. (2004). Junctional adhesion molecules (JAMs): more molecules with dual functions? Journal of cell science *117*, 19-29.

Edelblum, K.L., Yan, F., Yamaoka, T., and Polk, D.B. (2006). Regulation of apoptosis during homeostasis and disease in the intestinal epithelium. Inflammatory bowel diseases *12*, 413-424.

Elson, C.O., Cong, Y., McCracken, V.J., Dimmitt, R.A., Lorenz, R.G., and Weaver, C.T. (2005). Experimental models of inflammatory bowel disease reveal innate, adaptive, and regulatory mechanisms of host dialogue with the microbiota. Immunological reviews *206*, 260-276.

Eltzschig, H.K., and Carmeliet, P. (2011). Hypoxia and inflammation. The New England journal of medicine *364*, 656-665.

Engle, S.J., Ormsby, I., Pawlowski, S., Boivin, G.P., Croft, J., Balish, E., and Doetschman, T. (2002). Elimination of colon cancer in germ-free transforming growth factor beta 1-deficient mice. Cancer Res *62*, 6362-6366.

Espanel, X., and Sudol, M. (2001). Yes-associated protein and p53-binding protein-2 interact through their WW and SH3 domains. The Journal of biological chemistry *276*, 14514-14523.

Evans, W.H., and Martin, P.E. (2002). Gap junctions: structure and function (Review). Molecular membrane biology *19*, 121-136.

Fan, J., Frey, R.S., and Malik, A.B. (2003). TLR4 signaling induces TLR2 expression in endothelial cells via neutrophil NADPH oxidase. The Journal of clinical investigation *112*, 1234-1243.

Fang, S., Jensen, J.P., Ludwig, R.L., Vousden, K.H., and Weissman, A.M. (2000). Mdm2 is a RING finger-dependent ubiquitin protein ligase for itself and p53. The Journal of biological chemistry *275*, 8945-8951.

Fasano, A. (2011). Zonulin and its regulation of intestinal barrier function: the biological door to inflammation, autoimmunity, and cancer. Physiological reviews *91*, 151-175.

Fearon, E.R., and Vogelstein, B. (1990). A genetic model for colorectal tumorigenesis. Cell *61*, 759-767.

Fevr, T., Robine, S., Louvard, D., and Huelsken, J. (2007). Wnt/beta-catenin is essential for intestinal homeostasis and maintenance of intestinal stem cells. Molecular and cellular biology *27*, 7551-7559.

Fiocchi, C. (1998). Inflammatory bowel disease: etiology and pathogenesis. Gastroenterology *115*, 182-205.

Fiorentino, D.F., Zlotnik, A., Mosmann, T.R., Howard, M., and O'Garra, A. (1991). IL-10 inhibits cytokine production by activated macrophages. J Immunol *147*, 3815-3822.

Fish, E.M., and Molitoris, B.A. (1994). Alterations in epithelial polarity and the pathogenesis of disease states. The New England journal of medicine *330*, 1580-1588.

Fogal, V., Kartasheva, N.N., Trigiante, G., Llanos, S., Yap, D., Vousden, K.H., and Lu, X. (2005). ASPP1 and ASPP2 are new transcriptional targets of E2F. Cell death and differentiation *12*, 369-376.

Forcet, C., and Billaud, M. (2007). Dialogue between LKB1 and AMPK: a hot topic at the cellular pole. Science's STKE : signal transduction knowledge environment *2007*, pe51.

Forcet, C., Etienne-Manneville, S., Gaude, H., Fournier, L., Debilly, S., Salmi, M., Baas, A., Olschwang, S., Clevers, H., and Billaud, M. (2005). Functional analysis of Peutz-Jeghers mutations reveals that the LKB1 C-terminal region exerts a crucial role in regulating both the AMPK pathway and the cell polarity. Human molecular genetics *14*, 1283-1292.

Fournier, B.M., and Parkos, C.A. (2012). The role of neutrophils during intestinal inflammation. Mucosal immunology *5*, 354-366.

Fox, J.G., Ge, Z., Whary, M.T., Erdman, S.E., and Horwitz, B.H. (2011). Helicobacter hepaticus infection in mice: models for understanding lower bowel inflammation and cancer. Mucosal immunology *4*, 22-30.

Fre, S., Huyghe, M., Mourikis, P., Robine, S., Louvard, D., and Artavanis-Tsakonas, S. (2005). Notch signals control the fate of immature progenitor cells in the intestine. Nature *435*, 964-968.

Fujii, S., Fujimori, T., Kawamata, H., Takeda, J., Kitajima, K., Omotehara, F., Kaihara, T., Kusaka, T., Ichikawa, K., Ohkura, Y.*, et al.* (2004). Development of colonic neoplasia in p53 deficient mice with experimental colitis induced by dextran sulphate sodium. Gut *53*, 710-716.

Fujita, J. (1999). Cold shock response in mammalian cells. Journal of molecular microbiology and biotechnology *1*, 243-255.

Fukata, M., Chen, A., Vamadevan, A.S., Cohen, J., Breglio, K., Krishnareddy, S., Hsu, D., Xu, R., Harpaz, N., Dannenberg, A.J.*, et al.* (2007). Toll-like receptor-4 promotes the development of colitis-associated colorectal tumors. Gastroenterology *133*, 1869-1881.

Fukata, M., Michelsen, K.S., Eri, R., Thomas, L.S., Hu, B., Lukasek, K., Nast, C.C., Lechago, J., Xu, R., Naiki, Y.*, et al.* (2005). Toll-like receptor-4 is required for intestinal response to epithelial injury and limiting bacterial translocation in a murine model of acute colitis. American journal of physiology Gastrointestinal and liver physiology *288*, G1055-1065.

Fukushima, N., and Mukai, K. (1999). Pancreatic neoplasms with abundant mucus production: emphasis on intraductal papillary-mucinous tumors and mucinous cystic tumors. Advances in anatomic pathology *6*, 65-77.

Furuse, M., Hata, M., Furuse, K., Yoshida, Y., Haratake, A., Sugitani, Y., Noda, T., Kubo, A., and Tsukita, S. (2002). Claudin-based tight junctions are crucial for the mammalian epidermal barrier: a lesson from claudin-1-deficient mice. The Journal of cell biology *156*, 1099-1111.

Furuse, M., Hirase, T., Itoh, M., Nagafuchi, A., Yonemura, S., and Tsukita, S. (1993). Occludin: a novel integral membrane protein localizing at tight junctions. The Journal of cell biology *123*, 1777-1788.

Furuse, M., Itoh, M., Hirase, T., Nagafuchi, A., Yonemura, S., and Tsukita, S. (1994). Direct association of occludin with ZO-1 and its possible involvement in the localization of occludin at tight junctions. The Journal of cell biology *127*, 1617-1626.

Garabedian, E.M., Roberts, L.J., McNevin, M.S., and Gordon, J.I. (1997). Examining the role of Paneth cells in the small intestine by lineage ablation in transgenic mice. The Journal of biological chemistry *272*, 23729-23740.

Gardiol, D., Zacchi, A., Petrera, F., Stanta, G., and Banks, L. (2006). Human discs large and scrib are localized at the same regions in colon mucosa and changes in their expression patterns are correlated with loss of tissue architecture during malignant progression. International journal of cancer *119*, 1285-1290.

Gerard, A., van der Kammen, R.A., Janssen, H., Ellenbroek, S.I., and Collard, J.G. (2009). The Rac activator Tiam1 controls efficient T-cell trafficking and route of transendothelial migration. Blood *113*, 6138-6147.

Giatromanolaki, A., Sivridis, E., Maltezos, E., Papazoglou, D., Simopoulos, C., Gatter, K.C., Harris, A.L., and Koukourakis, M.I. (2003). Hypoxia inducible factor 1alpha and 2alpha overexpression in inflammatory bowel disease. Journal of clinical pathology *56*, 209-213.

Gilmore, T.D. (2006). Introduction to NF-kappaB: players, pathways, perspectives. Oncogene *25*, 6680-6684.

Gitter, A.H., Wullstein, F., Fromm, M., and Schulzke, J.D. (2001). Epithelial barrier defects in ulcerative colitis: characterization and quantification by electrophysiological imaging. Gastroenterology *121*, 1320-1328.

Goosney, D.L., DeVinney, R., and Finlay, B.B. (2001). Recruitment of cytoskeletal and signaling proteins to enteropathogenic and enterohemorrhagic Escherichia coli pedestals. Infection and immunity *69*, 3315-3322.

Gorina, S., and Pavletich, N.P. (1996). Structure of the p53 tumor suppressor bound to the ankyrin and SH3 domains of 53BP2. Science *274*, 1001-1005.

Goto, Y., and Kiyono, H. (2012). Epithelial barrier: an interface for the cross-communication between gut flora and immune system. Immunological reviews *245*, 147-163.

Green, K.J., Kowalczyk, A.P., Bornslaeger, E.A., Palka, H.L., and Norvell, S.M. (1998). Desmosomes: integrators of mechanical integrity in tissues. The Biological bulletin *194*, 374-376; discussion 376-377.

Gregorieff, A., and Clevers, H. (2005). Wnt signaling in the intestinal epithelium: from endoderm to cancer. Genes Dev *19*, 877-890.

Gregorieff, A., Pinto, D., Begthel, H., Destree, O., Kielman, M., and Clevers, H. (2005). Expression pattern of Wnt signaling components in the adult intestine. Gastroenterology *129*, 626-638.

Greten, F.R., Eckmann, L., Greten, T.F., Park, J.M., Li, Z.W., Egan, L.J., Kagnoff, M.F., and Karin, M. (2004). IKKbeta links inflammation and tumorigenesis in a mouse model of colitis-associated cancer. Cell *118*, 285-296.

Grivennikov, S., Karin, E., Terzic, J., Mucida, D., Yu, G.Y., Vallabhapurapu, S., Scheller, J., Rose-John, S., Cheroutre, H., Eckmann, L*., et al.* (2009). IL-6 and Stat3 are required for

survival of intestinal epithelial cells and development of colitis-associated cancer. Cancer cell *15*, 103-113.

Guarner, F., Bourdet-Sicard, R., Brandtzaeg, P., Gill, H.S., McGuirk, P., van Eden, W., Versalovic, J., Weinstock, J.V., and Rook, G.A. (2006). Mechanisms of disease: the hygiene hypothesis revisited. Nature clinical practice Gastroenterology & hepatology *3*, 275-284.

Guttman, J.A., and Finlay, B.B. (2009). Tight junctions as targets of infectious agents. Biochimica et biophysica acta *1788*, 832-841.

Hamazaki, Y., Itoh, M., Sasaki, H., Furuse, M., and Tsukita, S. (2002). Multi-PDZ domain protein 1 (MUPP1) is concentrated at tight junctions through its possible interaction with claudin-1 and junctional adhesion molecule. The Journal of biological chemistry *277*, 455-461.

Han, X., Fink, M.P., and Delude, R.L. (2003). Proinflammatory cytokines cause NO*-dependent and -independent changes in expression and localization of tight junction proteins in intestinal epithelial cells. Shock *19*, 229-237.

Hanada, N., Makino, K., Koga, H., Morisaki, T., Kuwahara, H., Masuko, N., Tabira, Y., Hiraoka, T., Kitamura, N., Kikuchi, A.*, et al.* (2000). NE-dlg, a mammalian homolog of Drosophila dlg tumor suppressor, induces growth suppression and impairment of cell adhesion: possible involvement of down-regulation of beta-catenin by NE-dlg expression. International journal of cancer *86*, 480-488.

Hardie, D.G., Carling, D., and Gamblin, S.J. (2011). AMP-activated protein kinase: also regulated by ADP? Trends in biochemical sciences *36*, 470-477.

Hardie, D.G., Hawley, S.A., and Scott, J.W. (2006). AMP-activated protein kinase--development of the energy sensor concept. The Journal of physiology *574*, 7-15.

Harpaz, N., Peck, A.L., Yin, J., Fiel, I., Hontanosas, M., Tong, T.R., Laurin, J.N., Abraham, J.M., Greenwald, B.D., and Meltzer, S.J. (1994). p53 protein expression in ulcerative colitis-associated colorectal dysplasia and carcinoma. Human pathology *25*, 1069-1074.

Harris, T.J., and Peifer, M. (2005). Decisions, decisions: beta-catenin chooses between adhesion and transcription. Trends in cell biology *15*, 234-237.

Haskins, J., Gu, L., Wittchen, E.S., Hibbard, J., and Stevenson, B.R. (1998). ZO-3, a novel member of the MAGUK protein family found at the tight junction, interacts with ZO-1 and occludin. The Journal of cell biology *141*, 199-208.

Haupt, Y., Maya, R., Kazaz, A., and Oren, M. (1997). Mdm2 promotes the rapid degradation of p53. Nature *387*, 296-299.

Hawley, S.A., Boudeau, J., Reid, J.L., Mustard, K.J., Udd, L., Makela, T.P., Alessi, D.R., and Hardie, D.G. (2003). Complexes between the LKB1 tumor suppressor, STRAD alpha/beta and MO25 alpha/beta are upstream kinases in the AMP-activated protein kinase cascade. Journal of biology *2*, 28.

Hawley, S.A., Davison, M., Woods, A., Davies, S.P., Beri, R.K., Carling, D., and Hardie, D.G. (1996). Characterization of the AMP-activated protein kinase kinase from rat liver and identification of threonine 172 as the major site at which it phosphorylates AMP-activated protein kinase. The Journal of biological chemistry *271*, 27879-27887.

Hayashi, F., Smith, K.D., Ozinsky, A., Hawn, T.R., Yi, E.C., Goodlett, D.R., Eng, J.K., Akira, S., Underhill, D.M., and Aderem, A. (2001). The innate immune response to bacterial flagellin is mediated by Toll-like receptor 5. Nature *410*, 1099-1103.

Hayashi, T., Hirshman, M.F., Kurth, E.J., Winder, W.W., and Goodyear, L.J. (1998). Evidence for 5' AMP-activated protein kinase mediation of the effect of muscle contraction on glucose transport. Diabetes *47*, 1369-1373.

He, F., Peng, J., Deng, X.L., Yang, L.F., Camara, A.D., Omran, A., Wang, G.L., Wu, L.W., Zhang, C.L., and Yin, F. (2012). Mechanisms of tumor necrosis factor-alpha-induced leaks in intestine epithelial barrier. Cytokine *59*, 264-272.

Helps, N.R., Barker, H.M., Elledge, S.J., and Cohen, P.T. (1995). Protein phosphatase 1 interacts with p53BP2, a protein which binds to the tumour suppressor p53. FEBS letters *377*, 295-300.

Hemminki, A., Markie, D., Tomlinson, I., Avizienyte, E., Roth, S., Loukola, A., Bignell, G., Warren, W., Aminoff, M., Hoglund, P*., et al.* (1998). A serine/threonine kinase gene defective in Peutz-Jeghers syndrome. Nature *391*, 184-187.

Hemminki, A., Tomlinson, I., Markie, D., Jarvinen, H., Sistonen, P., Bjorkqvist, A.M., Knuutila, S., Salovaara, R., Bodmer, W., Shibata, D*., et al.* (1997). Localization of a susceptibility locus for Peutz-Jeghers syndrome to 19p using comparative genomic hybridization and targeted linkage analysis. Nature genetics *15*, 87-90.

Hezel, A.F., Gurumurthy, S., Granot, Z., Swisa, A., Chu, G.C., Bailey, G., Dor, Y., Bardeesy, N., and Depinho, R.A. (2008). Pancreatic LKB1 deletion leads to acinar polarity defects and cystic neoplasms. Molecular and cellular biology *28*, 2414-2425.

Hirabayashi, S., Tajima, M., Yao, I., Nishimura, W., Mori, H., and Hata, Y. (2003). JAM4, a junctional cell adhesion molecule interacting with a tight junction protein, MAGI-1. Molecular and cellular biology *23*, 4267-4282.

Hirao, A., Kong, Y.Y., Matsuoka, S., Wakeham, A., Ruland, J., Yoshida, H., Liu, D., Elledge, S.J., and Mak, T.W. (2000). DNA damage-induced activation of p53 by the checkpoint kinase Chk2. Science *287*, 1824-1827.

Hirashima, M., Sano, K., Morisada, T., Murakami, K., Rossant, J., and Suda, T. (2008). Lymphatic vessel assembly is impaired in Aspp1-deficient mouse embryos. Developmental biology *316*, 149-159.

Hoffmann, A., Levchenko, A., Scott, M.L., and Baltimore, D. (2002). The IkappaB-NF-kappaB signaling module: temporal control and selective gene activation. Science *298*, 1241-1245.

Hofseth, L.J., Saito, S., Hussain, S.P., Espey, M.G., Miranda, K.M., Araki, Y., Jhappan, C., Higashimoto, Y., He, P., Linke, S.P*., et al.* (2003). Nitric oxide-induced cellular stress and p53 activation in chronic inflammation. Proceedings of the National Academy of Sciences of the United States of America *100*, 143-148.

Hollander, D., Vadheim, C.M., Brettholz, E., Petersen, G.M., Delahunty, T., and Rotter, J.I. (1986). Increased intestinal permeability in patients with Crohn's disease and their relatives. A possible etiologic factor. Annals of internal medicine *105*, 883-885.

Honda, R., Tanaka, H., and Yasuda, H. (1997). Oncoprotein MDM2 is a ubiquitin ligase E3 for tumor suppressor p53. FEBS letters *420*, 25-27.

Hooper, L.V. (2004). Bacterial contributions to mammalian gut development. Trends in microbiology *12*, 129-134.

Hooper, L.V. (2009). Do symbiotic bacteria subvert host immunity? Nature reviews Microbiology *7*, 367-374.

Hooper, L.V., Wong, M.H., Thelin, A., Hansson, L., Falk, P.G., and Gordon, J.I. (2001). Molecular analysis of commensal host-microbial relationships in the intestine. Science *291*, 881-884.

Horikoshi, Y., Suzuki, A., Yamanaka, T., Sasaki, K., Mizuno, K., Sawada, H., Yonemura, S., and Ohno, S. (2009). Interaction between PAR-3 and the aPKC-PAR-6 complex is indispensable for apical domain development of epithelial cells. Journal of cell science *122*, 1595-1606.

Hugot, J.P., Chamaillard, M., Zouali, H., Lesage, S., Cezard, J.P., Belaiche, J., Almer, S., Tysk, C., O'Morain, C.A., Gassull, M.*, et al.* (2001). Association of NOD2 leucine-rich repeat variants with susceptibility to Crohn's disease. Nature *411*, 599-603.

Huibregtse, I.L., van Lent, A.U., and van Deventer, S.J. (2007). Immunopathogenesis of IBD: insufficient suppressor function in the gut? Gut *56*, 584-592.

Humbert, P., Russell, S., and Richardson, H. (2003). Dlg, Scribble and Lgl in cell polarity, cell proliferation and cancer. BioEssays : news and reviews in molecular, cellular and developmental biology *25*, 542-553.

Hurd, T.W., Gao, L., Roh, M.H., Macara, I.G., and Margolis, B. (2003). Direct interaction of two polarity complexes implicated in epithelial tight junction assembly. Nature cell biology *5*, 137-142.

Hussain, S.P., Amstad, P., Raja, K., Ambs, S., Nagashima, M., Bennett, W.P., Shields, P.G., Ham, A.J., Swenberg, J.A., Marrogi, A.J.*, et al.* (2000). Increased p53 mutation load in noncancerous colon tissue from ulcerative colitis: a cancer-prone chronic inflammatory disease. Cancer Res *60*, 3333-3337.

Hutterer, A., Betschinger, J., Petronczki, M., and Knoblich, J.A. (2004). Sequential roles of Cdc42, Par-6, aPKC, and Lgl in the establishment of epithelial polarity during Drosophila embryogenesis. Developmental cell *6*, 845-854.

Iden, S., van Riel, W.E., Schafer, R., Song, J.Y., Hirose, T., Ohno, S., and Collard, J.G. (2012). Tumor type-dependent function of the par3 polarity protein in skin tumorigenesis. Cancer cell *22*, 389-403.

Ikeda, S., Kishida, S., Yamamoto, H., Murai, H., Koyama, S., and Kikuchi, A. (1998). Axin, a negative regulator of the Wnt signaling pathway, forms a complex with GSK-3beta and beta-catenin and promotes GSK-3beta-dependent phosphorylation of beta-catenin. The EMBO journal *17*, 1371-1384.

Insoft, R.M., Sanderson, I.R., and Walker, W.A. (1996). Development of immune function in the intestine and its role in neonatal diseases. Pediatric clinics of North America *43*, 551-571.

Ireland, H., Kemp, R., Houghton, C., Howard, L., Clarke, A.R., Sansom, O.J., and Winton, D.J. (2004). Inducible Cre-mediated control of gene expression in the murine gastrointestinal tract: effect of loss of beta-catenin. Gastroenterology *126*, 1236-1246.

Itoh, M., Morita, K., and Tsukita, S. (1999). Characterization of ZO-2 as a MAGUK family member associated with tight as well as adherens junctions with a binding affinity to occludin and alpha catenin. The Journal of biological chemistry *274*, 5981-5986.

Itoh, M., Sasaki, H., Furuse, M., Ozaki, H., Kita, T., and Tsukita, S. (2001). Junctional adhesion molecule (JAM) binds to PAR-3: a possible mechanism for the recruitment of PAR-3 to tight junctions. The Journal of cell biology *154*, 491-497.

Iwabuchi, K., Bartel, P.L., Li, B., Marraccino, R., and Fields, S. (1994). Two cellular proteins that bind to wild-type but not mutant p53. Proceedings of the National Academy of Sciences of the United States of America *91*, 6098-6102.

Iwasaki, A., and Medzhitov, R. (2004). Toll-like receptor control of the adaptive immune responses. Nature immunology *5*, 987-995.

Izcue, A., Coombes, J.L., and Powrie, F. (2006). Regulatory T cells suppress systemic and mucosal immune activation to control intestinal inflammation. Immunological reviews *212*, 256-271.

Jan, Y.N., and Jan, L.Y. (1998). Asymmetric cell division. Nature *392*, 775-778.

Jarriault, S., Brou, C., Logeat, F., Schroeter, E.H., Kopan, R., and Israel, A. (1995). Signalling downstream of activated mammalian Notch. Nature *377*, 355-358.

Jeghers, H., Mc, K.V., and Katz, K.H. (1949). Generalized intestinal polyposis and melanin spots of the oral mucosa, lips and digits; a syndrome of diagnostic significance. The New England journal of medicine *241*, 1031-1036.

Jenny, M., Uhl, C., Roche, C., Duluc, I., Guillermin, V., Guillemot, F., Jensen, J., Kedinger, M., and Gradwohl, G. (2002). Neurogenin3 is differentially required for endocrine cell fate specification in the intestinal and gastric epithelium. The EMBO journal *21*, 6338-6347.

Jensen, J., Pedersen, E.E., Galante, P., Hald, J., Heller, R.S., Ishibashi, M., Kageyama, R., Guillemot, F., Serup, P., and Madsen, O.D. (2000). Control of endodermal endocrine development by Hes-1. Nature genetics *24*, 36-44.

Ji, H., Ramsey, M.R., Hayes, D.N., Fan, C., McNamara, K., Kozlowski, P., Torrice, C., Wu, M.C., Shimamura, T., Perera, S.A*., et al.* (2007). LKB1 modulates lung cancer differentiation and metastasis. Nature *448*, 807-810.

Jishage, K., Nezu, J., Kawase, Y., Iwata, T., Watanabe, M., Miyoshi, A., Ose, A., Habu, K., Kake, T., Kamada, N*., et al.* (2002). Role of Lkb1, the causative gene of Peutz-Jegher's syndrome, in embryogenesis and polyposis. Proceedings of the National Academy of Sciences of the United States of America *99*, 8903-8908.

Johansson, M.E., Phillipson, M., Petersson, J., Velcich, A., Holm, L., and Hansson, G.C. (2008). The inner of the two Muc2 mucin-dependent mucus layers in colon is devoid of bacteria. Proceedings of the National Academy of Sciences of the United States of America *105*, 15064-15069.

Johnson-Leger, C.A., Aurrand-Lions, M., Beltraminelli, N., Fasel, N., and Imhof, B.A. (2002). Junctional adhesion molecule-2 (JAM-2) promotes lymphocyte transendothelial migration. Blood *100*, 2479-2486.

Ju, H., Lee, K.A., Yang, M., Kim, H.J., Kang, C.P., Sohn, T.S., Rhee, J.C., Kang, C., and Kim, J.W. (2005). TP53BP2 locus is associated with gastric cancer susceptibility. International journal of cancer *117*, 957-960.

Karuman, P., Gozani, O., Odze, R.D., Zhou, X.C., Zhu, H., Shaw, R., Brien, T.P., Bozzuto, C.D., Ooi, D., Cantley, L.C.*, et al.* (2001). The Peutz-Jegher gene product LKB1 is a mediator of p53-dependent cell death. Molecular cell *7*, 1307-1319.

Katoh, M. (2007). Notch signaling in gastrointestinal tract (review). Int J Oncol *30*, 247-251.

Katz, K.D., Hollander, D., Vadheim, C.M., McElree, C., Delahunty, T., Dadufalza, V.D., Krugliak, P., and Rotter, J.I. (1989). Intestinal permeability in patients with Crohn's disease and their healthy relatives. Gastroenterology *97*, 927-931.

Kausalya, P.J., Amasheh, S., Gunzel, D., Wurps, H., Muller, D., Fromm, M., and Hunziker, W. (2006). Disease-associated mutations affect intracellular traffic and paracellular Mg2+ transport function of Claudin-16. The Journal of clinical investigation *116*, 878-891.

Kazmierczak, B.I., Mostov, K., and Engel, J.N. (2001). Interaction of bacterial pathogens with polarized epithelium. Annual review of microbiology *55*, 407-435.

Kelly, D., Conway, S., and Aminov, R. (2005). Commensal gut bacteria: mechanisms of immune modulation. Trends in immunology *26*, 326-333.

Kemp, B.E., Mitchelhill, K.I., Stapleton, D., Michell, B.J., Chen, Z.P., and Witters, L.A. (1999). Dealing with energy demand: the AMP-activated protein kinase. Trends in biochemical sciences *24*, 22-25.

Kemp, C.J., Wheldon, T., and Balmain, A. (1994). p53-deficient mice are extremely susceptible to radiation-induced tumorigenesis. Nature genetics *8*, 66-69.

Kim, J.G., Lee, S.J., and Kagnoff, M.F. (2004). Nod1 is an essential signal transducer in intestinal epithelial cells infected with bacteria that avoid recognition by toll-like receptors. Infection and immunity *72*, 1487-1495.

Kim, J.M., Eckmann, L., Savidge, T.C., Lowe, D.C., Witthoft, T., and Kagnoff, M.F. (1998). Apoptosis of human intestinal epithelial cells after bacterial invasion. The Journal of clinical investigation *102*, 1815-1823.

Kinnebrew, M.A., and Pamer, E.G. (2012). Innate immune signaling in defense against intestinal microbes. Immunological reviews *245*, 113-131.

Knust, E., and Bossinger, O. (2002). Composition and formation of intercellular junctions in epithelial cells. Science *298*, 1955-1959.

Kobayashi, K.S., Chamaillard, M., Ogura, Y., Henegariu, O., Inohara, N., Nunez, G., and Flavell, R.A. (2005). Nod2-dependent regulation of innate and adaptive immunity in the intestinal tract. Science *307*, 731-734.

Kojouharoff, G., Hans, W., Obermeier, F., Mannel, D.N., Andus, T., Scholmerich, J., Gross, V., and Falk, W. (1997). Neutralization of tumour necrosis factor (TNF) but not of IL-1 reduces inflammation in chronic dextran sulphate sodium-induced colitis in mice. Clinical and experimental immunology *107*, 353-358.

Korinek, V., Barker, N., Moerer, P., van Donselaar, E., Huls, G., Peters, P.J., and Clevers, H. (1998a). Depletion of epithelial stem-cell compartments in the small intestine of mice lacking Tcf-4. Nature genetics *19*, 379-383.

Korinek, V., Barker, N., Willert, K., Molenaar, M., Roose, J., Wagenaar, G., Markman, M., Lamers, W., Destree, O., and Clevers, H. (1998b). Two members of the Tcf family implicated in Wnt/beta-catenin signaling during embryogenesis in the mouse. Molecular and cellular biology *18*, 1248-1256.

Kouklis, P.D., Hutton, E., and Fuchs, E. (1994). Making a connection: direct binding between keratin intermediate filaments and desmosomal proteins. The Journal of cell biology *127*, 1049-1060.

Kraehenbuhl, J.P., and Corbett, M. (2004). Immunology. Keeping the gut microflora at bay. Science *303*, 1624-1625.

Kruidenier, L., and Verspaget, H.W. (2002). Review article: oxidative stress as a pathogenic factor in inflammatory bowel disease--radicals or ridiculous? Alimentary pharmacology & therapeutics *16*, 1997-2015.

Kruse, J.P., and Gu, W. (2009). Modes of p53 regulation. Cell *137*, 609-622.

Kubbutat, M.H., Jones, S.N., and Vousden, K.H. (1997). Regulation of p53 stability by Mdm2. Nature *387*, 299-303.

Kucharzik, T., Walsh, S.V., Chen, J., Parkos, C.A., and Nusrat, A. (2001). Neutrophil transmigration in inflammatory bowel disease is associated with differential expression of epithelial intercellular junction proteins. The American journal of pathology *159*, 2001-2009.

Kuhn, R., Lohler, J., Rennick, D., Rajewsky, K., and Muller, W. (1993). Interleukin-10-deficient mice develop chronic enterocolitis. Cell *75*, 263-274.

Kuhnert, F., Davis, C.R., Wang, H.T., Chu, P., Lee, M., Yuan, J., Nusse, R., and Kuo, C.J. (2004). Essential requirement for Wnt signaling in proliferation of adult small intestine and colon revealed by adenoviral expression of Dickkopf-1. Proceedings of the National Academy of Sciences of the United States of America *101*, 266-271.

Kullberg, M.C., Ward, J.M., Gorelick, P.L., Caspar, P., Hieny, S., Cheever, A., Jankovic, D., and Sher, A. (1998). Helicobacter hepaticus triggers colitis in specific-pathogen-free interleukin-10 (IL-10)-deficient mice through an IL-12- and gamma interferon-dependent mechanism. Infection and immunity *66*, 5157-5166.

Laderoute, K.R., Amin, K., Calaoagan, J.M., Knapp, M., Le, T., Orduna, J., Foretz, M., and Viollet, B. (2006). 5'-AMP-activated protein kinase (AMPK) is induced by low-oxygen and glucose deprivation conditions found in solid-tumor microenvironments. Molecular and cellular biology *26*, 5336-5347.

Lakin, N.D., and Jackson, S.P. (1999). Regulation of p53 in response to DNA damage. Oncogene *18*, 7644-7655.

Lammi, L., Arte, S., Somer, M., Jarvinen, H., Lahermo, P., Thesleff, I., Pirinen, S., and Nieminen, P. (2004). Mutations in AXIN2 cause familial tooth agenesis and predispose to colorectal cancer. American journal of human genetics *74*, 1043-1050.

Laukoetter, M.G., Nava, P., Lee, W.Y., Severson, E.A., Capaldo, C.T., Babbin, B.A., Williams, I.R., Koval, M., Peatman, E., Campbell, J.A*., et al.* (2007). JAM-A regulates permeability and inflammation in the intestine in vivo. The Journal of experimental medicine *204*, 3067-3076.

Laurent-Puig, P., Beroud, C., and Soussi, T. (1998). APC gene: database of germline and somatic mutations in human tumors and cell lines. Nucleic acids research *26*, 269-270.

Lee, H.S., Nishanian, T.G., Mood, K., Bong, Y.S., and Daar, I.O. (2008). EphrinB1 controls cell-cell junctions through the Par polarity complex. Nature cell biology *10*, 979-986.

Lee, J., Mo, J.H., Katakura, K., Alkalay, I., Rucker, A.N., Liu, Y.T., Lee, H.K., Shen, C., Cojocaru, G., Shenouda, S*., et al.* (2006). Maintenance of colonic homeostasis by distinctive apical TLR9 signalling in intestinal epithelial cells. Nature cell biology *8*, 1327-1336.

Lee, J.H., Koh, H., Kim, M., Kim, Y., Lee, S.Y., Karess, R.E., Lee, S.H., Shong, M., Kim, J.M., Kim, J*., et al.* (2007). Energy-dependent regulation of cell structure by AMP-activated protein kinase. Nature *447*, 1017-1020.

Lee, M., and Vasioukhin, V. (2008). Cell polarity and cancer--cell and tissue polarity as a non-canonical tumor suppressor. Journal of cell science *121*, 1141-1150.

Lemmers, C., Medina, E., Delgrossi, M.H., Michel, D., Arsanto, J.P., and Le Bivic, A. (2002). hINADl/PATJ, a homolog of discs lost, interacts with crumbs and localizes to tight junctions in human epithelial cells. The Journal of biological chemistry *277*, 25408-25415.

Lemmers, C., Michel, D., Lane-Guermonprez, L., Delgrossi, M.H., Medina, E., Arsanto, J.P., and Le Bivic, A. (2004). CRB3 binds directly to Par6 and regulates the morphogenesis of the tight junctions in mammalian epithelial cells. Molecular biology of the cell *15*, 1324-1333.

Lennard-Jones, J.E. (1989). Classification of inflammatory bowel disease. Scandinavian journal of gastroenterology Supplement *170*, 2-6; discussion 16-19.

Li, Q., Zhang, Q., Wang, M., Zhao, S., Ma, J., Luo, N., Li, N., Li, Y., Xu, G., and Li, J. (2008). Interferon-gamma and tumor necrosis factor-alpha disrupt epithelial barrier function by altering lipid composition in membrane microdomains of tight junction. Clin Immunol *126*, 67-80.

Li, Y., Welm, B., Podsypanina, K., Huang, S., Chamorro, M., Zhang, X., Rowlands, T., Egeblad, M., Cowin, P., Werb, Z*., et al.* (2003). Evidence that transgenes encoding components of the Wnt signaling pathway preferentially induce mammary cancers from progenitor cells. Proceedings of the National Academy of Sciences of the United States of America *100*, 15853-15858.

Liang, T.W., Chiu, H.H., Gurney, A., Sidle, A., Tumas, D.B., Schow, P., Foster, J., Klassen, T., Dennis, K., DeMarco, R.A*., et al.* (2002). Vascular endothelial-junctional adhesion molecule (VE-JAM)/JAM 2 interacts with T, NK, and dendritic cells through JAM 3. J Immunol *168*, 1618-1626.

Lien, E., Chow, J.C., Hawkins, L.D., McGuinness, P.D., Miyake, K., Espevik, T., Gusovsky, F., and Golenbock, D.T. (2001). A novel synthetic acyclic lipid A-like agonist activates cells via the lipopolysaccharide/toll-like receptor 4 signaling pathway. The Journal of biological chemistry *276*, 1873-1880.

Liu, L.X., Liu, Z.H., Jiang, H.C., Qu, X., Zhang, W.H., Wu, L.F., Zhu, A.L., Wang, X.Q., and Wu, M. (2002). Profiling of differentially expressed genes in human gastric carcinoma by cDNA expression array. World journal of gastroenterology : WJG *8*, 580-585.

Lizcano, J.M., Goransson, O., Toth, R., Deak, M., Morrice, N.A., Boudeau, J., Hawley, S.A., Udd, L., Makela, T.P., Hardie, D.G.*, et al.* (2004). LKB1 is a master kinase that activates 13 kinases of the AMPK subfamily, including MARK/PAR-1. The EMBO journal *23*, 833-843.

Llanos, S., Royer, C., Lu, M., Bergamaschi, D., Lee, W.H., and Lu, X. (2011). Inhibitory member of the apoptosis-stimulating proteins of the p53 family (iASPP) interacts with protein phosphatase 1 via a noncanonical binding motif. The Journal of biological chemistry *286*, 43039-43044.

Logan, C.Y., and Nusse, R. (2004). The Wnt signaling pathway in development and disease. Annual review of cell and developmental biology *20*, 781-810.

Lorenz, R.G., and Newberry, R.D. (2004). Isolated lymphoid follicles can function as sites for induction of mucosal immune responses. Annals of the New York Academy of Sciences *1029*, 44-57.

Louvard, D., Kedinger, M., and Hauri, H.P. (1992). The differentiating intestinal epithelial cell: establishment and maintenance of functions through interactions between cellular structures. Annual review of cell biology *8*, 157-195.

Lowe, S.W. (1999). Activation of p53 by oncogenes. Endocrine-related cancer *6*, 45-48.

Lowenfels, A.B. (1973). Why are small-bowel tumours so rare? Lancet *1*, 24-26.

Lowry, W.E., Blanpain, C., Nowak, J.A., Guasch, G., Lewis, L., and Fuchs, E. (2005). Defining the impact of beta-catenin/Tcf transactivation on epithelial stem cells. Genes Dev *19*, 1596-1611.

Lu, W., Pochampally, R., Chen, L., Traidej, M., Wang, Y., and Chen, J. (2000). Nuclear exclusion of p53 in a subset of tumors requires MDM2 function. Oncogene *19*, 232-240.

Ludwig, R.L., Bates, S., and Vousden, K.H. (1996). Differential activation of target cellular promoters by p53 mutants with impaired apoptotic function. Molecular and cellular biology *16*, 4952-4960.

Ma, T.Y., Iwamoto, G.K., Hoa, N.T., Akotia, V., Pedram, A., Boivin, M.A., and Said, H.M. (2004). TNF-alpha-induced increase in intestinal epithelial tight junction permeability requires NF-kappa B activation. American journal of physiology Gastrointestinal and liver physiology *286*, G367-376.

MacPherson, G., Milling, S., Yrlid, U., Cousins, L., Turnbull, E., and Huang, F.P. (2004). Uptake of antigens from the intestine by dendritic cells. Annals of the New York Academy of Sciences *1029*, 75-82.

Madsen, K.L., Lewis, S.A., Tavernini, M.M., Hibbard, J., and Fedorak, R.N. (1997). Interleukin 10 prevents cytokine-induced disruption of T84 monolayer barrier integrity and limits chloride secretion. Gastroenterology *113*, 151-159.

Maggio-Price, L., Treuting, P., Zeng, W., Tsang, M., Bielefeldt-Ohmann, H., and Iritani, B.M. (2006). Helicobacter infection is required for inflammation and colon cancer in SMAD3-deficient mice. Cancer Res *66*, 828-838.

Makino, K., Kuwahara, H., Masuko, N., Nishiyama, Y., Morisaki, T., Sasaki, J., Nakao, M., Kuwano, A., Nakata, M., Ushio, Y*., et al.* (1997). Cloning and characterization of NE-dlg: a novel human homolog of the Drosophila discs large (dlg) tumor suppressor protein interacts with the APC protein. Oncogene *14*, 2425-2433.

Mankertz, J., and Schulzke, J.D. (2007). Altered permeability in inflammatory bowel disease: pathophysiology and clinical implications. Current opinion in gastroenterology *23*, 379-383.

Mankertz, J., Tavalali, S., Schmitz, H., Mankertz, A., Riecken, E.O., Fromm, M., and Schulzke, J.D. (2000). Expression from the human occludin promoter is affected by tumor necrosis factor alpha and interferon gamma. Journal of cell science *113 (Pt 11)*, 2085-2090.

Marchiando, A.M., Graham, W.V., and Turner, J.R. (2010). Epithelial barriers in homeostasis and disease. Annual review of pathology *5*, 119-144.

Margolis, B., and Borg, J.P. (2005). Apicobasal polarity complexes. Journal of cell science *118*, 5157-5159.

Marignani, P.A., Kanai, F., and Carpenter, C.L. (2001). LKB1 associates with Brg1 and is necessary for Brg1-induced growth arrest. The Journal of biological chemistry *276*, 32415-32418.

Marsh, V., and Clarke, A. (2007). Intestinal homeostasis and neoplasia studied using conditional transgenesis. Expert review of anticancer therapy *7*, 519-531.

Martin-Padura, I., Lostaglio, S., Schneemann, M., Williams, L., Romano, M., Fruscella, P., Panzeri, C., Stoppacciaro, A., Ruco, L., Villa, A*., et al.* (1998). Junctional adhesion molecule, a novel member of the immunoglobulin superfamily that distributes at intercellular junctions and modulates monocyte transmigration. The Journal of cell biology *142*, 117-127.

Martin, S.G., and St Johnston, D. (2003). A role for Drosophila LKB1 in anterior-posterior axis formation and epithelial polarity. Nature *421*, 379-384.

Massey, D.C., and Parkes, M. (2007). Genome-wide association scanning highlights two autophagy genes, ATG16L1 and IRGM, as being significantly associated with Crohn's disease. Autophagy *3*, 649-651.

Matsumoto, S., Hara, T., Mitsuyama, K., Yamamoto, M., Tsuruta, O., Sata, M., Scheller, J., Rose-John, S., Kado, S., and Takada, T. (2010). Essential roles of IL-6 trans-signaling in colonic epithelial cells, induced by the IL-6/soluble-IL-6 receptor derived from lamina propria macrophages, on the development of colitis-associated premalignant cancer in a murine model. J Immunol *184*, 1543-1551.

Matter, K., Aijaz, S., Tsapara, A., and Balda, M.S. (2005). Mammalian tight junctions in the regulation of epithelial differentiation and proliferation. Current opinion in cell biology *17*, 453-458.

Matter, K., and Mellman, I. (1994). Mechanisms of cell polarity: sorting and transport in epithelial cells. Current opinion in cell biology *6*, 545-554.

May, G.R., Sutherland, L.R., and Meddings, J.B. (1993). Is small intestinal permeability really increased in relatives of patients with Crohn's disease? Gastroenterology *104*, 1627-1632.

Mazaud-Guittot, S., Meugnier, E., Pesenti, S., Wu, X., Vidal, H., Gow, A., and Le Magueresse-Battistoni, B. (2010). Claudin 11 deficiency in mice results in loss of the Sertoli cell epithelial phenotype in the testis. Biology of reproduction *82*, 202-213.

McCarthy, K.M., Skare, I.B., Stankewich, M.C., Furuse, M., Tsukita, S., Rogers, R.A., Lynch, R.D., and Schneeberger, E.E. (1996). Occludin is a functional component of the tight junction. Journal of cell science *109 (Pt 9)*, 2287-2298.

McCracken, V.J., and Lorenz, R.G. (2001). The gastrointestinal ecosystem: a precarious alliance among epithelium, immunity and microbiota. Cellular microbiology *3*, 1-11.

Medzhitov, R. (2008). Origin and physiological roles of inflammation. Nature *454*, 428-435.

Medzhitov, R., Preston-Hurlburt, P., Kopp, E., Stadlen, A., Chen, C., Ghosh, S., and Janeway, C.A., Jr. (1998). MyD88 is an adaptor protein in the hToll/IL-1 receptor family signaling pathways. Molecular cell *2*, 253-258.

Michel, D., Arsanto, J.P., Massey-Harroche, D., Beclin, C., Wijnholds, J., and Le Bivic, A. (2005). PATJ connects and stabilizes apical and lateral components of tight junctions in human intestinal cells. Journal of cell science *118*, 4049-4057.

Milburn, C.C., Boudeau, J., Deak, M., Alessi, D.R., and van Aalten, D.M. (2004). Crystal structure of MO25 alpha in complex with the C terminus of the pseudo kinase STE20-related adaptor. Nature structural & molecular biology *11*, 193-200.

Mirouse, V., Swick, L.L., Kazgan, N., St Johnston, D., and Brenman, J.E. (2007). LKB1 and AMPK maintain epithelial cell polarity under energetic stress. The Journal of cell biology *177*, 387-392.

Miyoshi, H., Nakau, M., Ishikawa, T.O., Seldin, M.F., Oshima, M., and Taketo, M.M. (2002). Gastrointestinal hamartomatous polyposis in Lkb1 heterozygous knockout mice. Cancer Res *62*, 2261-2266.

Montagne, L., Piel, C., and Lalles, J.P. (2004). Effect of diet on mucin kinetics and composition: nutrition and health implications. Nutrition reviews *62*, 105-114.

Moore, R.J., Owens, D.M., Stamp, G., Arnott, C., Burke, F., East, N., Holdsworth, H., Turner, L., Rollins, B., Pasparakis, M.*, et al.* (1999). Mice deficient in tumor necrosis factor-alpha are resistant to skin carcinogenesis. Nature medicine *5*, 828-831.

Moreno-Bueno, G., Portillo, F., and Cano, A. (2008). Transcriptional regulation of cell polarity in EMT and cancer. Oncogene *27*, 6958-6969.

Mori, S., Ito, G., Usami, N., Yoshioka, H., Ueda, Y., Kodama, Y., Takahashi, M., Fong, K.M., Shimokata, K., and Sekido, Y. (2004). p53 apoptotic pathway molecules are frequently and simultaneously altered in nonsmall cell lung carcinoma. Cancer *100*, 1673-1682.

Morin, P.J., Sparks, A.B., Korinek, V., Barker, N., Clevers, H., Vogelstein, B., and Kinzler, K.W. (1997). Activation of beta-catenin-Tcf signaling in colon cancer by mutations in beta-catenin or APC. Science *275*, 1787-1790.

Moser, A.R., Luongo, C., Gould, K.A., McNeley, M.K., Shoemaker, A.R., and Dove, W.F. (1995). ApcMin: a mouse model for intestinal and mammary tumorigenesis. Eur J Cancer *31A*, 1061-1064.

Mostov, K., Apodaca, G., Aroeti, B., and Okamoto, C. (1992). Plasma membrane protein sorting in polarized epithelial cells. The Journal of cell biology *116*, 577-583.

Muth, T.R., and Caplan, M.J. (2003). Transport protein trafficking in polarized cells. Annual review of cell and developmental biology *19*, 333-366.

Muza-Moons, M.M., Koutsouris, A., and Hecht, G. (2003). Disruption of cell polarity by enteropathogenic Escherichia coli enables basolateral membrane proteins to migrate apically and to potentiate physiological consequences. Infection and immunity *71*, 7069-7078.

Muzio, M., Bosisio, D., Polentarutti, N., D'Amico, G., Stoppacciaro, A., Mancinelli, R., van't Veer, C., Penton-Rol, G., Ruco, L.P., Allavena, P*., et al.* (2000). Differential expression and regulation of toll-like receptors (TLR) in human leukocytes: selective expression of TLR3 in dendritic cells. J Immunol *164*, 5998-6004.

Nagafuchi, A. (2001). Molecular architecture of adherens junctions. Current opinion in cell biology *13*, 600-603.

Nagai-Tamai, Y., Mizuno, K., Hirose, T., Suzuki, A., and Ohno, S. (2002). Regulated protein-protein interaction between aPKC and PAR-3 plays an essential role in the polarization of epithelial cells. Genes to cells : devoted to molecular & cellular mechanisms *7*, 1161-1171.

Nakagawa, H., Koyama, K., Murata, Y., Morito, M., Akiyama, T., and Nakamura, Y. (2000). APCL, a central nervous system-specific homologue of adenomatous polyposis coli tumor suppressor, binds to p53-binding protein 2 and translocates it to the perinucleus. Cancer Res *60*, 101-105.

Nakagawa, S., Yano, T., Nakagawa, K., Takizawa, S., Suzuki, Y., Yasugi, T., Huibregtse, J.M., and Taketani, Y. (2004). Analysis of the expression and localisation of a LAP protein, human scribble, in the normal and neoplastic epithelium of uterine cervix. British journal of cancer *90*, 194-199.

Nakamura, T., Tsuchiya, K., and Watanabe, M. (2007). Crosstalk between Wnt and Notch signaling in intestinal epithelial cell fate decision. J Gastroenterol *42*, 705-710.

Naumovski, L., and Cleary, M.L. (1996). The p53-binding protein 53BP2 also interacts with Bc12 and impedes cell cycle progression at G2/M. Molecular and cellular biology *16*, 3884-3892.

Nishisho, I., Nakamura, Y., Miyoshi, Y., Miki, Y., Ando, H., Horii, A., Koyama, K., Utsunomiya, J., Baba, S., and Hedge, P. (1991). Mutations of chromosome 5q21 genes in FAP and colorectal cancer patients. Science *253*, 665-669.

Nitta, T., Hata, M., Gotoh, S., Seo, Y., Sasaki, H., Hashimoto, N., Furuse, M., and Tsukita, S. (2003). Size-selective loosening of the blood-brain barrier in claudin-5-deficient mice. The Journal of cell biology *161*, 653-660.

Noah, T.K., and Shroyer, N.F. (2012). Notch in the Intestine: Regulation of Homeostasis and Pathogenesis. Annual review of physiology.

Nolan, M.E., Aranda, V., Lee, S., Lakshmi, B., Basu, S., Allred, D.C., and Muthuswamy, S.K. (2008). The polarity protein Par6 induces cell proliferation and is overexpressed in breast cancer. Cancer research *68*, 8201-8209.

Nomura, F., Kawai, T., Nakanishi, K., and Akira, S. (2000). NF-kappaB activation through IKK-i-dependent I-TRAF/TANK phosphorylation. Genes to cells : devoted to molecular & cellular mechanisms *5*, 191-202.

Notari, M., Hu, Y., Koch, S., Lu, M., Ratnayaka, I., Zhong, S., Baer, C., Pagotto, A., Goldin, R., Salter, V.*, et al.* Inhibitor of apoptosis-stimulating protein of p53 (iASPP) prevents senescence and is required for epithelial stratification. Proceedings of the National Academy of Sciences of the United States of America *108*, 16645-16650.

O'Neill, L.A., and Dinarello, C.A. (2000). The IL-1 receptor/toll-like receptor superfamily: crucial receptors for inflammation and host defense. Immunology today *21*, 206-209.

Ogura, Y., Saab, L., Chen, F.F., Benito, A., Inohara, N., and Nunez, G. (2003). Genetic variation and activity of mouse Nod2, a susceptibility gene for Crohn's disease. Genomics *81*, 369-377.

Ohno, S. (2001). Intercellular junctions and cellular polarity: the PAR-aPKC complex, a conserved core cassette playing fundamental roles in cell polarity. Current opinion in cell biology *13*, 641-648.

Okayasu, I., Hatakeyama, S., Yamada, M., Ohkusa, T., Inagaki, Y., and Nakaya, R. (1990). A novel method in the induction of reliable experimental acute and chronic ulcerative colitis in mice. Gastroenterology *98*, 694-702.

Okayasu, I., Yamada, M., Mikami, T., Yoshida, T., Kanno, J., and Ohkusa, T. (2002). Dysplasia and carcinoma development in a repeated dextran sulfate sodium-induced colitis model. Journal of gastroenterology and hepatology *17*, 1078-1083.

Okoshi, R., Ozaki, T., Yamamoto, H., Ando, K., Koida, N., Ono, S., Koda, T., Kamijo, T., Nakagawara, A., and Kizaki, H. (2008). Activation of AMP-activated protein kinase induces p53-dependent apoptotic cell death in response to energetic stress. The Journal of biological chemistry *283*, 3979-3987.

Oliner, J.D., Kinzler, K.W., Meltzer, P.S., George, D.L., and Vogelstein, B. (1992). Amplification of a gene encoding a p53-associated protein in human sarcomas. Nature *358*, 80-83.

Oshitani, N., Watanabe, K., Nakamura, S., Fujiwara, Y., Higuchi, K., and Arakawa, T. (2005). Dislocation of tight junction proteins without F-actin disruption in inactive Crohn's disease. International journal of molecular medicine *15*, 407-410.

Ozinsky, A., Underhill, D.M., Fontenot, J.D., Hajjar, A.M., Smith, K.D., Wilson, C.B., Schroeder, L., and Aderem, A. (2000). The repertoire for pattern recognition of pathogens by the innate immune system is defined by cooperation between toll-like receptors. Proceedings of the National Academy of Sciences of the United States of America *97*, 13766-13771.

Pamer, E.G. (2007). Immune responses to commensal and environmental microbes. Nature immunology *8*, 1173-1178.

Partanen, J.I., Tervonen, T.A., Myllynen, M., Lind, E., Imai, M., Katajisto, P., Dijkgraaf, G.J., Kovanen, P.E., Makela, T.P., Werb, Z.*, et al.* (2012). Tumor suppressor function of Liver kinase B1 (Lkb1) is linked to regulation of epithelial integrity. Proceedings of the National Academy of Sciences of the United States of America *109*, E388-397.

Pearson, H.B., McCarthy, A., Collins, C.M., Ashworth, A., and Clarke, A.R. (2008). Lkb1 deficiency causes prostate neoplasia in the mouse. Cancer Res *68*, 2223-2232.

Pearson, H.B., Perez-Mancera, P.A., Dow, L.E., Ryan, A., Tennstedt, P., Bogani, D., Elsum, I., Greenfield, A., Tuveson, D.A., Simon, R.*, et al.* (2011). SCRIB expression is deregulated in human prostate cancer, and its deficiency in mice promotes prostate neoplasia. The Journal of clinical investigation *121*, 4257-4267.

Pellegrinet, L., Rodilla, V., Liu, Z., Chen, S., Koch, U., Espinosa, L., Kaestner, K.H., Kopan, R., Lewis, J., and Radtke, F. (2011). Dll1- and dll4-mediated notch signaling are required for homeostasis of intestinal stem cells. Gastroenterology *140*, 1230-1240 e1231-1237.

Petersson, J., Schreiber, O., Hansson, G.C., Gendler, S.J., Velcich, A., Lundberg, J.O., Roos, S., Holm, L., and Phillipson, M. (2011). Importance and regulation of the colonic mucus barrier in a mouse model of colitis. American journal of physiology Gastrointestinal and liver physiology *300*, G327-333.

Pino, M.S., and Chung, D.C. (2010). The chromosomal instability pathway in colon cancer. Gastroenterology *138*, 2059-2072.

Pinto, D., Gregorieff, A., Begthel, H., and Clevers, H. (2003). Canonical Wnt signals are essential for homeostasis of the intestinal epithelium. Genes Dev *17*, 1709-1713.

Plant, P.J., Fawcett, J.P., Lin, D.C., Holdorf, A.D., Binns, K., Kulkarni, S., and Pawson, T. (2003). A polarity complex of mPar-6 and atypical PKC binds, phosphorylates and regulates mammalian Lgl. Nature cell biology *5*, 301-308.

Podolsky, D.K. (1991). Inflammatory bowel disease (1). The New England journal of medicine *325*, 928-937.

Polakis, P. (1999). The oncogenic activation of beta-catenin. Current opinion in genetics & development *9*, 15-21.

Popivanova, B.K., Kitamura, K., Wu, Y., Kondo, T., Kagaya, T., Kaneko, S., Oshima, M., Fujii, C., and Mukaida, N. (2008). Blocking TNF-alpha in mice reduces colorectal carcinogenesis associated with chronic colitis. The Journal of clinical investigation *118*, 560-570.

Poritz, L.S., Harris, L.R., 3rd, Kelly, A.A., and Koltun, W.A. (2011). Increase in the tight junction protein claudin-1 in intestinal inflammation. Dig Dis Sci *56*, 2802-2809.

Porter, E.M., Bevins, C.L., Ghosh, D., and Ganz, T. (2002). The multifaceted Paneth cell. Cell Mol Life Sci *59*, 156-170.

Potten, C.S. (1992). The significance of spontaneous and induced apoptosis in the gastrointestinal tract of mice. Cancer metastasis reviews *11*, 179-195.

Potten, C.S. (1997). Epithelial cell growth and differentiation. II. Intestinal apoptosis. The American journal of physiology *273*, G253-257.

Potten, C.S., and Loeffler, M. (1990). Stem cells: attributes, cycles, spirals, pitfalls and uncertainties. Lessons for and from the crypt. Development *110*, 1001-1020.

Potten, C.S., and Morris, R.J. (1988). Epithelial stem cells in vivo. Journal of cell science Supplement *10*, 45-62.

Potten, C.S., Wilson, J.W., and Booth, C. (1997). Regulation and significance of apoptosis in the stem cells of the gastrointestinal epithelium. Stem Cells *15*, 82-93.

Radtke, F., Wilson, A., and MacDonald, H.R. (2004). Notch signaling in T- and B-cell development. Current opinion in immunology *16*, 174-179.

Rakoff-Nahoum, S., and Medzhitov, R. (2007). Regulation of spontaneous intestinal tumorigenesis through the adaptor protein MyD88. Science *317*, 124-127.

Rakoff-Nahoum, S., Paglino, J., Eslami-Varzaneh, F., Edberg, S., and Medzhitov, R. (2004). Recognition of commensal microflora by toll-like receptors is required for intestinal homeostasis. Cell *118*, 229-241.

Ramachandran, A., Madesh, M., and Balasubramanian, K.A. (2000). Apoptosis in the intestinal epithelium: its relevance in normal and pathophysiological conditions. Journal of gastroenterology and hepatology *15*, 109-120.

Ramos, Y.F., Stad, R., Attema, J., Peltenburg, L.T., van der Eb, A.J., and Jochemsen, A.G. (2001). Aberrant expression of HDMX proteins in tumor cells correlates with wild-type p53. Cancer Res *61*, 1839-1842.

Redston, M.S., Papadopoulos, N., Caldas, C., Kinzler, K.W., and Kern, S.E. (1995). Common occurrence of APC and K-ras gene mutations in the spectrum of colitis-associated neoplasias. Gastroenterology *108*, 383-392.

Regala, R.P., Weems, C., Jamieson, L., Khoor, A., Edell, E.S., Lohse, C.M., and Fields, A.P. (2005). Atypical protein kinase C iota is an oncogene in human non-small cell lung cancer. Cancer Res *65*, 8905-8911.

Rehfeld, J.F. (1998). The new biology of gastrointestinal hormones. Physiological reviews *78*, 1087-1108.

Reifenberger, G., Liu, L., Ichimura, K., Schmidt, E.E., and Collins, V.P. (1993). Amplification and overexpression of the MDM2 gene in a subset of human malignant gliomas without p53 mutations. Cancer Res *53*, 2736-2739.

Reinecker, H.C., Steffen, M., Witthoeft, T., Pflueger, I., Schreiber, S., MacDermott, R.P., and Raedler, A. (1993). Enhanced secretion of tumour necrosis factor-alpha, IL-6, and IL-1 beta by isolated lamina propria mononuclear cells from patients with ulcerative colitis and Crohn's disease. Clinical and experimental immunology *94*, 174-181.

Reya, T., Duncan, A.W., Ailles, L., Domen, J., Scherer, D.C., Willert, K., Hintz, L., Nusse, R., and Weissman, I.L. (2003). A role for Wnt signalling in self-renewal of haematopoietic stem cells. Nature *423*, 409-414.

Rhodes, J.M., and Campbell, B.J. (2002). Inflammation and colorectal cancer: IBD-associated and sporadic cancer compared. Trends in molecular medicine *8*, 10-16.

Riccio, O., van Gijn, M.E., Bezdek, A.C., Pellegrinet, L., van Es, J.H., Zimber-Strobl, U., Strobl, L.J., Honjo, T., Clevers, H., and Radtke, F. (2008). Loss of intestinal crypt progenitor cells owing to inactivation of both Notch1 and Notch2 is accompanied by derepression of CDK inhibitors p27Kip1 and p57Kip2. EMBO Rep *9*, 377-383.

Rodrigues, N.R., Rowan, A., Smith, M.E., Kerr, I.B., Bodmer, W.F., Gannon, J.V., and Lane, D.P. (1990). p53 mutations in colorectal cancer. Proceedings of the National Academy of Sciences of the United States of America *87*, 7555-7559.

Roh, M.H., Makarova, O., Liu, C.J., Shin, K., Lee, S., Laurinec, S., Goyal, M., Wiggins, R., and Margolis, B. (2002). The Maguk protein, Pals1, functions as an adapter, linking mammalian homologues of Crumbs and Discs Lost. The Journal of cell biology *157*, 161-172.

Roose, J., Huls, G., van Beest, M., Moerer, P., van der Horn, K., Goldschmeding, R., Logtenberg, T., and Clevers, H. (1999). Synergy between tumor suppressor APC and the beta-catenin-Tcf4 target Tcf1. Science *285*, 1923-1926.

Rosenberg, D.W., Giardina, C., and Tanaka, T. (2009). Mouse models for the study of colon carcinogenesis. Carcinogenesis *30*, 183-196.

Rotem, S., Katz, C., and Friedler, A. (2007). Insights into the structure and protein-protein interactions of the pro-apoptotic protein ASPP2. Biochemical Society transactions *35*, 966-969.

Rowan, A., Churchman, M., Jefferey, R., Hanby, A., Poulsom, R., and Tomlinson, I. (2000). In situ analysis of LKB1/STK11 mRNA expression in human normal tissues and tumours. The Journal of pathology *192*, 203-206.

Rustgi, A.K. (2007). The genetics of hereditary colon cancer. Genes Dev *21*, 2525-2538.

Rutgeerts, P., Van Assche, G., and Vermeire, S. (2004). Optimizing anti-TNF treatment in inflammatory bowel disease. Gastroenterology *126*, 1593-1610.

Saitou, M., Fujimoto, K., Doi, Y., Itoh, M., Fujimoto, T., Furuse, M., Takano, H., Noda, T., and Tsukita, S. (1998). Occludin-deficient embryonic stem cells can differentiate into polarized epithelial cells bearing tight junctions. The Journal of cell biology *141*, 397-408.

Salzman, A.L. (1995). Nitric oxide in the gut. New Horiz *3*, 352-364.

Samuels-Lev, Y., O'Connor, D.J., Bergamaschi, D., Trigiante, G., Hsieh, J.K., Zhong, S., Campargue, I., Naumovski, L., Crook, T., and Lu, X. (2001). ASPP proteins specifically stimulate the apoptotic function of p53. Molecular cell *8*, 781-794.

Sanchez-Cespedes, M., Parrella, P., Esteller, M., Nomoto, S., Trink, B., Engles, J.M., Westra, W.H., Herman, J.G., and Sidransky, D. (2002). Inactivation of LKB1/STK11 is a common event in adenocarcinomas of the lung. Cancer Res *62*, 3659-3662.

Sanchez-Munoz, F., Dominguez-Lopez, A., and Yamamoto-Furusho, J.K. (2008). Role of cytokines in inflammatory bowel disease. World journal of gastroenterology : WJG *14*, 4280-4288.

Sancho, E., Batlle, E., and Clevers, H. (2004). Signaling pathways in intestinal development and cancer. Annual review of cell and developmental biology *20*, 695-723.

Sangiorgi, E., and Capecchi, M.R. (2008). Bmi1 is expressed in vivo in intestinal stem cells. Nature genetics *40*, 915-920.

Sansom, O.J., Reed, K.R., Hayes, A.J., Ireland, H., Brinkmann, H., Newton, I.P., Batlle, E., Simon-Assmann, P., Clevers, H., Nathke, I.S*., et al.* (2004). Loss of Apc in vivo immediately perturbs Wnt signaling, differentiation, and migration. Genes Dev *18*, 1385-1390.

Santarosa, M., and Ashworth, A. (2004). Haploinsufficiency for tumour suppressor genes: when you don't need to go all the way. Biochimica et biophysica acta *1654*, 105-122.

Sapkota, G.P., Boudeau, J., Deak, M., Kieloch, A., Morrice, N., and Alessi, D.R. (2002). Identification and characterization of four novel phosphorylation sites (Ser31, Ser325, Thr336 and Thr366) on LKB1/STK11, the protein kinase mutated in Peutz-Jeghers cancer syndrome. The Biochemical journal *362*, 481-490.

Sapkota, G.P., Kieloch, A., Lizcano, J.M., Lain, S., Arthur, J.S., Williams, M.R., Morrice, N., Deak, M., and Alessi, D.R. (2001). Phosphorylation of the protein kinase mutated in Peutz-Jeghers cancer syndrome, LKB1/STK11, at Ser431 by p90(RSK) and cAMP-dependent protein kinase, but not its farnesylation at Cys(433), is essential for LKB1 to suppress cell vrowth. The Journal of biological chemistry *276*, 19469-19482.

Sato, T., van Es, J.H., Snippert, H.J., Stange, D.E., Vries, R.G., van den Born, M., Barker, N., Shroyer, N.F., van de Wetering, M., and Clevers, H. (2011). Paneth cells constitute the niche for Lgr5 stem cells in intestinal crypts. Nature *469*, 415-418.

Sato, T., Vries, R.G., Snippert, H.J., van de Wetering, M., Barker, N., Stange, D.E., van Es, J.H., Abo, A., Kujala, P., Peters, P.J.*, et al.* (2009). Single Lgr5 stem cells build crypt-villus structures in vitro without a mesenchymal niche. Nature *459*, 262-265.

Sawa, Y., Oshitani, N., Adachi, K., Higuchi, K., Matsumoto, T., and Arakawa, T. (2003). Comprehensive analysis of intestinal cytokine messenger RNA profile by real-time quantitative polymerase chain reaction in patients with inflammatory bowel disease. International journal of molecular medicine *11*, 175-179.

Schmitz, H., Fromm, M., Bentzel, C.J., Scholz, P., Detjen, K., Mankertz, J., Bode, H., Epple, H.J., Riecken, E.O., and Schulzke, J.D. (1999). Tumor necrosis factor-alpha (TNFalpha) regulates the epithelial barrier in the human intestinal cell line HT-29/B6. Journal of cell science *112 (Pt 1)*, 137-146.

Schonhoff, S.E., Giel-Moloney, M., and Leiter, A.B. (2004). Minireview: Development and differentiation of gut endocrine cells. Endocrinology *145*, 2639-2644.

Schottenfeld, D., and Beebe-Dimmer, J. (2006). Chronic inflammation: a common and important factor in the pathogenesis of neoplasia. CA: a cancer journal for clinicians *56*, 69-83.

Schreiber, D.S., Apstein, M., and Hermos, J.A. (1978). Paneth cells in Barrett's esophagus. Gastroenterology *74*, 1302-1304.

Schroder, N., and Gossler, A. (2002). Expression of Notch pathway components in fetal and adult mouse small intestine. Gene expression patterns : GEP *2*, 247-250.

Schulzke, J.D., Gitter, A.H., Mankertz, J., Spiegel, S., Seidler, U., Amasheh, S., Saitou, M., Tsukita, S., and Fromm, M. (2005). Epithelial transport and barrier function in occludin-deficient mice. Biochimica et biophysica acta *1669*, 34-42.

Schwandner, R., Dziarski, R., Wesche, H., Rothe, M., and Kirschning, C.J. (1999). Peptidoglycan- and lipoteichoic acid-induced cell activation is mediated by toll-like receptor 2. The Journal of biological chemistry *274*, 17406-17409.

Sebbagh, M., Santoni, M.J., Hall, B., Borg, J.P., and Schwartz, M.A. (2009). Regulation of LKB1/STRAD localization and function by E-cadherin. Current biology : CB *19*, 37-42.

Selbach, M., Moese, S., Hauck, C.R., Meyer, T.F., and Backert, S. (2002). Src is the kinase of the Helicobacter pylori CagA protein in vitro and in vivo. The Journal of biological chemistry *277*, 6775-6778.

Sellon, R.K., Tonkonogy, S., Schultz, M., Dieleman, L.A., Grenther, W., Balish, E., Rennick, D.M., and Sartor, R.B. (1998). Resident enteric bacteria are necessary for development of spontaneous colitis and immune system activation in interleukin-10-deficient mice. Infection and immunity *66*, 5224-5231.

Sgroi, D.C., Teng, S., Robinson, G., LeVangie, R., Hudson, J.R., Jr., and Elkahloun, A.G. (1999). In vivo gene expression profile analysis of human breast cancer progression. Cancer Res *59*, 5656-5661.

Shaw, R.J., Bardeesy, N., Manning, B.D., Lopez, L., Kosmatka, M., DePinho, R.A., and Cantley, L.C. (2004a). The LKB1 tumor suppressor negatively regulates mTOR signaling. Cancer cell *6*, 91-99.

Shaw, R.J., Kosmatka, M., Bardeesy, N., Hurley, R.L., Witters, L.A., DePinho, R.A., and Cantley, L.C. (2004b). The tumor suppressor LKB1 kinase directly activates AMP-activated kinase and regulates apoptosis in response to energy stress. Proceedings of the National Academy of Sciences of the United States of America *101*, 3329-3335.

Shin, K., Fogg, V.C., and Margolis, B. (2006). Tight junctions and cell polarity. Annual review of cell and developmental biology *22*, 207-235.

Shorning, B.Y., Zabkiewicz, J., McCarthy, A., Pearson, H.B., Winton, D.J., Sansom, O.J., Ashworth, A., and Clarke, A.R. (2009). Lkb1 deficiency alters goblet and paneth cell differentiation in the small intestine. PloS one *4*, e4264.

Sipos, F., and Muzes, G. (2011). Isolated lymphoid follicles in colon: switch points between inflammation and colorectal cancer? World journal of gastroenterology : WJG *17*, 1666-1673.

Slee, E.A., O'Connor, D.J., and Lu, X. (2004). To die or not to die: how does p53 decide? Oncogene *23*, 2809-2818.

Smith, D.P., Rayter, S.I., Niederlander, C., Spicer, J., Jones, C.M., and Ashworth, A. (2001). LIP1, a cytoplasmic protein functionally linked to the Peutz-Jeghers syndrome kinase LKB1. Human molecular genetics *10*, 2869-2877.

Smith, D.P., Spicer, J., Smith, A., Swift, S., and Ashworth, A. (1999). The mouse Peutz-Jeghers syndrome gene Lkb1 encodes a nuclear protein kinase. Human molecular genetics *8*, 1479-1485.

Snoeck, V., Goddeeris, B., and Cox, E. (2005). The role of enterocytes in the intestinal barrier function and antigen uptake. Microbes and infection / Institut Pasteur *7*, 997-1004.

Sottocornola, R., Royer, C., Vives, V., Tordella, L., Zhong, S., Wang, Y., Ratnayaka, I., Shipman, M., Cheung, A., Gaston-Massuet, C*., et al.* (2010). ASPP2 binds Par-3 and controls the polarity and proliferation of neural progenitors during CNS development. Developmental cell *19*, 126-137.

Specian, R.D., and Oliver, M.G. (1991). Functional biology of intestinal goblet cells. The American journal of physiology *260*, C183-193.

St Johnston, D., and Nusslein-Volhard, C. (1992). The origin of pattern and polarity in the Drosophila embryo. Cell *68*, 201-219.

Stein, S.C., Woods, A., Jones, N.A., Davison, M.D., and Carling, D. (2000). The regulation of AMP-activated protein kinase by phosphorylation. The Biochemical journal *345 Pt 3*, 437-443.

Su, J.Y., Erikson, E., and Maller, J.L. (1996). Cloning and characterization of a novel serine/threonine protein kinase expressed in early Xenopus embryos. The Journal of biological chemistry *271*, 14430-14437.

Su, L., Shen, L., Clayburgh, D.R., Nalle, S.C., Sullivan, E.A., Meddings, J.B., Abraham, C., and Turner, J.R. (2009). Targeted epithelial tight junction dysfunction causes immune activation and contributes to development of experimental colitis. Gastroenterology *136*, 551-563.

Sun, Y., Connors, K.E., and Yang, D.Q. (2007). AICAR induces phosphorylation of AMPK in an ATM-dependent, LKB1-independent manner. Molecular and cellular biochemistry *306*, 239-245.

Sussman, D.A., Santaolalla, R., Strobel, S., Dheer, R., and Abreu, M.T. (2012). Cancer in inflammatory bowel disease: lessons from animal models. Current opinion in gastroenterology *28*, 327-333.

Sutcliffe, J.E., and Brehm, A. (2004). Of flies and men; p53, a tumour suppressor. FEBS letters *567*, 86-91.

Suzuki, K., Fukui, H., Kayahara, T., Sawada, M., Seno, H., Hiai, H., Kageyama, R., Okano, H., and Chiba, T. (2005). Hes1-deficient mice show precocious differentiation of Paneth cells in the small intestine. Biochemical and biophysical research communications *328*, 348-352.

Tabuse, Y., Izumi, Y., Piano, F., Kemphues, K.J., Miwa, J., and Ohno, S. (1998). Atypical protein kinase C cooperates with PAR-3 to establish embryonic polarity in Caenorhabditis elegans. Development *125*, 3607-3614.

Tajima, M., Hirabayashi, S., Yao, I., Shirasawa, M., Osuga, J., Ishibashi, S., Fujita, T., and Hata, Y. (2003). Roles of immunoglobulin-like loops of junctional cell adhesion molecule 4; involvement in the subcellular localization and the cell adhesion. Genes to cells : devoted to molecular & cellular mechanisms *8*, 759-768.

Takayama, S., Reed, J.C., and Homma, S. (2003). Heat-shock proteins as regulators of apoptosis. Oncogene *22*, 9041-9047.

Tamboli, C.P., Neut, C., Desreumaux, P., and Colombel, J.F. (2004). Dysbiosis in inflammatory bowel disease. Gut *53*, 1-4.

Tamura, A., Hayashi, H., Imasato, M., Yamazaki, Y., Hagiwara, A., Wada, M., Noda, T., Watanabe, M., Suzuki, Y., and Tsukita, S. (2011). Loss of claudin-15, but not claudin-2, causes Na+ deficiency and glucose malabsorption in mouse small intestine. Gastroenterology *140*, 913-923.

Tamura, A., Kitano, Y., Hata, M., Katsuno, T., Moriwaki, K., Sasaki, H., Hayashi, H., Suzuki, Y., Noda, T., Furuse, M*., et al.* (2008). Megaintestine in claudin-15-deficient mice. Gastroenterology *134*, 523-534.

Tanaka, M., Kamata, R., and Sakai, R. (2005). Phosphorylation of ephrin-B1 via the interaction with claudin following cell-cell contact formation. The EMBO journal *24*, 3700-3711.

Tanaka, T., Kohno, H., Suzuki, R., Yamada, Y., Sugie, S., and Mori, H. (2003). A novel inflammation-related mouse colon carcinogenesis model induced by azoxymethane and dextran sodium sulfate. Cancer science *94*, 965-973.

Tarmin, L., Yin, J., Harpaz, N., Kozam, M., Noordzij, J., Antonio, L.B., Jiang, H.Y., Chan, O., Cymes, K., and Meltzer, S.J. (1995). Adenomatous polyposis coli gene mutations in ulcerative colitis-associated dysplasias and cancers versus sporadic colon neoplasms. Cancer Res *55*, 2035-2038.

ten Klooster, J.P., Jansen, M., Yuan, J., Oorschot, V., Begthel, H., Di Giacomo, V., Colland, F., de Koning, J., Maurice, M.M., Hornbeck, P.*, et al.* (2009). Mst4 and Ezrin induce brush borders downstream of the Lkb1/Strad/Mo25 polarization complex. Developmental cell *16*, 551-562.

Terzic, J., Grivennikov, S., Karin, E., and Karin, M. (2010). Inflammation and colon cancer. Gastroenterology *138*, 2101-2114 e2105.

Thukral, S.K., Blain, G.C., Chang, K.K., and Fields, S. (1994). Distinct residues of human p53 implicated in binding to DNA, simian virus 40 large T antigen, 53BP1, and 53BP2. Molecular and cellular biology *14*, 8315-8321.

Tiainen, M., Vaahtomeri, K., Ylikorkala, A., and Makela, T.P. (2002). Growth arrest by the LKB1 tumor suppressor: induction of p21(WAF1/CIP1). Human molecular genetics *11*, 1497-1504.

Tiainen, M., Ylikorkala, A., and Makela, T.P. (1999). Growth suppression by Lkb1 is mediated by a G(1) cell cycle arrest. Proceedings of the National Academy of Sciences of the United States of America *96*, 9248-9251.

Tian, H., Biehs, B., Warming, S., Leong, K.G., Rangell, L., Klein, O.D., and de Sauvage, F.J. (2011). A reserve stem cell population in small intestine renders Lgr5-positive cells dispensable. Nature *478*, 255-259.

Turner, J.R. (2009). Intestinal mucosal barrier function in health and disease. Nature reviews Immunology *9*, 799-809.

Ueo, T., Imayoshi, I., Kobayashi, T., Ohtsuka, T., Seno, H., Nakase, H., Chiba, T., and Kageyama, R. (2012). The role of Hes genes in intestinal development, homeostasis and tumor formation. Development *139*, 1071-1082.

Ullman, T.A., and Itzkowitz, S.H. (2011). Intestinal inflammation and cancer. Gastroenterology *140*, 1807-1816.

Umar, S. (2010). Intestinal stem cells. Current gastroenterology reports *12*, 340-348.

Unno, N., Menconi, M.J., Smith, M., and Fink, M.P. (1995). Nitric oxide mediates interferon-gamma-induced hyperpermeability in cultured human intestinal epithelial monolayers. Critical care medicine *23*, 1170-1176.

van de Wetering, M., Sancho, E., Verweij, C., de Lau, W., Oving, I., Hurlstone, A., van der Horn, K., Batlle, E., Coudreuse, D., Haramis, A.P.*, et al.* (2002). The beta-catenin/TCF-4

complex imposes a crypt progenitor phenotype on colorectal cancer cells. Cell *111*, 241-250.

van der Flier, L.G., and Clevers, H. (2009). Stem cells, self-renewal, and differentiation in the intestinal epithelium. Annual review of physiology *71*, 241-260.

Van der Sluis, M., De Koning, B.A., De Bruijn, A.C., Velcich, A., Meijerink, J.P., Van Goudoever, J.B., Buller, H.A., Dekker, J., Van Seuningen, I., Renes, I.B.*, et al.* (2006). Muc2-deficient mice spontaneously develop colitis, indicating that MUC2 is critical for colonic protection. Gastroenterology *131*, 117-129.

van Dullemen, H.M., van Deventer, S.J., Hommes, D.W., Bijl, H.A., Jansen, J., Tytgat, G.N., and Woody, J. (1995). Treatment of Crohn's disease with anti-tumor necrosis factor chimeric monoclonal antibody (cA2). Gastroenterology *109*, 129-135.

van Es, J.H., van Gijn, M.E., Riccio, O., van den Born, M., Vooijs, M., Begthel, H., Cozijnsen, M., Robine, S., Winton, D.J., Radtke, F.*, et al.* (2005). Notch/gamma-secretase inhibition turns proliferative cells in intestinal crypts and adenomas into goblet cells. Nature *435*, 959-963.

Van Itallie, C.M., and Anderson, J.M. (2006). Claudins and epithelial paracellular transport. Annual review of physiology *68*, 403-429.

Vetrano, S., Rescigno, M., Cera, M.R., Correale, C., Rumio, C., Doni, A., Fantini, M., Sturm, A., Borroni, E., Repici, A.*, et al.* (2008). Unique role of junctional adhesion molecule-a in maintaining mucosal homeostasis in inflammatory bowel disease. Gastroenterology *135*, 173-184.

Viloria-Petit, A.M., David, L., Jia, J.Y., Erdemir, T., Bane, A.L., Pinnaduwage, D., Roncari, L., Narimatsu, M., Bose, R., Moffat, J.*, et al.* (2009). A role for the TGFbeta-Par6 polarity pathway in breast cancer progression. Proceedings of the National Academy of Sciences of the United States of America *106*, 14028-14033.

Vives, V., Slee, E.A., and Lu, X. (2006a). ASPP2: a gene that controls life and death in vivo. Cell Cycle *5*, 2187-2190.

Vives, V., Su, J., Zhong, S., Ratnayaka, I., Slee, E., Goldin, R., and Lu, X. (2006b). ASPP2 is a haploinsufficient tumor suppressor that cooperates with p53 to suppress tumor growth. Genes Dev *20*, 1262-1267.

von Kries, J.P., Winbeck, G., Asbrand, C., Schwarz-Romond, T., Sochnikova, N., Dell'Oro, A., Behrens, J., and Birchmeier, W. (2000). Hot spots in beta-catenin for interactions with LEF-1, conductin and APC. Nature structural biology *7*, 800-807.

Voth, D.E., and Ballard, J.D. (2005). Clostridium difficile toxins: mechanism of action and role in disease. Clinical microbiology reviews *18*, 247-263.

Wang, Y., Wang, X.D., Lapi, E., Sullivan, A., Jia, W., He, Y.W., Ratnayaka, I., Zhong, S., Goldin, R.D., Goemans, C.G.*, et al.* (2012). Autophagic activity dictates the cellular response to oncogenic RAS. Proceedings of the National Academy of Sciences of the United States of America *109*, 13325-13330.

Wang, Z.J., Churchman, M., Avizienyte, E., McKeown, C., Davies, S., Evans, D.G., Ferguson, A., Ellis, I., Xu, W.H., Yan, Z.Y.*, et al.* (1999). Germline mutations of the LKB1 (STK11) gene in Peutz-Jeghers patients. Journal of medical genetics *36*, 365-368.

Watson, A.J., Duckworth, C.A., Guan, Y., and Montrose, M.H. (2009). Mechanisms of epithelial cell shedding in the Mammalian intestine and maintenance of barrier function. Annals of the New York Academy of Sciences *1165*, 135-142.

Watts, J.L., Morton, D.G., Bestman, J., and Kemphues, K.J. (2000). The C. elegans par-4 gene encodes a putative serine-threonine kinase required for establishing embryonic asymmetry. Development *127*, 1467-1475.

Wei, C., Amos, C.I., Stephens, L.C., Campos, I., Deng, J.M., Behringer, R.R., Rashid, A., and Frazier, M.L. (2005). Mutation of Lkb1 and p53 genes exert a cooperative effect on tumorigenesis. Cancer Res *65*, 11297-11303.

Wells, J.M., Rossi, O., Meijerink, M., and van Baarlen, P. (2011). Epithelial crosstalk at the microbiota-mucosal interface. Proceedings of the National Academy of Sciences of the United States of America *108 Suppl 1*, 4607-4614.

Willert, K., Brown, J.D., Danenberg, E., Duncan, A.W., Weissman, I.L., Reya, T., Yates, J.R., 3rd, and Nusse, R. (2003). Wnt proteins are lipid-modified and can act as stem cell growth factors. Nature *423*, 448-452.

Wills-Karp, M., Santeliz, J., and Karp, C.L. (2001). The germless theory of allergic disease: revisiting the hygiene hypothesis. Nature reviews Immunology *1*, 69-75.

Wingo, S.N., Gallardo, T.D., Akbay, E.A., Liang, M.C., Contreras, C.M., Boren, T., Shimamura, T., Miller, D.S., Sharpless, N.E., Bardeesy, N.*, et al.* (2009). Somatic LKB1 mutations promote cervical cancer progression. PloS one *4*, e5137.

Woodfin, A., Reichel, C.A., Khandoga, A., Corada, M., Voisin, M.B., Scheiermann, C., Haskard, D.O., Dejana, E., Krombach, F., and Nourshargh, S. (2007). JAM-A mediates neutrophil transmigration in a stimulus-specific manner in vivo: evidence for sequential roles for JAM-A and PECAM-1 in neutrophil transmigration. Blood *110*, 1848-1856.

Woods, A., Dickerson, K., Heath, R., Hong, S.P., Momcilovic, M., Johnstone, S.R., Carlson, M., and Carling, D. (2005). Ca2+/calmodulin-dependent protein kinase kinase-beta acts upstream of AMP-activated protein kinase in mammalian cells. Cell metabolism *2*, 21-33.

Woods, A., Johnstone, S.R., Dickerson, K., Leiper, F.C., Fryer, L.G., Neumann, D., Schlattner, U., Wallimann, T., Carlson, M., and Carling, D. (2003). LKB1 is the upstream kinase in the AMP-activated protein kinase cascade. Current biology : CB *13*, 2004-2008.

Wooten, R.M., Ma, Y., Yoder, R.A., Brown, J.P., Weis, J.H., Zachary, J.F., Kirschning, C.J., and Weis, J.J. (2002). Toll-like receptor 2 plays a pivotal role in host defense and inflammatory response to Borrelia burgdorferi. Vector Borne Zoonotic Dis *2*, 275-278.

Wu, X., Bayle, J.H., Olson, D., and Levine, A.J. (1993). The p53-mdm-2 autoregulatory feedback loop. Genes Dev *7*, 1126-1132.

Wullaert, A., Bonnet, M.C., and Pasparakis, M. (2011). NF-kappaB in the regulation of epithelial homeostasis and inflammation. Cell research *21*, 146-158.

Xiao, B., Sanders, M.J., Underwood, E., Heath, R., Mayer, F.V., Carmena, D., Jing, C., Walker, P.A., Eccleston, J.F., Haire, L.F.*, et al.* (2011). Structure of mammalian AMPK and its regulation by ADP. Nature *472*, 230-233.

Xie, S., Wang, Q., Wu, H., Cogswell, J., Lu, L., Jhanwar-Uniyal, M., and Dai, W. (2001). Reactive oxygen species-induced phosphorylation of p53 on serine 20 is mediated in part by polo-like kinase-3. The Journal of biological chemistry *276*, 36194-36199.

Yamamoto, N., Tanigaki, K., Han, H., Hiai, H., and Honjo, T. (2003). Notch/RBP-J signaling regulates epidermis/hair fate determination of hair follicular stem cells. Current biology : CB *13*, 333-338.

Yamanaka, T., Horikoshi, Y., Sugiyama, Y., Ishiyama, C., Suzuki, A., Hirose, T., Iwamatsu, A., Shinohara, A., and Ohno, S. (2003). Mammalian Lgl forms a protein complex with PAR-6 and aPKC independently of PAR-3 to regulate epithelial cell polarity. Current biology : CB *13*, 734-743.

Yang, A., Schweitzer, R., Sun, D., Kaghad, M., Walker, N., Bronson, R.T., Tabin, C., Sharpe, A., Caput, D., Crum, C.*, et al.* (1999a). p63 is essential for regenerative proliferation in limb, craniofacial and epithelial development. Nature *398*, 714-718.

Yang, J.P., Hori, M., Takahashi, N., Kawabe, T., Kato, H., and Okamoto, T. (1999b). NF-kappaB subunit p65 binds to 53BP2 and inhibits cell death induced by 53BP2. Oncogene *18*, 5177-5186.

Yang, Q., Bermingham, N.A., Finegold, M.J., and Zoghbi, H.Y. (2001). Requirement of Math1 for secretory cell lineage commitment in the mouse intestine. Science *294*, 2155-2158.

Yeaman, C., Grindstaff, K.K., and Nelson, W.J. (1999). New perspectives on mechanisms involved in generating epithelial cell polarity. Physiological reviews *79*, 73-98.

Yoo, L.I., Chung, D.C., and Yuan, J. (2002). LKB1--a master tumour suppressor of the small intestine and beyond. Nat Rev Cancer *2*, 529-535.

Youakim, A., and Ahdieh, M. (1999). Interferon-gamma decreases barrier function in T84 cells by reducing ZO-1 levels and disrupting apical actin. The American journal of physiology *276*, G1279-1288.

Yu, A.S., Enck, A.H., Lencer, W.I., and Schneeberger, E.E. (2003). Claudin-8 expression in Madin-Darby canine kidney cells augments the paracellular barrier to cation permeation. The Journal of biological chemistry *278*, 17350-17359.

Zen, K., Yasui, K., Gen, Y., Dohi, O., Wakabayashi, N., Mitsufuji, S., Itoh, Y., Zen, Y., Nakanuma, Y., Taniwaki, M.*, et al.* (2009). Defective expression of polarity protein PAR-3 gene (PARD3) in esophageal squamous cell carcinoma. Oncogene *28*, 2910-2918.

Zhang, L., Li, J., Young, L.H., and Caplan, M.J. (2006). AMP-activated protein kinase regulates the assembly of epithelial tight junctions. Proceedings of the National Academy of Sciences of the United States of America *103*, 17272-17277.

Zheng, B., and Cantley, L.C. (2007). Regulation of epithelial tight junction assembly and disassembly by AMP-activated protein kinase. Proceedings of the National Academy of Sciences of the United States of America *104*, 819-822.

Zhu, Y., Michelle Luo, T., Jobin, C., and Young, H.A. (2011). Gut microbiota and probiotics in colon tumorigenesis. Cancer letters *309*, 119-127.